Cytokinin interconversion by StCKP1 controls potato tuber dormancy

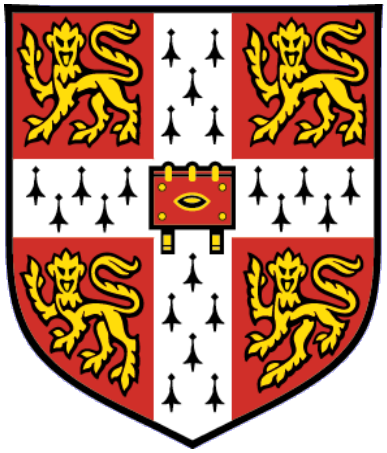

This dissertation is submitted
for the degree of Doctor of Philosophy by

Jennifer Rachael Bromley
St Catharine's College
June 2009

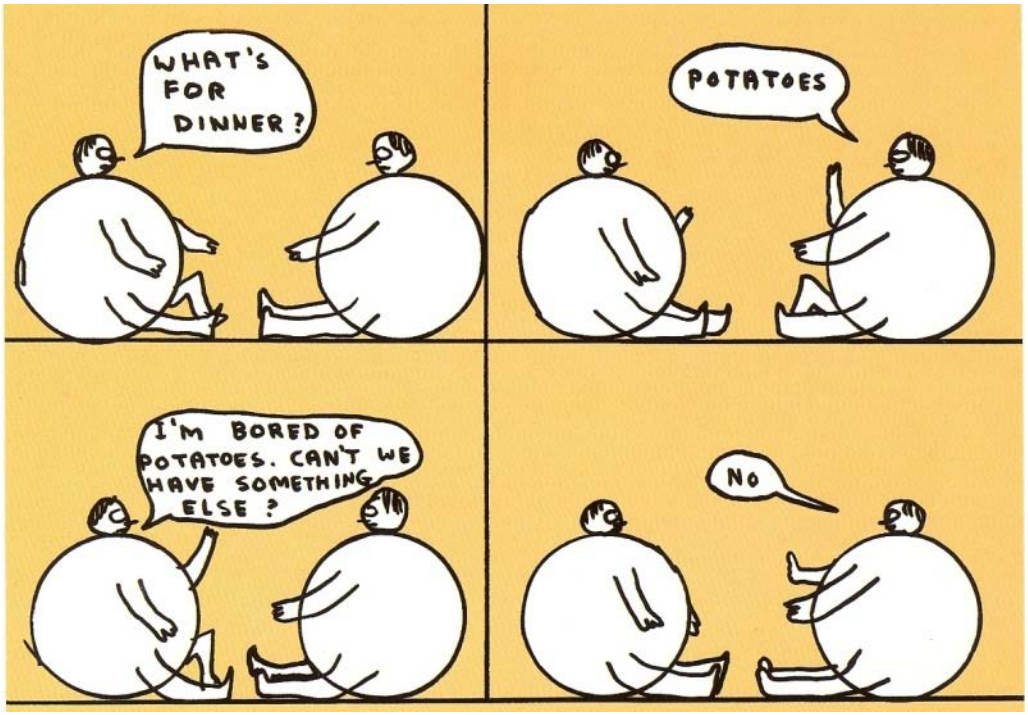

Potatoes by David Shrigley

Table of Contents

Declaration

The work described in this thesis was carried out in the Department of Plant Sciences, University of Cambridge between April 2006 and June 2009, under the supervision of Dr. David E. Hanke. The work is original except where indicated by reference. This work has not been submitted for any other degree at this or any other university and the thesis does not exceed 300 pages in length.

Jennifer Rachael Bromley

St Catharine's College

29th June 2009

Acknowledgements

Top of the list of people to say thank you to is my supervisor, Dr. David Hanke for his passion for potatoes, his constant encouragement, his approach towards my tight deadlines with the energy of someone half my age, and his encyclopaedic knowledge of language without which this thesis would not read half as well. Coming a close second is Dr. Barbara Warnes who not only helped me learn all the techniques I needed to get started, but also for the work that she put into the project before, and after I joined the lab. Also to Dr. Sue Cowgill, my supervisor at the Potato Council who has allowed me the freedom to direct this investigation.

Thanks also to all the past and present members of the Developmental Botany Group: Dr Alex Murphy, guru of all things chromatographic; Dr Christine Newell who helped me with potato transformations and offered general encouragement at all times; Dr. Natalia Mielnichuk who has been such fun to work with and always offers a different perspective when things are going a bit wrong. Thanks also to Sue Green who could always fix the HPLC, which was good as it frequently broke. Also thanks to Dr. Jo Winwood and Adrienne Pate for their help with ELISAs and to Olga Sedelnikova for her help with the laborious task of enzyme assay development. Finally thanks must go to all the members of the Signal Transduction group that have made sharing a lab enjoyable.

I would also like to thank the members of the Virology lab for practically adopting me as a member of their group, always offering help and letting me borrow equipment, particularly Dr. Mat Lewsey and Dr. Fiona Robertson for helping me with RNA blots. Also to Dr. Colin Turnbull and Mark Bennett at Imperial College for their help with LC-MS-MS, and to Dr. Michael Moulin for his help when I was running two HPLCs in tandem. Thanks must also go to the members of Supergroup for helpful advice and comments over the last year. I also acknowledge the BBSRC, Potato Council, Frank Smart Fund, Company of Biologists and St Catharine's College for funding.

Special thanks must go to all the people that have kept me sane over the last three years, particularly to Claire, Ella and Tamzin for always knowing when it was time for a gin or a margarita; to everyone at CUW for giving me a competitive outlet, but particularly to Katie, Chiara, Fi and Sabrina for their five-sided coolness; and to the residents of Elsworth who didn't object to the installation of skysports. Also to Gez who has supported and fed me, taken me on exciting adventures to homebase and beyond, and generally been a brilliant person to be around while I've been writing. Finally to my Mum and Dad who have helped me get this far with their encouragement and support, I promise I'm not planning on any more degrees!

Abstract

Worldwide production of potatoes is in excess of 350 million metric tonnes per annum, of which 60% is intended for human consumption. Since the period of tuber dormancy before tuber buds sprout is usually shorter than the optimal market storage period, control of sprouting is essential. To prolong dormancy, tubers are either stored at low temperatures and/or are treated with chemical sprout inhibitors, the use of which subject to increasing scrutiny in the European Union due to their impact upon the environment. Cytokinins, a group of plant growth regulators, are known to play a central role in tuber bud sprouting and tuber initiation from stolon tips in *Solanum tuberosum* L. although it is unclear when and how cytokinins act to regulate dormancy.

The interconversion of cytokinins is incompletely understood. Enzymes identified to date have higher affinities for aminopurines than their cytokinin equivalents. A novel cytokinin binding protein *Solanum tuberosum* Cytokinin Phosphorylase 1 (StCKP1), has been identified in tuberising stolon tips which shares regions of homology with members of the nucleosidase and phosphoribosyl transferase family. The composition of cytokinin N^9 conjugates in tuber bud and surrounding tissue is known to change on transition from a dormant state, with an increase in base and riboside types observed. Analysis of transcripts indicates an increase in abundance of *StCKP1* on tuberisation of stolon tips, and high abundance in the periderm of dormant tubers. Analysis of protein abundance by immunoblotting echoes this finding and indicates StCKP1 begins to accumulate in stolon tips shortly before tuberisation, matching binding activity. Transgenic analysis of the cytological reporter gene *uidA* under the control of two identified promoter regions indicates *StCKP1* is expressed predominantly in tuber tissue. Analysis of StCKP1 activity by HPLC and LC-MS-MS shows that StCKP1 catalyses the interconversion of free base and riboside. K_Ms determined for cytokinin and aminopurine substrates indicate that StCKP1 has a higher affinity for cytokinin substrates and, of these cytokinins, displays a higher affinity for the free base catalysing ribosylation of the N^9 to form the corresponding riboside.

Desiree cultivars over-expressing *StCKP1* under the CaMV 35S promoter exhibited an increased rate of tuberisation of stolon tips and an increase in the length of the dormant period following lifting. Over-expression of *StCKP1* was found in particular to increase the chill sensitive period of dormancy, confirming results of *StCKP1* knock-down by RNAi. Transcript abundance of StCKP1 at tuberisation in other cultivars including King Edward and Maris Peer was found to correlate with the dormancy characteristics prescribed by the European Cultivated Potato Database and the British potato variety database.

List of Figures

List of Tables

List of Abbreviations

ABA	Abscisic acid
Ade	Adenine
Ado	Adenosine
ADP	Adenosine diphosphate
AK	Adenine kinase
AMP	Adenosine monophosphate
ARR	Arabidopsis response regulator
AP	Adenine phosphorylase
APRT	Adenine-phosphoribosyltransferase
ATP	Adenosine triphosphate
AU	Absorbance unit
BA	Benzyladenine
[9G]BA	Benzyladenine 9-glucoside
[9R]BA	Benzyladenosine
[9R-MP]BA	Benzyladenine ribotide
BLAST	Basic local alignment search tool
BSA	Bovine serum albumin
BSP	Bark storage protein
BT	Before tuberisation
CaMV 35S	Cauliflower mosaic virus 35S promoter
CBP	Cytokinin binding protein
cDNA	Complementary deoxyribonucleic acid
CIAP	Calf intestinal alkaline phosphatase
CIPC	Chloropropham
CK	Cytokinin
CKI1	Cytokinin independent 1
CRE1	Cytokinin response 1 (AHK4/WOL)
CRF	Cytokinin response factor
CTAB	Cetrimonium bromide ($(C_{16}H_{33})N(CH_3)_3Br$)
DMAPP	Dimethylallyl diphosphate
DNA	Deoxyribonucleic acid
dNTP	Deoxynucelotides
DZ	Dihydrozeatin
[9G]DZ	Dihydrozeatin 9-glucoside
[9R]DZ	Dihydrozeatin riboside
[9R-MP]DZ	Dihydrozeatin ribotide
EDTA.Na_2	Diaminoethanetetra-acetic acid disodium salt
ELISA	Enzyme linked immunosorbent assay
EPI	Enhanced product ion
EST	Expressed sequence tag
FM	Fresh mass
FPLC	Fast performance liquid chromatography

g	Force due to gravity
gDNA	Genomic deoxyribonucleic acid
GC-MS	Gas chromatography-mass spectrometry
GFP	Green fluorescent protein
GUS	β-glucuronidase
HEPES	4-(2-hydroxyethyl)-1-piperazineethanesulfonic acid
HMBDP	1-hydroxy-2-methyl-2-(E)-butenyl 4 diphosphate
HPLC	High pressure liquid chromatography
HRP	Horseradish peroxidase
IAA	Indol-3-ylacetic acid
IPTG	Isopropyl-*β*-D-thiolgalactopyranoside
iP	Isopentenyladenine
[9G]iP	Isopentenyladenine 9-glucoside
[9R]iP	Isopentenyladenosine
[9R-MP]iP	Isopentenyladenosine 5′-monophosphate
ipt	Isopentenyltransferase
K_{CAT}	Catalytic efficiency
K_D	Binding affinity constant
K_M	Michaelis constant
LC-MS/MS	Liquid chromatography-tandem mass spectrometry
MEP	Methylerythritol phosphate pathway
MBP	Maltose binding protein
MOPS	3-[N-morpholino]-propane sulphonic acid
MQH_2O	Milli-Q water
MRM	Multiple reaction monitoring
mRNA	Messenger ribonucleic acid
MS	Murashige and Skoog
MU	4-methyl-umbelliferone
MUG	4-methyl-umbelliferyl-glucuronide
NCBI	National centre for biotechnology information
OD	Optical density
OsLOG	*Oryza sativa* Lonely Guy
PAGE	Polyacrylamide gel electrophoresis
PAR	Photosynthetically active radiation
PBS	Phosphate buffered saline
PBST	Phosphate buffered saline + Tween 20
PCR	Polymerase chain reaction
PNP	Purine nucleoside phosphorylase
PNPP	*Para*-nitrophenylphosphate
PVPP	Polyvinylpolypyrrolidone
PVX	Potato virus X
R 1-P	D-Ribose 1-phosphate Bis(cyclohexylamine)
RNA	Ribonucleic acid
RNAi	Ribonucleic acid interference
RT	Room temperature

RT-PCR	Reverse transcript polymerase chain reaction
SDS	Sodium dodecyl sulphate
SE	Standard error
SGN	Sol genomic network
SSC	Standard saline citrate
T	Tween-20
TAE	Tris-acetate-EDTA
TBS	Tris buffered saline
TBST	Tris buffered saline + Tween 20
T-DNA	Transfer deoxyribonucleic acid
TE	Tris-EDTA
TEA	Triethylamine
TEAA	Triethylammonium acetate
TIC	Total ion chromatogram
TLC	Thin layer chromatography
tRNA	Transfer RNA
UV	Ultra violet
VIGS	Virus induced gene silencing
V_0	Initial reaction velocity
V_{max}	Maximum initial velocity
XIC	Extracted ion chromatogram
X-Gluc	5-bromo-4-chloro-3-indolyl-β-D-glucuronic acid
Z	trans-Zeatin
(OG)Z	trans-Zeatin O-glucoside
[9R]Z	trans-Zeatin riboside
[9R](OG)Z	trans-Zeatin riboside O-glucoside
[9R-MP]Z	trans-Zeatin riboside 5′-monophosphate

Chapter 1

Introduction

1.1 Plant Development

Virtually every aspect of the dynamic process of plant development, from embryogenesis to senescence is strictly co-ordinated by endogenous plant hormones at submicromolar concentrations (Bishopp et al., 2006). In general this developmental control is exerted by controlling cell division, expansion, differentiation and death. Numerous plant growth regulators (PGRs) have been identified to date, with strigolactones recently emerging as a new class of PGRs (Gomez-Roldan et al., 2008). The roles of the identified PGRs in plant development is well characterised, particularly for the five classic PGRs. However, the exact mechanisms of biosynthesis, perception, and inactivation, are still not well understood.

1.2 Plant Growth Regulators

Plant growth regulators, often referred to as hormones or phytohormones, are essential for the growth and development of tissues and organs which they contact. They elicit a wide range of developmental responses, some promoting, others retarding, processes dependent upon the environmental opportunity or challenge to which the hormonal signal relates. Alterations in hormone responses have been responsible for several important agricultural advances, such as the breeding of semi-dwarf varieties and increased grain production (Ashikari et al., 2005). At present, there are five recognised major classes of "classic" non-peptide hormones: auxins, gibberellins (GA), ethylene, abscisic acid (ABA) and cytokinins. Jasmonates, salicylic acid (SA), brassinosteroids and strigolactones have more recently come to be accepted as universal plant hormones.

1.3 Cytokinins

Cytokinins were defined as agents that promote cell division, cytokinesis, in the presence of auxin (Mok and Mok, 2001). They have diverse regulatory effects on many physiological processes (Mok, 1994; Hare and van Staden, 1997), playing a central role in development in the promotion of cytokinesis (Miyawaki et al., 2004), activation of dormant lateral buds, and increasing sink strength (Kakimoto, 2003a). Study of transgenic plants with decreased levels of cytokinins revealed that these and many other developmental processes are regulated by endogenous cytokinins (Werner et al., 2001). Levels of cytokinins are spatially and temporally regulated within the plant. Sites of abundance can be found in the root tip, the shoot apical meristem and immature seeds (Letham, 1994). It is generally assumed that the root tip is the major site of synthesis as xylem exudates from roots of diverse plant species contain relatively large amounts of cytokinins, and because root organs are still capable of production after decapitation (Oka, 2003). The cambium, shoot apex and immature seeds and other such proliferative tissues are also thought to be active in cytokinin

synthesis (Kakimoto, 2003b), although cytokinins are found throughout the plant due to vascular transport.

Naturally occurring cytokinins are N^6-substituted adenine derivatives and are classified into one of four basic molecules: N^6-(Δ^2- isopentenyl)adenine (iP), zeatin (Z) the side chain of which occurs in either the *cis* (c) or *trans* (t) conformation dependent upon the stereo-isomeric position of the hydroxylated methyl group, dihydrozeatin (DHZ) and benzyladenine (BA). They are classified by the configuration of the N^6-side chain as either isoprenoid or aromatic, although aromatic cytokinins are considered to be uncommon in plant tissue (Kakimoto, 2003b). Each isoprenoid cytokinin molecule is distinguished by characteristics of the side chain, namely the presence or absence of a hydroxyl group at the end of the prenyl chain and its stereoisomeric position (figure 1.1). Differences have been found between the activity and *in vivo* stability of the structural variants described. The structure and conformation of the side chain are critical for the activity of the cytokinin (Mok and Mok, 2001). Relative biological activities of cytokinins have been determined by measuring their ligand affinity to identified cytokinin receptors (section 1.3.4). Assays carried out indicate biological activity of cytokinin varies by molecular species. *In vitro* and *in vivo* studies carried out using the Arabidopsis receptors AHK3 and AHK4/CRE1/WOL showed that iP and tZ have much higher affinities than cZ and DZ (Inoue et al., 2001; Suzuki et al., 2001; Yamada et al., 2001; Spichal et al., 2004; Romanov et al., 2006). In bioassays using cucumber and *Amaranthus caudatus*, tZ was found to be most active and cZ least (Kaminek et al., 1979), while a cytokinin receptor from maize, ZmHK1 responded to cZ and tZ with similar sensitivity (Yonekura-Sakakibara et al., 2004). The *trans* form is generally regarded as having greater activity in bioassays and abundance in plant cells than the *cis* isomer (Kakimoto, 2003b). Concurrent with this finding is that cytokinins with an unsaturated isoprenoid side chain are by far the most abundant *in planta*.

Alongside the nucleobase form, cytokinins also occur as the corresponding sugar derivatives: ribosides and ribotides (figure 1.1). Since the initial isolation of the first natural cytokinin, zeatin, as a causative agent of cytokinesis in the presence of auxin in immature maize kernels, numerous natural and synthetic compounds have been identified to promote cell division in a manner that fits with the definition of a cytokinin. Synthetic cytokinins include adenine derivatives, such as kinetin, as well as compounds apparently structurally unrelated to natural cytokinins, e.g. certain phenylureas and thidiazuron (Mok et al., 2000).

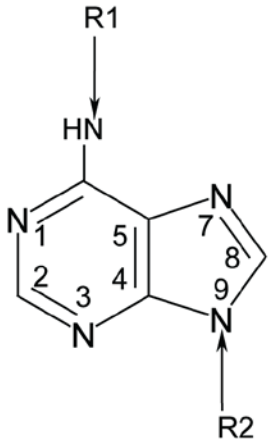

R_1	R_2	Common Name	Abbreviation
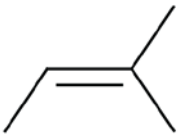	H	isopentenyladenine	iP
	ribosyl	isopentenyladenosine	[9R]iP
	ribotidyl	isopentenyladenosine ribotide	[9R-MP]iP
	glucosyl	isopentenyladenosine 9-glucoside	[9G]iP
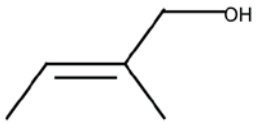	H	zeatin	Z
	ribosyl	zeatin riboside	[9R]Z
	ribotidyl	zeatin ribotide	[9R-MP]Z
	glucosyl	zeatin 9-glucoside	[9G]Z
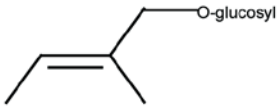	H	zeatin O-glucoside	(OG)Z
	ribosyl	zeatin riboside O-glucoside	[9R](OG)Z
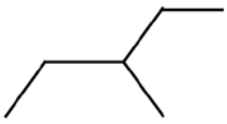	H	dihydrozeatin	DHZ
	ribosyl	dihydrozeatin riboside	[9R]DHZ
	ribotidyl	dihydrozeatin ribotide	[9R-MP]DHZ
	glucosyl	dihydrozeatin 9-glucoside	[9G]DHZ
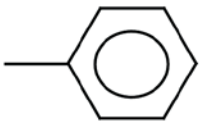	H	benzyladenine	BA
	ribosyl	benzyladenosine	[9R]BA
	ribotidyl	benzyladenine ribotide	[9R-MP]BA
	glucosyl	benzyladenine 9-glucoside	[9G]BA

Figure 1.1 Isoprenoid and aromatic cytokinin structures
Isoprenoid are the most common forms, aromatics are considered to be rare. Adapted from Warnes (2005)

1.3.1 Cytokinin biosynthesis

Although isoprenoid type cytokinins are ubiquitously found in various plant species, it is still not clear to date whether aromatic cytokinins are common in plants or not. As a result, the majority of studies have focussed upon isoprenoid cytokinin synthesis and metabolism, recently reviewed by Hirose et al. (2007) and Kamada-Nobusada and Sakakibara (2009).

Three biosynthetic pathways have been proposed to operate in cytokinin biosynthesis which, alongside metabolism and degradation, regulate the levels of cytokinins found in tissues (Prinsen et al., 1997; Mok et al., 2000; Kakimoto, 2003b; Hwang and Sakakibara, 2006). In the classically recognised [9R-MP]iP-dependent, often referred to as the iPMP-dependent pathway, iP is the initial cytokinin type formed by the conjugation of dimethylallyl pyrophosphate (DMAPP), a 2-isopentenyl hydrocarbon chain, to the N^6 of adenosine-5′-tri-, -di-, or monophosphate (ATP, ADP, AMP) to produce isopentenyladenosine-5′-tri- or –diphosphate ([9R-TP]iP or [9R-DP]iP) or isopentenyladenine ribotide ([9R-MP]iP), catalysed by an isopentenyltransferase (IPT). The prenyl-donor for the IPT reaction, DMAPP, can be produced by both the methylerythritol phosphate (MEP) pathway in plastids and the mevalonate (MVA) pathway in the cytosol. Isotope labelling experiments in Arabidopsis seedlings have shown that the prenyl group of tZ and iP is mainly produced by the MEP pathway (Kasahara et al., 2004). In agreement with this finding is the localisation of four Arabidopsis IPTs: AtIPT1, AtIPT3, AtIPT5 and AtIPT8 to the plastids (Miyawaki et al., 2004). AtIPT4 and AtIPT7 are found to localise to the cytosol and mitochondria respectively suggesting the MVA pathway also provides DMAPP for cytokinin biosynthesis. Åstot et al. (2000) proposed a second pathway of biosynthesis, the iPMP-independent pathway in which the initial product of conjugation is a zeatin-type cytokinin. Their research suggested that tZ types are formed by the direct addition of a hydroxylated side chain, 4-hydroxy-3-methyl-2-(*E*)-butenyl diphosphate (HMBDP), an intermediate product of the MEP pathway by IPT (Figure 1. 2).

[9R-MP]iP produced by IPT in the classically recognised biosynthetic pathway undergoes hydroxylation of the prenyl side chain to synthesise [9R-MP]tZ. In Arabidopsis this step is catalysed by two cytochrome P450 monooxygenases, CYP735A1 and CYP735A2 (Takei et al., 2004). CYP735As are found to preferentially catalyse the stereo-specific hydroxylation of [9R-MP]iP and [9R-DP]iP to produce [9R-MP]tZ and [9R-DP]tZ over [9R-TP]iP indicating the hydrolysis of the terminal phosphate of [9R-TP]iP is required to yield [9R-DP]iP before tZ type cytokinins can be formed.

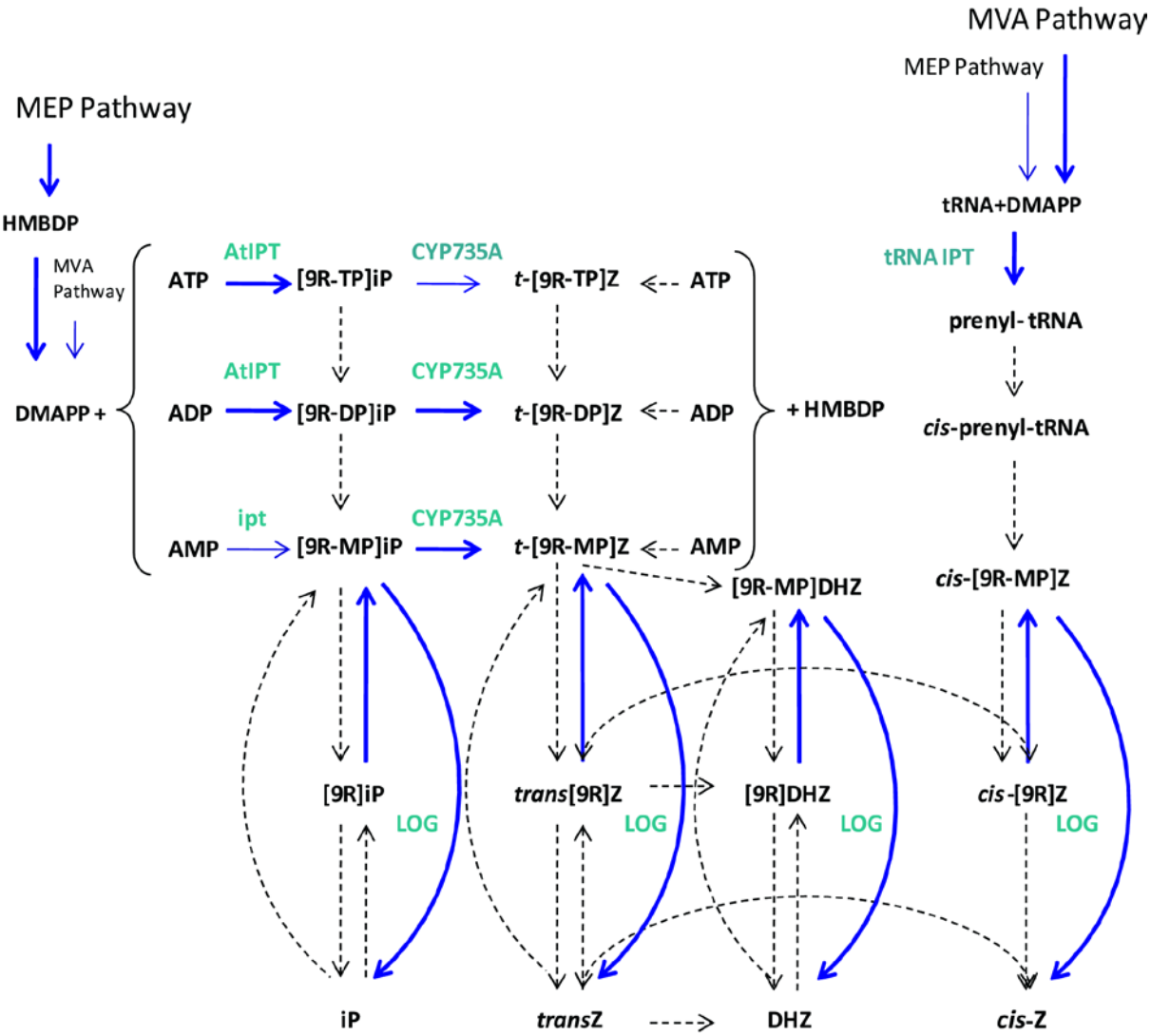

Figure 1.2 Current model of isoprenoid cytokinin biosynthesis and interconversion in higher plants
The isoprenoid side chain of iP and tZ predominantly comes from the MEP pathway, whereas that of cZ mostly originates from the MVA pathway. Isopentenyltransferases (IPTs) in higher plants preferably use ATP and ADP as isoprenoid acceptors. The cytokinin nucleotides are converted into the corresponding tZ nucleotides by CYP735A, which prefers [9R-DP]iP and [9R-MP]iP. Dephosphorylation by phosphatase may occur in di- or tri-phosphorylated cytokinin nucleosides. An alternative biosynthetic pathway uses IPTs to catalyse the conjugation of HMBDP as an isoprenoid donor to an ATP, ADP or AMP acceptor. The tRNA IPTs catalyse prenylation of tRNA that leads to the production of [9R-MP]cZ. The cytokinin ribotides are directly catalysed to the biologically active free base by LOG, or thought to undergo a two step interconversion by 5'-nucleotidase and Adenosine Kinase. cZ and tZ may be enzymatically interconverted by zeatin cis-trans isomerase. The width of the lines indicates the strength of metabolic flow. Blue arrows indicate flow for which enzymes have been identified. Dashed arrows show flow in which the related enzymes have not yet been identified. Adapted from Kamada-Nobusada and Sakakibara (2009).

A third pathway of cytokinin biosynthesis has been proposed to utilise tRNAs as a source of cytokinins as N^6-isopentenyladenosine occurs on the 3' side next to the anticodon in tRNA species for codons beginning with U. Prenylated tRNA has a *cis*-hydroxyl group, so degradation of prenylated tRNA generates cZ. In some bacteria, cytokinins have been found to be derived from isopentenylated tRNA (Gray et al., 1996) and two of the identified Arabidopsis IPTs, IPT2 and IPT9 are implicated in the tRNA biosynthetic pathway which is thought to be responsible for the majority of cZ formed (Golovko et al., 2002; Miyawaki et al., 2006). The Arabidopsis mutant deficient in both tRNA IPTs was found to contain cZ below detectable limits while levels of iP and tZ cytokinins were unaffected (Miyawaki et al., 2006). It is possible that *cis-trans* isomerase may interconvert tZ and cZ type cytokinins to contribute to the pool, however it is considered as either inactive or not expressed normally as interconversion between tZ and cZ does not readily occur (Bassil et al., 1993). In agreement with the cytosolic location of AtIPT2, it is thought that the prenyl group donor in the tRNA biosynthetic pathway derives from the MVA pathway in Arabidopsis (Kasahara et al., 2004). However, in plants, it is generally considered that isopentenylated tRNAs do not constitute a significant source of active cytokinin. Calculations carried out by Barnes et al. (1980) indicated that tRNA turnover rate could not account for a significant part of cytokinin production, particularly in potato which was used as a model, although this calculation cannot be considered to be conclusive evidence as the rate of tRNA turnover and cytokinin production cannot be determined accurately enough.

Sequence analysis has revealed seven genes closely resembling the bacterial *ipt* in the *Arabidopsis thaliana* genome, and different tissues vary in respect of which combination of these they express. Biochemical characterization of IPT proteins from higher plants demonstrated that IPTs have distinct substrate specificities. IPTs from higher plants preferentially utilize ADP or ATP over AMP as prenyl acceptors and DMAPP almost exclusively as a prenyl donor, producing [9R-DP]iP or [9R-TP]iP respectively (Takei et al., 2001). This contrasts with the activity of one of the first IPTs to be identified in the slime mould *Dictyostelium discoideum* (Taya et al., 1978) which was referred to as DMAPP:AMP isopentenyltransferase as it used AMP and not ADP or ATP as the isopentenyl acceptor as is found in higher plants. Two further IPTs have been isolated from *Agrobacterium tumefaciens* which have also been demonstrated to use only AMP as the isopentenyl acceptor (Kakimoto, 2003b).

1.3.2 Cytokinin Interconversion

Interconversion, producing structural modifications to natural cytokinins that influence their function, stability, activity and transport in plants, alongside biosynthesis is an important regulator of

cytokinin content of plant tissues (Auer, 2002). It is, however, unclear where the former begins and the latter concludes (figure 1.2). Whereas free bases are considered to be the most biologically active forms, cytokinin nucleosides have been proposed as the major transport form (Mok and Mok, 2001). Several transporter-like proteins have been reported to associate non-specifically with free base cytokinins (Burkle et al., 2003) however, free bases are sufficiently non-polar as to move freely across membranes without the need for transporters (Laloue and Pethe, 1982). Adenosine (Ado) has been found to be transported into the cell by equilibrative nucleoside transporters such as AtENT1 (Mohlmann et al., 2001) which have been hypothesised to be involved in a pathway salvaging extracellular ATP. Molecular and genetic studies carried out by Sun et al. (2005) provide evidence to support the hypothesis that SOI33 (AtENT8) and AtENT3 are functional transporters specific to [9R]iP as mutations in either gene cause a substantially reduced uptake of [9R]iP *in planta*. Plants also posses purine permeases (PUPs) which have been shown to transport Ade into the cell along a H^+ gradient, it has been hypothesised that apoplastic Ado could be further converted to Ade by an apoplastic nucleosidase and imported by PUPs (Burkle et al., 2003). Cell membranes are impermeable to purine ribotides and so the formation and breakdown of ribotides after unloading from the xylem may have a role in controlling the flow of cytokinin ribotides into and out of the cell (Laloue & Pethe, 1982).

Enzymes of purine metabolism have been identified as functioning in the interconversion of cytokinins by catalysing reactions involving the substituent at the N^9 position on the adenine ring (figure 1.3). A number of enzymes involved in purine metabolism have been isolated from plants, including adenosine kinase which catalyses the phosphorylation of ribosides to produce the corresponding ribotide (Chen and Eckert, 1977); adenine phosphoribosyltransferase found to catalyse conjugation of the base to form its ribotide (Chen et al., 1982b; Schnorr et al., 1996); 5'-nucleotidase which catalyses dephosphorylation of the ribotide to produce the riboside (Chen and Kristopeit, 1981b); adenosine phosphorylase which acts to transfer a ribosyl group to the base, producing a riboside (Chen and Petschow, 1978); adenine nucleosidase which cleaves the ribosyl group to yield the free base (Chen and Kristopeit, 1981a); and 5'-monophosphate phosphoribohydrolase which cleaves the ribotidyl group from the N^9 position to yield the base (Kurakawa et al., 2007); and have been shown to have an affinity for cytokinins and to act in the interconversionary pathway.

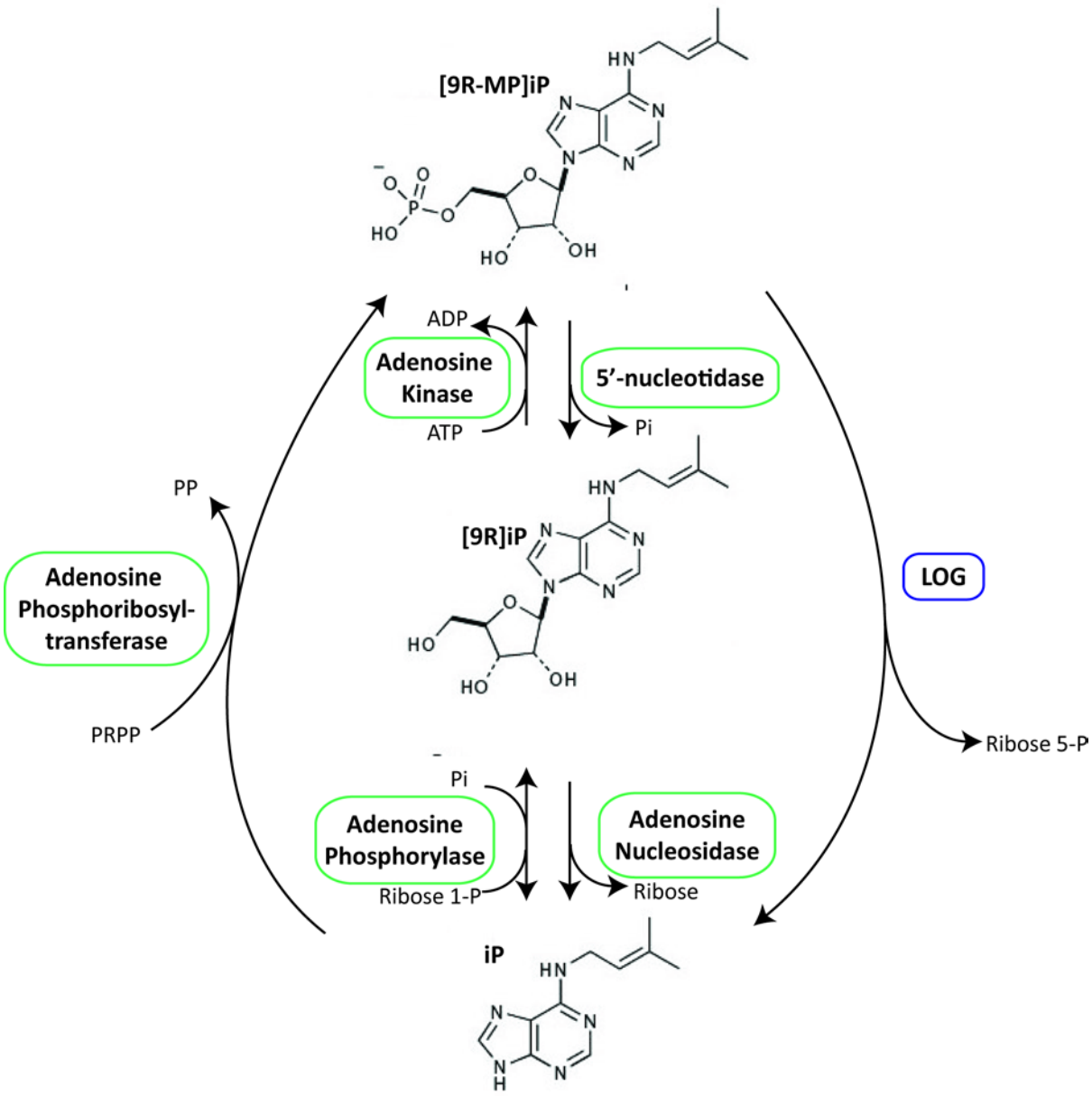

Figure 1.3 The pathway of interconversion between cytokinin N^9 conjugates
Enzymes involved in cytokinin interconversion are boxed; those in green are known to have a higher affinity for aminopurines over cytokinin substrates, those in blue are known to act specifically in the interconversion of cytokinins. The pathway is illustrated with isopentenyladenine type cytokinin conjugate forms, however is equally applicable to the interconversion of both *cis*- and *trans*-zeatin and to dihydrozeatin type cytokinins.

Of the enzymes of purine metabolism identified to date only one, OsLOG a 5'-monophosphate phosphoribohydrolase, is involved specifically in cytokinin metabolism (Hirose et al., 2007). Revising the long-held idea of multistep reactions to interconvert newly synthesised cytokinin ribotide to the free base form, LOG directly converts inactive cytokinin ribotides to the biologically active free base form. When presented with AMP, no phosphoribohydrolytic activity could be measured, however when offered [9R-MP]iP and [9R-MP]Z as substrates, K_Ms were determined to be 11.7µM and 22.0µM respectively. AtApt2, an adenine phosphoribosyltransferase which catalyses the reverse reaction to that catalysed by LOG forming the ribotide from the base, was found to catalyse the conjugation of both BA and adenine (Ade) substrates but had a higher affinity for BA over Ade (Schnorr et al., 1996). Other enzymes identified, notably those identified by Chen and co-workers, in general show a low degree of specificity for the exact structure of the aminopurine ring and are active for adenine and N^6-substituted adenine derivative substrates including, but not limited to, cytokinins. It is not known if these enzymes acting in the cytokinin interconversionary pathway function predominantly in adenine salvage, with any action on cytokinin metabolism largely incidental to the predominant function (Mok and Mok, 2001).

1.3.3 Cytokinin Degradation

The turnover of cytokinins appears to be mainly controlled by an irreversible degradation reaction catalysed by a small, conserved group of cytokinin oxidases/dehydrogenases (CKX). Over-expression of *CKX* resulted in a cytokinin-deficiency syndrome similar to that observed in triple receptor mutants. Members of both the IPT and CKX gene families display distinctive expression patterns, suggesting cytokinin levels are fine tuned by genetic and developmental cues (Werner *et al*. 2003; Miyawaki *et al*. 2004). Major quantitative trait loci for grain yield in rice have been identified as two CKX genes (Mameaux, pers. comm.) underlining their importance in plant development.

1.3.4 Perception

A first glimpse into cytokinin perception and signalling was provided by the identification of *CKI1* (*cytokinin-independent 1)*, a receptor histidine kinase in *Arabidopsis* whose over-expression induces typical cytokinin responses, notably growth and greening, in the absence of exogenous cytokinins (Kakimoto, 1996). Initially proposed as a receptor due to its similarity to two-component regulators such as the membrane-spanning ethylene receptor ETR1, further investigation into the function of CKI1 revealed an inability to bind cytokinin itself but a role in activating the cytokinin response gene *ARR6* (Hwang and Sheen, 2001). Sequence analysis of CKI1 shows low amino acid sequence similarity to CRE1 with only 25% identity and the putative extracellular domain, putatively the ligand-binding

domain, of CKI1 is completely different from that of the known cytokinin receptor CRE1. This sequence divergence and the failure of cytokinin binding to CKI1 in yeast argue against the function of CKI1 as a cytokinin receptor (Yamada et al., 2001). In Arabidopsis protoplasts, however, the expression of CKI1 activated the cytokinin-responsive *ARR6* promoter in the absence of exogenous cytokinin, indicating that CKI1 is a constitutively active His protein kinase connected to cytokinin signalling. However, the identification of CKI1 as a histidine kinase initiated the investigation of the two-component systems, which use a histidine kinase as an environmental sensor and rely on a phosphorelay in signal transduction, in the perception of cytokinins. Perception and transmission involves the autophosphorylation of a His residue on the sensor histidine-kinase upon binding of a cytokinin with the N-terminal extra-cellular CHASE region of this sensor kinase (Anantharaman and Aravind, 2001). The phosphoryl group is then transferred to a central Asp residue on the cognate response regulator (ARR) which is activated as a result of phosphorylation (Hutchison and Kieber, 2002) (section 1.3.5).

Three highly homologous transmembrane cytokinin receptor histidine kinases; AHK2, AHK3 and CRE1 (AHK4) have been identified in Arabidopsis in recent years (Ueguchi et al., 2001; Kakimoto, 2003a). The three differ in their expression pattern with CRE1 mainly found to be expressed in the roots, while AHK2 and AHK3 are present in all major organs (Schmulling, 2001; Ueguchi et al., 2001; Heyl and Schmulling, 2003). The first of which to be discovered was *CRE1*, later found to be identical to the loci *WOL* (*wooden leg*) and *AHK4*. Arabidopsis plants were mutagenised and subsequently calli were screened for impaired sensitivity to exogenous cytokinins. The *cre1* mutants were found to respond normally to auxin, ethylene and ABA in root elongation assays in that root elongation was inhibited, but were less sensitive to exogenous BA. T-DNA knockouts in the *CRE1* translation initiation site showed the same apparent resistance to cytokinins, in that they were less sensitive to cytokinin (Inoue et al., 2001). Expression of *CRE1* in the fission yeast *Schizosaccharomyces pombe*, isolation of the membrane and subsequent SDS-PAGE revealed CRE1 to be present in the membrane. Such CRE1-containing membranes were used in *in vitro* binding assays with ^{3}H-IP, showing that the radio-labelled cytokinin was specifically retained on the membrane (Yamada et al., 2001). It is however important to remember that other downstream signalling components such as AHPs may be bound to membrane bound histidine kinases. Nishimura et al. (2004) investigated the functional redundancy of *AHK2/3/CRE1* through the study of double and triple mutants in these cytokinin receptor genes. The phenotype observed in *cre1* mutants containing an intact *AHK2* or *AHK3* gene was slight, strongly suggesting complete overlap of their biological roles with *CRE1* with *AHK2* and *AHK3* putatively functioning as the main cytokinin receptors in the support of growth and development. However in *ahk2/3* double mutants and *ahk2/3/cre1* triple mutants, impaired leaf and

root development was observed as cells lost the ability to divide and differentiate compared to wild type and single mutants. Triple mutants were found to exhibit near-complete insensitivity to cytokinin in various assays, including the induction of type-A ARR transcription, indicating that at least one of these three AHKs is required for perception of and response to cytokinins *in planta*. In addition, shoots of *ahk* receptor mutants were found to accumulate higher levels of cytokinin than found in the wild type, suggesting a role for AHKs in feedback modulation to regulate cytokinin homeostasis (Riefler et al., 2006).

1.3.5 Signal Transduction

Signal transduction downstream of cytokinin perception is carried out by proteins capable of His-Asp phospho-transfer which can translocate to the nucleus where they can transfer the phosphoryl group to a conserved Asp on either type-A or type-B ARR receivers or to cytokinin response factors (CRFs) (Rashotte et al., 2006). At least five AHPs are known in Arabidopsis, various studies have identified AHPs in phospho-transfer cytokinin signalling downstream of perception by AHK receptors (To and Kieber, 2008). Single and double *ahp* mutants generally show no defects in cytokinin responses, indicating a high level of redundancy. Quadruple and quintiple *ahp* mutants show reduced cytokinin induction of transcription of type-A ARRs, the transcriptional outcome of cytokinin signalling. However, quintuple mutants still exhibit a residual response to cytokinin indicating redundancy or that other pathways may compensate for loss of AHPs in phosphotransfer (Hutchison et al., 2006).

The final output of this transduction system in cytokinin signalling is the response regulator (ARR), of which two major classes have been recognised through analysis of the Arabidopsis genome. Arabidopsis has 22 genes for response regulators, 11 Type-A ARRS, recognised by their short C-terminal receiver domain; and 11 Type-B ARRs which contain a DNA binding domain that has features associated with transcription factors (Ferreira and Kieber, 2005). Cytokinin mediated induction of type-A ARRs has been demonstrated in a variety of tissues in Arabidopsis, maize and rice (To and Kieber, 2008). Characterisation of cytokinin responses in type-A ARR loss and gain of function Arabidopsis mutants indicates type-A ARRs are negative regulators of cytokinin signalling. Sextuple loss of function mutants in type-A ARR genes resulted in an increase in induction of cytokinin primary response genes, including type-A ARR transcripts (To et al., 2004). Exogenous application of cytokinin results in the up-regulation of transcript levels of at least 9 Type-A ARRs with *ARR4* and *ARR* induced within 10 minutes of treatment.

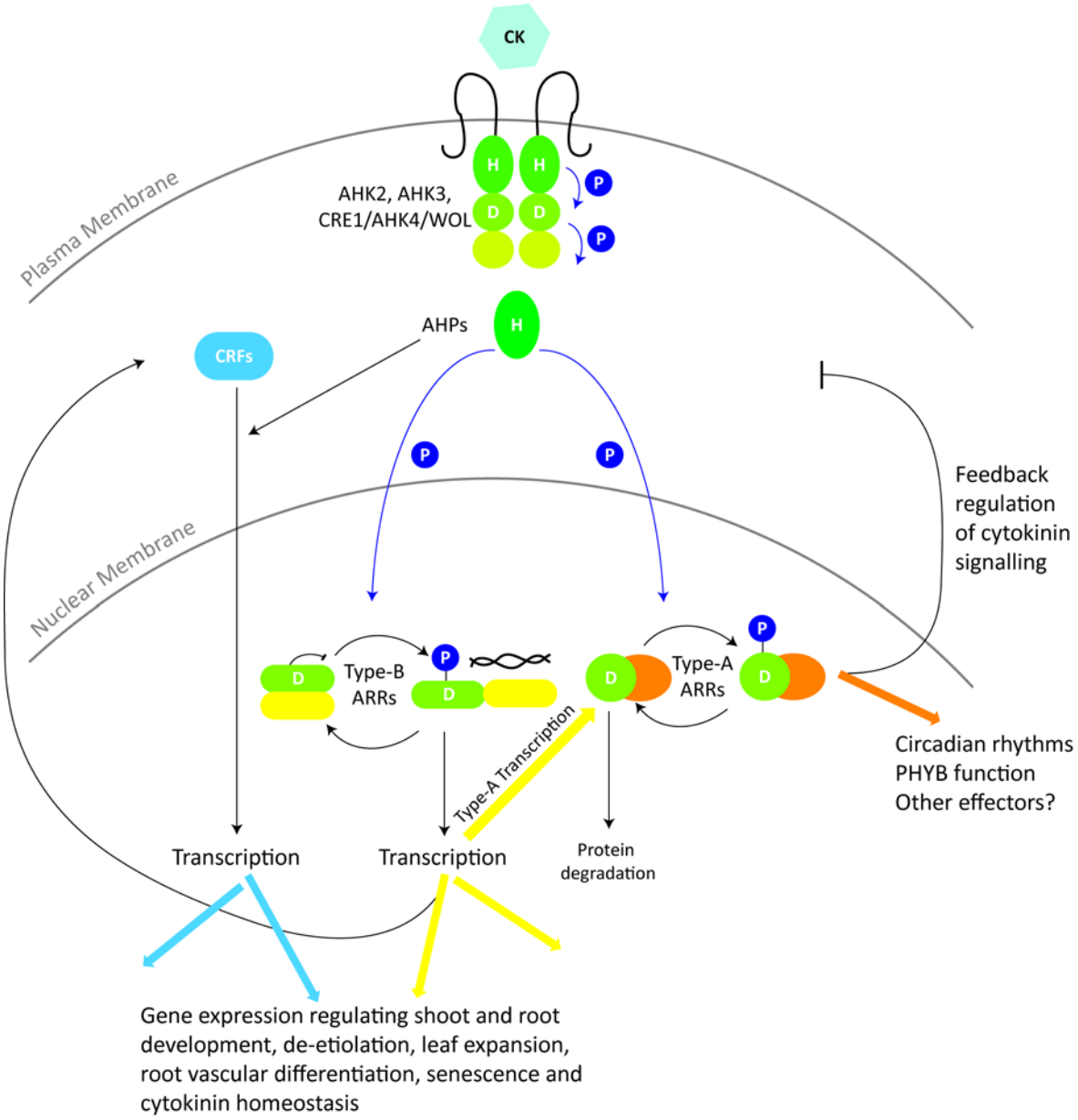

Figure 1.4 Cytokinin perception and signal transduction
Cytokinin (CK) is perceived by receptors AHK2, AHK3 and CRE1/AHK4/WOL at the plasma membrane activating a multistep phosphorelay indicated by dark blue arrows. AHPs receive the phosphoryl group (P) at a conserved His residue (H) in the cytosol. AHPs can translocate to the nucleus to transfer the P to a type-A ARR or type-B ARR receiver domain on a conserved Asp (D). Type-B ARRs contain a C-terminal DNA binding domain (yellow) which is inactivated by binding to the unphosphorylated N-terminal receiver domain. Phosphorylation relieves inactivation/inhibition to induce transcription of a subset of CK regulated targets (yellow arrows) including type-A ARRs and CRFs. CRF proteins are also activated via AHPs to accumulate in the nucleus and activate transcription (light blue arrows). Type-A ARRs contain the conserved receiver domain and a short C-terminal region (orange). Activated type-A ARRs mediate downstream processes (orange arrows) including feedback regulation of CK signalling. Adapted from To and Kieber (2007).

Type-B ARRs are expressed constitutively and expression does not increase upon application of cytokinin (or nitrate or other plant hormones), yet they are considered to be key regulators of cytokinin signalling as a result of their role in activation of transcription of type-A ARRs following treatment with cytokinin (Kakimoto, 2003a). Analysis of loss and gain of function mutants in Arabidopsis indicates at least six of the eleven type-B ARRs are positive regulators of response to cytokinin. A triple type-B ARR loss of function mutant was found to be insensitive to cytokinin, showing a strong reduction in accumulation of type-A ARR transcripts indicating type-B ARRs are required for the primary cytokinin transcriptional response (Mason et al., 2005).

Cytokinin response factors (CRFs) have been identified as targets of cytokinin regulated transcription by microarray analysis of Arabidopsis transcript pre and post cytokinin treatment. Found to belong to the AP2-like class of transcription factors, CRFs are found to rapidly accumulate in the nucleus in response to cytokinin treatment. Nuclear accumulation was found to be dependent upon perception by AHKs and phospho-transfer by AHPs, but not upon either type of response regulator (Rashotte et al., 2006). The regulation of CRF proteins by cytokinin signalling represents a novel branching point from the cytokinin-activated two component phosphorelay. Cytokinin perception and signal transduction is summarised in figure 1.4.

1.4 Potato - *Solanum tuberosum* L.

The potato (figure 1.5) originates from the Andean region of Peru and has been in cultivation for more than 6000 years. It is believed that this practice was initiated by the ancestors of the Incas (Zuckerman, 1998). After introduction to Europe by the Spanish explorers of the 1500s, the potato has become a staple food and is one of the top four crops in the world (Sonnewald, 2001) behind the cereals wheat, maize and rice. In 2004, worldwide production was in excess of 327 million metric tonnes, 37 million of which was subsequently used as seed stock (FAOstats data, 2004). Between 50 and 60% of potato production is intended for human consumption with the remainder used as animal feed, for industrial products, or as seed tubers (Sonnewald, 2001). In Europe and North America potatoes are most commonly used in the form of processed products, but for subsistence farmers, especially in some areas of Southeast Asia and Latin America, potatoes provide the primary staple food (Farre et al., 2001). In addition to starch, tubers contain high quality proteins, substantial amounts of vitamins, including water soluble vitamins lacking from cereals, minerals and trace elements. As such, there is a strong, year round demand.

Potato plants are grown from seed potatoes to produce tubers, the lifecycle of which is illustrated in figure 1.6. Current farming practice sees over-wintered seed tubers planted in early spring after

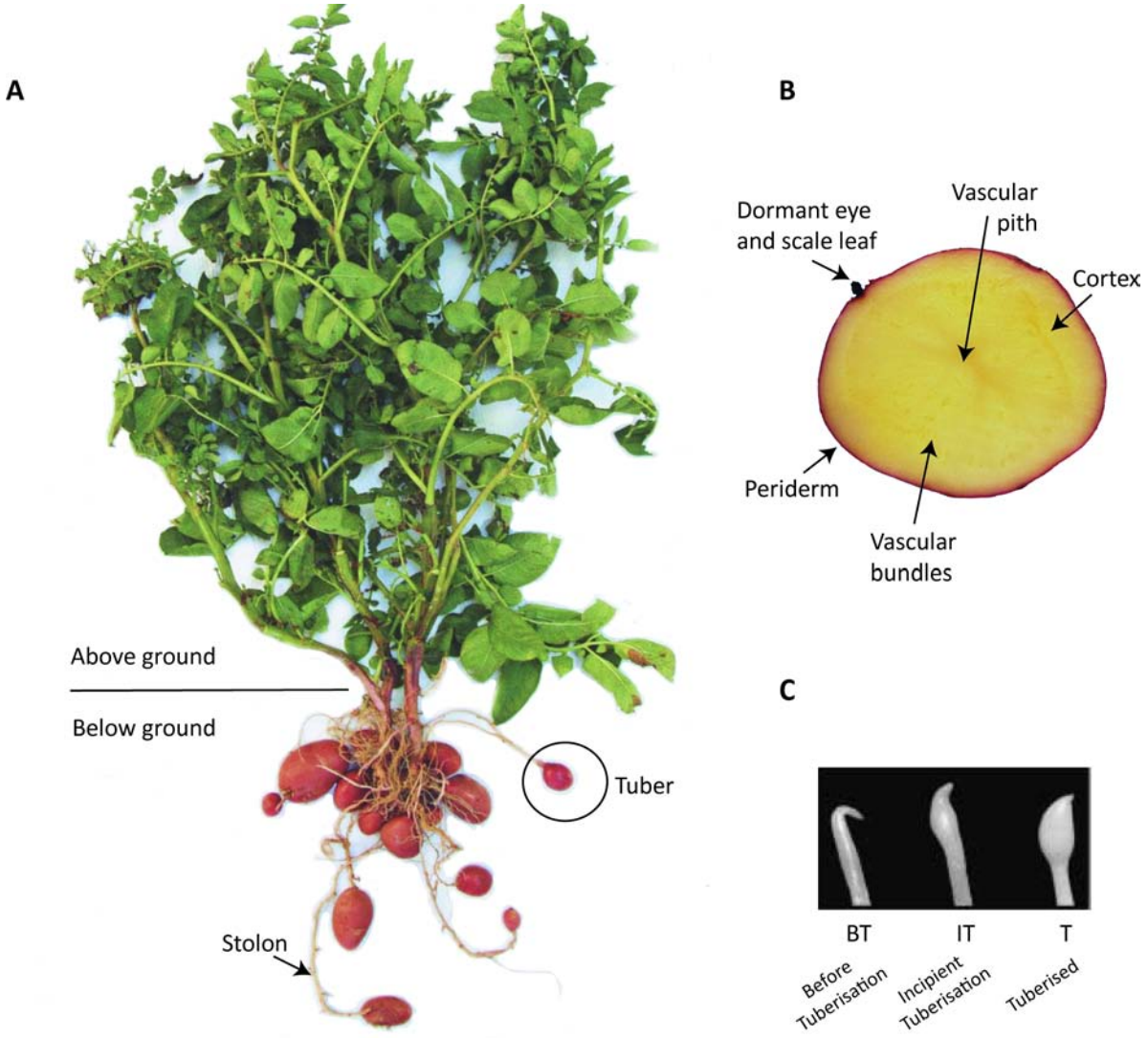

Figure 1.5 Anatomy of a potato
A. The potato plant. Tubers are modified stems, below ground storage organs which are capable of producing stolons, which themselves may enter tuberisation through a change in metabolism at the tip, resulting in the cessation of longitudinal growth while cell division and radial expansion continue. **B.** The tuber. The apical eye tends to release from dormancy prior to those basal to it, producing a sprout from which multiple stolons emerge. The tuber is classified into different tissue types depending upon their location within the mature tuber. **C.** Stolon tips at the three stages of tuberisation analysed in this study. **BT** = Before tuberisation, **IT** = Incipient tuberisation, **T** = Tuberised

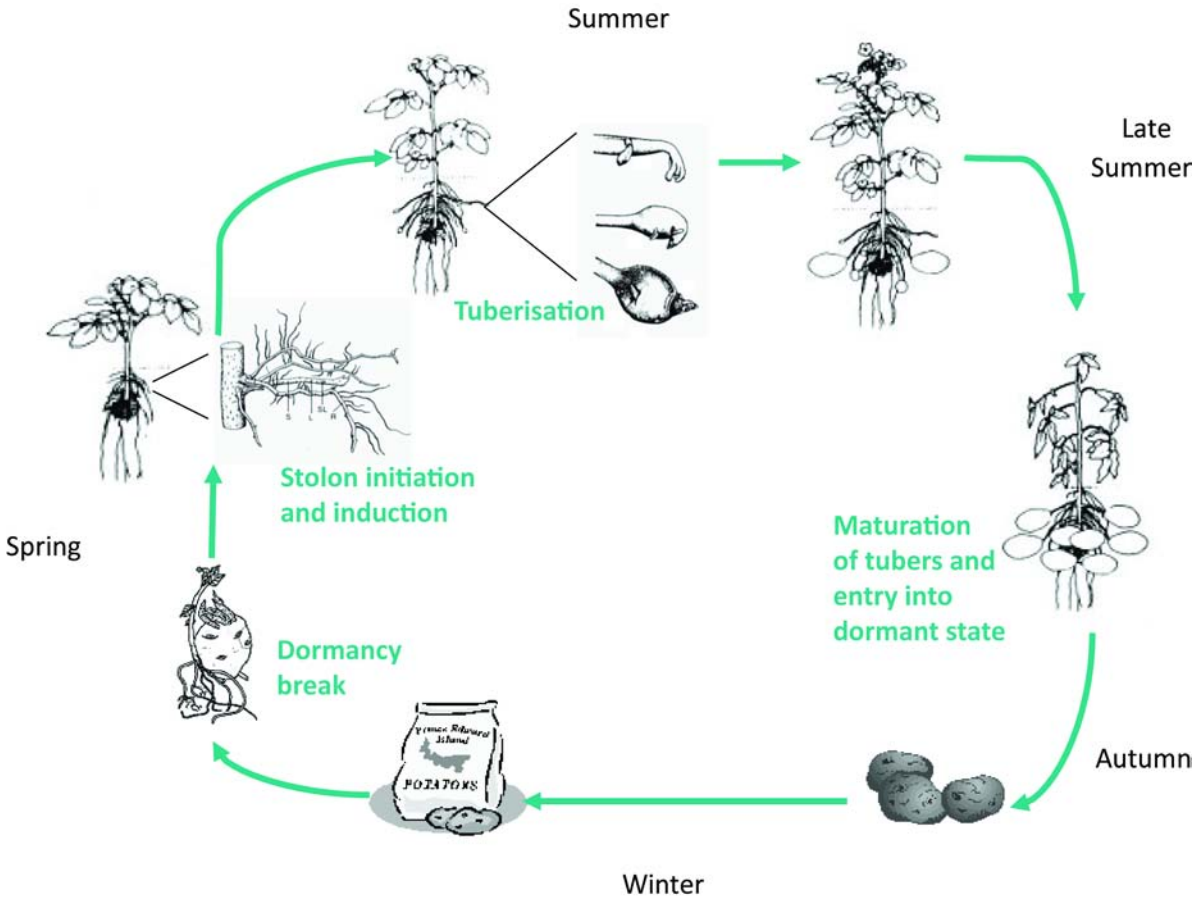

Figure 1.6 Potato vegetative lifecycle
The vegetative lifecycle is used in commercial production of tubers. Mature tubers are harvested in late summer/early autumn (depending upon cultivar) and seed tubers stored over winter. Upon sprouting of tuber buds in spring, seed tubers are sown. Initially aerial organs are established before lateral shoots emerge below ground level. These stolons continue elongating until a signal for tuberisation is received which causes a change in growth pattern, and swelling behind the stolon apex. Tubers swell by a further changes in cell division to produce randomly oriented planes concurrent with enlargement of cells.

tuber buds have begun to break dormancy. These tuber sprouts go on to form aerial stems and a few form below ground stems, known as stolons, from which tubers are produced although these are generally produced after aerial growth has become established. At the base of the main aerial stem of the plant, a number of lateral shoots are formed which usually remain growing below soil level. Unilke the aboveground stems, stolons grow diagravitropically with retarded leaf development and elongated internodes. When conditions are favourable, tubers are formed at the tip of the stolons, or from axillary buds formed along the stolon length (section 1.5.1). At the onset of tuberisation, the elongation of stolons ceases and cells in the pith and cortex enlarge radially and divide periclinally, resulting in subapical swelling. When these young tubers reach a certain size, there is a shift from longitudinal to random cell division coupled with cell enlargement in the perimedullary region (Xu et al., 1998).

As the potato of commerce, *S. tuberosum* is best grown in a temperate climate where continuous cultivation is impossible, tuber storage is required. Roughly 70% of the US autumn crop is placed into medium-long-term storage, but unlike cereal crops, tubers are stored in a fully hydrated, highly perishable form (Suttle, 2004) and so are subject to a wider array of challenges during this period. Seed potatoes are generally stored between 2 and 4°C in order to suppress sprouting, however ware potatoes, those intended for consumption, are stored between 8 and 12°C in order to maintain the tuber quality as at lower storage temperatures, a greater proportion of starch degrades to reducing sugars. It is at this stage that great losses in marketable biomass are incurred, with annual post-harvest losses typically 10-15% of the harvested crop but occasionally as high as 30%. Tuber deterioration during storage can result from both disease-related and physiological processes. Of the physiological, the unregulated break of dormancy in sprouting of the tuber buds is one of the most important as break of dormancy is accompanied by many physiological changes including increases in reducing sugar content, respiration, water loss, and glycoalkaloid content (Suttle, 1996).

Since the period of innate dormancy is usually shorter than the storage period optimal for the market, control of sprouting is essential (Wiltshire and Cobb, 1996).To prolong the dormancy period, tubers are either stored at low temperatures (for retail) and/or are treated with chemical sprout inhibitors such as chloropropham (CIPC) and propham (for processing only). Notably in the UK, there is a heavy dependency upon CIPC with 94% of all chemically treated tubers being fumigated with this sprout suppressant. Low temperatures however cause the conversion of starch to sugars, a process known as cold-induced sweetening, and result in a discoloration of tuber flesh due to the Maillard reaction between the reducing sugars and amino acids, an important consideration in many downstream food processing applications (Burton et al., 1992). Also acrylamide is released by

thermal treatment, such as roasting or frying, of certain amino acids, particularly in combination with reducing sugars and early Maillard reaction products (Stadler et al., 2002). Acrylamide is a potent carcinogen, and increased dietary acrylamide has been linked to increased risk of human endometrial and ovarian cancer (Mucci and Adami, 2009). The use of sprout suppressants is currently subject to increasing scrutiny in the EU due to their impact upon the environment. CIPC is also known to have an inhibitory effect on the equilibrium between assembly and disassembly of preformed microtubules in porcine brains (Albertini et al., 1988), leading to a recommendation for a reduction in reliance on CIPC in the suppression of sprouting to reduce CIPC residues on potatoes for consumption or processing (Bradshaw, 2006). For growers, the situation is reversed with the desired outcome being accelerated, synchronously breaking dormancy (Sonnewald, 2001). However as yet an effective, safe method for sprout-induction has not been developed.

1.4.1 Tuber Dormancy

Dormancy is a block on vegetative growth during conditions favourable to growth, associated with the diversion of resources to the establishment of dormant adversity-resistant structures including seeds, corns, buds and tubers, resistant to biotic and abiotic stresses. Dormancy is defined as a temporary suspension of visible growth of any plant structure containing a meristem (Lang et al., 1987). In potato tubers, there is considerable debate over the correct interpretation of when dormancy is initiated. It has been proposed that there is in fact no true dormancy, with microscopic growth occurring continuously from harvest with the visible sprout representing a fast macroscopic growth feature. Others have argued that dormancy is initiated upon top-kill, lifting or death of mother plant. However the most favoured model proposed is that dormancy begins at onset of tuber initiation and ends with the resumption of active bud growth under favourable growing conditions (Coleman, 1987; Claassens and Vreugdenhil, 2000; Vreugdenhil, 2007).

Two main states of potato tuber dormancy have been characterised: innate, often referred to as endodormancy; and imposed, often referred to as ecodormancy. Although the superficial result is the same in both cases, the underlying physiological states are quite different (Turnbull and Hanke, 1985a). In the state of innate dormancy, growth is prevented by internal inhibition imposed by factors arising within the meristem itself, even in a favourable external environment; while imposed dormancy is incurred when the requirements for growth, usually warmth and water, are not met (Turnbull and Hanke, 1985a). The duration of the innate dormancy period largely depends upon the cultivar (British Potato Variety Database, European Cultivated Potato Database) and to some extent biotic and abiotic conditions during tuber growth. During prolonged low temperature storage,

potatoes gradually exit the innate dormant state and enter into a low temperature imposed state of dormancy. Upon transfer to warmer temperatures, imposed dormancy is rapidly lifted and tubers resume active growth. Of the environmental conditions investigated only temperature seems to have a major influence. Some reports present evidence to support chilling shortening dormancy, while others suggest that higher storage temperatures can prematurely terminate dormancy. This suggests that multiple mechanisms can act to break of tuber dormancy. Campbell et al. (1996) found the endodormant block on cell division in tuber buds was released during storage at 3°C, resulting in a replacement of endodormancy with that of ecodormancy.

1.4.1.1 Physiological regulation of dormancy

Dormant potato tubers are metabolically active and responsive to external stimuli but currently little is understood concerning the mechanisms of suppression of tuber bud growth. Many studies have been undertaken in an attempt to understand the mechanisms that govern dormancy and sprouting.

Cell division in tuber buds ceases with the onset of dormancy, placing meristematic cells in the G_0/G_1 phase of the cell cycle (Campbell et al., 1996). Termination of innate dormancy by low temperature storage was found not to alter the cell cycle position of tuber bud cells, indicating mitotic arrest in endodormancy involves processes upstream from the immediate mechanisms of cell cycle regulation. Other studies have demonstrated major changes in gene expression that occur during progression between innate and imposed dormancy. As would be expected during a transition from quiescence to active growth, many of the transcripts and proteins associated with non-dormant meristems are related to basic cellular processes (Suttle, 2004).

Farré et al. (2001) proposed that starch breakdown and subsequent formation of various metabolites needed for growth are of importance in the control of the duration of dormancy and the promotion of sprouting. Expression of an *E.coli* inorganic pyrophosphatase under the tuber specific patatin promoter caused transgenic tubers produced to sprout earlier than non transformed controls. Pyrophosphatase activity was increased threefold, resulting in a 20-60% reduction in tuber pyrophosphate, accompanied by elevated sucrose and UDPglucose levels.

As with many aspects of plant development, the five major PGRs have been assigned principle roles in the regulation of the innate period of tuber dormancy and the subsequent induction and growth following break of dormancy. In general, tuber endodormancy is thought to be regulated by a balance between dormancy promoting and inhibiting PGRs (Coleman, 1987) (Table 1.1). However, as

Table 1.1 Summary of the role of hormones in potato tuber dormancy.
+ = internal levels increase; **0** = no change; **-** = internal levels decrease. Adapted from Suttle (1996)

	Exogenous effects on sprout growth	**Dormancy**	**Sprouting**	**Proposed Role in Sprout Growth**
Abscisic Acid (ABA)	Inhibitory	+/-	-	Inhibitor
Auxin (IAA)	Inhibitory/ Promotive	+/0/-	+/-	Unknown
Cytokinin	Promotive	+	+	Promoter
Ethylene (C_2H_4)	Inhibitory/ Promotive	?	+	Unknown
Gibberellin (GA)	Promotive	-/+	+	Promoter

Table 1.1 reveals, much of the evidence is conflicting (Claassens and Vreugdenhil, 2000). It is thought that the innate dormancy held by tuber buds six weeks after initiation is unlikely to involve apical dominance since the apical bud of the tuber is the first to enter dormancy after tuberisation of the stolon (Leshem and Clowes, 1972).

1.4.1.2 Regulation of dormancy by cytokinin

Hemberg (1970) demonstrated that treatment of apical buds of dormant tubers with kinetin or zeatin could induce sprouting in innately dormant tubers. It was later shown that potato tuber buds cv. Majestic have periods of sensitivity to applied zeatin during the innate period of dormancy. In these sprouts, initiated due to a response to injected cytokinin, rates of cell division within 48 hours of injection were similar to those in which dormancy had been broken naturally. The first of these periods of sensitivity was in the first six weeks after tuber initiation, while the second was in the three weeks preceding the break of dormancy, although this was only observed in tubers stored at the artificially high temperature of 10°C (Turnbull and Hanke, 1985a). In parallel with this, endogenous zeatin-type cytokinin was measured during tuber growth and storage (Turnbull and Hanke, 1985b). It was found that young tubers, less than six weeks after initiation that had previously been shown to be induced to break dormancy on application of exogenous cytokinin, contained naturally high [9R]Z, with measured concentrations reaching 1300 pmol g^{-1}. In mature tuber tissue, [9R]Z content was found to be as low as 2% of the value at earlier stages, coinciding with a period in which sprouting could not be induced by exogenous application of cytokinin. A 20- to 50-fold increase in bud zeatin-type cytokinin was detected in a 4 week period after harvest at 2°C which coincided with the timing of the transition from innate dormancy to a non-dormant but non-growing state, indicating a strong association between a dramatic rise in endogenous cytokinin and the natural transition out of innate dormancy. An increase in bud cytokinin was also observed in tubers stored at 10°C over the same period of time, although the level of cytokinin measured was lower at 210-260pmol g^{-1} FM compared to 460-510pmol g^{-1} FM in tubers stored at 2°C (Turnbull and Hanke, 1985b).

From these results, they reached the conclusion that cytokinins could be the primary trigger releasing tuber buds from innate dormancy. However the concentration of cytokinins in bud tissue offered no guide to the state of dormancy or its responsiveness to applied cytokinin. Suttle & Banowetz (2000), on the basis of evidence to show *cis*-[9R]Z exhibits biological activity in potatoes, applied exogenous *cis*-zeatin to dormant potato tubers. Repeating the findings of Turnbull & Hanke (1985a), in warm stored tubers they found a gradual acquisition of cytokinin sensitivity post tuber initiation with the efficacy of *cis*-zeatin at the highest concentrations applied for dormancy release

increasing with storage time. This observation fits with Turnbull & Hanke's (1985a) hypothesis that the sensitivity of the tissue to the available cytokinin is an important factor in breaking dormancy when cytokinin is present at active levels. For chilled tubers however, it seems more likely to be increased cytokinin rather than a greatly heightened sensitivity that breaks dormancy.

Endogenous levels of cytokinins in both tubers and buds was found to fall immediately after harvest and remain at a constant level in storage tissue. In bud tissue though, a 20-50 fold increase in total cytokinin content over a six week (2°C) storage period was observed (Turnbull and Hanke, 1985b). Koda (1982a) found a decrease in Z and [9R]Z immediately after harvest and an increase preceding the break of dormancy. The level of [9R-MP]Z showed an opposite pattern, building up during storage then going into decline. On the basis of this, it was suggested that the increases in base and riboside content observed prior to the break of dormancy were the result of metabolism of the stored ribotide. Mauk & Langille (1978), consistent with the results presented by Koda (1982a), demonstrated [9R]Z levels to be 10-100 times greater in the swelling stolon tip than any other cytokinin detected in non-dormant tissues.

Over-expression of genes encoding plant (Zubko et al., 2005) and bacterial (Macháčková et al., 1997) IPTs resulted in increased cytokinin biosynthesis in transgenic tubers. Concurrent with this increase, the length of the dormant period decreased dramatically. Tubers transformed to constitutively express the *Sho* isopentenyltransferase from Petunia showed almost no dormancy, sprouting and vegetatively producing new plants before top kill of the parent plant (Zubko et al., 2005). Morris et al. (2006) produced tubers of cultivar Desiree over-expressing a bacterial 1-deoxy-D-xylulose 5-phosphate synthase (*dxs*) gene which acts in the MEP pathway of isoprenoid biosynthesis. These tubers were found to have increased [9R]Z at harvest relative to wild type, and were found to have emerged from innate dormancy before harvest. Like the results of Zubko (2005), it seems increased cytokinin biosynthesis results in a decrease in duration of tuber dormancy.

1.4.2 Tuberisation

Tuberisation of stolon tips is a complex developmental process involving interactions between several environmental, biochemical and genetic factors. (Sarkar, 2008). For formation of tubers, stolons must first be induced and initiated. An axillary bud is activated on the stem base, the first visible outgrowth of the tuber bud is as a diagravitropically growing shoot. Growth and branching is maintained until a signal is received causing cessation of longitudinal growth. This is in concert with tuber induction and initiation, the stimulus for which results in radial growth of the stolon tip. The

order of these steps of tuberisation is not necessarily chronological, under rare, specific conditions, tubers can form without prior stolon initiation.

1.4.2.1 Regulation of tuberisation

There are numerous factors that affect tuber formation. Stimuli are both abiotic and biotic, and of the biotic stimuli can include bacteria in the rhizosphere. There is a general consensus that, of the abiotic stimuli, nitrogen levels, temperature, and light have the greatest effect upon the timing of tuberisation. Although the overall effects of various environmental factors are generally consistent, the genotype, physiological age of the plant and derivation of the plant, either from a mother tuber or derived from cuttings, can cause considerable variations in the degree to which a plant responds to abiotic stimuli (Jackson, 1999). High light and high sucrose, the latter of which is often exploited when inducing microtubers in tissue culture, are known to promote tuberisation. High sucrose results in an increase in leaf starch accumulation, and so export of sucrose from the leaf to the forming sink organ. High nitrogen in the medium was found to inhibit tuberisation (Krauss, 1985), alongside high temperatures which were found to be inhibitory in both short and long day photoperiods, but much greater in long day photoperiods (Ewing and Struik, 1992). Phytochrome B (PHYB) has been strongly implicated in the photoperiodic response (Jackson et al., 1996) with short days being the favoured photoperiod for tuberisation. Analysis of the signal transduction pathways involved in tuberisation indicate tuberisation is a photomorphogenic event with PHYB controlling diagravitropic growth in the apical region of the stolon.

Of the PGRs, GA is generally considered to be the most influential upon timing of tuberisation. The abiotic factors discussed: nitrogen, temperature and day length, are all thought to affect GA levels. In many cultivars, GA content of tissues is lower in short days compared to the relatively high levels in long day conditions where they act to inhibit tuberisation (Vreugdenhil and Struik, 1989). Of the remaining PGRS, numerous studies have been carried out where differences exist between phases of tuberisation measured, number of time points, cultivar used and whether the study was carried out *in vivo* or *in vitro*. The result of this is conflicting evidence for the timing of involvement and the extent of up or down regulation of each PGR at the time points measured (Vreugdenhil and Struik, 1989; Claassens and Vreugdenhil, 2000).

1.4.2.2 Regulation of tuberisation by cytokinin

Palmer and Smith (1969) were the first to demonstrate an involvement of cytokinins in tuber initiation. Stolons in *in vitro* culture, treated with cytokinins showed indications of tuber formation

after ten days of incubation in exogenous cytokinin with kinetin being more effective than BA. These indications included apical swelling and swelling of lateral buds of stolons alongside starch accumulation that occurs before any visible signs of tuber formation. Since their initial implication in tuberisation, the level of endogenous cytokinin has been observed to increase in roots and stolons on transfer of potato plants to short day conditions, the photoperiod known to stimulate tuberisation (Koda, 1982a). Cytokinin applied to a stolon tip converts it into a negatively gravitropic shoot (Kumar and Wareing, 1972). Regulation of this growth most likely occurs via regulation of the distribution of root produced cytokinins. Vreugdenhil and Struik (1989) noted that although cytokinins have been shown to stimulate tuberisation, they are also capable of converting a stolon into a leafy shoot, indicating that the response to elevated cytokinin depends upon the interaction with other hormones.

Transgenic potatoes over-expressing bacterial *dxs*, involved in isoprenoid biosynthesis via the MEP pathway was found to cause stolon tips produced in *in vitro* culture to initiate and tuberise significantly earlier than non-transformed and non-expressing controls when induced on media not supplemented with a cytokinin source (Morris et al., 2006). This early tuberisation resulted in a reduced mean stolon length relative to non-transformed controls. When induced on media supplemented with cytokinin, no significant difference was observed between transgenic lines over-expressing *dxs* and non-transformed controls in stolon initiation or tuberisation indicating a role for cytokinin in tuberisation of stolon tips.

1.5 Identification of StCKP1 from tuberising stolon tips

If tuber tissue is more sensitive to cytokinins at certain periods during dormancy (Turnbull and Hanke, 1985a), it follows that something must be causing this change in tissue responsiveness. Thomson (1994) noted that cytokinin binding activity in extracts of stolon tips was upregulated eight-fold immediately prior to spontaneous tuberisation, and isolated a 37kDa cytokinin-binding protein with a K_D of 1.7µM for [9R]Z from stolon tips at this stage. A 19 amino acid N-terminal sequence was subsequently determined (James, pers.comm.).

The full sequence of this novel cytokinin binding protein, *StCKP1*, has since been determined (Warnes, 2005). Analysis of transcript abundance of *StCKP1* in the Majestic cultivar indicates the expression pattern is associated with the onset of tuberisation. Southern blotting and sequence analysis revealed *StCKP1* to be a member of a largely prokaryotic superfamily of enzymes which also includes a group of bark storage proteins (BSPs) and wound-induced proteins, alongside bacterial nucleosidases and nucleotidases (Mushegian and Koonin, 1994). Homology between these proteins

occurs in three distinct, conserved motifs, the second of which is predicted to be a nucleoside-binding site although the putative nucleosidase activity of BSPs and VSPs is yet to be shown (figure 4.1).

Transgenic lines with *StCKP1* under the control of an estradiol-inducible promoter have given further insight on StCKP1 activity. Callus tissue of over-expressers (OE) of StCKP1 was observed to increase in fresh mass at a greater rate relative to empty vector (EV) controls and antisense (AS) lines respectively. This phenotype indicates that StCKP1 may be acting to increase the availability of cytokinin and hence OE lines show increased growth rates. The tuberisation phenotype, determined by *in vitro* tuberisation of axillary buds showed OE lines formed terminal tubers almost as soon as the stolon had been initiated. Inducible antisense (AS) lines by contrast formed no terminal tubers, and possessed an over-extended stolon. Some explants initiated axillary tubers possibly as a result of the actively growing stolon tip acting as a strong nutrient sink. As a result, the preferential accumulation of oestrogen from the medium in this apical growing point would then result in less AS induction in axillary buds, hence the production of axillary tubers was attributed to unsuppressed expression of *StCKP1*. The tuberisation phenotype of inducible OE *StCKP1* transgenics is similar to that of OE *dxs* potatoes, indicating over-expression of *StCKP1* may result in alteration of cytokinin availability in responsive tissue, having phenotypic effects on tuberisation and possibly upon tuber dormancy (Warnes, pers. comm.).

1.6 Outline of thesis

Homology between *StCKP1* and nucleosidase members of the enzyme superfamily may indicate that StCKP1 functions as an enzyme in the metabolism of adenine and adenine derivatives such as cytokinins. Implicit in the phenotypes of transgenics produced by Warnes (pers. comm.), but not yet shown directly, is StCKP1's putative activity in the metabolism of cytokinins. The amino acid sequence homology shown between bacterial nucleosidases and StCKP1 lead Warnes (2005) to propose that StCKP1 is likely to have nucleosidase activity.

It is possible that StCKP1 could be involved in the control of sprouting of potato tuber buds and in the timing of tuberisation. Both systems involve the shoot apical meristem and have been shown to be responsive to applied cytokinin at certain sensitive periods during the tuber lifecycle (figure 1.6). The aims of this project were to determine activity for the cytokinin binding protein StCKP1, and to investigate the function of StCKP1 in the processes of tuberisation and maintenance of tuber dormancy through production of transgenic over-expressing lines and assay of commercial cultivars.

StCKP1 transcript abundance was assayed in dormant and non dormant tuber tissues and at defined stages during tuberisation of stolon tips of the cultivar Desiree. Cytokinin was extracted from stolon tips harvested at the same stages of tuberisation and analysed by HPLC-ELISA. The full amino acid sequence of StCKP1 determined by Warnes (2005) was used to produce a recombinant fusion protein for bacterial expression and purification. Purified StCKP1 after cleavage from the recombinant protein was used to assay for nucleosidase activity. Once enzymatic activity had been determined, the purified protein was used to determine K_Ms for cytokinin and aminopurine substrates. *StCKP1* under the transcriptional control of the CaMV 35S promoter was transformed into a Desiree background, and tuberisation and dormancy phenotypes characterised with reference to over-expression of *StCKP1*. Relative transcript abundance of StCKP1 was measured in commercial cultivars and correlated with dormancy duration data from the British Potato Variety Database and the European Cultivated Potato Database. Finally, a proposed model of action for StCKP1 and its roles in tuberisation and the maintenance of tuber dormancy are presented alongside ideas for future work.

Chapter 2

Materials and Methods

2.1 Experimental Reagents, Materials and General Information

Except where specifically stated otherwise, methods were based on those of Sambrook, Fritsch and Maniatis (Sambrook et al., 1989).

2.1.1 Reagents and Materials

All laboratory reagents used were of the highest grade were obtained from Sigma-Aldrich (Gillingham, UK), BDH (Poole, UK) and Fisons (Ipswich, UK). For all solutions and solvent mixtures, the water used as a diluent was deionised (dIH_2O) or, if required dIH_2O which had been filtered and UV treated using the Millipore Milli-Q Quantum IX system, and then subsequently autoclaved (MQH_2O) (Millipore, Billerica, MA, USA). Bactotryptone and yeast extract were obtained from Oxoid (Basingstoke, UK). Preparation of plasmid DNA from *E. coli* was carried out using Sigma GenElute Miniprep kits (Sigma-Aldrich) and according to the manufacturer's instructions. pT7-Blue3 from Novagen (Beeston, UK) was used to carry out blunt cloning. First strand cDNA synthesis was carried out using Revert Aid H Minus M-MuLV reverse transcriptase (Fermentas, Burlington, Ontario, Canada) according to manufacturer's instructions. Restriction enzymes, calf intestinal alkaline phosphatase (CIAP) and Xa cleavage factor were bought from New England Biolabs (Ipswich, MA, USA), Roche (Burgess Hill, UK), and Novagen respectively. Acrylamide and Protein Assay Dye Reagent Concentrate were acquired from Severn Biotech (Worcs, UK) and BioRad (Hemel Hempstead, UK) respectively. 3mm filter paper was bought from Waterman (Maidstone, UK), Protran BA 83 nitrocellulose was obtained from Whatman GmbH (Dassel, Germany) and positively charged nylon membrane from Roche Diagnostics (Mannheim, Germany). FPLC columns were purchased from Amersham Biosciences (St. Giles, UK). 5-bromo-4-chloro-3-indolyl-*β*-D-glucuronic acid (X-Gluc), 4-methyl-umbelliferyl-glucuronide (MUG), Isopropyl-β-D-1-thiogalactopyranoside (IPTG) and antibiotics were obtained from Melford Laboratories Ltd (Ipswich, UK). DNA molecular markers (1 kb) and pre-stained PageRuler™ protein molecular markers (10 - 170 kDa) used for gel electrophoresis were obtained from Fermentas.

2.1.2 Measurement of pH

pH measurements were carried out on a Hanna Instruments pH 210 Microprocessor pH Meter, fitted with a Russell Standard glass electrode.

2.1.3 Centrifugation

Centrifugations were carried out in an MSE Microcentaur Centrifuge, an Hettich Mikro 20 Centrifuge and a Beckman Coulter Avanti J-25 centrifuge using JA20 and JLA10.500 rotors and appropriate plasticware. Centrifugation at 4℃ were performed in a Howe, Sigma Laboratories, Centrifuge 3K10.

2.1.4 Sterilisation of Solutions

The majority of solutions used in this study were sterilised by autoclaving (121℃ for 20 mins). All solutions sensitive to heat were sterilised through 0.2 µm sterile filters (Minisart).

2.1.5 Antibiotics

Filter sterilised antibiotics were prepared at the stock concentrations and used at the final concentrations in Appendix 1, Table 1.6. unless otherwise stated.

2.1.6 Bacterial Strains

For the strains used in this study refer to table 2.1.

2.1.7 Plasmids

For the plasmids used in this study refer to table 2.2.

2.1.8 Oligonucleotides

Oligonucleotides used in this study are listed in table 2.3. with their sequence and section reference. Oligonucleotides were custom made by either Invitrogen Life Technologies (Paisley,UK) or VH Bio (Gateshead, UK) as stated.

2.1.9 Antibodies

For a list of antibodies used in this study refer to table 2.4.

2.1.10 Computer Analysis

All *Solanum tuberosum* L. sequences were obtained from the Sol Genomic Network (SGN) expressed sequence tag (EST) database website. Other sequences required were found on the National Centre for Biotechnology Information (NCBI) website. A number of computer programs were used to carry out bioinformatics. For nucleotide and protein sequence searches and alignments, BLAST (Altschul *et*

Table 2.1 Table of bacterial strains used in this study

Organism	Strain	Genotype
E.coli	TB1	F-*ara Β(lac-proAB) [Φ80dlac Β(lacZ)M15] rpsL(StrR) thi hsdR*. (NEB pMal Protein Fusion and Purification System Users manual)
E.coli	DH5α	As described in Sambrook et al. (1989)
E.coli	BL21 (DE3)pLysS	F–,*omp*T,*hsd*S_B(r_B–, m_B–),*dcm*,*gal*, λ(DE3), pLysS, Cm^r
E.coli	UT6500	*F– ara-14 leuB6 secA6 lacY1 proC14 tsx-67 Δ(ompT-fepC)266 entA403 trpE38 rfbD1 rpsL109(Str*R*) xyl-5 mtl-1 thi-1* (NEB pMal Protein Fusion and Purification System Users manual)
E.coli	ER2508	F-*ara-14 leuB6 fhuA2 Δ(argF-lac)U169 lacY1 lon::miniTn*10(Tet^R) *glnV44 galK2 rpsL20*(Str^R) *xyl-5 mtl-5 Δ(malB) zjc::Tn*5(Kan^R) *Δ(mcrC-mrr)* (NEB pMal Protein Fusion and Purification System Users manual)
Agrobacterium tumefaciens	LBA4404	As described in Hoekema et al. (1983)

Table 2.2 Table of plasmids used in this study

Plasmid Name	Description	Size	Cloning Site	Reference
pT7Blue-3	Linear cloning vector with A overhangs, used for blunt cloning of PCR products. Amp^R and Kan^R	3.8kb	N/A	Novagen
pMalc2x	Cloning vector provided in pMal protein fusion and purification system producing a translational fusion between maltose binding protein and a protein of interest. Amp^R	6.6kb	N/A	New England Biolabs
pGADT7 AD	Cloning Vector provided in Clontech's Matchmaker™ Gold Yeast and Two-Hybrid Screening System. Amp^R	8.0kb	N/A	Clontech
pGADT7CKPCDS	*StCKP1* cDNA sequence cloned into pGADT7 AD. Amp^R	9.0kb	N/A	Gift from Barbara Warnes
pc2xCKP	*StCKP1* cloned into pMalc2x from PGADT7 AD producing a translational fusion between maltose binding protein and StCKP1. Amp^R	7.6kb	*Eco*RI and *Bam*HI	This study
pGreen0029:35SS	A binary Ti vector containing a CaMV 35S promoter. Kan^R	6.1kb	N/A	(Hellens et al., 2000)
pSOUP	Helper plasmid used in transformation of *Agrobacterium tumefaciens* with pGreen derived vectors. Tet^R	9.2kb	N/A	(Hellens et al., 2000)
pG35SSCKP	*S.tuberosum CKP1* cloned into pGreen0029:35SS from PGADT7 AD under the transcriptional control of a double CaMV 35S promoter. Kan^R	7.1kb	*Eco*RI and *Bam*HI	This study
pGGUS	A binary Ti vector containing a promoterless *uidA* gene. Kan^R	6.8kb	N/A	(Hellens et al., 2000)

Plasmid Name	Description	Size	Cloning Site	Reference
pG35SGUS	A binary Ti vector containing *uidA* gene under the transcriptional control of the CaMV 35S promoter. Kan^R	8.3kb	N/A	(Wilkins, 2004)
pTAIL256	*StCKP1* pro1 promoter cloned into pCR2.1-TOPO linear cloning vector. Amp^R and Kan^R	4.9kb	N/A	(Warnes, 2005)
pTAIL128	*StCKP1* pro2 promoter cloned into pCR2.1-TOPO linear cloning vector. Amp^R and Kan^R	3.5kb	N/A	(Warnes, 2005)
pT7B-3Cp1	*StCKP1* pro1 from pTAIL256 blunt cloned into pT7Blue-3 linear vector. Amp^R and Kan^R	4.8kb	N/A	This study
pT7B-3Cp2	*StCKP1* pro2 from pTAIL128 blunt cloned into pT7Blue-3 linear vector. Amp^R and Kan^R	3.4kb	N/A	This study
pGpro1GUS	A binary Ti plasmid based on pGGUS with the *uidA* gene under the transcriptional control of the StCKP1 pro1 promoter from pT7B-3Cp1. Kan^R	7.8kb	*Bam*HI and *Xba*I	This study
pGpro2GUS	A binary Ti plasmid based on pGGUS with the *uidA* gene under the transcriptional control of the StCKP1 pro2 promoter from pT7B-3Cp2. Kan^R	7.4kb	*Bam*HI and *Xba*I	This study

Table 2.3 Table of oligonucleotides used in this study

Primer Name	Primer sequence 5′-3′	T_m (°C)	Reference
C1 F	GCT TCT CTC AAA CTC AAA GTG TCT ACC	58	3.3
C1 R	GAG ATC ACC AGG TTT GTA ACT AGG ATG	57	3.3
C2 F	AGC AAA TGG TGC TAT TAG TGG AAA GAC	55	3.3, 4.2
C2 R	AGC AAA TGG TGC TAT TAG TGG AAA GAC	55	3.3, 4.2
C912F	TGA AAT GGA AAG TGC TGC TG	45	6.2
F Tub	AGT GCC AGA GCT TAC TCA AC	50	3.3
R Tub	CAC CTG TCT ACC AAT GCA AG	50	3.3
Prom F	GGT AGA CAC TTT GAG TTT GAG AGA AGA GAG	60	3.4.1
Prom R	AGT GGA GTA ACA CAG AGC CAA TAG AAG AC	60	3.4.1
CP2 F	ACG CGT CGA CTG TCG AGT GAG ATG AAA AAA AAT G	63	3.4.1
CP2 R	TTG ACG TCA ATA GTA TTG ACA AGG GAA ACT AA	59	3.4.1
GUS F	TTA CGT CCT GTA GAA ACC CCA	52	3.4.2
GUS R	TGT AAC GCG CTT TCC CAC CAA C	57	3.4.1, 3.4.2
35S F	CTA TCC TTC GCA AGA CCC TTC CTC T	60	6.2
Nos R	TTA TCC TAG TTT GCG CGC TA	54	6.2
R20-mer	ATG ACC ATG ATT ACG CCA AG	51	3.4.1
U19-mer	GTT TTC CCA GTC ACG TTG T	48	3.4.1
NptII F	TGA ATG AAC TGC AGG ACG AG	52	6.2
NptII R	AGC CAA CGC TAT GTC CTG AT	52	6.2
pGEM R	TGT GGA ATT GTG AGC GGA TA	50	3.4.1
M13/pUC R	CGC CAG GGT TTT CCC AGT CAC GAC	60	3.4.1, 4.2
MalE F	GGT CGT CAG ACT GTC GAT GAA GCC	60	4.2
18SF	CGC AAA TTA CCC AAT CCT GAC	52	3.2, 3.3
18SR	CTA TGA AAT ACG AAT GCC CCC	52	3.2, 3.3
U292623F	ATT GTG GTG GTC ATG GGA GT	60	3.2
U292623R	ATG CAT CGA CCC ATA GGA AA	60	3.2

Table 2.4 Table of antibodies used in this study

Antibody	Host Raised In	Section Reference	Reference
Anti-MBP	Rabbit	4.2	New England Biolabs
Anti-*Solanum tuberosum* CKP1	Rabbit	4.2	Unpublished; Developmental Botany laboratory, University of Cambridge
Anti-[9R]Z	Rabbit	3.2, 6.7	(Collier et al., 2003)
Anti-[9R]iP	Rabbit	3.2	(Collier et al., 2003)
Anti-[9R]DZ	Rabbit	3.2	(Collier et al., 2003)

al., 1990), CLUSTALW (Thompson *et al.*, 1994) and CLUSTALX (Thompson *et al.*, 1997) were used. All statistical analysis was carried out using Microsoft Excel, SigmaPlot, MiniTab and GenStat.

2.2 Growth of Organisms

2.2.1 Plant Material

2.2.1.1 Growth of *Solanum tuberosum* L.

Certified seed tubers of *Solanum tuberosum* L. cv. Desiree were planted in the Botanic Gardens, Cambridge in April and grown, with no spray or chemicals applied during cultivation. The resulting tubers were lifted in September, washed and left to dry. Other cultivars used in this study were grown at Cambridge University Farm or Babraham Home Farm (stated) using commercial farming practice.

2.2.1.2 Growth of *S.tuberosum* L. harbouring transgenes

S.tuberosum L. cv. Desiree lines harbouring transgenes were grown at the Plant Growth Facility, Botanic Gardens, Cambridge. Plants were transferred from aseptic culture (section 2.2.1.5) to a 7:1 mix of Levington M3 compost to medium grade vermiculite pre-treated with intercept according to manufacturer's instructions, initially in 20cm diameter pots. Following a period of 8 to 10 weeks growth, plants were transferred to pots of 40cm diameter where they remained until aerial organs began to senesce, indicating tuber maturation. Plants were grown at a constant temperature of 22°C under a long day photoperiod at 350µM intensity. Light was predominantly fluorescent but some red light was supplied from 10 15W incandescent bulbs per shelf. Humidity remained constant at 65%. Soil moisture was monitored hourly by probe and water delivered to all plants if the soil moisture was detected to be less than 45%.

2.2.1.3 Production of stolon tips

Tubers of *Solanum tuberosum* L. cv. Desiree were selected on the basis of size (tubers >4cm, <10cm diameter were selected), lack of disease and damage and placed into paper sacks; around 30 tubers in each; tied at the neck and sealed with aluminium foil to prevent light penetrating the opening. Bags were kept in a basement room in ambient conditions (approximately 15°C) until after 10 weeks in storage when tubers began sprouting, producing a mass of stolon tips. Stolon tips were harvested at two different time points, classified into three different categories:

1. Three months before signs of tuberization, shortly after stolons had been produced (BT)

2a. Non-tuberizing stolon tips from tubers some of whose stolon tips were showing signs of tuberization. As stolon tips from a single tuber tuberize within a short period of time, it is reasonable to presume this tissue is at incipient tuberization (IT).

2b. Stolon tips having just begun tuberization (T), defined by the tip of the stolon having swollen to three times the mean diameter of BT stolon tips.

Harvested stolon tips were subsequently flash frozen in liquid nitrogen and stored at -80°C prior to analysis unless otherwise stated.

2.2.1.4 Harvest of tuber tissue

Sprouts from non-dormant tubers approximately 10cm in length were harvested. Tissue was excised at the tip, base to include the bud which had broken dormancy, and mid-way along the sprout; cut into 3mm portions and flash frozen in liquid nitrogen. Dormant bud tissue was excised to include the scale leaves and some cortical tissue just below the bud, cut into $3mm^3$ portions and flash frozen in liquid nitrogen. Cortical tuber tissue was harvested from both dormant and non-dormant tubers using a sterile 6mm diameter cork borer, cut into slices approximately 3mm in depth, and flash frozen in liquid nitrogen. Periderm from both dormant and non-dormant tubers was harvested using a scalpel blade to remove only the characteristically pink tissue of Desiree skin and the few cell layers below that, encompassing the periderm. Tissue was flash frozen in liquid nitrogen and stored, like all tissue samples, at -80°C prior to analysis.

2.2.1.5 Aseptic culture of *Solanum tuberosum* L.

Aseptic stocks of *S. tuberosum* L. cv. Desiree were kept as shoot cultures in 250ml metal lid pots (Bibby Sterilin, Stone, UK) containing approximately 50ml MS30 medium (Appendix 1, Table A1.2,), with three shoots per pot. Pots were closed so the lid remained loose (tightened then turned back ¼ turn) and sealed with micropore tape. After four weeks in culture, plants were sub-cultured by transferring approximately 2cm nodal sections into fresh MS30 media. Cultures were grown at 21°C with a 16 hour light / 8 hour dark cycle with 200µmol m^{-2} s^{-1} photosynthetically active radiation (PAR) from fluorescent tubes (Phillips TLD 36W/33).

2.2.1.5.1 Microtuber Induction

Microtubers were induced from single nodes taken from aseptic stocks in 100mm square petri dishes (Bibby Sterilin) containing approximately 150ml PMM+6% sucrose supplemented with 2.5mg/l BA (Appendix 1, Table A1.2.) using methods adapted from Gopal *et al*. (1998). Single nodal segments (0.5–1.0 cm) with subtending leaf were subcultured aseptically from the central portion of six to eight week old plantlets as explants and incubated at 21°C in darkness for 35 days.

2.2.1.5.2 Callus Induction

Callus was induced from 0.5cm internodal stem sections taken from sterile stocks in 90mm diameter petri dishes containing approximately 75ml Gamborg's B-5 callus induction media (Blackhall, 1992; Wee et al., 1998) (G B-5; Appendix 1, Table A1.2.). Sections were subcultured aseptically and 4 were placed equidistantly on a single dish. Callus was moved to fresh G B-5 media every 2 weeks to prevent nutrient deficiency. Calli were cultured with a 16 hour light / 8 hour dark cycle with 200µmol m^{-2} s^{-1} PAR from fluorescent tubes (Phillips TLD 36W/33).

2.2.2 Growth of Bacteria

2.2.2.1*Escherichia coli*

All bacterial cultures were grown using autoclaved LB media (Appendix 1, Table A1.1.) unless stated otherwise. The solution was allowed to cool to 55℃ before the addition of the appropriate antibiotic, if required. Liquid cultures were grown at 37℃ at 3Hz, unless otherwise stated. For growth of bacterial colonies, 20ml molten LB Agar (LBA) plus appropriate antibiotics was poured into 90mm petri dishes in the flow hood to prevent contamination, and stored at 4℃ once set. Bacteria were plated or streaked over the media and incubated at 37℃, overnight or until colonies could be seen.

2.2.2.2*Agrobacteria tumefaciens*

Strains of *Agrobacterium tumefaciens* used in this study was LBA4404 (table 2.1) and was grown using TYNG media (Appendix 1, Table A1.1.) at 28℃ and 2.5Hz unless otherwise stated. On solid media the *A. tumefaciens* required 96 hours to form visible colonies whilst in liquid media 48 hours was required to reach mid log phase. The required antibiotics for selection of each strain are shown in table 2.1.

2.3 Nucleic Acid Manipulations

2.3.1 DNA extraction

2.3.1.1CTAB DNA extraction

Genomic DNA (gDNA) was extracted and precipitated from potato tissue based on a method described by Murray and Thompson (1980). 0.3g leaf tissue excised from tissue grown in aseptic culture was ground to a fine powder using a pestle and mortar pre-chilled to -20°C using liquid nitorgen and transferred to a sterile 1.5ml microcentrifuge tube. 3ml CTAB extraction buffer (Appendix 1, Table A1.3) was added to the ground tissue and vortexed. The tube was then incubated at 65°C for 30 minutes. Following incubation, 1.2ml chloroform was added and mixed well before being centrifuged at 4000*g* for 30 minutes. The upper, aqueous phase was transferred to a new tube and nucleic acids precipitated by adding 2ml ice cold isopropanol and incubating at -20°C for 30 minutes. The pellet was obtained by centrifugation at 4000*g* for 15 minutes and resuspended in 1.2ml autoclaved MQH_2O then extracted once with 0.5 volumes of phenol before centrifuging at 13400*g* for 5 minutes. The upper phase was then transferred to a new tube and extracted with 0.5 volumes chloroform before centrifuging at 13400*g* for 5 minutes. The upper phase was transferred to a new tube and the DNA precipitated.

2.3.1.2'Shorty' DNA extraction

100mg tissue was ground to a fine powder in an eppendorf and 0.5ml Shorty DNA extraction buffer (Appendix 1, Table A1.3.) was added. The ground tissue and extraction buffer were mixed thoroughly by vortexing then centrifuged at 12000*g* for 5 minutes. 350µl of the supernatant was transferred to a fresh tube carrying an equal volume of isopropanol. The tubes were inverted 10 times then centrifuged at 12000*g* for 10 minutes to pellet the precipitated DNA. The pellet was washed twice with 500µl 70% (v/v) ethanol, vortexed and centrifuged at 12000*g* for 2 minutes. The ethanol was removed by vacuum siphon and the pellet left to air dry before resuspending in 250µl MQH_2O.

2.3.2 Nucleic acid precipitation

Nucleic acid was precipitated from the crude nucleic acids extracted by adding 2.5 volumes 96% (v/v) ethanol and 0.1 volume 3M sodium acetate, pH 5.2 and incubating overnight at -20°C. After centrifugation at 13400*g* for 15 minutes, the supernatant was discarded and the pellet washed in 70% (v/v) ethanol and allowed to dry on a laminar flow hood. The pellet was resuspended in 300µl MQH_2O overnight at 4°C.

2.3.3 Nucleic acid quantification

The concentration of nucleic acid in a 1:50 dilution in TE buffer (Appendix 1, Table A1.3.) of total extract was determined by measuring the absorbance at 260nm using a BioPhotometer (Eppendorf, USA) where an A_{260} of 1.0 is equivalent to 40µg ml^{-1} RNA and an A_{280} of 1.0 is equivalent to 50 µg ml^{-1} dsDNA. The purity of nucleic acids was measured by calculating the ratio of A260nm:A280nm, as contaminating proteins typically show an absorbance maximum at 280 nm. Nucleic acids with ratios of 1.8-2.1 were considered pure enough to be used.

The quality of total RNA extracted was also determined by separation of the RNA on 1.5% (w/v) agarose gels (Agarose Ultra Pure electrophoresis grade, Invitrogen) in 1xTAE buffer (Appendix 1, Table A1.3.) diluted from a 50x stock (section 2.3.7). RNA of good quality was identified by the presence of two distinct bands of rRNA (28S and 18S).

2.3.4 Primer design

Primers were designed using either the Primer 3 tool on SDSC Biology Workbench (http://workbench.sdsc.edu) or using the Invitrogen OligoPerfect™ Designer (http://www.invitrogen.com/content).

2.3.5 Polymerase chain reaction (PCR)

All PCR reactions were carried out in a GeneAmp 2400 thermocycler (Perkin Elmer). PCR products to be cloned or sequenced were amplified using a proof-reading Phusion High-Fidelity DNA Polymerase (Finnzymes, New England Biolabs). For all other purposes, BioMix Red (Bioline), which contains BIOTAQ DNA polymerase, 2mM dNTPs, 32mM $(NH_4)_2SO_4$, 125mM Tris-HCl (pH 8.8), 0.02% (v/v) Tween 20, 3mM $MgCl_2$, a stabiliser and an inert dye for gel loading was used. Reactions were carried out in a total volume of 20µl and conditions for the two polymerases are detailed in Table 2.5. Thermal cycling conditions, notably the T_m for annealing required were determined on the basis of primer size using the nearest-neighbour method (http://www.finnzymes.com). General cycling parameters are detailed in Table 2.6.

Table 2.5 Reaction conditions for PCR according to DNA polymerase used.

Component	Phusion High-Fidelity	BioMix Red
Template	10-100ng	10-100ng
Buffer	5x Phusion HF Buffer: 4µl	2x BioMix Red: 10µl
dNTPs	200µM each NTP	
Primers	0.5µM each primer	0.8µM each primer
DNA Polymerase	0.4U	

Table 2.6 Cycling parameters for PCR according to polymerase used.

Polymerase	Phusion High-Fidelity			BioMix Red		
Step	**Temp. (°C)**	**Time (s)**	**Nr Cycles**	**Temp. (°C)**	**Time (s)**	**Cycles (No)**
Initial Denaturation	98	120	1	94	120	1
Denaturation	98	10	30-40	94	30	30-40
Annealing	44-51	30		50-55	30	
Extension	72	60		72	60	
Final Extension	72	120	1	72	300	1
Hold	10	α	1	4	α	1

Table 2.7 Colony PCR thermal cycling conditions

Step	Temp. (°C)	Time (min)	Cycles (No)
Initial Denaturation	94	10	1
Denaturation	94	1	30
Annealing	50-55	1	
Extension	72	1	
Final Extension	72	10	1
Hold	4	α	1

2.3.6 Multiplex PCR

Reaction conditions for multiplex PCR with BioMix Red were as in section 2.3.5, together with the thermal cycling conditions, but using two primer pairs. Primers designed to amplify a 450bp fragment of tubulin were used to standardize the amount of cDNA (therefore RNA) incorporated into the PCR reaction mix throughout all experimental samples, alongside the primers designed to *StCKP1* (Table 2.3.) whose expression is unknown and likely to vary.

2.3.7 Agarose gel electrophoresis

Individual targets were separated on 1.5% (w/v) agarose gels. Agarose was melted in 1xTAE (Appendix 1, Table A1.3.) and left to cool before 0.5µg ml^{-1} ethidium bromide was added and mixed by swirling. The mixture was then poured into gel running equipment (Mini-horizontal gel system, Major Science, Pan-Chiao City, Taiwan) and allowed to set. Samples prepared using BioMix Red were loaded straight onto the gel while those prepared with Phusion were mixed with $1/6^{th}$ volume 6x Loading Buffer (Fermentas). All gels were electrophoresed in a 1x TAE running buffer at 70V with 0.5µg GeneRuler™ 1kb DNA Ladder (Fermentas) and visualized using a UV transilluminator. Digitized data were collected and analyzed with the ImageQuantTL analysis package (GE Healthcare, Chalfont St Giles, UK). For multiplex reactions both products were corrected against the background and amplified β-tubulin was used as a standard against which amplified *StCKP1* was quantified.

2.3.8 RNA extraction

All spatulas, mortars and pestles used in the extraction of RNA were wrapped in aluminium foil and baked at 180°C for 2 hours. Sterile, certified, disposable plastics were used. All water used for elution was RNase-free (either supplied in a kit or MQH_2O). All work was carried out on a tray, and gloves and pipettes were replaced frequently and regularly wiped with RNase *ZAP* (Sigma, Gillingham, UK) solution during use.

RNA was extracted from 100mg tissue using TriPure Isolation Reagent (Roche Applied Science) according to manufacturer's instructions. Tissue was ground to a fine powder in a pre-cooled mortar using liquid nitrogen, to this 1ml TriPure Isolation Reagent was added and mixed well throughout thawing. 0.2ml chloroform was added to the thawed isolate in a 1.5ml microfuge tube, vortexed to mix and the mixture kept at room temperature (RT) for 15 minutes. The sample was centrifuged at 12,000*g* for 15 minutes at 4°C. The upper aqueous phase was removed to a fresh tube and RNA precipitated by addition of an equal volume of isopropanol followed by several inversions and left at RT for 10 minutes. Precipitated RNA was pelleted by centrifugation at 12,000*g* for 10 minutes and

4°C. The pellet was washed twice using 75% ethanol, allowed to air dry and resuspended in 50µl MQH_2O before storing at -80°C.

2.3.9 DNase Treatment of RNA

If required, RNA was incubated with 0.1 volume 10x DNaseI buffer (Ambion) and 1U DNaseI (Ambion) at 37°C for 30 minutes. Subsequently, 0.1 volume DNase Inactivation Reagent (Ambion) was added and incubated at RT for 2 minutes. DNase Inactivation Reagent was pelleted by centrifugation at 9000*g* for 1 minute. RNA was removed and DNaseI and buffer were removed using the RNeasy Plant Mini kit (Qiagen) according to manufacturer's instructions.

2.3.10 First strand cDNA synthesis

2µg total RNA was transcribed to cDNA using Revert Aid H Minus M-MuLV reverse transcriptase (Fermentas) according to the manufacturer's instructions using an oligo(dT) primer (Table 2.3.). cDNA produced was then used in PCR (section 2.3.5.) or multiplex PCR (section 2.3.6.) reactions.

2.3.11 RNA blotting

RNA samples were denatured by incubation at 65°C for 15 minutes in 3x volumes of RNA loading dye (Appendix 1, Table A1.3.). Samples were electrophoresed in 1.2% (w/v) 1x MOPS, diluted from a 10x stock, (Appendix 1, Table A1.3.) agarose gel. The gel was run at 80V in 1x MOPS buffer until the bromophenol blue dye had moved an appropriate distance down the gel.

Gels were then equilibrated in 2x standard saline citrate buffer (SSC), diluted from a 20x stock, for 5 minutes and RNA transferred to nylon membrane by capillary blotting. The membrane was rinsed in 2x SSC and allowed to air-dry. Transferred RNA was covalently linked to the membrane by exposure to 120,000µJ UV light in a Stratalinker 1800 UV cross-linker (Stratagene, La Jolla USA). Blots were stored dry at room temperature between sheets of 3MM paper until probed.

2.3.12 Radiolabelled [α-^{32}P]dCTP probe preparation

The Prime-It® II Random Primer Labelling kit (Stratagene) was used to label 50ng PCR product (section 2.3.5) with 5µl [α-^{32}P]dCTP (111 TBq mmol^{-1}, Perkin Elmer) according to manufacturer's instructions. The labelled probe was purified from unincorporated [α-^{32}P]dCTP using a 1ml Sephadex G-25 column prepared in JOB buffer (Appendix 1, Table A1.3.).

2.3.13 Hybridisation of RNA blots

Prehybridisation of membranes was carried out in a Techne Roller-Blot Hybridiser HB-3D (Duxford, Cambridgeshire UK) at 42°C with 20ml ULTRAhyb Ultrasensitive Hybridization Buffer (Ambion) for at least 1 hour. To the hybridization solution, a [α-^{32}P]dCTP-labelled probe was added and allowed to hybridise for at least 16 hours at 42°C. The blots were washed three times with 2x SSC/0.1%(w/v) SDS at 65°C for 15 minutes. The background radiation was measured using a Geiger-Muller counter, and if found to be above 5-10 counts per second they were washed twice with 1x SSC/0.1%(w/v) SDS at 65°C for 15 minutes. If the background radiation was still above 5-10 counts per second the stringency of washing was increased until it had been reduced to an acceptable level. The washed blots were double sealed in two plastic bags to keep them moist and hybridisation intensity was measured by phosphorimaging analysis (section 2.3.14).

If membranes were to be re-probed, the membrane was washed 5 times for 5 minutes each in boiled stripping solution (Appendix 1, Table A1.3). Blots were dried and stored at RT between sheets of 3MM paper for later use.

2.3.14 Phosphorimaging analysis

Hybridised blots were exposed to a storage phosphor screen (GE Healthcare) for periods up to 48 hours depending upon strength of the probe and quantity of mRNA crosslinked to the membrane. Phosphor imaging was carried out using a Typhoon 8610 Variable Mode Imager (GE Healthcare) and images were processed using ImageQuantTL analysis software (GE Healthcare).

2.4 Transformation Methods

2.4.1 Plasmid construction

2.4.1.1 Gel purification of PCR products

Amplified regions were purified from agarose gels using the QIAquick PCR purification kit (Qiagen, Crawley) using a microcentrifuge according to the manufacturer's instructions. The kit uses a column containing an activated membrane which binds nucleic acids. DNA was eluted in 30µl 10mM Tris, pH 8.5 (supplied).

2.4.1.2 Blunt cloning of PCR products

Purified PCR products were cloned into a pT7Blue-3 vector using the Perfectly Blunt® Cloning kit (Novagen). Initially, products were subject to an end conversion reaction by which product ends

were converted to blunt, phosphorylated ends. 0.05pmol purified PCR product (section 2.4.1.1.) was added to 5µl End Conversion mix (supplied) and made up to 10µl with nuclease-free water. The mixture was then incubated at 22°C for 15 minutes. The reaction was halted by heating to 75°C for 5 minutes, to inactivate the kinase in the End Conversion mix. The reaction was cooled on ice for 2 minutes before adding 1µl pT7Blue-3 blunt vector followed by 1µl T4 DNA ligase (Novagen) then incubated at 22°C for 15 minutes. The product of the ligation reaction was then stored on ice, or at -20°C for longer periods, before transforming into *Escherichia coli* (section 2.4.3).

2.4.1.3 Conventional cloning

2.4.1.3.1 Restriction endonuclease digestion of DNA

The desired fragment was excised from the donor vector by digestion with the appropriate restriction endonucleases (Roche, Burgess Hill, UK), or was amplified from a DNA template incorporating the desired restriction sites at the 3′ and 5′ ends of the PCR product using appropriately designed primers. Expression vectors were cut by the same methods. Digests were always performed in a reaction volume of 50µl containing less than 10% enzyme. Double digests were performed if the two enzymes used had a compatible buffer. If the two enzymes shared no compatible buffer, the DNA was first cleaved with the restriction endonuclease that required the lower salt reaction conditions. Digestions were incubated at 37°C for 2 hours, then heat inactivated for 10 minutes at 65°C in a water bath. The cut DNA was then purified using the QIAquick PCR purification kit (Qiagen, Crawley, UK) to remove restriction endonucleases, and this cleaned DNA used in a second digest.

2.4.1.3.2 Dephosphorylation of cut plasmid DNA

Dephosphorylation was carried out in order to prevent self-religation of cut ends. 0.1U calf intestinal alkaline phosphatase (CIAP) (Promega) per pmol ends was added to the digested DNA based on equation 2-1:

Equation 2-1

$$\text{pmol ends} = \left(\frac{\text{mass of DNA (µg)}}{\text{size of DNA (kb)}}\right) \times 3.04$$

The appropriate number of units of CIAP were incubated with 1x CIAP buffer (supplied), the digested DNA and nuclease-free water to a total volume of 200µl at 37°C for 30 minutes. After 30 minutes, a

further 0.01U CIAP per pmol ends was added to the reaction and incubated at 37°C for a further 30 minutes. The reaction was stopped by adding 0.5M EDTA.Na_2 and heating at 65°C for 20 minutes, and purified using the QIAquick PCR purification kit, eluting in 30µl water.

2.4.1.3.3 Ligation of insert DNA and cloning vector

The appropriate amount of vector and insert to be ligated was determined using equation 2-2:

Equation 2-2

$$\text{size of vector (kb)} = \frac{(\text{mass of vector (ng)} \times \text{size of insert (kb)})}{\text{mass of insert (ng)}}$$

The digested vector and insert in a volume made up to 10µl in a 0.2ml PCR tube with water were heated together at 65°C for 10 minutes to break any unwanted insert-insert and vector-vector associations, increasing the probability of achieving more successful transformants, then cooled to 4°C and centrifuged briefly to collect any condensate. Ligation was carried out using Quick Ligase (New England Biolabs, Boston, MA, USA). Briefly, 10µl 2x reaction buffer and 1µl T4 Quick Ligase were added to the vector and insert preparation and incubated at room temperature for 5 minutes. The ligated preparation was then chilled on ice for transformation into chemically competent *E. coli* (section 2.4.3), or stored at -20°C.

Colonies were selected and screened for presence of the prepared plasmid (section 2.4.4.) using both vector- and insert-specific primers. A plasmid preparation was carried out on colonies containing the desired plasmid (section 2.4.5.) and 500µl of the liquid culture used for glycerol stock.

2.4.2 Preparation of chemically competent *E. coli*

Cells were streaked onto LBA plates (Appendix 1, Table A1.1.) and cultured overnight at 37°C. From this culture, a single colony, selected and inoculated into 5ml LB broth and shaken overnight at 37°C and 3Hz. 1ml of this overnight liquid culture was harvested and inoculated into 100ml LB broth and incubated at 3Hz for 2 hours at 37°C. The stock culture was transferred to two 50ml falcon tubes and placed on ice for 5 minutes. Following this, the culture was subject to centrifugation at 4000*g* at 4°C for 5 minutes. Cells were drained for 1 minute then resuspended in 40ml transformation buffer (TBI) (Appendix 1, Table A1.1.) per tube and cooled on ice for 5 minutes. Cells were then pelleted by centrifugation at 4000*g* at 4°C for 5 minutes. The pellet was resuspended in 2ml transformation buffer 2 (TBII) (Appendix 1, Table A1.1). The cell suspension was placed on ice for 15 minutes prior to dividing into 50µl aliquots. Cells were snap frozen in liquid nitrogen and stored at -80°C.

2.4.3 Transformation of *E. coli*

Competent cells were thawed on ice for 2-5 minutes and gently flicked to evenly redistribute cells. Either 1µl plasmid or 5µl ligation mix was added and stirred with a pipette tip to mix. The cells were incubated on ice for 30 minutes prior to a 45 second heat shock at 42°C before returning to ice for a further 2 minutes. While on ice, 500µl LB was added to the cells followed by recovery at 37°C for at least 1 hour at 3Hz. Cells were lawn plated into LBA plates containing the appropriate antibiotic for selection of strain (table 2.1.) and plasmid (table 2.2).

2.4.4 Colony PCR

Prior to growing bacterial colonies for plasmid preparation (section 2.4.5.), the presence of the appropriate insert was ascertained using colony PCR. A single colony was picked from an agar plate using a sterile toothpick and streaked inside a PCR tube. This was repeated for as many colonies as required. 10µl PCR master mix (5µl 2x BioMix Red, 0.4mM per primer, water to 10µl) was added to each tube. Cycling conditions are described in table 2.7.

2.4.5 Plasmid Preparation

Colonies with the desired insert were inoculated into 5ml LB broth with the appropriate antibiotic and grown overnight at 37°C in an orbital shaker at 3Hz. The following day, the plasmid was purified from 4.5ml of the overnight culture using GenElute™ Plasmid Miniprep kit (Sigma-Aldrich) following the manufacturer's instructions. The plasmid was eluted in 50µl water, then re-eluted using the first eluate to avoid further dilution of the plasmid.

2.4.6 Sequence analysis

Plasmid preparations were sequenced using an Applied Biosystems 3730xl DNA Analyser by Geneservice, Cambridge, UK using appropriate primers designed to both plasmid backbone and insert.

2.4.7 Preparation of chemically competent *Agrobacterium tumefaciens*

Cells of *A. tumefaciens* strain LBA4404 were made chemically competent and transformed according to methods published on www.bioinformatics.us/methods/agrotransformationf.htm. A starter culture was prepared with appropriate antibiotics (Table 2.1). Following incubation at 30°C for 24 hours at 2.5Hz, 0.5ml was inoculated into 60ml TYNG (Appendix 1, Table A1.1) supplemented with the same antibiotics and incubated under the same conditions overnight. The culture was

transferred to ice for 10 minutes prior to centrifugation at 4000*g* for 6 minutes at 4°C. Pelleted cells were rinsed with 1ml ice cold 20mM filter sterilised $CaCl_2$ before a second centrifugation for 1 minute. Cells were resuspended in 1ml ice cold filter sterilised 20mM $CaCl_2$, aliquoted into 150µl fractions and snap frozen before storing at -80°C.

2.4.8 Transformation of *A.tumefaciens*

5µl plasmid was pipetted onto frozen cells and thawed using the warmth of the hand. The cells and added plasmid were evenly distributed by flicking 5-10 times and incubated in liquid nitrogen for 5 minutes. The cells were then thawed at RT and added to 1ml TYNG before incubating at 3.3Hz for 16 hours at room temperature. LBA4404 were liable to clumping so cells were vortexed prior to plating on TYNGA then incubated at 30°C for 96 hours. Successful transformants were identified by colony PCR (section 2.4.4)

2.4.9 Transformation of S.tuberosum L.

Explants of *S. tuberosum* L. cv. Desiree were transformed according to the methods of Visser (1991). All media used in the transformation protocol is detailed in Appendix 1, Table A1.2. Unless otherwise stated, cultures were grown at 20-22°C with a 16 hour light/8 hour dark cycle with 200µmol m^{-2} s^{-1} PAR from fluorescent tubes (Phillips TLD 36W/33).

Pre-culture

Stem segments, devoid of axillary meristems together with halved leaves were put into pre-culture on MC plates, each overlaid with 2ml M100. 20-25 explants per 90mm diameter plate were laid onto filter paper to wick M100 pre-culture media towards them and incubated in moderate light for 2 days at 25°C.

Transformation

4.5ml of a 5ml overnight starter culture of *A.tumefaciens* harbouring the desired plasmid was inoculated into 50ml of TYNG containing the appropriate antibiotics and incubated at 30°C overnight at 2.5Hz. One culture was prepared for each plate of explants. 3ml of *A.tumefaciens* culture was suspended in a total volume of 30ml MS10 to give an OD at A_{600} of 0.3. To this, 1 pre-culture plate of explants was added and incubated for 10 minutes at RT with gentle agitation every 2 minutes to ensure even distribution of culture in the inoculation media. After 10 minutes incubation, explants were briefly blotted on sterile Whatman Number 1 filter paper to remove excess inoculant before

transferring back to MC plates for incubation under light diffused using tissue paper at 25°C for 2 days.

Culture and production of transgenic callus

After 2 days on MC plates, explants were transferred to M400 plates containing 400mg l^{-1} carbenicillin to kill off uninfiltrated bacteria and incubated at 25°C for 5 days. Explants were then transferred to M400 plates containing 400mg l^{-1} carbenicillin and 50 mg l^{-1} plasmid selective antibiotic (table 2.2) and incubated under the same conditions. Explants were transferred to new M400 plates containing carbenicillin and selective antibiotic fortnightly until shoots began to develop from callus tissue.

Shoot elongation and rooting

To encourage shoot elongation, when shoots were approximately 1 to 2cm in length, callus was transferred to M13 media in 60ml Sterilin pots (Bibby Sterilin) containing the same antibiotics and cultured until the shoots reached 4-6cm. To induce roots, shoots free from callus were transferred to MS30 in 250ml Sterilin pots (Bibby Sterilin) with the same antibiotics and cultured for 4-6 weeks before harvesting tissue for subculture to MS30 containing only the selective antibiotic. Tissue was also harvested at this stage for DNA extraction (section 2.3.1.2) to confirm presence of the transgene by PCR (section 2.3.5), or for RNA extraction (section 2.3.8) for quantification of transgene expression by RNA blotting (section 2.3.11).

2.5 Protein Methods

2.5.1 Protein extraction from plant tissue

0.1-1g tissue was ground in an eppendorf tube with a pinch of acid washed sand in 500µl protein extraction buffer (Appendix 1, Table A1.4). The homogenate was centrifuged at 12000*g* at 4°C for 10 minutes to pellet insoluble matter. The supernatant was removed and protein content ascertained using BioRad Protein Assay Dye Concentrate (section 2.7.2). Protein samples were used immediately for SDS-PAGE.

2.5.2 SDS-Polyacrylamide gel electrophoresis (SDS-PAGE)

Protein samples were boiled for 5 minutes in 1x SDS-PAGE loading buffer (Appendix 1, Table A1.4) and then briefly centrifuged at 12000*g* to pellet any insoluble material. Samples were loaded onto a 12% SDS polyacrylamide gel and protein separation achieved at a constant voltage of 200 V. Following electrophoresis, gels were either stained with Coomassie blue (Appendix 1, Table A1.4)

overnight at room temperature and destained in Coomassie destain (Appendix 1, Table A1.4) at room temperature or the proteins were electro-blotted onto nitrocellulose and used to carry out western blot analysis.

2.5.3 Western blot

For western blot analysis, the proteins separated by SDS-PAGE were transferred onto a nitrocellulose membrane. The gel and nitrocellulose were pre-equilibrated in semi-dry transfer buffer (Appendix 1, Table A1.4) for 15 minutes, sheets of Whatman 3MM paper cut to size were pre-wetted in the same buffer. The gel was then placed in the Semi-Dry Transfer Blotter (Bio-Rad) in the following configuration: platinum anode; 5x pieces 3MM paper; nitrocellulose membrane; gel; 5x pieces 3MM paper; cathode. The protein was transferred using an electrical current of 15V for 45 minutes. Visualisation of the blotted protein was achieved by incubating the membrane in Ponceau Stain (Appendix 1, Table A1.4) for 5 minutes. Excess stain was rinsed off using dIH_2O. The gel was also incubated in Coomassie blue to check for total transfer.

Following confirmation of successful blotting, the membrane was washed in blocking solution of 5% (w/v) Marvel dried skimmed milk powder in PBST (Appendix 1, Table A1.4) overnight. The membrane was twice washed in PBST, 5 minutes each,then incubated for 1 hour in the required primary antibody solution (PBSTM (Appendix 1, Table A1.4) plus antibody) at a concentration of 1:10,000 unless otherwise stated. Following incubation, the membrane was washed for 15 minutes, and 4 times subsequently for 5 minutes, in PBST followed by incubation of the membrane for an hour with a horse radish peroxidise (HRP) labelled secondary antibody solution at a concentration of 1:10,000 (as above). Finally the membrane was subject to a 15 minute wash followed by four 5 minute washes in PBST before visualisation by chemiluminescence using Western Lightening Chemiluminescence Reagent Plus (PerkinElmer) according to manufacturer's instructions. If nitrocellulose membranes were to be re-probed with a second antibody, the membrane was incubated in stripping buffer (Appendix 1, Table A1.4) according to manufacturer's instructions.

2.5.4 Over-expression and purification of MBP-CKP recombinant protein

The MBP-CKP fusion protein was produced using the pMal protein fusion and purification system (NEB) and unless otherwise stated, expressed and purified according to manufacturer's instructions. A 50ml starter culture of ER2508 (table 2.1) containing pc2XCKP (table 2.2) was grown in LB containing carbenicillin at 50mg l^{-1} overnight at 37°C at 3Hz. A 500ml culture of Rich Media (RM,

Appendix 1, Table A1.1) containing 50mg l^{-1} carbenicillin was inoculated with 10ml of the starter culture and allowed to grow at 37°C for 5 hours at 3Hz. Induction of the recombinant protein was carried out by addition of 0.4mM IPTG followed by overnight incubation at 16°C and 3Hz to prevent induced protein being sequestered into exclusion bodies. Cells were harvested by centrifugation at 8000*g* for 10 minutes and resuspended in 10ml pMal column buffer (Appendix 1, Table A1.4) before snap freezing in liquid nitrogen and incubating at -80°C for 1 hour. Cells were defrosted in iced water then lysed by sonication at a wavelength of 14 microns, and the soluble fraction separated from the insoluble fraction by centrifugation at 30,000*g* for 25 minutes. MBPCKP was purified from other soluble proteins by affinity chromatography. The soluble fraction was added to a 10ml slurry of amylose which bound 3mg recombinant protein ml^{-1} and allowed to bind at 4°C overnight with gentle agitation. Following binding, the amylose was loaded onto a column, produced using substituents from the Pierce Avidin Kit (Pierce Protein Research Products, Thermo Fisher), with glass wool packed between the outlet and filter to reduce the flow rate, and washed with 5 volumes of chilled column buffer to remove any unbound and non-specifically bound protein. The fusion protein was eluted from the column by application of 1.5 column volumes of chilled pMal elution buffer (Appendix 1, Table A1.4). 1ml fractions were collected and tested for the presence of protein using BioRad Protein Dye Reagent Concentrate. Following elution, the amylose slurry was regenerated for re-use according to manufacturer's instructions. The procedure was scaled up as required.

2.5.5 Cleavage of fusion protein

All fractions showing presence of the fusion protein, by the BioRad assay were pooled and concentrated in a Vivaspin centrifugal filter device with a molecular weight cut off of 10kDa (Sartorius, Goettingen, Germany) by centrifugation at 4000*g* until the final volume was approximately 5 ml. Buffer exchange from the pMal elution buffer to Xa cleavage buffer was carried out using the same centrifugal filter device, adding Xa cleavage buffer (Appendix 1, Table A1.4) to 20ml volume and concentrating to 5ml. This was carried out 3 times to ensure buffer replacement had an efficiency >95%. The concentration of protein was determined using the BioRad assay (section 2.7.2). Cleavage of the fusion protein was carried out using Xa Cleavage factor (Novagen) at 1% (w/w) the amount of fusion protein. The reaction was mixed by pipetting and incubated at 4°C overnight.

2.5.6 Purification

2.5.6.1 Affinity chromatography

Affinity purification of StCKP1 was from the products of the cleavage reaction was carried out by adding the cleavage reaction mix to prepared amylose slurry and incubated with gentle agitation at 4°C overnight. The amylose was pelleted by centrifugation at 800*g* at 4°C for 1 minute and the supernatant containing StCKP1 carefully removed to a fresh tube. The StCKP1 fraction was concentrated to 1mg ml^{-1} for use in nucleosidase assays (section 2.7.3) using a Centricon centrifugal filter device.

2.5.6.2 Gel filtration

The StCKP1 containing protein solution purified by affinity chromatography was applied to a Superdex 200 FPLC column (GE Healthcare), pre-equilibrated with pMal column buffer. Protein was eluted on the basis of size in 2 column volumes of pMal column buffer at a flow rate of 1ml min^{-1} in 0.5ml fractions. Fractions containing StCKP1 were concentrated using a centrifugal filter device.

2.6 Extraction, purification and quantification of cytokinins

All glassware used in extraction of cytokinins was silanised by rinsing with 2% dimethyldichlorosilane solution in 1,1,1-trichloroethane (BDH) to prevent adsorption of cytokinins onto glass surfaces. Cytokinin standards were obtained from Apex Organics (Devon, UK). The protocol described is based on the extraction, purification and quantification protocols described by Collier *et al*. (2003) and Winwood(2007).

2.6.1 Extraction of cytokinins

1 g fresh weight of tissue was ground to a fine powder in a pestle and mortar pre-chilled to -20°C under liquid nitrogen. 30ml ice cold 90% (v/v) ethanol was added to the tissue along with 833Bq HPLC-purified [^{3}H]Z (specific activity 1.1 TBq $mmol^{-1}$) to enable overall cytokinin recoveries to be determined at the end of the procedure. The homogenate was extracted on ice for a period of 30 minutes, with stirring at 10 min intervals to aid the extraction process. The homogenate was then centrifuged at 800*g* at 4°C for 10 min and the supernatant poured into a silanised round-bottomed flask. To improve recoveries, the pellet was washed with a further 10 ml 90 % (v/v) ethanol, centrifuged, and the supernatant added to the first. The combined supernatants were then reduced to 5ml under rotary evaporation at 30°C.

2.6.2 Purification

2.6.2.1 Removal of phenolic compounds

1.5 g g^{-1}FM of insoluble polyvinylpolypyrrolidone (PVPP) was added to a centrifuge tube together with 20 ml of 10 mM acetic acid, pH 3.5. The tube was shaken and left for 15 min for the solution to clear. The supernatant containing fine PVPP particles was discarded and replaced with a further 20 ml of 10 mM acetic acid, shaken, and left for a further 20 min; this was repeated an additional three times. Once the final 20 ml of acetic acid had been discarded, the extract was added to the tube. The mixture was then placed on an orbital shaker at 0.8-1.0 Hz for 30 min. The mixture was centrifuged at 4000*g* at 4 °C for 30 min and the supernatant reserved (first supernatant). The pellet was washed with 20 ml of 10 mM acetic acid, shaken for 20 min on an orbital shaker and centrifuged as before. After centrifugation, the wash supernatant was added to the first supernatant, poured into a silanised round-bottomed flask and reduced to 200 μl under rotary evaporation at 35 °C. The extract was then re-suspended in 1 ml of H_2O.

2.6.2.2 Sep-Pak purification

A C_{18} Sep-Pak cartridge (Waters, Millipore, Billerica, MA, USA) was activated by passing 10 ml of ice-cold methanol at 10ml min^{-1} through it followed by 10 ml of 10 mM triethylammonium acetate (TEAA), pH 7.4. The extract was applied to the column and washed through with a further 10 ml of 10 mM TEAA. Cytokinins were eluted with 10 ml 50 % (v/v) methanol/ H_2O into a silanised round-bottomed flask. The partially purified extract was then reduced to a volume of 500 μl under rotary evaporation at 30°C and re-suspended to a final volume of 1ml using HPLC grade H_2O.

2.6.3 Separation of cytokinins

2.6.3.1 High pressure liquid chromatography (HPLC)

The HPLC system consisted of a Spectraphysics SP8750 pump linked to a SP8700 solvent delivery system. UV-absorbing substances were detected using an LC871 UV-VIS detector set at 254 nm. Samples were loaded using a manual injection port with 1 ml sample loop. A 15 cm, 4.6 mm i.d., column of 5 μm octadecylsilica (Varian Microsorb 100) was used, together with a C_{18} guard column, in order to separate cytokinins on the basis of their polarity. Chromatograms were analysed using Chrom Perfect Chromatography Data System (Justice Laboratory Software, Fife, UK).

A methanol gradient based on that used by Turnbull and Hanke (1985b) was used to separate the isoprenoid cytokinins with a flow rate of 1ml min^{-1}. Solvents used were as follows: Cytokinin

separation A. 10% Methanol, 4.6ml glacial acetic acid, pH 3.6 with Triethylamine (TEA), B. 80% Methanol, 6ml glacial acetic acid, C. 100% Methanol (figure 4.5). For adenine separation, solvent A was replaced with one containing 5% Methanol, 4.6ml glacial acetic acid, 200mM ammonium acetate, 0.5ml TEAA and adjusted to pH 5 (section 5.4.2 & figure 5.11) All solvents used were of HPLC grade, diluted with dIH_2O and degassed with helium at a flow rate of 1ml min^{-1}. Before the extract was applied to the column, a solution of cytokinin standards, 500pmol each, was applied to the column.

500µl of purified extract diluted in 500µl HPLC grade water was loaded into the sample loop using a blunt ended needle. If required, 1ml fractions were collected for the duration of the gradient and dried to remove all solvents using a Univap centrifugal evaporator and refrigerated solvent trap (Uniscience, UK) at a temperature less than 40°C. The dried fraction was resuspended in 1ml HPLC grade water and stored at 4°C prior to quantification by ELISA (section 2.7.1).

2.6.3.2 Tandem liquid chromatography - mass spectrometry (LC-MS-MS)

LC-MS-MS was carried out in collaboration with Dr. Colin Turnbull, Imperial College. LC-MS-MS analyses were performed largely as described by Morris et al. (Morris et al., 2001). Samples analysed by LC-MS-MS were initially filtered through a nylon membrane with a pore size of 0.2µm then taken to dryness using a Univap centrifugal evaporator connected to a refrigerated solvent trap. Samples were resuspended in 10µl HPLC grade acetonitrile then diluted with 190µl 10mM ammonium acetate pH 3.4. To each sample the following [2H]-labeled cytokinin internal standards were added: $[^2H_5]$Z, $[^2H_5]$[9R]Z, $[^2H_3]$dihydrozeatin ($[^2H_3]$DHZ), $[^2H_3]$[9R]DHZ, $[^2H_6]$iP, $[^2H_6]$isopentenyl adenosine-9-glucoside, $[^2H_6]$[9R]iP, and $[^2H_3]$[9G]DHZ (OlChemIM, Olomouc, Czech Republic). Cytokinins were chromatograpically separated using gradient of acetonitrile in 10mM ammonium acetate, pH 3.4, initially running isocratically at 5% solvent for 4 minutes, rising to 14% solvent at 20 minutes and 32% solvent at 35 minutes with a flow rate of 200µl min^{-1}. A Phenomenex 3µm C18 Luna 100 x 2mm column on an Agilent 1100 Binary LC system, coupled to an Applied Biosystems Q-Trap hybrid mass spectrometer fitted with a TurboIonspray (electrospray) source operating in positive ion multiple reaction monitoring mode was used. Dwell time was 30ms for each MS-MS ion pair.

2.6.4 Recovery analysis

In order to quantify recovery of cytokinin from the purification procedure described, the proportion of added $[^3H]$Z recovered from the extract was determined by liquid scintillation counting. 1ml

Optiphase-Hisafe 3 liquid scintillation cocktail (Perkin Elmer) was added to 50µl of purified extract or to 50µl resuspended fractionated extract. Samples were mixed by vortexing and counted for 20 minutes in a Tri-Carb 2100TR Liquid Scintillation Analyzer (Packard, GMI, Ramsey, MN, USA).

2.6.4.1Re-purification of tritiated zeatin

Tritiated compounds at high specific activity stored in solution are sensitive to decomposition. Self-decomposition can be accelerated by the effect of molecular clustering on storage of frozen solutions. Some tritiated compounds are prone to gradual loss of the label as tritiated water by exchange with the aqueous solution. For these reasons, the [^{3}H]Z and [^{3}H]iP stocks were re-purified and the specific radioactivity checked at three-monthly intervals.

For purification, 20 µl of [^{3}H]Z stock (approximately 3 x 10^5 Bq) was added to 1 ml of H_2O. 900µl of this solution was applied to the HPLC column in a 50 min methanol gradient at a flow rate of 1 ml min^{-1} and thirty 1 ml fractions were collected. The retention time of the zeatin fraction was determined using a prior run with a standard solution, and the radioactivity in the zeatin fraction was measured by liquid scintillation counting (section 2.6.4.). The remaining fractions, which contained any dissociated radioactivity, were discarded. The purified stock was diluted to 830 Bq per 50 µl and stored at 4 °C. The chemical concentration was estimated from the extinction coefficient and specific radioactivity calculated.

2.7 Assays

2.7.1 Competitive Enzyme Linked Immunosorbance Assay (ELISA)

The protocol was based on that described by Strnad *et al.* (1992), which can be used to detect ribotides, ribosides, free bases and 9-glucosides. For all cytokinin antisera, the 'whole serum' was used and for one Maxisorp F96 immunoplate (Nunc, Roskilde, Denmark), 1 µl of antiserum diluted in 15 ml of 50 mM sodium bicarbonate, pH 9.6, was required. 150µl of the solution was added to each well - except wells 1A and 1B, which were used as reagent blanks. The plates were incubated overnight at 4 °C to allow the protein to bind the surface of the wells.

Following incubation, the plates were washed three times with TBS+T (Appendix 1, Table A1.5.). In order to block any vacant protein-binding sites, 200 µl of 0.02 % BSA in TBS (Appendix 1, Table A1.5.) was added to each well. The plates were then incubated at 4 °C for 1 hour and washed three times with TBS+T.

To each well: 50µl of TBS, 50µl of a cytokinin riboside standard, or 50µl of a sample fraction, together with 50µl of tracer were then added, including wells 1A and 1B. Each was prepared in duplicate. The tracer was a solution of alkaline phosphatase-linked cytokinin (section 2.7.1.1). A single plate required 1 µl of stock tracer diluted in 5 ml of 0.02% BSA in TBS. The plates were then incubated at room temperature for 1 hour for the binding reaction to approach equilibrium. After this time, the plates were washed three times with TBS+T.

The amount of bound tracer was quantified by the addition of 150 µl of *para*-nitrophenylphosphate (PNPP) solution to each well (1 mg ml^{-1} in 50 mM $NaHCO_3$, pH 9.6). The absorbance of the product was measured at 405 nm using a Titretek Multiscan PLUS MK11 plate reader (ICN). The amount of cytokinin in each well was calculated from the standard curve produced for each plate by the Deltasoft programme (BioMetallics Inc., New Jersey, USA). Values were background corrected and, for each sample, the calculated values for all non-cytokinin fractions (determined by retention time) were averaged and this average was subtracted from the calculated values for each cytokinin-containing well. The background-corrected values were adjusted for recovery based on the percentage of [^{3}H]Z remaining at the end of the procedure (section 2.6.4). Data presented in this thesis have not been adjusted for differences in cross-reactivity of the antisera for free bases, ribosides and ribotides and results are therefore presented as riboside equivalents (for cross-reactivities see Table 2.8.).

2.7.1.1 Preparation of cytokinin-alkaline phosphatase tracers

The protocol for the conjugation of cytokinins to alkaline phosphatase (AP) was based on Erlanger and Beiser (Erlanger and Beiser, 1964). 0.7mg of cytokinin riboside was dissolved in 50µl of dimethylformamide in a screw-cap eppendorf tube covered with aluminium foil and 150 µl of H_2O added. 200µl of $NaIO_4$(10.7 mg/5 ml H_2O) was added in 10µl aliquots in order to oxidise the ribose moiety. The tube was shaken at approximately 0.04 Hz for 8 min, and the reaction then stopped by the addition of 10µl of ethanediol to inactivate the remaining periodate.

The tube was again shaken for 5 minutes and the solution divided in half. Half was coupled to AP for use in the ELISA, and the other half was coupled to BSA to allow the coupling reaction to be monitored. One half of the solution was added to an eppendorf tube covered in aluminium foil containing 1 mg of BSA in 200µl of 10 mM Na_3BO_3, pH 9.4. The other half was added to an eppendorf tube covered in aluminium foil containing 1 mg of CIAP in 200µl of 10mM Na_3BO_3, pH 9.4. The tubes were shaken for 1 hour at 4 °C. 30µl of $NaCNBH_4$ solution (3.14 mg $NaCNBH_4$/1 ml H_2O) was then

added to stabilise the bond formed between the cytokinin and the amino group of the enzyme. The tubes were shaken for a further 1 hour, and a further 20µl of $NaCNBH_4$ solution added.

The solutions were then transferred to individual 500µl micro-dialysers and dialysed in 1l of chilled TBS, pH 7.4 at 4 °C for 48 h, to remove substances of low molecular weight. The TBS was changed every 12 hours and was stirred continuously. After dialysis, the volume of each of the solutions was determined and an equal volume of 0.1% BSA in TBS added. An amount of glycerol equivalent to the volume of the combined solutions was also added to each solution. The conjugates were snap frozen in liquid nitrogen and stored at -20 °C in 200µl aliquots. Conjugation of the cytokinin and BSA was confirmed by UV-VIS spectrophotometry, scanning from 310 to 210nm, and the CIAP conjugates were tested in standard ELISAs.

The alkaline phosphatase tracers used in this study were made by several people in the laboratory over the course of this study: [9R]iP (J. Bromley), [9R]Z & [9R]DZ (J. Winwood).

2.7.2 Bradford assay

Determination of protein concentration was carried out using BioRad protein reagent, based on that of Bradford (Bradford, 1976), according to the manufacturer's instructions. Calibration of the assay was achieved by the use of protein concentration standards using BSA diluted in the appropriate extraction or elution buffer.

2.7.3 Nucleosidase assay

An assay for nucleosidase activity was developed based on the methods of Chaudhary *et al*. (2006) and Kicska *et al*. (2002) and Moshides (1988). A stock reaction mix containing a final concentration of: 50mM HEPES buffer, pH 5.2; 1mM $MgCl_2$; 4mM phosphate donor of either D-Ribose 1-phosphate Bis(cyclohexylamine) (R 1-P) or K_2HPO_4; 30mM NaF, a known phosphatase inhibitor; 0.5mg ml^{-1} BSA

Table 2.8 Cross reactivities of isoprenoid cytokinins with ELISA antisera.
Values are percentage ratios of molar concentrations of cytokinins required for 50% inhibition of tracer binding. The midpoint concentration for each cytokinin is relative to the midpoint concentration of the competitor, which is assigned the value of 100. '-' means no detectable cross reactivity. From Dent (1996).

Cytokinin	Antibody against		
	[9R]iP	[9R]Z	[9R]DZ
[9R-MP]iP	61.0 ± 12.6	1.6 ± 0.1	0.8 ± 0.1
[9R]iP	100	3.0 ± 1.7	1.4 ± 0.5
iP	38.3 ± 12.8	0.7 ± 0.3	0.8 ± 0.1
[9G]iP	46.2 ± 4.8	1.3 ± 0.2	1.0 ± 0.2
[9R](OG)iP	-	-	-
(OG)iP	-	-	-
[9R-MP]Z	0.5 ± 0.2	66.3 ± 1.7	2.0 ± 0.4
[9R]Z	0.5 ± 0.1	100	2.9 ± 2.1
Z	0.3 ± 0.1	44.6 ± 2.1	2.3 ± 0.6
[9G]Z	0.5 ± 0.003	65.9 ± 6.9	1.3 ± 0.01
[9R](OG)Z	-	0.467 ± 0.07	-
(OG)Z	-	-	-
[9R-MP]DHZ	0.1 ± 0.002	1.3 ± 0.1	61.5 ± 4.0
[9R]DHZ	0.2 ± 0.04	0.8 ± 0.3	100
DHZ	<0.5	0.8 ± 0.1	67.2 ± 162
[9G]DHZ	0.1 ± 0.03	1.0 ± 0.5	83.9 ± 3.5
[9R](OG)DHZ	-	-	-
(OG)DHZ	-	-	-

was used and warmed to 30°C before adding cytokinin or adenine derivative, 10µg extracted protein and HPLC grade water to a volume of 50µl. For HPLC (section 2.6.3.1) or LC-MS-MS (section 2.6.3.2) analysis, the reaction was incubated at 30°C then stopped after the required time by adding 250µl 95% (v/v) ethanol. Before injection, the products were filtered using a syringe filtered through a 0.2µm pore nylon membrane (Chromacol, Welwyn Garden City, UK) and diluted in HPLC grade water to a lower percentage (v/v) solvent than initially used in separation. For the continuous assay, carried out using a BioTek Powerwave XS microplate spectrophotometer (BioTek, Winooski, VT, USA) monitoring each well at 285nm at 5 second intervals, the reaction was allowed to proceed to completion at 30°C over a 20 minute period.

2.7.4 Fluorometric Assay of Plants Expressing GUS

The fluorometric visualisation of plants expressing the *uidA* reporter gene, encoding β-glucuronidase (GUS), was carried out according to Jefferson *et al.* (1987). Plant tissue was homogenised in extraction buffer (Appendix 1) and the insoluble fraction was pellet by centrifugation at 12,000*g* at 4°C for 5 minutes. The supernatant was retained and assayed for protein concentration using BioRad reagent (2.7.2.). Plant extracts were all normalised to protein concentrations of 0.1mg ml^{-1}. The expression levels of the genes of interest were determined by assaying the fluorescence produced from the conversion of 4-methylumbelliferyl β-D-glucuronide (MUG) to methylumbelliferone (MU), catalysed by GUS. The fluorescence was measured with excitation at 385nm and emission at 448nm in a 96-well microtitre plates using a BioTek Powerwave XS plate reader. A range of different concentrations of MU in extraction buffer were used to produce a standard curve and the reaction was stopped using MUG stop buffer (Appendix 1, Table A1.4.). The time points taken during the assay varied with the different promoters used. Triplicate tissue samples were taken from each plant and assayed further in duplicate.

2.7.5 Histochemical Assay of Plants Expressing GUS

The colorimetric visualisation of plants expressing the *uidA* reporter gene, encoding β-glucuronidase, was carried out according to Jefferson *et al.* (1987) .Plant samples were harvested and subjected to vacuum infiltration in the staining solution (Appendix 1). The tissue was incubated for 24 to 48 hours in the dark at 37°C. Tissue fixation was carried out by removing the staining solution, and incubating in 5% (v/v) formaldehyde, 5% (v/v) acetic acid and 20% (v/v) ethanol for 10 minutes, and finally washing the tissue in 50% (v/v) ethanol for 5 minutes. Removal of chlorophyll, if necessary was achieved by incubating the tissue in several changes of absolute ethanol at 65°C.

Chapter 3

Analysis of stolon tip cytokinin and StCKP1 localisation

3.1 Introduction

Much work has been undertaken to determine the role of cytokinin in potato tuberisation. Many studies have focused upon measuring cytokinin levels prior to tuberisation in order to determine whether increased cytokinin concentrations trigger tuberisation (Koda, 1982a; Turnbull, 1982; Jameson et al., 1985; Turnbull and Hanke, 1985b; Vreugdenhil and Struik, 1989). Mauk and Langille (1978) proposed [9R]Z to be the stimulus required to promote tuber formation. Studies of the levels of different cytokinins in stolon tips indicate that [9R]Z is the predominant cytokinin species. However, results obtained indicate that [9R]Z levels increase after tuberisation and are not involved in triggering of tuberisation. This information, together with the finding of Turnbull and Hanke (Turnbull and Hanke, 1985b) that stolons have periods of heightened sensitivity to applied cytokinins indicates that an increase in sensitivity of the tissue to active cytokinins rather than an increase in cytokinin itself seems the likely trigger for spontaneous tuberisation. Turnbull (1982) proposed that spontaneous tuberisation of stolon tips in June, having been stored in darkness at 10°C for a period of nine months, is due to cytokinin hypersensitivity. This hypersensitivity could be due to increased receptor activity or an increase in processing of cytokinins to their active form, thus not changing the total tissue cytokinin content but increasing the proportion of active cytokinin.

Thomson (1994) monitored cytokinin binding activity of stolon tips at different stages of development to find a 37kDa protein that was upregulated in stolons immediately prior to spontaneous tuberisation. This protein was found to have a K_D of 1.7µM for [9R]Z, and its upregulation was found to result in an eight-fold increase in cytokinin binding activity of this tissue. This figure for cytokinin affinity was found to be of the same order of magnitude as for high-affinity binding sites found in maize and corn shoot. A protein of the same size was purified by [9R]Z linked affinity chromatography (James, pers. comm.) and a partial amino acid sequence determined.

StCKP1, a putative cytokinin binding protein, was purified from incipiently tuberising potato stolon tips and its full length sequence comprising coding region, 5′ and 3′ untranslated regions and two putative promoter regions (designated pro1 and pro2) were determined by Warnes (2005) (figure 3.1, 3.9 and 3.10). The aim of this study was to characterise the localisation of StCKP1 to relate to its putative role in tuberisation of stolon tips of *Solanum tuberosum* L. cv. Desiree.

The two promoter regions isolated by Warnes (2005) were found to contain a number of potential transcription factor binding sites by use of the PATCH and PLACE databases. The promoters pro1 and pro2 were found to contain 11 sequences recognised in other light regulated promoters including

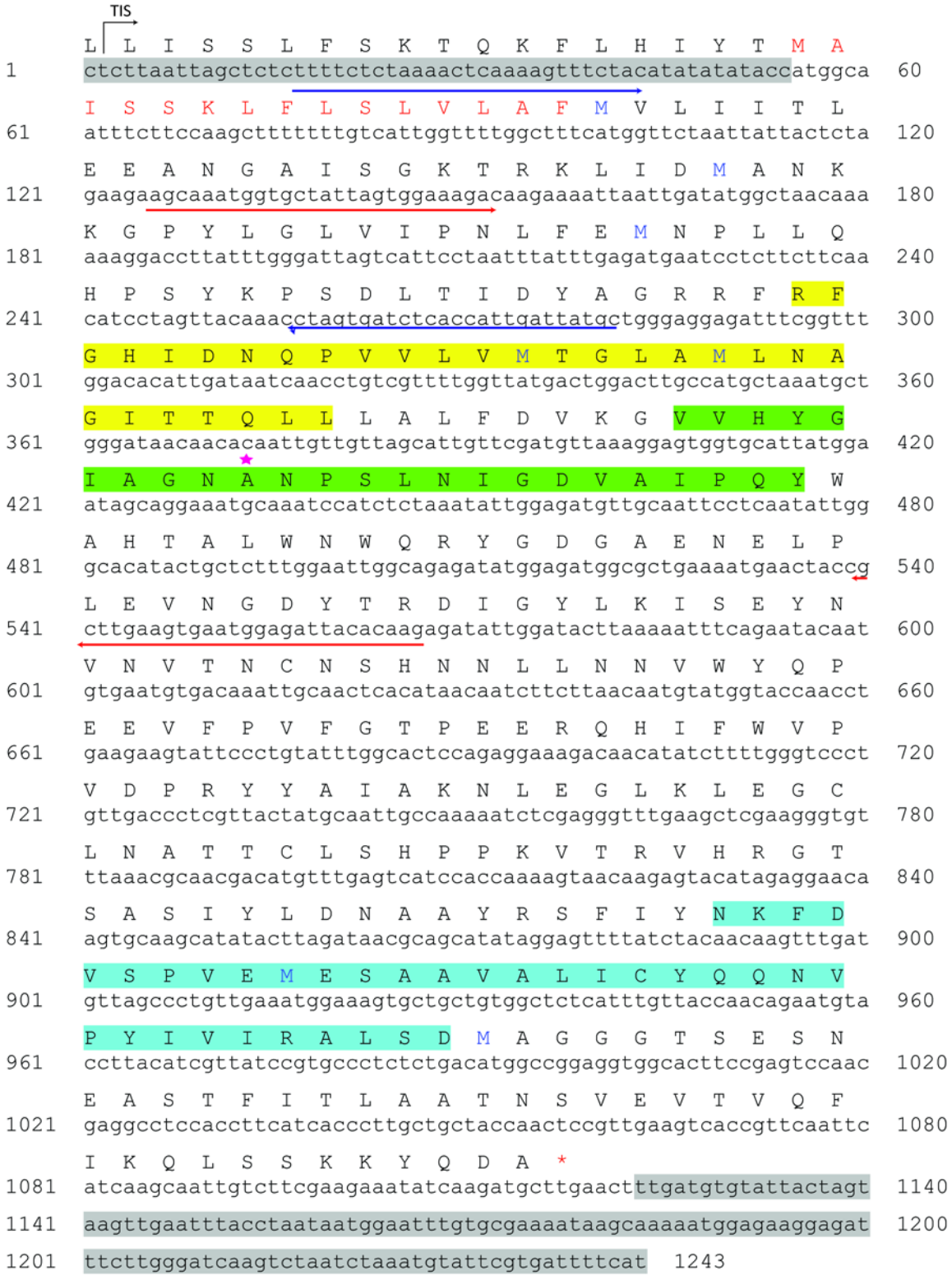

Figure 3.1 Nucleotide sequence of StCKP1 cDNA and putative amino acid sequence of StCKP1
Bases are numbered from the start of the cDNA sequence, amino acids (above nucleotide sequence) are not numbered, internal methionine residues are in blue type. 5' and 3' untranslated regions are highlighted in grey. Amino acids comprising motifs I (yellow) II (green) and III (blue) are highlighted, the position of the alanine residue is marked with ★. The predicted signal sequence is depicted in red. Primer binding sites are marked with arrows: blue - C1F/R, red - C2F/R. TIS=transcription initiation site.

GT-2, CCA1 and GT1-b, and consensus sequences found in many light-regulated genes (Terzaghi and Cashmore, 1995), suggesting transcription of *StCKP1* may be regulated by light. This is unsurprising as if StCKP1 does indeed play a role in tuberisation and dormancy as has been predicted (Thomson, 1994; Warnes, 2005), it is known that tuberisation of *S.tuberosum* L. is regulated by photoperiod, particularly phytochrome B (Martinez-Garcia et al., 2002; Rodriguez-Falcon et al., 2006). The two putative promoter regions identified also contained sequences found in the promoters of gibberellin, auxin, ABA and cytokinin-induced genes. If StCKP1 plays a role in tuberisation and dormancy, the presence of these cis-elements is consistent with a role in mobilisation of starch to end the dormant period and promote tuber sprouting as, for example, gibberellins induce expression of hydrolytic enzymes which are capable of degrading starch and storage proteins to a mobile form fuelling growth of embryos (Sun and Gubler, 2004). Auxin and ABA responsive motifs were found in both pro1 and pro2, notably cis-elements found in ABI3, FUS3 and VP1 which are thought to be key ABA-responsive regulators of genes during seed development, consistent with the proposed role of StCKP1 in tuberisation of stolon tips and the release of dormancy. The PLACE search identified six ARR1 binding sites in each of pro1 and pro2. ARR1 is a known type-B cytokinin response regulator, itself directly activated by those of the type-A class. Multiple copies of the ARR1 target sequence in both pro1 and pro2 indicate the likely regulation of StCKP1 expression by ARR1 and so plant responses to cytokinin. This would fit with the findings of Turnbull (1982) that, depending on the stage of development, the application of cytokinin to a dormant tuber is sufficient to break dormancy, and that exogenous cytokinin treatment of stolon tips can induce tuberisation (Palmer and Smith, 1969).

It has previously been shown that *StCKP1* transcript is present in cytokinin-responsive tissues, particularly the shoot apex, root and stolon tips in *Solanum tuberosum* L. cv. Majestic (Warnes, 2005). As StCKP1 was originally isolated from stolon tips (James, pers. comm.), and the cytokinin-binding activity of an extract of protein from potato stolon tips was shown to increase by eight times prior to tuberisation (Thomson, 1994), it was decided to further investigate the localisation of StCKP1 to tuber tissues and in stolon tips progressing towards tuberisation, and the cytokinin content of these stolon tips, to look for a correlation between cytokinin and StCKP1 abundance.

3.2 Cytokinin content of potato stolon tips

Cytokinins were extracted from 2g FM stolon tips at three defined stages of tuberisation (Viola et al., 2001) termed: before tuberisation, incipiently tuberised and. Stolon tips had been produced in a bag system (Turnbull, 1982; Thomson, 1994; Warnes, 2005), harvested at the appropriate time and

frozen at -80°C prior to use (section 2.2.1.3). The protocol previously described (section 2.6) was used to extract, purify and calculate recovery of cytokinins. Following purification, the sample was resuspended in a final volume of 1.5ml of which 500µl was separated using HPLC (section 2.6.3.1) over a methanol gradient of 35 minutes with a flow rate of 1ml min^{-1} (figure 4.5). 36 x 1ml fractions were collected, taken to dryness and resuspended in 1ml dIH_2O. 50µl of each resuspended fraction was added to 1ml Optiphase-Hisafe 3 liquid scintillation cocktail and scintillation counted for 20 minutes to estimate recovery after purification.

Cytokinin content of each of the fractions was determined by ELISA using a protocol adapted from Strnad (1992) as previously described (section 2.7.1). 3 microtitre plates were set up to quantify cytokinin content of each sample, one with each of anti-[9R]iP, anti-[9R]Z and anti-[9R]DZ bound. To each plate, a set of appropriate standards: 6250, 3125, 1562, 780, 390, 195, 97.5, 48.8, 24.4 & 12.2 fmol, was included for quantification (figure 3.2). 50µl each sample or standard was added to each well together with 50µl diluted cytokinin-linked alkaline phosphatase and 50µl TBS and allowed to equilibrate before assaying for alkaline phosphatase activity, thus the greater the alkaline phosphatase activity, the less cytokinin in the sample loaded. Plates were incubated for between 30 minutes and 3 hours depending on signal strength, and read at 405nm. The amount of cytokinin in each well was calculated from the standard curve produced for each plate by the Deltasoft programme (BioMetallics Inc., New Jersey, USA). For each sample values were background corrected as follows. The calculated values for all non-cytokinin fractions as determined by retention time of the twelve cytokinin standards (1µM each zeatin (Z), zeatin riboside ([9R]Z), zeatin ribotide ([9R-MP]Z), zeatin 9-glucoside ([9G]Z), dihydrozeatin (DZ), dihydrozeatin riboside ([9R]DZ), dihydrozeatin ribotide ([9R-MP]DZ), dihydrozeatin 9-glucoside ([9G]DZ), isopentenyladenine (iP), isopentenyladenosine ([9R]iP), isopentenyladenosine 5'-monophosphate ([9R-MP]iP), and isopentenyladenine 9-glucoside ([9G]iP))(figure 4.5) were averaged and this average was subtracted from the calculated values for each cytokinin-containing well. The background-corrected values were adjusted for recovery based on the percentage of [^{3}H]Z remaining at the end of the procedure (section 2.6.4). As one cytokinin may have spanned two fractions, integration was carried out to determine peak area and thus cytokinin content. An extraction was made from three different harvests of stolon tips for each tuberisation stage studied, the data collected from each set of replicates averaged, and standard error calculated. Results presented are as riboside equivalents.

An increase in cytokinin content was observed as tuberisation progressed from untuberised stolon tips to those that have undergone tuberisation. This finding is in line with previous observations that

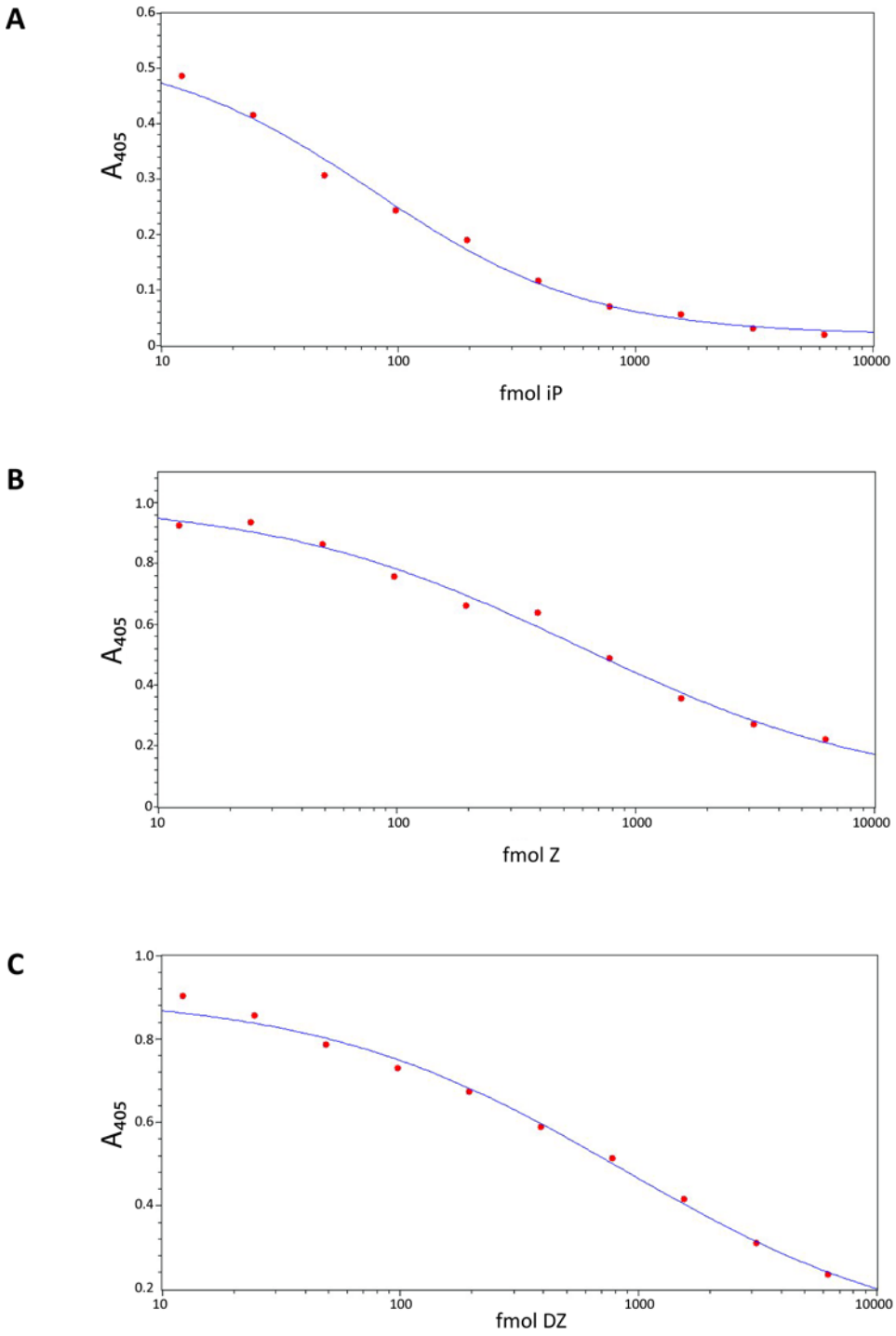

Figure 3.2 Standard curves produced for quantification of cytokinins by HPLC-ELISA
50µl cytokinin standard plus 50µl cytokinin linked alkaline phosphatase tracer were added to each well plus 50µl TBS. Cytokinins were allowed to competitively bind to the antibody coating the plate wall for 1 hour before washing and adding 150µl PNPP tracer solution, a substrate for alkaline phosphatase which cleaves PNPP to produce a soluble yellow product which was quantified by absorbance at 405nm. **A.** Isopentenyladenine standards. **B.** Zeatin standards. **C.** Dihydrozeatin standards.

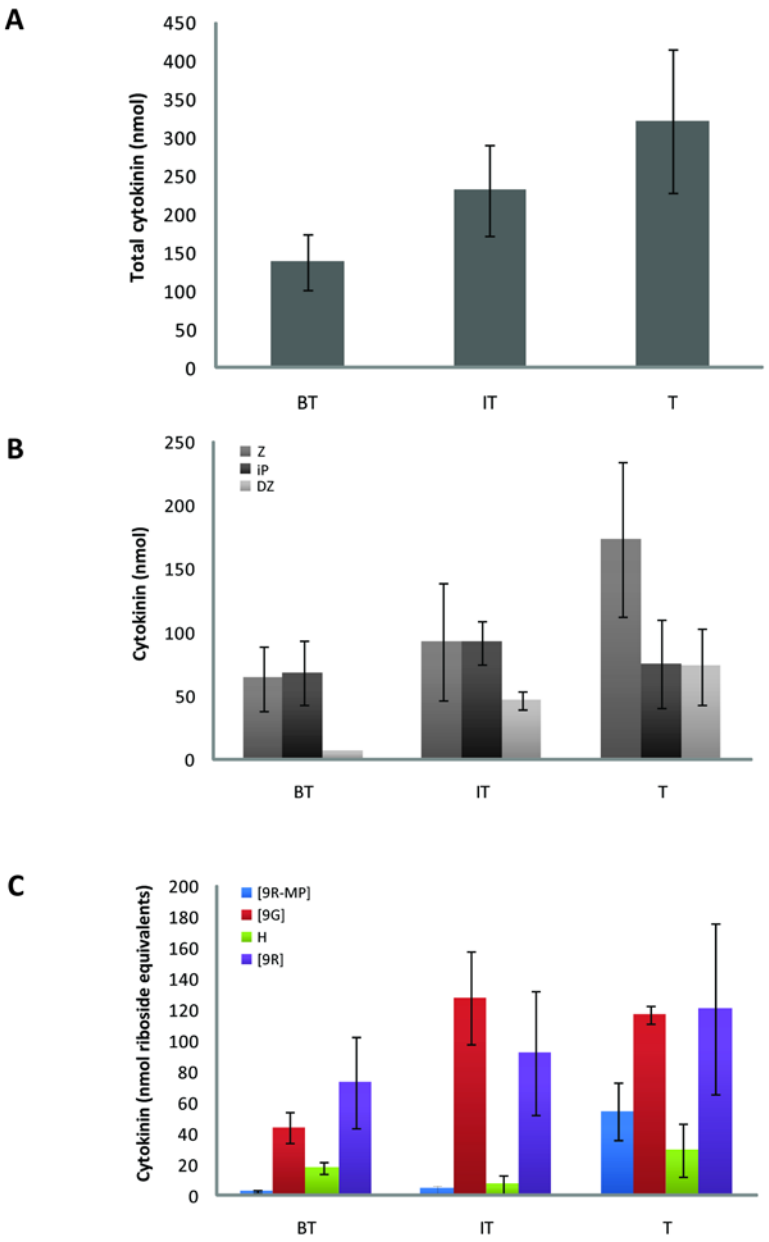

Figure 3.3 Cytokinin content of stolon tips progressing through tuberisation

Tuberisation stages analysed are defined as: BT=Before tuberisation, IT=Incipient tuberisation, T=Tuberised. **A.** Total cytokinin content.. **B**. Total cytokinin by N^6 substituent. **C.** Total cytokinin by N^9 conjugate. Data are means of duplicate assays on three HPLC analyses of each of three samples extracted from approximately 1g stolon tips ±SE. Values are corrected for background and recovery, but not for cross-reactivity

endogenous cytokinin is higher after tuberisation (Mauk and Langille, 1978; Turnbull and Hanke, 1985b). This increase is seen to progress steadily as the putative signal for tuberisation is received in incipiently tuberising stolon tips, an observation which has previously been reported by Sattlemacher and Marschner (1978) which the authors correlated with a shift in the pattern of cell division and regulation of carbohydrate storage in the forming tuber (figure 3.3a).

Analysis of cytokinin type, as determined by the N^6 conjugate, indicates that zeatin and isopentenyladenine type cytokinins predominate in stolon tissue before the stolon is fully tuberised, however once tuberised, zeatin types come to dominate (figure 3.3b). Quantities of dihydrozeatin type cytokinins were found to increase as stolons progressed throughout the process of tuberisation, although as dihydrozeatin types are generally considered inactive, or to have a low activity (Mok and Mok, 2001), the significance of this observation it is not clear. In concert with the observations of Mauk and Langille (1978), cytokinin ribosides were found to be the dominant active cytokinin, particularly zeatin riboside (figure 3.4). Inactive N^9 glucoside conjugates were also found in similar abundance to cytokinin ribosides increasing as the postulated signal for tuberisation is received in incipiently tuberising stolons and remaining at this level once tuberised (figure 3.3c). This is in line with the finding reported by Van Staden and Dimalla (1978) that zeatin glucoside content of potato tubers increase upon entering dormancy. This could indicate stolon tissue undergoes a process of cytokinin sequestration as tuberisation proceeds in order to facilitate entry to the dormant state, although there are no known plant enzymes that hydrolyse cytokinin N-glucosides to release the active free base. However, it is known that the hydrolysis of cytokinin O-glucosides is involved in the breaking of dormancy and apical growth in potato tubers (Van Staden and Dimalla, 1978) and so inactivation and sequestration of cytokinins by N-glycosylation for release on dormancy break is not an unlikely mechanism. This shift in cytokinin spectrum from untuberised stolons to those that are considered to have tuberised could signify that it is not an increase in cytokinins in general that regulate tuberisation and more notably dormancy, but an increase in a certain fraction of cytokinin conjugates that is important.

In order to determine if the changes in cytokinin abundance seen were due to changes in expression of cytokinin biosynthetic enzymes, notably isopentenyltransferases, it was decided to probe RNA blots used in determination of *StCKP1* expression (section 3.3.1) with radio-labelled probes raised to fragments of potato isopentenyltransferases (IPTs). To determine the sequence required, a BLASTn search was carried out using the Sol Genomics Network (SGN) EST database with the DNA sequence of the Arabidopsis isopentenyltransferase3 (IPT3). This search identified a unigene build, SGN-U292623 of 656bp which had high sequence homology to the *AtIPT3* sequence, an IPT functional in

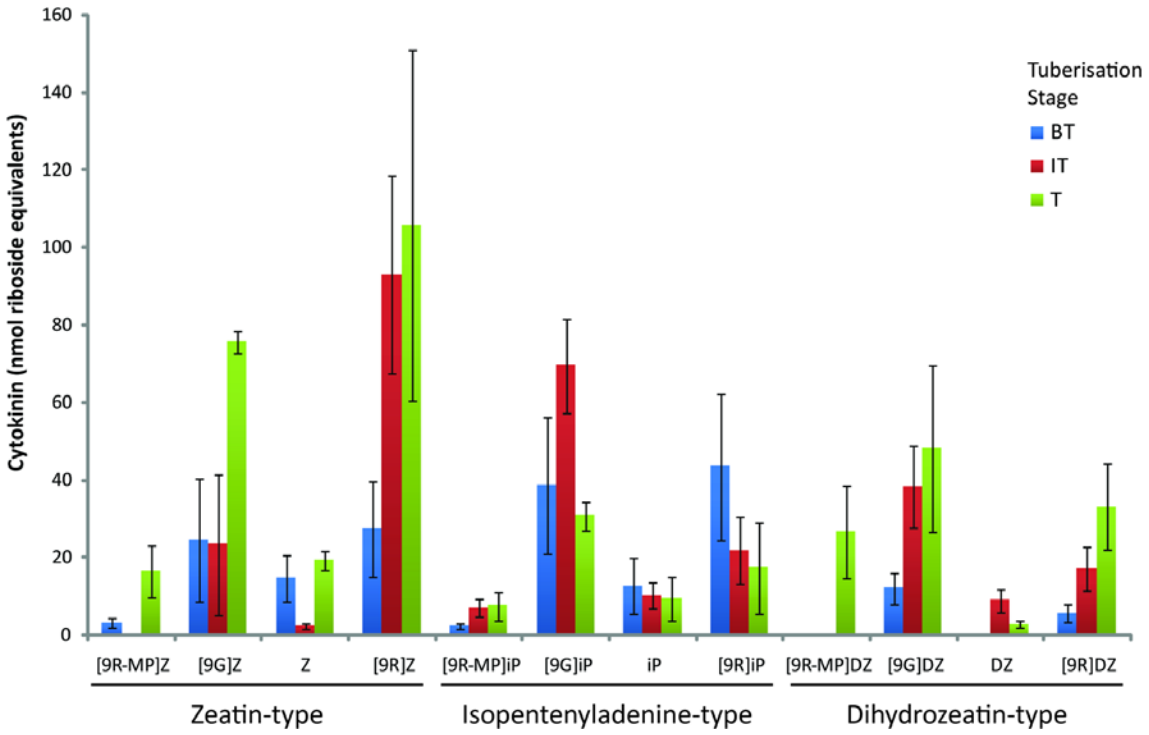

Figure 3.4 Total cytokinin content by N^6 substituent (Z, iP, DZ) and N^9 conjugate ([9R-MP]CK, [9G]CK, H-CK and [9R]CK)

Data are means of duplicate assays on 3 HPLC-ELISA analyses of 3 samples of approximately 2g stolon tips ±SE. Values are corrected for background and recovery, but not for cross-reactivity.

the shoot vasculature. SGN-U292623 was found to be a member of the SGN 102000 unigene family which allowed identification of a further three candidate potato isopentenyltransferase unigene builds. Of these SGN-U277317 was found to share homology with *AtIPT9*, a tRNA IPT(Miyawaki et al., 2004). The remaining two were found to be more closely related to the Arabidopsis shikimate kinase, a phosphotransferase involved in phenylalanine, tyrosine and tryptophan biosynthesis (Herrmann and Weaver, 1999)(figure 3.5). Primers were designed to a 380bp fragment of SGN-U292623 (U292623F and U292623R, table 2.3) and a DNA probe amplified by PCR. Probes were labelled with [α-^{32}P]dCTP as previously described (section 2.3.12) and abundance of transcripts was quantified by hybridisation of these DNA probes to 10µg extracted RNA immobilised on a nylon membrane, and normalised relative to abundance of 18S rRNA. Attempts were made to amplify a DNA probe from SGN-U277317 however these were unsuccessful.

As figure 3.5 shows, no significant difference was found in transcript abundance for either of the putative IPTs as tuberisation progressed. This indicates that there may be no change in cytokinin biosynthetic activity. However, to date seven IPTs: IPT1 and 3 to 8, have been identified as functioning via the DMAPP/HMBDP biosynthetic pathway, and 2 via the tRNA biosynthetic pathway: IPT2 and 9 (Miyawaki et al., 2006). It may be that different isopentenyl transferases are dominant in cytokinin biosynthesis in potato by comparison with roles known in Arabidopsis where AtIPT3 predominates in shoot cytokinin biosynthesis throughout development. Alternatively, import of cytokinin from elsewhere, such as root tissue may be a key source. There may also be a degree of post-transcriptional or -translational modification of IPTs which alters their biosynthetic activity during development.

3.3 Analysis of StCKP1 abundance

3.3.1 Transcript

In this study, the abundance of transcript in the tissues of the tuber at different stages of development, in which StCKP1 is thought to influence the break of dormancy, was examined for the first time. Total RNA was extracted from tissues as previously described (section 2.3.8). These included the cortex, periderm and buds of *S. tuberosum* L. cv. Desiree tubers in both the dormant and non-dormant state, and from stolon tips at three defined stages of tuberisation (Viola et al., 2001), termed: before tuberisation (BT), incipiently tuberised (IT) and tuberised (T). Primers designed by Warnes (2005) to sequenced regions of *StCKP1* which shared 100% homology with EST sequences within the database were used in RT-PCR to measure transcript abundance in the mature tuber whilst dormant, and after dormancy had been broken. 2µg of total RNA was used to produce

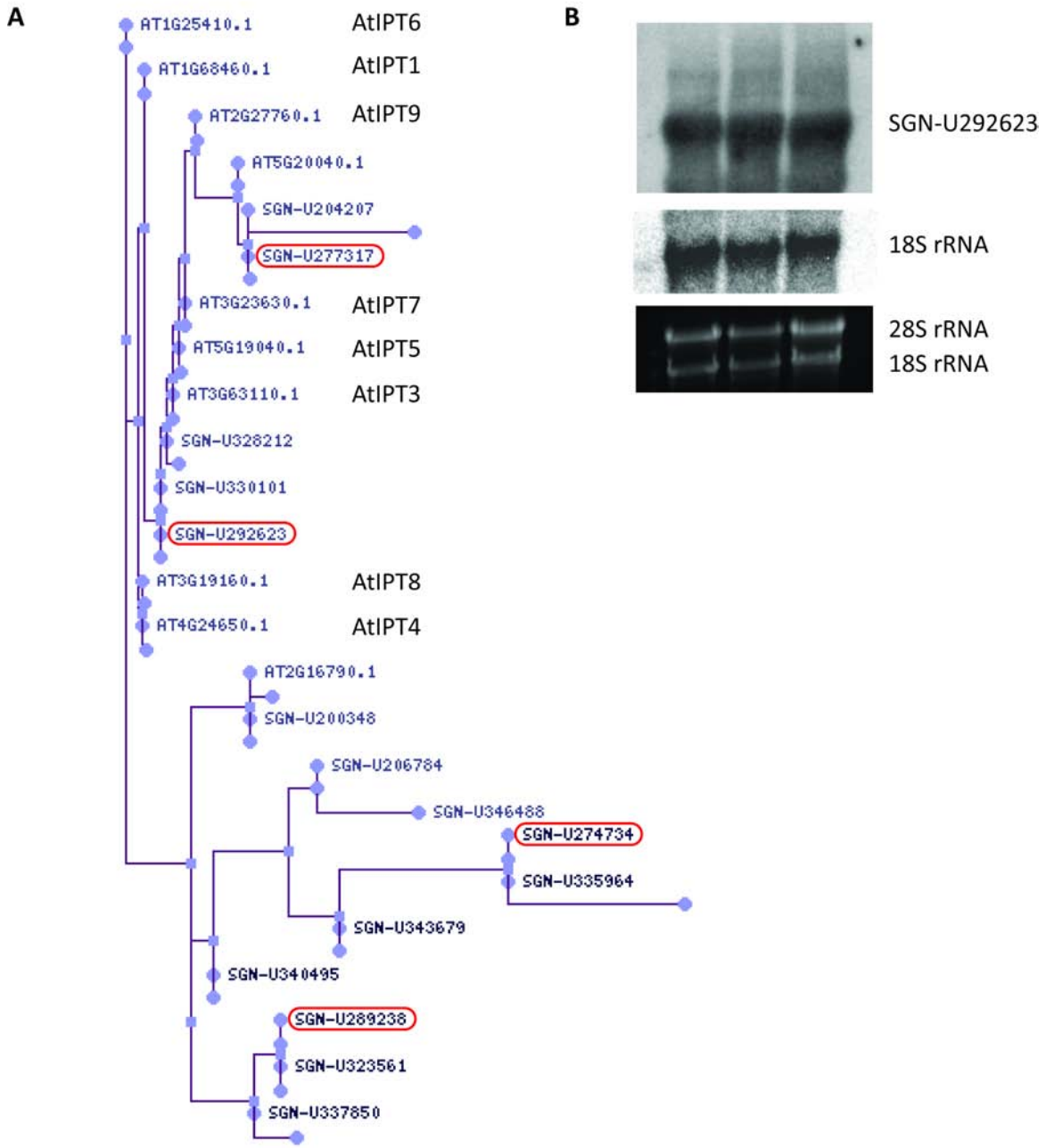

Figure 3.5 Analysis of isopentenyl transferase expression in stolon tips progressing through tuberisation
A. SGN unigene family 102000 - 'isopentenyl transferase like'. *A.thaliana IPT* genes are labelled accordingly. Potato unigene builds are outlined in red. **B.** RNA blots hybridised with DNA probes for SGN-U292623, a putative potato homologue of *AtIPT3*, and 18S rRNA.

cDNA as previously described (section 2.3.10) of which 10-100ng was subject to multiplex PCR (section 2.3.6) using BioMix Red polymerase reaction conditions as previously described (table 2.5). Primers were designed to a 437bp region of *StCKP1* (C1F & C1R, table 2.3) (Warnes, 2005) and a 346bp region of the β-tubulin gene *TUBST1* (FTUB & RTUB, table 2.3) (Taylor et al., 1994). To overcome variation in the DNA concentration between samples post cDNA synthesis, standardisation of template content by dilution was carried out to *TUBST1* transcript and *StCKP1* content quantified relative to *TUBST1*. Reactions were carried out three times, each with freshly extracted RNA, and the mean calculated. Results presented are ± standard error (SE).

As shown in figure 3.6, analysis of *StCKP1* transcript abundance by RT-PCR on RNA extracts from tuber tissues revealed conspicuously high expression levels in the sprout apex of non-dormant tubers, this correlates with analyses carried out by Warnes (2005) in which *StCKP1* transcript was found to be higher in cytokinin responsive tissues such as the shoot apex, roots, leaves carpels and stolon tips. Detectable levels of expression were also found in the mid and basal tissues of the sprout and dormant bud. Notably, a decrease in expression was seen in the peridermal tissues on break of dormancy relative to that seen in dormant periderm.

Warnes (2005) has previously identified *StCKP1* transcript to be present in *S. tuberosum* L. cv. Majestic stolon tips at the three defined stages of tuber development. However, it is proposed that StCKP1 is the 37kDa protein discovered by Thomson (1994) and thought to be responsible for the eight fold increase in cytokinin binding observed in tuberising stolon tips. To investigate *StCKP1* transcript abundance throughout tuberisation of stolon tips, total RNA was extracted from stolon tips which had been previously harvested from a bag production system (section 2.2.1.3) and frozen at -80°C. Multiplex RT-PCR was carried out as for tuber tissue extracts, and the result obtained validated by RNA blotting using a [α-^{32}P]dCTP labeled probe synthesised using a 441bp fragment of *StCKP1* produced by PCR with C2F and C2R primers (table 2.3) (section 2.3.11). Abundance of *StCKP1* transcript was quantified by hybridisation of this DNA probe to 10µg extracted RNA immobilised on a nylon membrane, and normalised relative to abundance of 18S rRNA determined by hybridisation of an [α-^{32}P]dCTP labeled 18S probe. Three biological replicates were carried out for each method undertaken to calculate mean transcript abundance at each stage of tuberisation.

Figure 3.7 shows the agarose gel and phosphor images of hybridised blots and quantification. Detectable amounts of *StCKP1* transcript were observed in extracts at all stages of stolon

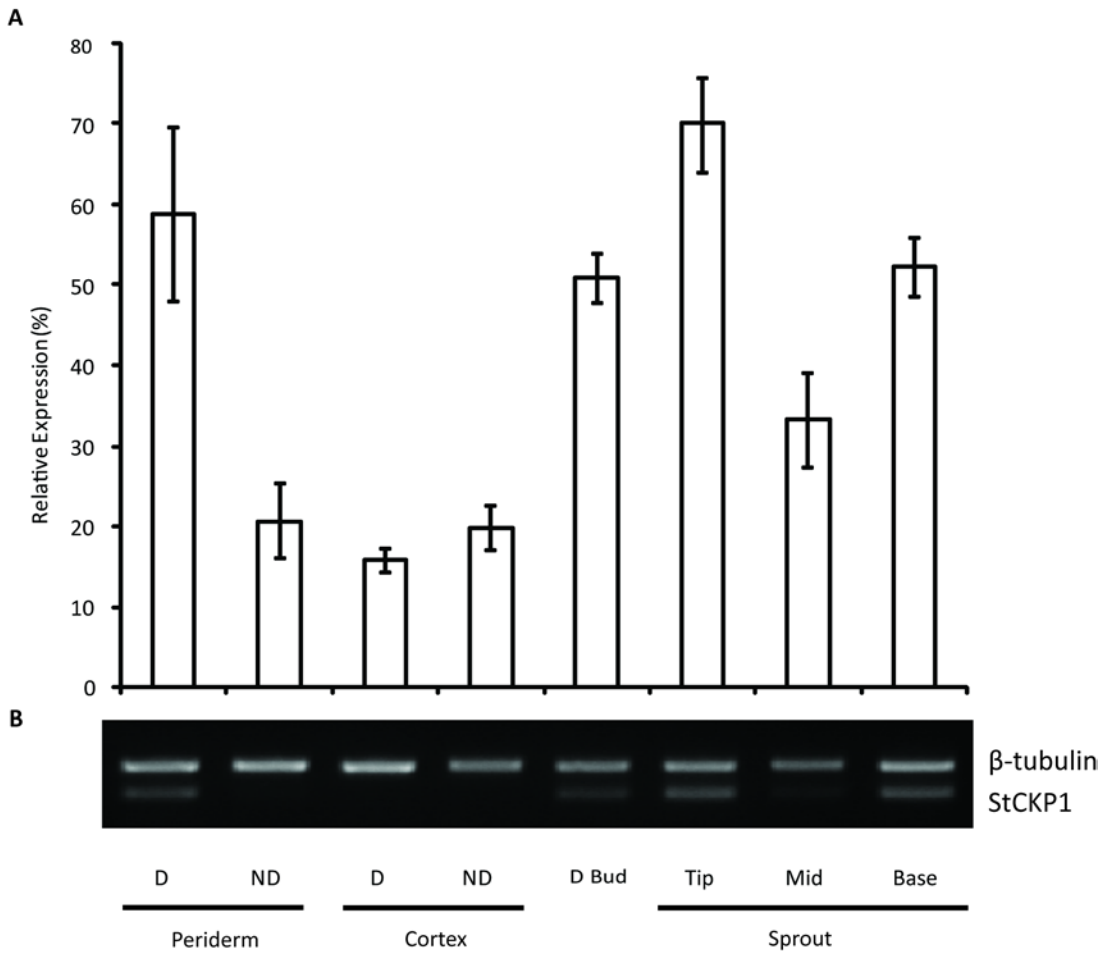

Figure 3.6. RT-PCR analysis of *StCKP1* in dormant and non-dormant tuber tissue
A. Quantification of *StCKP1* abundance, normalised to *TUBST1* transcript visualised by **B.** Agarose gel electrophoresis. D=Dormant, ND=Non-dormant. Data presented are means of triplicate reactions, each carried out with freshly extracted RNA ± SE (n=3).

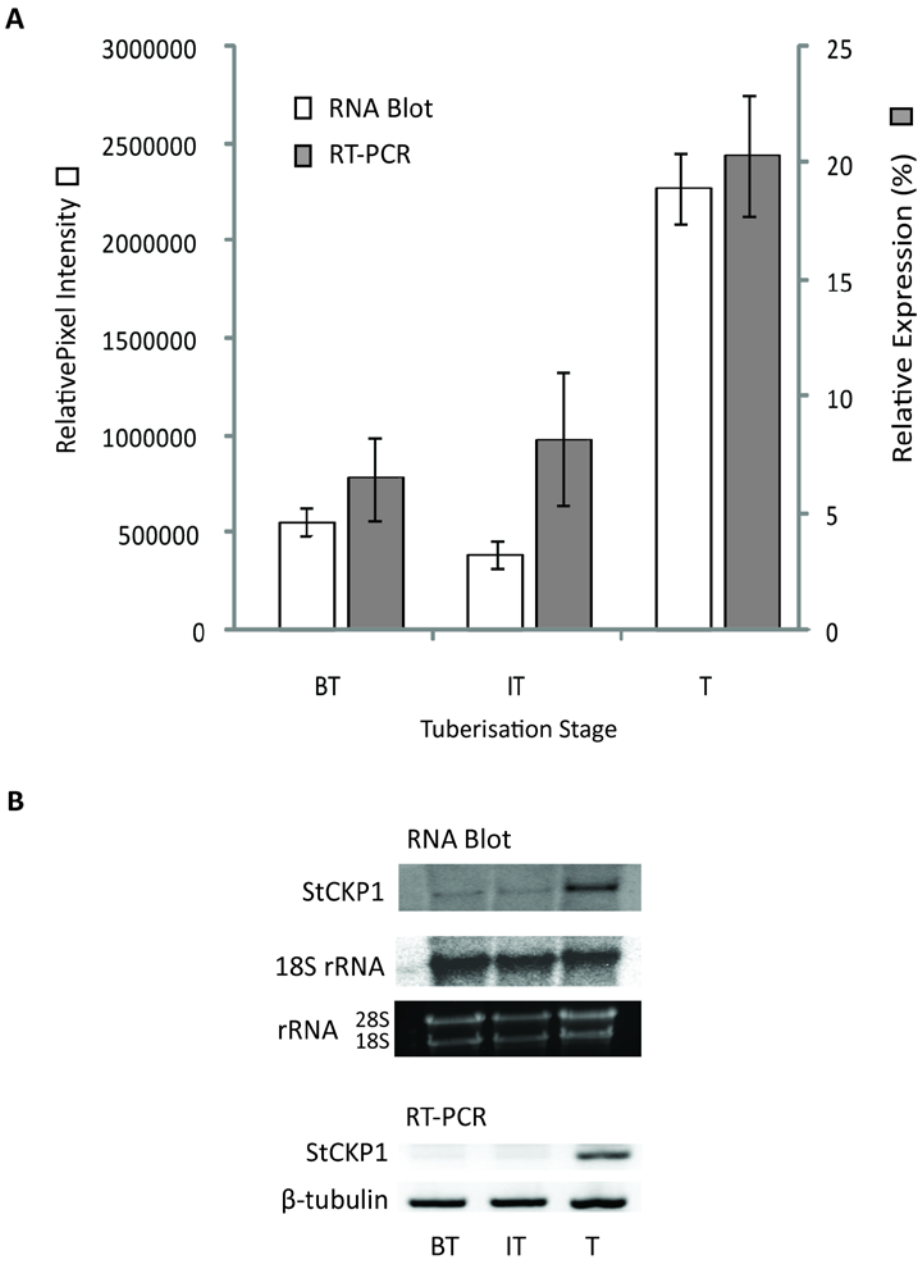

Figure 3.7 Expression of StCKP1 transcript in stolon tips at three defined stages of tuberisation
A. Quantification of *StCKP1* abundance by RNA blotting (white bars), normalised to 18S rRNA; and by RT-PCR, normalised to *TUBST1* transcript visualised by agarose gel electrophoresis. Data presented are means ± SE (n=3), each carried out with freshly extracted RNA. **B.** Representative RNA blots to which [^{32}P]-labelled *StCKP1* or 18S rRNA DNA probes were hybridised and; representative multiplex RT-PCR visualised by agarose gel electrophoresis (inverted).

development. Calculation of the standard error of the mean (SEM) for both RNA blotting and RT-PCR transcript measurements reveals no significant difference between *StCKP1* abundance before and at incipient tuberisation, while tuberised stolon tips contain significantly elevated levels of *StCKP1* by comparision with those before and at incipient tuberisation. The quantification of transcript for both transcript detection methods indicated that RNA-blotting is a more precise method of measuring abundance as error is much reduced.

3.3.2 Protein

StCKP1 protein abundance was also quantified by immunoblotting to assess the correlation of protein and transcript abundance. Protein was extracted from 1g of stolon tips for each of the three previously defined stages of tuberisation as previously described (section 2.5.1) and protein content of each sample determined by Bradford assay (Bradford, 1976) before standardising to 100mg ml^{-1} each. 10µg total protein was loaded onto two 12% SDS-polyacrylamide gels and run for 1 hour 15 minutes at 200V. One gel was subject to staining with Coomassie blue, while the other was used in a chemiluminescent immunoblot with an antibody previously raised to a short synthetic peptide derived from the StCKP1 sequence, anti-CKP (Warnes, 2005) . It was found a 1:50,000 dilution of anti-CKP was required to achieve a degree of specificity in binding to transferred proteins. As figure 3.8 shows, a protein of 37kDa is detected by anti-CKP in both incipiently tuberising and tuberised stolon tips, but is absent from stolon tips before signs of tuberisation are evident, indicating that StCKP1 has low turnover like the bark storage proteins with which it shares homology.

3.4 Promoter driven expression of β-glucuronidase (GUS)

3.4.1 Generation of promoter::GUS fusions

As a tetraploid, it is likely that there are two copies of StCKP1, termed StCKP1a and StCKP1b, encoded in the genome. Putative promoter regions of the StCKP1a and StCKP1b, pro1 (figure 3.9) and pro2 (figure 3.10) (renamed for this study from CP1 and CP2 respectively) were isolated and sequenced by Warnes (2005) who used the PLACE and PATCH databases to find putative cis-acting regulatory DNA elements for regulation of gene expression as annotated on figures 3.9 and 3.10. In order to investigate the activity of these two putative promoters, it was decided to drive expression of the *E.coli* protein GUS encoded by *uidA* using pro1 and pro2 as promoter::GUS fusions are known to be a reliable method for promoter assay in plants.

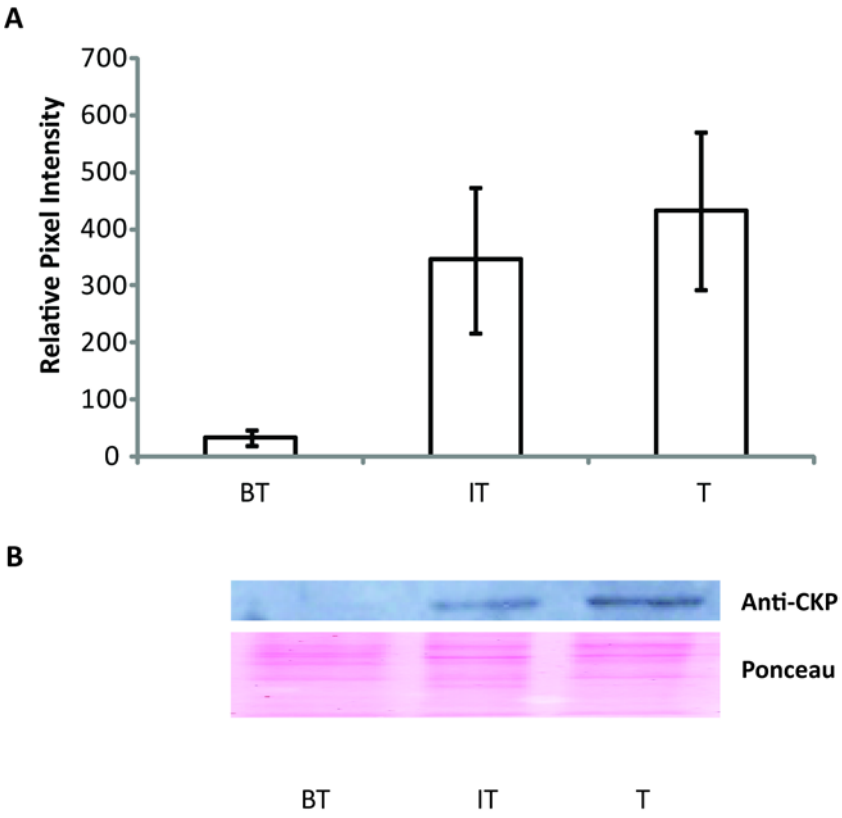

Figure 3.8 StCKP1 protein abundance estimated by immunoblotting at three defined stages of tuberisation
10µg transferred protein was probed with 1:50,000 dilution of anti-CKP whole serum for 1 hour before washing and probing with 1:10,000 dilution of HRP-linked anti-rabbit. A. Data presented is mean relative pixel intensity estimated using Image J ±SE (n=3). B. StCKP1 immunoblot and ponceau stain as loading control. Bands detected were of the expected size of 37kDa for StCKP1 according to sequence data and size determination of previously extracted protein (Warnes, 2005)

```
1    AGTGGAGTAACACAGAGCCAATAGAAGACTCATCTATCAGAGTAACAATG  50
51   AAAAAAAGCTTCATTTGAATGTTAATTCATGGTTTACTTGAATTACTTAT 100
101  CATTTAGGATGAATTCCTTCATGCTGAAGGAGAACAGTAAGAACTATTGA 150
151  AGACTCCAAAGATATTACATATCATAAACAAGAAGAATGAGGCTCAGATC 200
201  TCTCTATAACCAGGTACTTATATTTCTCAGAAATGCTATGGCTGCAACCT 250
251  AGAGCAGGTTGTCCTGCCAAGTTACTGAGTCTTGTATCATATCAACAATG 300
301  CAAACCAATATTGCTATTTGTCAAAAACTATATCATTACTGCCTCAATTT 350
351  TTCACATTTTCTTTATTTTGAGCATGATTATCACTGTTTATGTGTTAATG 400
401  CAGCCACACAGCAGCAAGGCAAGAACCAATAGCAGTAAAAGATAATTAAT 450
451  TATGTGCATCTTCTCAAGCTAGAGTTACAAGAAAGAGCTAGCCACTGTTA 500
501  CTTTCTTCCAGCAAGATTTCACATCTTGGCCTTACCAGCAAAACGAAATG 550
551  AAAAAATAAATTATTCACATTTCTCATTGATGATGTCTCATACTCTCATT 600
601  TATGGGCTAGCTGTCTAAGAAACGATTTTTCCATCAAACAATGTCCAGAA 650
651  GGACTGCTTGCAATTTTGACACTCACAACTGGCTACTAATGAATGGGTCA 700
701  AAGAGTGAAGAAGACTACGCCATGGCTGCAAAAGAACCAGTTGCATGTGA 750
751  TAGAGGAGTCTCAAATCACATATCATCATGGGTTTTTGCCAAGCCAAGAT 800
801  ACAGATCTACTCGTCTATAAACCCGAACAACCTTTTTTTAAGCCAAGATA 850
851  ACCAAATATTATCTGCCTCATTGATAACTGGTAGCATAGGATTCGAGGAA 900
901  TTTGAGGTGCTTTGGACCTGAGCTCATAAATCAGAACGAGGTCCANGGNC 950
951  TACTACTGCTGCTGCTGATGTCAATGCT                       978
```

Figure 3.9 *StCKP1a* promoter sequence 1 (pro1)
Putative transcription factor binding sites identified by PATCH are underlined. Light responsive *cis*-acting elements underlined in black. Auxin responsive elements are underlined in blue ARR1 binding elements found in Arabidopsis are highlighted in purple. Adapted from Warnes (2005)

```
1   TGTCGAGTGAGATGAAAAAAAATGATATGTGGCATTGTTTAATTTAGTTG  50
51  AATCTTTAAGAAAGAAAATCAAATTAGTTTCATAGATTTATTTTCATGCA 100
101 AAAATACAGAGAAATCTAAAAAAATAATATTATTATTTCAAAAAAAAAAT 150
151 CGATGTTCGTTAGTTAATTTTTATTTTTAAAAAATGAAATTAACAGACAC 200
201 GACAATTGAAGAACATAAATAAAAGAATAAAGAAATCATAAAAATAATAT 250
251 TTCGTGTTTAAATGGTACATAAAAAATAGAGTTTAAGGGTTAATTAAAAT 300
301 GAAATAAGACTAAGATAGAGTGTCAAAATGAAAAATAAGGACAAGTGTGA 350
351 GAGTTTGTATATGTGTTTGGCCTTATACAAAAGTTTTACATGACAAAAAT 400
401 ATATATATTAAAAAAATAGTCAAATTATTGATGGATGATGCAACGTAATAT 450
451 AATTATAATTTTACTATAAATATGAGGGCTTTGTTATTAGTTTCCCTTGT 500
501 CAATACTATTCT                                       512
```

Figure 3.10 *StCKP1b* promoter sequence 2 (pro2)
Putative transcription factor binding sites identified by PATCH are underlined. Light responsive *cis*-acting elements underlined in black. Hormone responsive elements are underlined in blue: auxin single underline, gibberellin double underlined, ABA underlined by a dashed line. ARR1 binding elements found in Arabidopsis are highlighted in purple. Adapted from Warnes (2005)

Pro1 and pro2 had previously been cloned into the pCR 2.1-TOPO vector (Warnes, 2005), however the restriction sites this vector provided were not suitable for the sub-cloning of promoter regions into pGGUS. In order to clone the promoter regions for expression of GUS, it was decided to subclone from the sequencing vectors to pT7Blue-3 which contained appropriate restriction sites on either side of the blunt insertion site. The pro1 putative promoter region was amplified by PCR from the sequencing plasmid pTAIL256 (table 2.2) using the Phusion proof reading DNA polymerase with the primer pair Pro1F and Pro1R (table 2.8), while pro2 was amplified from the sequencing plasmid pTAIL128 (table 2.2) using CP2F and CP2R primers (table 2.3). The products were gel purified from a 1.2% agarose gel using the QIAquick PCR purification kit (Qiagen) as previously described (section 2.4.1.1) and 0.05pmol cloned into pT7Blue-3 (Novagen) (section 2.4.1.2) to produce pT7B-3Cp1 and pT7B-3Cp2. The newly ligated plasmids were transformed into *E.coli* strain TB1 (section 2.4.3) and plated onto LBA plates containing kanamycin (appendix 1, table A1.6). Colony PCR (section 2.4.4 & table 2.7) with primers designed to the flanking regions of the insertion site (R20-mer & U19-mer, table 2.3) was undertaken to check for success of transformation of colonies selected. Two successful transformants were selected for each ligation reaction carried out, placed in LB liquid culture supplemented with kanamycin and allowed to grow overnight at 37°C at 3Hz for plasmid preparation (section 2.4.5). Purified plasmids, pT7B-3Cp1 and pT7B-3Cp2 were subject to a restriction digest with *Nco*I and *Cla*I for pro1 and pro2 respectively, to ascertain that promoters had ligated into the cloning vector in the desired direction before sequencing with R20-mer (table 2.3).

Using methods described in section 2.4.1.3, the promoter regions pro1 and pro2 were excised from their respective sub-cloning vectors; pT7B-3Cp1 and pT7B-3Cp2, by restriction digest with *Bam*HI and *Xba*I. The products of digest were purified from a 1.2% agarose gel using the QIAquick PCR purification kit and quantified by UV spectrophotometry. The destination vector, pGGUS was digested with the same enzymes and cut ends dephosphorylated using CIAP, purified and quantified as before (section 2.4.1.3). Using a 3:1 molar ratio of insert to vector, the cut pGGUS backbone and promoter insert were ligated using NEB Quick Ligase to produce pGpro1GUS and pGpro2GUS (figure 3.11), and transformed into *E.coli* strain TB1. Colony PCR of transformed bacteria using pGEMR and GUSR primers was carried out in order to determine if ligation reactions had been successful. Colonies yielding a PCR product of the expected size (1.2kb for pro1 insert, 700bp for pro2 insert) were selected, grown in LB liquid culture supplemented with kanamycin and used for plasmid preparation. Plasmids were sequenced to confirm presence of the appropriate promoter in the 5′ region of *uidA* using M13R and GUSR primers (table 2.3) and 500µl of bacterial liquid culture put into glycerol stock for each confirmed plasmid.

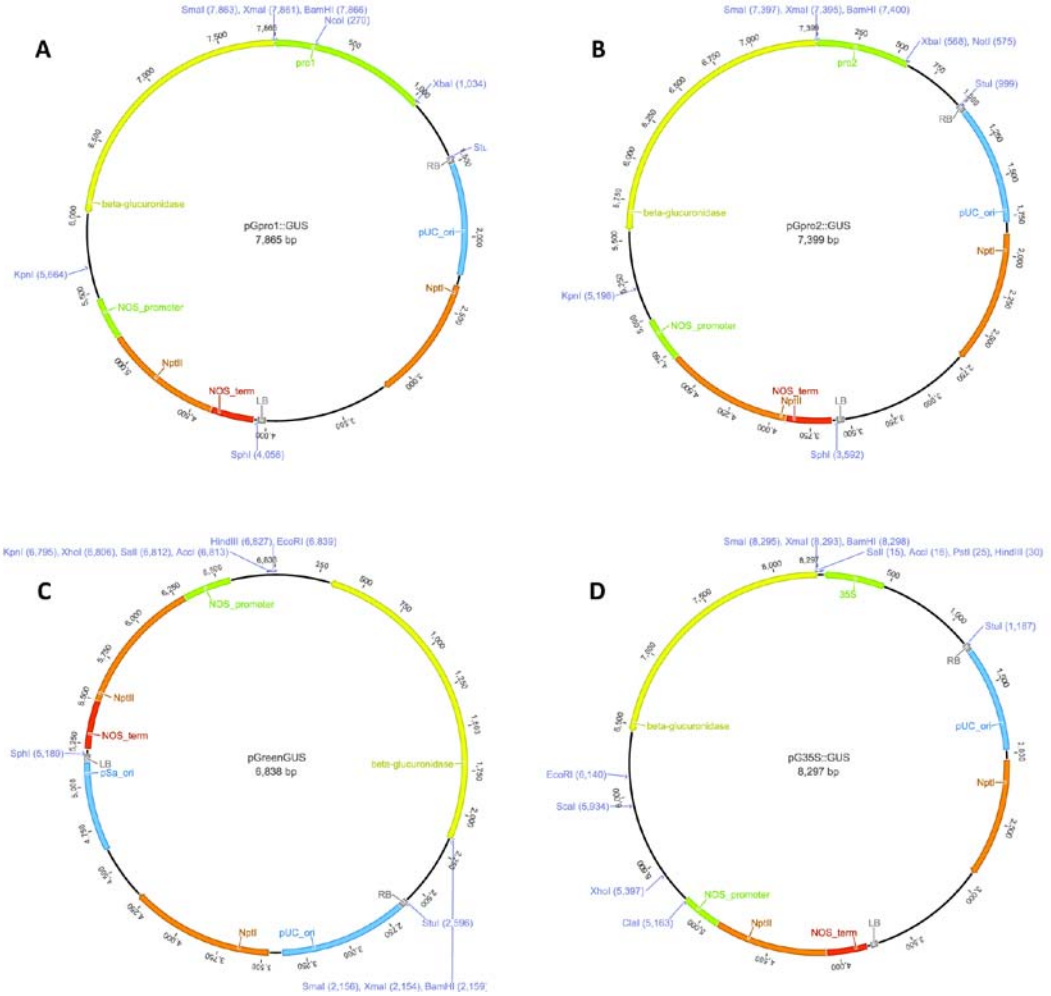

Figure 3.11 Maps of plasmids used in the production of promoter::GUS fusions
A. constructedpGpro1::GUS, **B.** constructed pGpro2::GUS, **C.** pGreenGUS plasmid backbone (Hellens et al., 2000). **D.** pG35S::GUS (Wilkins, 2004).

3.4.2 Transformation of *S.tuberosum* and selection of transformants

pGpro1GUS and pGpro2GUS plasmids were transformed into *A.tumefaciens* strain LBA4404 already harbouring the pSOUP plasmid as previously described (section 2.4.8) along with the empty vector pGGUS and an over-expressing vector, pG35SGUS as controls. Transformed Agrobacteria were cultured on TYNGA (Appendix 1, table A1.1) containing kanamycin, tetracyclin and streptomycin at appropriate concentrations (appendix 1, table A1.6). Successful transformants were identified by colony PCR using M13R and GUSR primers (table 2.3). One positive colony for each of the four transformations was selected and placed into 5ml liquid culture in TYNG supplemented with appropriate antibiotics. Transformation of *S.tuberosum* was carried out as described in section 2.4.9, using six plates of 20-25 explants per transformation and 50µg ml^{-1} kanamycin as a selective antibiotic. Once on MS30 media containing selective antibiotics, leaf tissue was harvested and DNA extracted (section 2.3.1.2) to screen for positive transformants by PCR with GUSF and GUSR primers (table 2.3). All lines transformed with one of the four vectors and showing kanamycin resistance were found to be positive for the *uidA* transgene, indicating the transformation and selection process was successful. Positive transformants were each sub-cultured into two new pots of MS30 containing kanamycin as the sole antibiotic, at a concentration of 50µg ml^{-1}. One of these pots was sub-cultured every 6-8 weeks onto fresh MS30 media containing kanamycin while the other was allowed to mature for 7 weeks before transfer to pot culture at the Plant Growth Facility for tuber production (section 2.2.1.2). Tuberising stolon tips and mature tubers were harvested from non-sterile material after 12 weeks culture in 7:1 mix of Levington M3 compost to medium grade vermiculite in 20cm diameter pots after aerial plant organs had begun to senesce. Stolon tips were snap frozen in liquid nitrogen and stored at -80°C while tubers were cleaned of soil by washing in RO water then allowed to dry at RT before moving to dry storage in the dark at 16°C.

3.4.3 Screening for GUS activity

In order to determine which lines of promoter::GUS fusions would be most appropriate to use in histochemical assay, the fluorometric assay for GUS activity was employed using harvested stolon tips as a source of protein as it has previously been shown that tuberising stolon tips have high *StCKP1* transcript abundance. It is also known that fluorescence quenching by chlorophyll can interfere in fluorometric assays for GUS activity and so the choice of stolon tissue for preliminary screening of GUS expression was additionally justified by the low chlorophyll content of stolons. Preliminary studies were performed using 1g tuberising stolon tips. Stolons were ground in extraction buffer and assayed for protein concentrations using BioRad reagent. The samples were normalised to a protein concentration of 0.1mg ml^{-1} before being assayed for GUS activity (figure

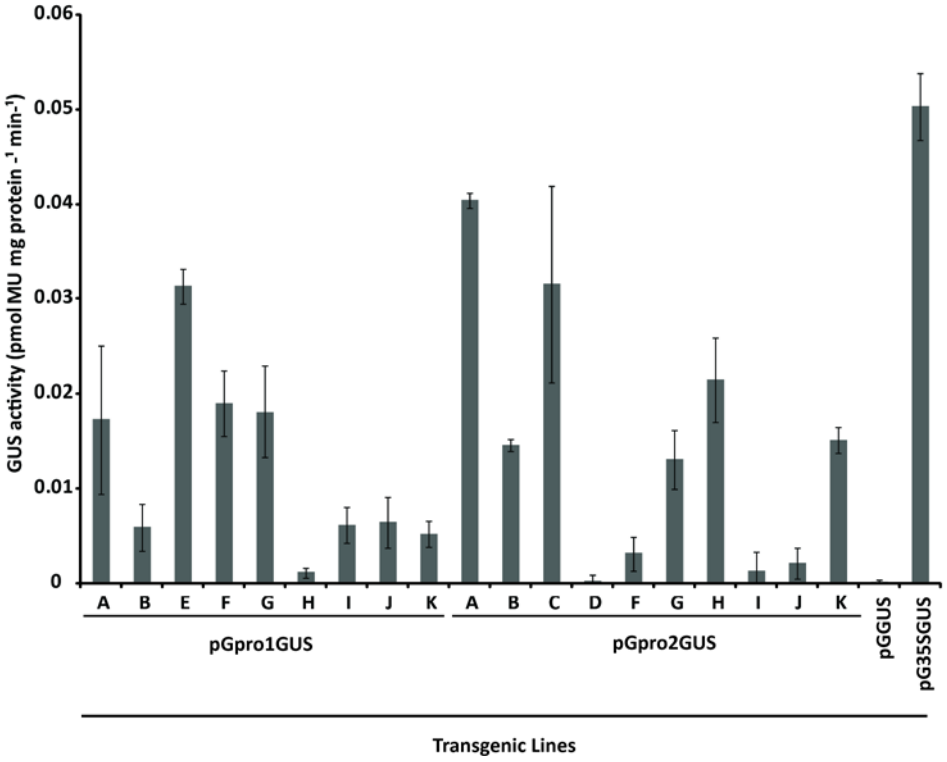

Figure 3.12 Screening independent pGpro1GUS and pGpro2GUS lines for GUS activity
Tuberising stolon tips of all pGpro1GUS and pGpro2GUS lines that had successfully grown to tuber maturation were ground in extraction buffer and protein concentration of extracts normalised to 0.1mg ml^{-1}. The protein extract was used to carry out the fluorometric GUS assay to determine which lines showed GUS activity. NT tuberising stolon tips were used as a negative control to determine inherent background fluorescence which was found to be 0.004pmol MU mg $protein^{-1}$ $min^{-1.}$ Mean values presented have been corrected for background fluorescence ±SE (n=3).

3.12). To obtain reproducible rates, assays were carried out immediately after protein extraction over a period of 24 hours to detect low levels of activity. Stolons transgenic for the CaMV35S::GUS fusion were used as a positive control for GUS activity, and those harbouring the *uidA* gene without a promoter (empty vector, EV) were used as a negative control. Non-transformed (NT) Desiree stolons were assayed to determine the background fluorescence reading, expected to be negligible.

Data shown in figure 3.12 have been normalised relative to the zero time point for each sample initially, and then corrected against the background fluorescence emitted by NT samples which was found to be 0.004pmol 4-methyl-umbelliferone (MU) $mg^{-1}min^{-1}$. Screening of the pGpro1GUS lines using the fluorometric assay revealed all 9 lines demonstrated GUS activity greater than the background level found in NT stolon tips. However, line H was significantly lower in activity than other transformed lines and so was not analysed further. Screening of the pGpro2GUS lines indicated a greater GUS activity than that of NT in 9 out of 10 lines. Lines I and J were found have lower GUS activity than other transformants for the pGpro2GUS construct and so these were also excluded from further study. As expected, the pG35SGUS line assayed showed high GUS activity and the EV negative control had activity on a par with NT. The lines chosen for further investigation of these two putative *StCKP1* promoters were: pGpro1GUS A, B and E, and pGpro2GUS A, C and K, as these had the highest measurable GUS activity by fluorometric assay.

3.4.4 Determination of promoter activity by histochemical assay

2mm slices of mature tuber from soil cultivated lines; leaves from the shoot apex, and root stocks of 6 week old plants from aseptic culture; and stolons from 1 week old microtuber inductions, were excised and placed immediately into GUS staining solution. The staining solution was vacuum infiltrated into all tissue then placed at 37°C. Following an overnight incubation for two of the pGpro2GUS lines selected, staining of the vascular tissue and periderm of mature tubers was evident (figure 3.14). After 48 hours of incubation, two of the pGpro1GUS lines showed evidence of staining in tuber vasculature (figure 3.13). On examination under a dissecting microscope (Leica DFC310 FX, Leica Microsystems GmbH, Wetzlar, Germany), staining in the dormant bud of the tuber (figure 3.13) and light staining at the stolon tip was evident (figure 3.13). No staining was found in the leaves or roots of either of pGpro1GUS or pGpro2GUS lines (data not shown), which was unexpected as *StCKP1* transcript analysis carried out by Warnes (2005) predicts promoter activity in these tissues. Infiltration of the tuber and leaf tissues by the staining solution had been thorough as lines expressing GUS under the control of the CaMV 35S promoter were stained throughout (figure 3.14).

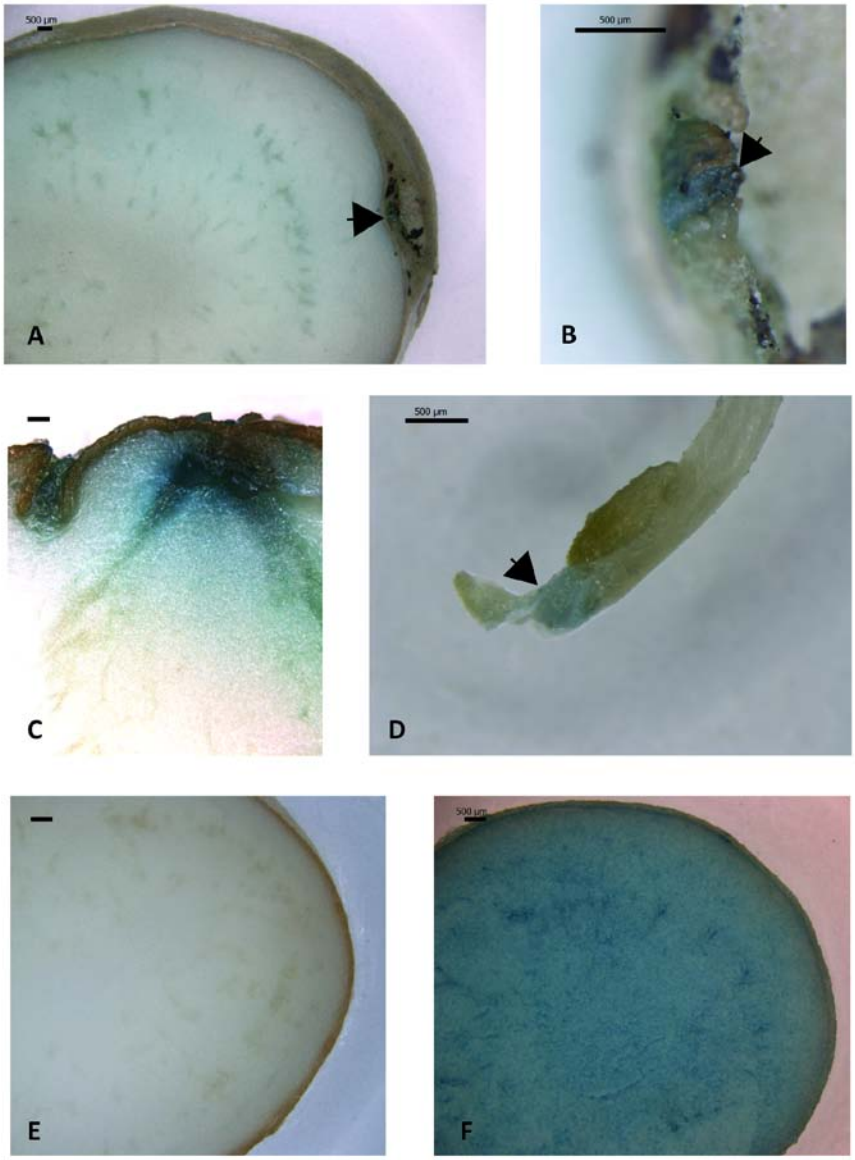

Figure 3.13 Histochemical GUS stained tuber sections of tubers transformed with pro1::GUS construct
2mm slices of tuber were vacuum infiltrated with, and incubated in GUS staining solution for a period of up to 48 hours. Tuber slices were fixed in 50% ethanol and imaged using a Leica DFC310 FX dissecting microscope. **A**. Cross-section of a pro1::GUS transgenic tuber. Arrow indicates GUS expressing tuber bud. **B**. Close up of tuber bud in A. **C.** Vascular tissue immediately below tuber buds expressing GUS transgene. **D.** Stolon tip apex expressing GUS transgene. **E.** Empty vector negative control transformed with pGGUS. **F.** Positive staining control constitutively expressing GUS under control of CaMV 35S promoter. Scale bar=500µm.

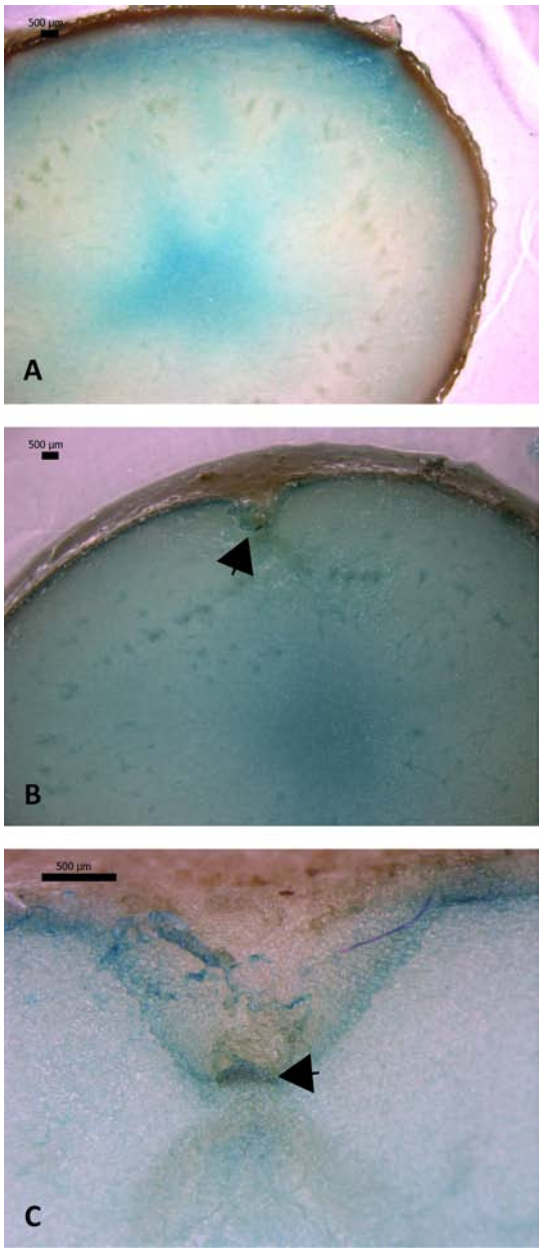

Figure 3.14 Histochemical GUS stained tuber sections of tubers transformed with pro2::GUS construct
2mm slices of tuber were vacuum infiltrated with, and incubated in GUS staining solution for a period of up to 48 hours. Tuber slices were fixed in 50% ethanol and imaged using a Leica DFC310 FX dissecting microscope. **A.** Cross-section of a pro2::GUS transgenic tuber**. B.** Staining in periderm and tuber bud. Arrow points to tuber bud. **C**. Close up of tuber bud in B. Arrow points to the meristem. Scale bar=500µm.

3.5 Discussion

The cytokinin content of stolon tips quantified for different stages of tuberisation was found to be in line with previous observations of increasing cytokinin upon tuberisation of stolon tips (Mauk and Langille, 1978; Sattelmacher and Marschner, 1978; Turnbull and Hanke, 1985b) with the predominating active cytokinin being zeatin riboside as previously discussed (section 3.2). However, the amounts of cytokinin as determined by HPLC-ELISA in each biological replicate were variable, leading to a larger than expected standard error. In order to test if this variability between biological replicates is real or a factor of the numerous purification steps, and so potential loss points in extraction and separation of cytokinin, it would be wise to carry out LC-MS-MS using stolon extracts which had undergone only the initial extraction and Sep-Pak purification. Combined with the tissue specific data gathered by transcript analysis and promoter analysis through reporter fusions, it would be of great interest to look at the cytokinin abundance in the periderm of dormant mature tubers and those exiting dormancy, and also from dormant tuber buds. Extraction and quantification of cytokinin from such a small mass of tissue is virtually impossible, so it would be of interest to study the transcript abundance of orthologs of the Arabidopsis Response Regulators (ARR) by either RT-PCR or RNA blotting. This method has been successfully implemented in the study of response to applied cytokinin in cytokinin metabolic *log* mutants of *Oryza sativa* using the response regulators OsRR1 and OsRR5 (Kurakawa et al., 2007). Putative response regulator orthologues have been found by carrying out BLAST searches of the SGN EST database with ARR nucleotide sequences. Three unigene builds have been found to share homology with two Arabidopsis Type-A response regulators, of which StU277247 shares most homology with AtARR3 and 4, and StU279600 shares most homology with AtARR8 and 9. Although these ARR3,4,8 and 9 are known to have high basal expression in Arabidopsis, exploratory experiments indicate transcript of StU277247 and StU279600 are cytokinin responsive (Mielnichuk, pers. comm.).

Analysis of transcript abundance indicated that *StCKP1* RNA is present in periderm of dormant mature tubers, much like *bspA,* with which *StCKP1* shares close sequence homology, is found in the bark of poplar. BSPA is one of the few proteins that has been well characterised which shares sequence homology with StCKP1 (Zhu and Coleman, 2001). It is one of a family of bark storage proteins (BSP) known to accumulate in the inner bark and parenchyma and xylem rays during autumn and decline during spring growth (Wetzel et al., 1989). BSPs are thought to store nitrogen translocated from autumnal senescence for supply of nitrogen during commencement of growth the following spring. This observation of decline of BSPs during the transition to growth is in line with the observation of a decline in *StCKP1* transcript in the periderm of tubers on break of dormancy.

StCKP1 transcript and protein are also seen to increase upon tuberisation of stolon tips, although the data collected by immunoblotting with an antibody raised to a synthetic peptide sequence derived from StCKP1 may not be robust as this antibody is not specific. Indeed it produces numerous bands of 30-50kDa which may represent StCKP1 paralogs or orthologues. As stolon tips tuberise, they enter the period of innate dormancy (Turnbull and Hanke, 1985b) and, much like the increase in BSPA upon entering the overwinter period, StCKP1 may be increasing as a storage protein for mobilisation upon break of dormancy. Analysis of pro1 and pro2 driven expression of GUS indicates that it is pro2 that drives the expression of *StCKP1b* in the periderm resulting in the accumulation of *StCKP1b* during onset and throughout the dormant period, while it is likely that pro1 is responsible for driving expression of *StCKP1a* in dormant tuber buds and in stolon tips.

To quantify promoter activity in these different tissues, it would be of interest to carry out the fluorometric GUS assay from extracts of these different tissues, notably the periderm and stolon tips. However, as GUS is highly stable, it may well persist in the tissue after the promoter has ceased to be active in driving transcription, thus the promoter::GUS system used in this study is unlikely to be of much use in studying activity of the two promoters during tuberisation of stolon tips and their entry into innate dormancy and, as tubers break dormancy. One method of ensuring non-persistence of the reporter protein is to use promoter::luciferase fusions which have been demonstrated to function well in potato microtubers (Vreugdenhil et al., 2006). However this system has drawbacks in that identification of promoter activity in a single internal tissue such as the periderm would be much more difficult. Another possible method of ensuring non-persistence of the reporter protein is to use a degradation tagged reporter. Degradation tags are short peptide sequences that mark a protein for degradation by the cell's protein recycling machinery. Numerous green fluorescent proteins (GFP) have been produced with degradation tags of between 3 and 11 amino acids (Andersen et al., 1998; Triccas et al., 2002) and would be of use as GFP can be localised to individual cells and tissues using confocal microscopy. However, to date this technology has only been utilised in bacteria and its use *in planta* may require changes to the tag in order to facilitate degradation by the plant cell machinery.

However, having now produced these reporter linked lines, it would be of great interest to test the putative transcription factor binding sites identified by Warnes (2005) and their activity in response to changes in signal perceived. Of particular interest would be the application of cytokinin as there are numerous ARR1 regulatory sites present in both pro1 and pro2 (figures 3.9 and 3.10). An auxin response factor binding site is also seen in the pro1 promoter region, while the pro2 promoter contains gibberellin- and ABA-responsive elements thus an investigation into the effect of hormonal

signal would be of interest in further determining the process of induction of StCKP1. Also of interest would be photoperiod as numerous cis-elements from promoter regions of photoperiodic transcriptional regulation are present in both pro1 and pro2 and previous studies have shown that tubers are induced in *S.tuberosum* L. under short day conditions (Jackson, 1999), and that *S.tuberosum* ssp. *andigena* is a qualitative short day plant that requires day lengths of 12 hours or less to tuberise, and so is frequently used in laboratory studies of tuberisation (Martinez-Garcia et al., 2002; Espinosa et al., 2004; Rodriguez-Falcon et al., 2006).

Chapter 4

Functional characterisation of StCKP1

4.1 Introduction

In an investigation that identified the full sequence of *StCKP1*, Warnes (2005) identified a conserved domain in the C-terminal region of the predicted translated protein which shared high similarity with members of a family of phosphorylases including purine-nucleoside phosphorylase (Marchler-Bauer et al., 2003). A BLASTp search with the full sequence of *StCKP1* identified similarity with the Phosphorylase superfamily (PNP_UDP_1) of proteins whose members include purine nucleoside phosphorylase (PNP), uridine phosphorylase (UdRPase), and 5'-methylthioadenosine phosphorylase (MTA phosphorylase) (Figure 4.1a)(Marchler-Bauer and Bryant, 2004; Marchler-Bauer et al., 2005; Marchler-Bauer et al., 2007). The member of the superfamily with which StCKP1 shares highest similarity is Pfs, a 5′-methylthioadenosine/S-adenosylhomocysteine nucleosidase from *E.coli* (Figure 4.1a). Pfs is responsible for hydrolysis of the glycosidic bond in both 5′methylthioadenosine and S-adenoslhomocysteine to yield adenine and the corresponsing thiopentose (Cornell and Riscoe, 1998). The predicted protein sequence of StCKP1 was also found to share structural similarity with a class of bacterial nucleosidases originally described by Mushegian & Koonin (1994). The family consists of both bacterial and eukaryotic enzymes including *E.coli* purine phosphorylase (DeoD), UdRPase and AMP glycosidase, a variety of as yet to be characterised bacterial proteins, and a group of plant stress-inducible proteins including bark storage proteins (BSPs) and wound induced (win4) proteins from poplar. It is hypothesized that these plant proteins have evolved from nucleosidases and will most likely possess nucleosidase activity as the probability of obtaining each of the conserved motifs alone was below 10^{-5}. The proteins in this family contain three conserved motifs (I,II & III), of which motif II corresponds to the ribose binding part of the nucleoside-binding site found in eukaryotic purine nucleosidases (Figure 4.1b). The central feature of this ribose binding site, as characterised in human PNP, is a distorted β-barrel and the conserved motif is part of the active centre. Motif II included 3 β-sheets of which the interface is directly involved in nucleoside binding, notably the backbone amino group of alanine which forms a hydrogen bond with the 3′ hydroxyl region of the ribose (Ealick et al., 1990). This conserved alanine residue (marked with a * in Figure 4.1.B) is present in StCKP1 between two β-sheets, indicating that this protein may also contain a nucleoside binding site. Warnes (2005) noted that the predicted translated amino acid sequence of StCKP1 differed from the consensus sequence at two positions in both motifs I and II. In motif I a hydrophobic residue is replaced by a hydrophilic R residue and a relatively small N residue replaces the predicted G or A. In motif II, another N residue replaces a predicted G, A or S, all small residues, while the aliphatic A is in place of the predicted bulky aliphatic I, L, V or M. It is unclear as to how these residue substitutions will affect the functionality of StCKP1.

A

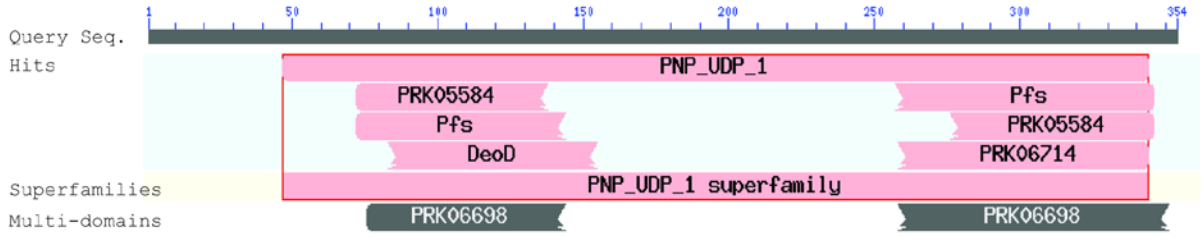

B

Motif I

```
StCKP1 57 RFGHIDNQPVVLVMTGLAMLNAGITTQLLL 86
Con       h···h·G··U··h··G·············hh
                A

StCKP1 57 EECCCCCCCEEEEEEHHHHHHHCHHHHHHH 86
Con       EECCCCCCCEEEEECCCCCCCCCHHHHHHHH
```

Motif II

```
                  *
StCKP1 94 VVHYGIAGNANPSLNIGDVAIPQY 117
Con       hh·····GsU·····h·D&·h···

StCKP1 94 EEEEEECCCCCCCCCCCCEEECCC 117
Con       EEEEE?CCC?????????????
```

Motif III

```
StCKP1  279 NKFDVSPVEMESAAVALICYQQNVPYIVIRALSD 312
Con           ····h··hE··s··&h·········h··I··h··

StCKP1  279 CCCCCCCHHHHHHHHHHHHHCCCCCEEEEEEEC 312
Con           HHHHHHHHHHHHHHHHCCC???EEEEEEEEC
```

Figure 4.1 Comparison of StCKP1 amino acid sequence with nucleosidases, and structural homology with motifs common to nucleosidases

A. Blastp output indicating putative conserved domains between StCKP1 (Query seq.) and a number of proteins (Hits) and known superfamilies and multi-domains. Numbers designate StCKP1 amino acid residues. **B.** Alignment of StCKP1 with predicted consensus (con) sequence for structural motifs I, II and III (**h** designates any hydrophobic residue I, L, V, M, F, Y, W, C or A; **U** designates a bulky aliphatic residue I, L, V, M; **s** designates a small residue G, A or S; **&** designates a bulky hydrophobic residue I, L, V, M, F, Y or W; · designates any residue). The predicted secondary structure of StCKP1 is aligned with the consensus (Con) of predictions of secondary structure from individual proteins in the nucleosidase family (Mushegian & Koonin, 1994) **E** - beta sheet, **C** - random coil, **H** - alpha helix, **?** - unknown. The position of the alanine residue in Motif II is marked *. Adapted from Warnes (2005).

Many plant nucleoside phosphorylases have been identified to date, particularly of note are those characterised by Chen and co-workers (Chen et al., 1980; Chen and Kristopeit, 1981a, b; Chen et al., 1982b) which have all been shown to catalyse hydrolysis of the N^9 riboside of cytokinins and adenine-type substrates; and OsLOG1, recently identified to hydrolyse N^9 ribotides to release the base of cytokinin substrates (Kurakawa et al., 2007). Katahira and Ashihara (2006) carried out a comprehensive analysis of purine biosynthesis, salvage and degradation in potato tuber tissue. This included radiochemical determination of enzyme activities for phosphoribosyltransferases, nucleoside kinases, nucleoside phosphotransferases and nucleoside nucleosidases using a variety of radiolabelled purine substrates. Adenosine kinase activity was found to be eight times higher than adenosine nucleosidase activity, while adenine phosphoribosyltransferase activity were found to be 10 times higher than adenosine nucleosidase. Their findings led to the conclusion that AMP can be formed either directly by adenosine kinase, or by the two step conversion via adenine by adenosine nucleosidase and adenine phosphoribosyltransferase. As this study did not investigate the interconversion of cytokinin substrates, it is not clear whether the enzymes identified in this study will play a significant role in cytokinin metabolism.

Using a short sequence of *StCKP1* isolated by Hanke lab (unpublished), Warnes (2005) amplified a partial length nucleotide sequence from cDNA isolated from stolon tips before tuberisation. Rapid amplification of cDNA ends (RACE) PCR was used to amplify 5′ and 3′ regions of *StCKP1*. Analysis of the sequence obtained indicated StCKP1 shared close homology with a number of bark storage proteins, and members of a superfamily of phosphorylases. Structural homology was identified between StCKP1 and three motifs known to be common to nucleosidases. This investigation set out to characterise the activity of StCKP1 biochemically as sequence data and homology between StCKP1 and members of the Phosphorylase superfamily suggest that it functions as a nucleoside phosphorylase.

4.1.1 Purification of enzymes involved in cytokinin interconversion

In a study carried out by Chen and co-workers, a number of cytokinin binding proteins were purified from wheat germ by [9R]iP-sepharose affinity chromatography (Chen et al., 1980). In follow up studies they sought to purify and characterise enzymes involved in metabolism of cytokinins, adenine and adenine derivatives. Enzymes including adenosine nucleosidase (Chen and Kristopeit, 1981a), adenosine 5′-nucleotidase (Chen and Kristopeit, 1981b), adenosine phosphorylase (Chen and Petschow, 1978), adenine kinase (Chen and Eckert, 1977) and adenine phosphoribosyltransferase (Chen et al., 1982b) were purified directly from wheat germ extracts using a combination of low pH fractionation, ammonium sulphate fractionation, DEAE-cellulose chromatography, followed by

Sephadex G-200 chromatography. Throughout this process, losses of activity were incurred during purification up to 46-fold by comparison with the crude extract. Following purification, enzymes were assayed at pH 4.7 in a Tris-citrate buffer using [8-^{14}C]Ade, Ado or AMP; or [8-^{14}C][9R]iP, iP or [9R-MP]iP as substrates. Following stopping the reaction by addition of 95% ethanol, products were separated using thin layer chromatography (TLC), visualised at 254nm and appropriate bands cut out and scintillation counted to measure amounts of radio label in each UV-absorbing compound found. Characterisation of these purified enzymes is discussed in section 4.7.

4.1.2 Identification, over-expression and purification of recombinant *Oryza sativa* LOG (OsLOG)

In a screen for defects in shoot meristem maintenance, the *lonely guy* (*log*) mutant was identified in *Oryza sativa* (rice) by Kurakawa and colleagues (2007). The *LOG* gene was isolated by positional cloning to a 35kb region on chromosome 1 which contained four putative genes. Of these genes, mutations were found in only one of the four in the six *log* mutant alleles. Their finding was confirmed by complementation of the phenotype of the *log-2* mutant with a full length *LOG* cDNA driven by a 1.5kb promoter region of *LOG*. The coding regions of LOG were ligated into pCOLD1 (Takara) to express His-tagged recombinant proteins in an *E.coli* host system. Enzyme activity of LOG as a cytokinin nucleoside 5′-monophosphate phosphoribohydrolase was measured by incubating the enzyme with 50µM substrate at 30°C for the appropriate period followed by HPLC separation and LC-MS-MS analysis of reaction products.

4.2 Generation of StCKP1 pMal expression vector

Purification of StCKP1 direct from potato stolon tips by affinity chromatography with biotinylated [9R]Z and subsequent removal of naturally biotinylated proteins was not reliably efficient and gave variable yields (Warnes, 2005), this study sought to utilise a bacterial expression system in order to express and purify sufficient quantities of pure protein. One use of this purified protein was to assay for its activity. The pMal expression system (Riggs, 2000) was chosen as it is known to aid the purification of proteins with solubility problems and with a single transmembrane span in its predicted structure, the system allowed for manipulation of expression of StCKP1 depending upon the preferred conditions.

The pMal expression system requires the in-frame cloning of a gene of interest down-stream of *malE*, an *E. coli* gene encoding maltose binding protein (MBP). The gene fusion is expressed under the control of the *tac* promoter, a composite of the *lac* and *trp* promoters. The use of the *tac*

promoter and the translation initiation signals of *malE* results in high levels of expression of the cloned sequence. Expression from the promoter yields a fusion protein made up of MBP and the protein of interest. It is thought that the highly soluble MBP acts as a chaperone to aid correct folding and improve the solubility of the foreign protein in the *E. coli* cell. The method of purification of the fusion protein from the crude cell lysate is a one-step affinity purification. The cell lysate is passed down an amylose column, to which the MBP binds. The column is then washed to remove the unbound protein and elution of the fusion protein from the column is achieved by competitive binding through washing with column buffer containing maltose. The polylinker between MBP and the protein of interest has been built in such a way that it can be cleaved by addition of Xa cleavage factor. The protein of interest can then be purified further to homogeneity, using the appropriate steps.

The *Solanum tuberosum* L. gene *StCKP1*, without the signal sequence coding for the predicted transit peptide, was cloned into the expression vector pMalc2x from pGADT7CKPCDS (produced by Barbara Warnes) by restriction digest of the donor plasmid using *Eco*RI and *Bam*HI. The pMalc2x vector was digested with the same enzymes and treated with CIAP to remove 5′ phosphates and thus prevent self religation. Following transformation into chemically competent *E.coli* strain TB1, colonies obtained were screened for the presence of the *StCKP1* coding region using C2F and C2R primers. Many colonies showed the presence of the StCKP1 sequence and a small number were selected for plasmid preparation and 5′ and 3′ sequencing using MalE F and M13/pUC R primers respectively to check *StCKP1* had been correctly cloned downstream and in-frame with *malE* (figure 4.2a).

4.3 Expression and purification of MBP-CKP from pMal

Initial construction of the pc2xCKP was carried out in the *E.coli* host strain TB1 (see table 2.1) supplied with the pMal system (NEB). However, the yield of fusion protein produced (5l culture yielding 3mg StCKP1 after affinity chromatography) was not as high as would be expected and so reasons for low yield were investigated. It is known that over-expression of recombinant protein in *E.coli* can be severely diminished if the open reading frame (ORF) that codes for the protein uses “rare” tRNA codons infrequently used by *E.coli*. Codons for arginine (Arg), leucine (Leu), isoleucine (Ile) and proline (Pro) are known to be a problem, particularly when present as tandem repeats. In order to determine the number of rare tRNA codons in the StCKP1 ORF, the cDNA sequence was analysed using the Rare Codon Calculator (RaCC) (http://nihserver.mbi.ucla.edu/RACC/). 11 Arg

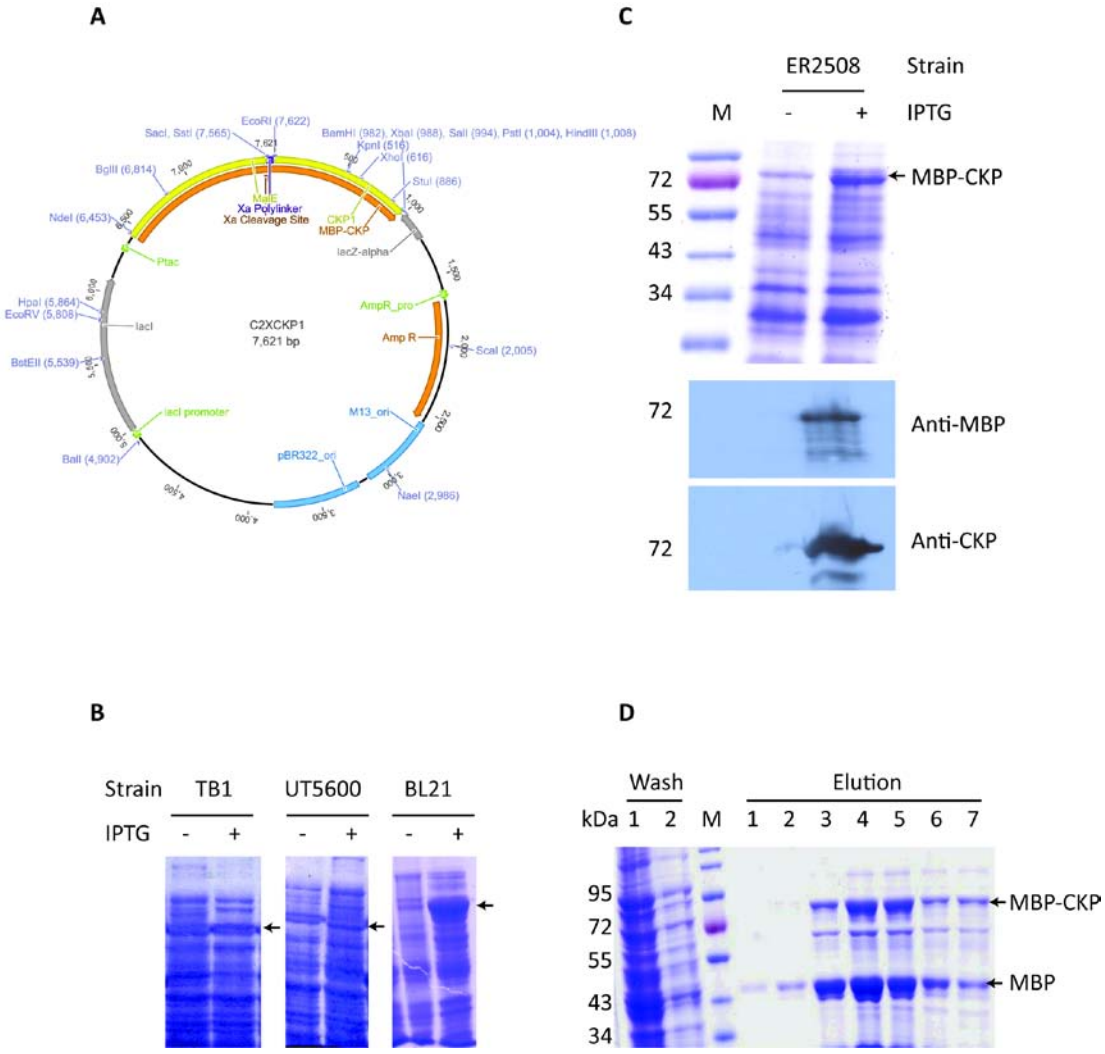

Figure 4.2 Production of recombinant StCKP1 using pMal fusion protein production system
A. pc2xCKP vector constructed. **B.** Coomassie stained SDS-PAGE gels of induction of expression of MBP-CKP fusion protein in *E.coli* strains TB1, UT5600 and BL21. Arrows point to 79kDa, the expected size of MBP-CKP. - no IPTG, **+** 0.4mM IPTG. **C.** Induction of MBP-CKP in *E.coli* strain ER2508 (NEB), Coomassie stained SDS-PAGE and immunoblot probed twice with anti-MBP and anti-CKP. **D.** Affinity purification of MBP-CKP from ER2508 on amylose resin. Wash = pMal column buffer, Elution = pMal column buffer + 10mM maltose, M = Molecular weight marker.

codons, of which 2 were found in double tandem repeat, 4 Ile codons and 6 Leu codons were identified. To ascertain if expression had been impaired due to a reduced pool of rare tRNA codons in the TB1 strain, pc2xCKP was transformed into E.coli strain BL21 harbouring pLysSRARE which contains the rare tRNA genes on the same plasmids that carries T7 lysozyme (table 2.1). Expression of the MBP-CKP fusion protein in this strain was not much different from that observed in TB1 at 4.5mg/5l culture. Following purification by affinity chromatography, a number of bands smaller than 37kDa were detected by SDS-PAGE of bacterial proteins indicating reduced yields may have been due to the action of bacterial proteases, although strain BL21 is deficient in OmpT and Ion proteases. Subsequently, strains UT5600 and ER2508 were sourced (NEB) and transformed with pc2xCKP. *E.coli* strain UT5600 is deficient in the periplasmic protease OmpT, so a negative result with this strain would indicate that it is a protease or proteases other than OmpT responsible for the apparent reduced expression seen in TB1 and BL21 pLysSRARE strains. *E.coli* strain ER2508 is carries a *lon* mutation, resulting in the knock out of the major ATP-dependent protease in the *E.coli* cytoplasm. ER2508 also carries a chromosomal deletion in *malB* which results in the deletion of *malE* and thus no constitutive expression. Expression of the MBP-CKP fusion protein was increased in strain ER2508 yielding 7mg/5l culture after affinity chromatography relative to strain UT6500 yielding 5mg/5l culture following affinity chromatography indicating the reduced protease activity conferred by knocking out the *lon* is preferable for expression of MBP-CKP (figure 4.2b).

Induction of the MBP-CKP fusion protein in *E.coli* strain ER2508 was initially checked by harvest of 1ml cell culture prior to and 16 hours after induction at 16°C by addition of IPTG to a final concentration of 0.4mM. Cells were pelleted and resuspended in 50µl 2x Sample Buffer before boiling to denature for 5 minutes and loading onto a 12% SDS-PAGE gel. Gels were subject to Coomassie stain and Western blot (see sections 2.5.2 and 2.5.3. respectively)(figure 4.2c). Purification of MBP-CKP fusion protein from *E.coli* ER2508 was carried out by release of the soluble fraction, as described in section 2.5.4 and mixing it with a slurry of amylose resin suspended in pMal column buffer to allow MBP-CKP to bind the amylose (Appendix 1, Table A1.4). Following binding the resin was poured into a column, and unbound plus non-specifically bound proteins washed through with 2 volumes pMal column buffer before eluting the fusion protein by application of column buffer containing 10mM maltose. One ml fractions of eluate were collected and assayed for presence of protein using BioRad protein assay dye reagent concentrate (50µl BioRad reagent, 550µl dIH_2O, 20µl fraction) and analysis of fraction content carried out by SDS-PAGE (figure 4.2d). Fractions containing fusion protein were pooled, and concentrated to 1.5mg ml^{-1} concentrated using Vivaspin centrifugal filter device with a molecular weight cut off of 10kDa, as determined by Bradford assay (section 2.7.2).

4.4 Cleavage of MBP-CKP fusion protein

Cleavage of MBP-CKP fusion protein was carried out by addition of 1% (w/w MBP-CKP as detected by Bradford assay) Factor Xa and incubating overnight at 4°C. Factor Xa is a protease that cleaves after the arginine residue in its preferred cleavage site Ile-(Glu or Asp)-Gly-Arg which is embedded into the polylinker sequence of the fusion protein. What remains of the polylinker on StCKP following cleavage is a small number of vector derived residues, isoleucine, serine, glutamate and phenylalanine added to the C-terminal of StCKP.

Optimal conditions were determined for cleavage of the MBP-CKP fusion protein by addition of low concentrations of SDS to the reaction as, in some cases, the fusion protein has been known to fold to make the Xa cleavage site inaccessible. Perturbation of the structure with low concentrations of SDS, ranging from 0.01% to 0.05% is known to relax the structure sufficiently to allow access to the cleavage site without altering the activity of the protein following cleavage (Ellinger et al., 1991). Addition of SDS to 0.04% was found to be optimal, increasing efficacy of cleavage without affecting the activity of the protein. 0.05% SDS was also found to be effective, however as SDS acts to disrupt protein structure, the lowest effective concentration was preferred. There is some evidence to suggest that a substrate or cofactor analogue could aid the cleavage of the fusion protein by Xa. To test this hypothesis, 100µM BAR or Ado was added to 250µg MBP-CKP with 1% (w/w) Xa and the reaction allowed to proceed at 4°C overnight. The addition of predicted StCKP substrate in such excess did not have a positive effect on the cleavage (figure 4.3) indicating that the conformation change exerted by binding of the MBP-CKP fusion protein to a substrate or substrate analogue did not relax the protein about the Xa cleavage site.

When analysed by SDS-PAGE, MBP-CKP fusion protein cleavage resulted in four major bands of approximately 79, 60, 43 and 37 kDa. The band of 43kDa represented MBP and the 37kDa band was thought to be StCKP1 while the band of 79kDa represents uncleaved fusion protein. The band at 60kDa, was not detected using antibodies raised to either MBP or StCKP1 and is thought to be a result of protein degradation (figure 4.3). There were a number of much smaller, less dense bands smaller than 37kDa which are assumed to be a result of protein degradation by contaminating bacterial proteases as upon storage at 4°C without addition of P2714 protease inhibitor cocktail (Sigma-Aldrich), which has broad specificity for the inhibition of serine, cysteine, and metalloproteases, these fragments increased in abundance.

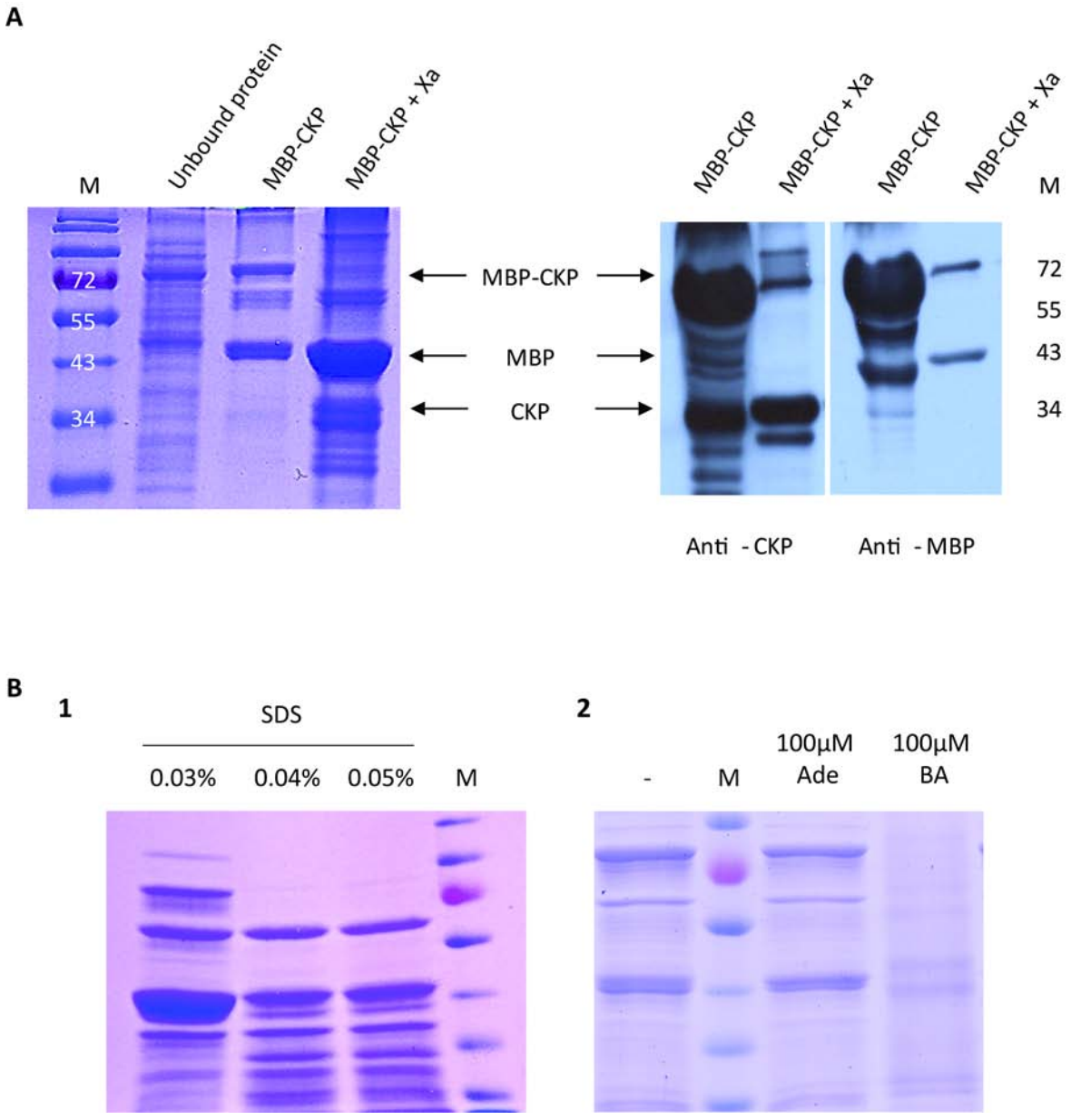

Figure 4.3 Cleavage of MBP-CKP fusion protein by Xa protease
A. Basic cleavage reaction by addition of 1%(w/w) Xa protease. Coomassie stain and immunoblot with anti-CKP and anti-MBP. **B.** Cleavage reaction in the presence of **1**. SDS or **2**. putative substrate to relax the protein about the Xa target site. M = Molecular weight marker, kDa.

4.5 Purification of StCKP1

4.5.1 Purification by affinity chromatography

Products of Xa cleavage were purified by affinity chromatography, yielding up to 7.6mg total protein/5l culture, according to methods outlined previously (section 2.5.6.1). This method of purification decreased the abundance of MBP by binding to the amylose resin. However MBP was not completely removed. The 60kDa contaminating fragment also remained, presumably as this is a product of degradation of the MBP-CKP fusion protein which no longer has a maltose binding site, or that degradation has caused sufficient change in conformation of the protein that the maltose binding site is no longer accessible (figure 4.4a).

4.5.2 Purification by gel filtration

The protein solution produced by cleavage of the MBP-CKP fusion protein which had already been part-purified by affinity chromatography was concentrated to approximately 1ml. The protein solution was applied to a Superdex 200 FPLC column packed as previously described (section 2.5.6.2). The fractions collected from each elution step containing protein were concentrated approximately 10 fold and analysed by SDS-PAGE (figure 4.4b). Yields of StCKP1 were however not high enough at less than 0.2mg StCKP1/5l culture to carry out full kinetic characterisation of the enzyme and so this method of purification was only used for initial enzyme assays described in this chapter. For kinetic characterisation (see chapter 5) StCKP1 was purified by two rounds of affinity chromatography (section 4.5.1) resulting in yields between 6.2 and 7.6mg total protein/5l culture.

4.6 Purification of MBP

In order to test that the activity measured in assays was due to purified StCKP1 and not an artefact of possible contaminating proteins remaining in the suspension after purification, the pMalc2x vector was transformed into the same *E.coli* ER2508 host. MBP was purified in the same way as described in section 4.3 and this protein used as a control in assays carried out with StCKP1 purified from the MBP-CKP fusion protein.

4.7 Determination of StCKP1 activity

As discussed earlier (section 4.1), according to protein sequence and the presence of three conserved domains of protein structure, StCKP1 is predicted to have nucleoside phosphorylase activity. It would be of great interest and potential use to identify a nuceloside phosphorylase involved in interconversion of cytokinin. From a purely scientific view point, to date only LOG has

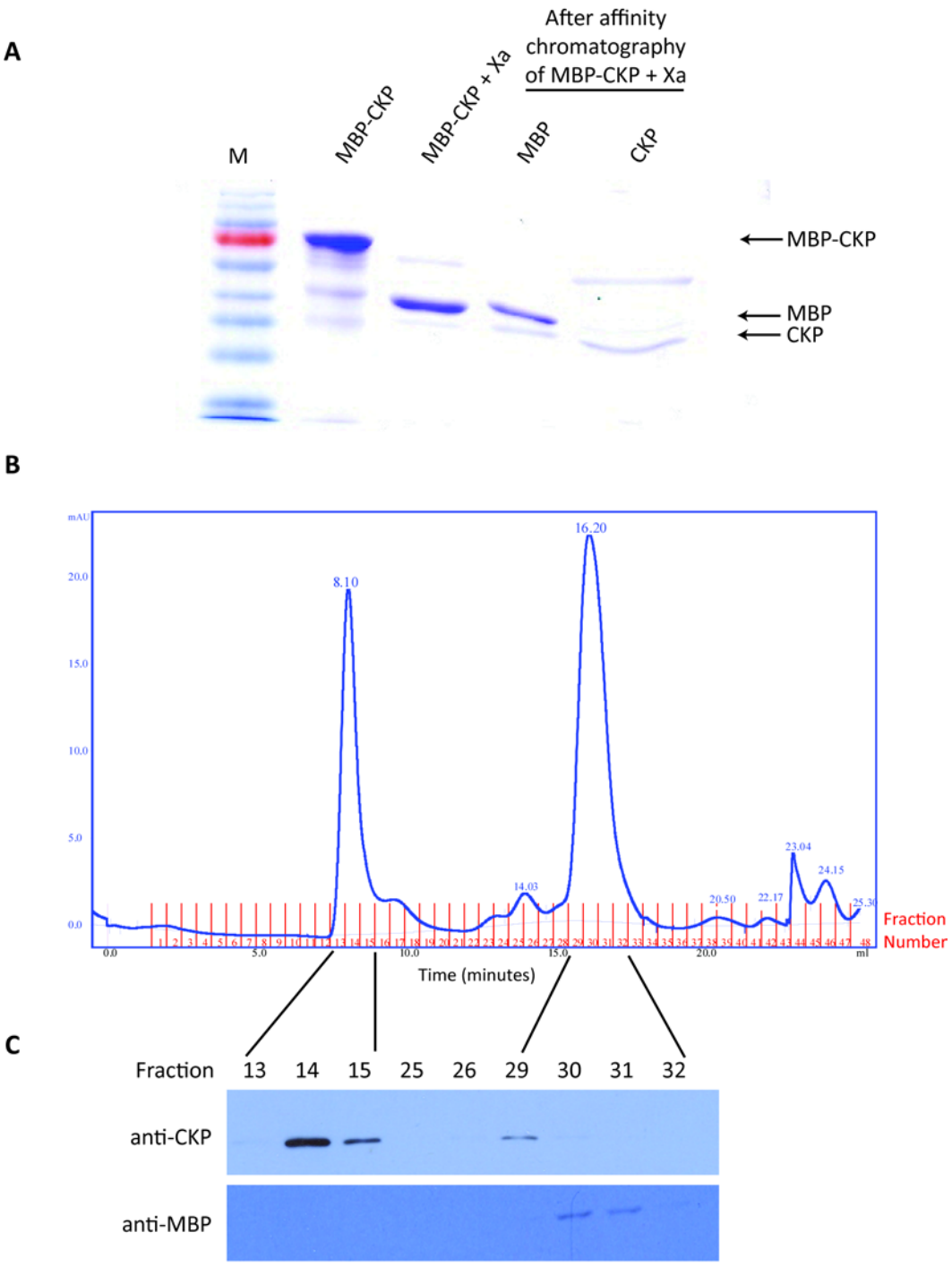

Figure 4.4 Purification of StCKP1 after cleavage from MBP-CKP with Xa
A. Products of affinity chromatography purification on amylose resin. 5mg total protein separated by SDS-PAGE and Coomassie stained. **B.** Superdex 200 FPLC purification of 'CKP' fraction yielded by affinity chromatography. **C.** Immunoblot indicates FPLC peak at 8.10 minutes (fractions 14 and 15) is StCKP1 while the peak at 16.20 (fractions 30 and 31) is MBP.

been identified as an enzyme specifically interconverting cytokinins by hydrolysis at the N^9 residue (Kurakawa et al., 2007). Other enzymes shown to interconvert cytokinins have had a higher affinity for adenine and adenine conjugates and so are considered to be primarily involved in the adenine salvage pathway (Chen and Kristopeit, 1981a, b; Chen et al., 1982b). The identification and characterisation of another enzyme in the interconversionary pathway would aid an increase in the understanding of cytokinin interconversion and its regulation.

An end-point assay for nucleosidase activity was developed from the methods of Chaudhary et al. (2006), Kicska et al. (2002) and Moshides (1988). The substrates and donors were adapted depending on nucleosidase activity being assayed. When assaying for phosphorolytic activity, the assay mix (section 2.7.3.) was supplemented with 40mM K_2HPO_4 as a phosphate donor and 20µM cytokinin riboside substrate of [9R]iP, [9R]Z or [9R]DZ. When assaying for ribosyltransferase activity, the same base assay mix was supplemented with 40mM D-ribose 1-phosphate Bis(cyclohexylamine) (R 1-P) as a ribosyl donor and 20µM cytokinin base substrate of iP, Z or DZ. The assay mix was warmed to 30°C before adding 10µg StCKP1 purified by gel filtration to give a final reaction volume of 50µl. Following incubation of the assay at 30°C for 10 minutes, 5 volumes ice cold 95% (v/v) ethanol was added to precipitate the protein and thus halt the reaction. Before loading onto the HPLC, protein was removed from the reaction mix by filter sterilisation using a pore size of 0.2µm and the reaction mix was diluted to contain less than 10% ethanol to allow cytokinins to partition in to the stationary phase. 1ml of diluted reaction mix, devoid of protein, was loaded onto the column and retention times provided by UV absorption compared to those of the standards run.

A methanol gradient (figure 4.5 B) adapted from that used by Turnbull and Hanke (1985a) was employed to separate cytokinins over an elution period of 35 minutes (figure 4.5). Initially and after every 4-5 sample gradients run, 0.5ml of a cytokinin standard solution was applied to the column. The solution comprised twelve cytokinins each at 1µM (zeatin (Z), zeatin riboside ([9R]Z), zeatin ribotide ([9R-MP]Z), zeatin 9-glucoside ([9G]Z), dihydrozeatin (DZ), dihydrozeatin riboside ([9R]DZ), dihydrozeatin ribotide ([9R-MP]DZ), dihydrozeatin 9-glucoside ([9G]DZ), isopentenyladenine (iP), isopentenyladenosine ([9R]iP), isopentenyladenosine 5′-monophosphate ([9R-MP]iP), and isopentenyladenine 9-glucoside ([9G]iP)). Figure 4.5 shows a typical UV absorption trace obtained for this set of cytokinin standards and their retention times and the percentage change in methanol throughout the gradient. By running a set of standards after initialisation of the HPLC system and again after every 4-5 extracts, retention times under the prevailing temperature and pH (solvent) conditions were determined.

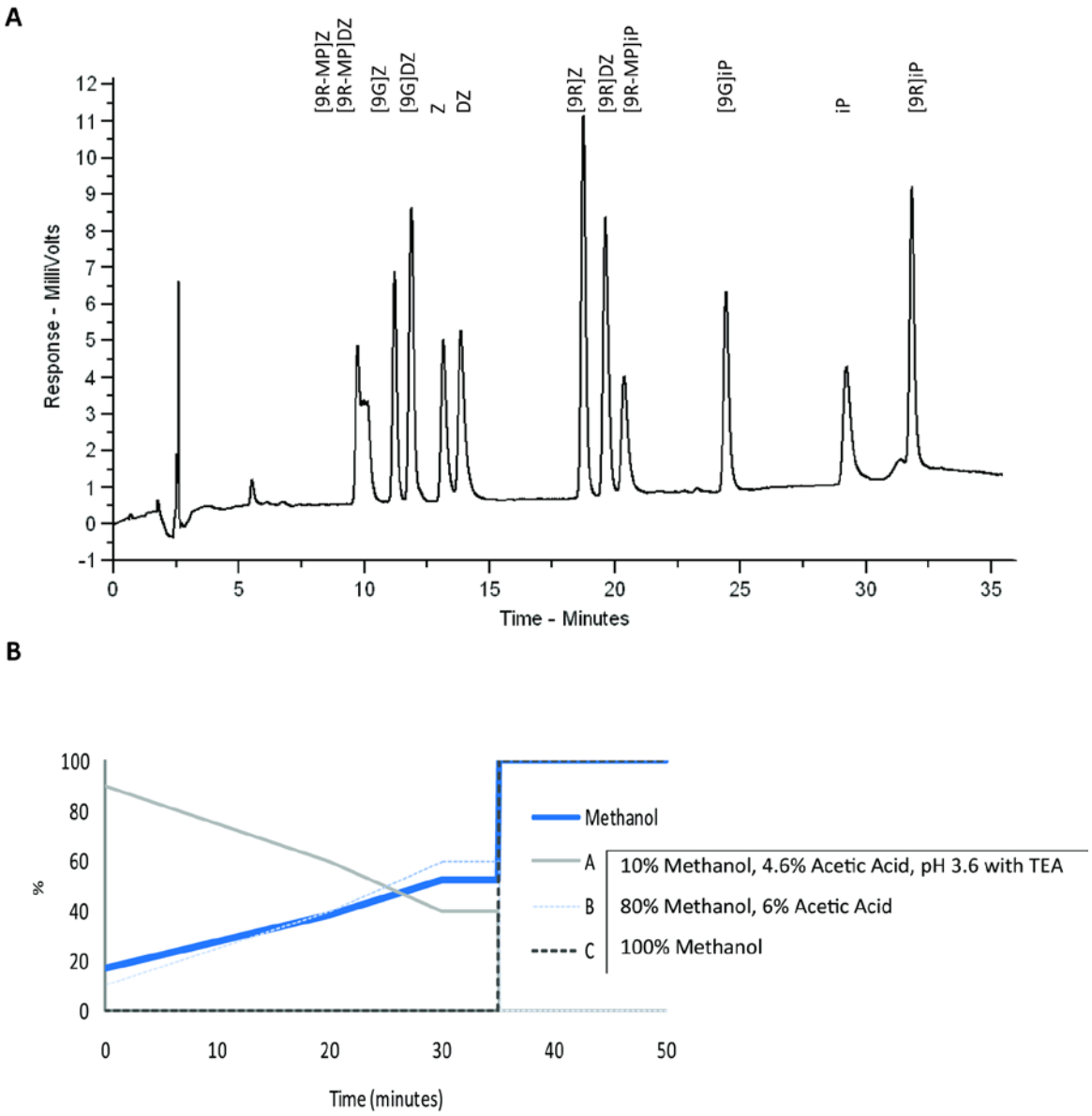

Figure 4.5 Cytokinin separation over a methanol gradient
A. Typical chromatogram of twelve isoprenoid cytokinin standards of 500pmol each. **B.** Methanol gradient and solvent used as previously described by Turnbull and Hanke (1985b)

Stock solutions at 10µM were prepared for each of the twelve constituent cytokinin standards by dissolving a small amount of the solid cytokinin in a small amount of methanol, and making up to 100 ml in H_2O. The concentration of the solution was determined spectrophotometrically at a wavelength of 270nm, using the methanol extinction coefficients specified by Apex Organics. The solution was then diluted to 10µM using H_2O and stored at -20 °C.

4.8 Determination of phosphorolytic activity

Reaction products of four different reactions were purified and diluted as described previously (section 4.7), together with a set of standards, containing base, riboside, ribotide and 9-glucoside for each of iP, Z and DZ cytokinin types respectively and were loaded onto a primed C18 HPLC column. The reaction products were eluted over a 35 minute methanol gradient (section 4.7 & figure 4.5) and UV absoption traces obtained by HPLC separation and UV detection at 254nm were compared. With 20µM [9R]iP as a substrate in the presence of excess inorganic phosphate, purified StCKP1 catalysed the transfer of the ribosyl moiety from [9R]iP (figure 4.6 A). In the absence of inorganic phosphate, [9R]iP was not cleaved detectably (figure 4.6 E). A control reaction using MBP purified from pMalc2x vector showed no activity (figure 4.6 C). When presented with 20µM [9R]Z, and in the presence of an excess of inorganic phosphate donor, StCKP1 catalysed the same phosphorolysis reaction as with [9R]iP as substrate (figure 4.7 A). Again, both in the absence of inorganic phosphate (figure 4.7 E) and with a negative control provided by purified MBP from the pc2x vector (figure 4.7 C), phosphorolysis of the ribosyl moiety did not occur. When offered 20µM [9R]DZ with an excess of inorganic phosphate in the reaction mix, the ribose moiety was again transferred from the nucleoside substrate (figure 4.8 A) while the control reactions carried out were unsuccessful in cleaving the ribose moiety from [9R]DZ (figure 4.8 C & E).

4.9 Validation of phosphorolytic activity

In addition to the results obtained by HPLC separation and UV detection of products of reaction, liquid chromotography coupled to tandem mass spectrometry (LC-Ms-MS) was used to identify the compounds generated unambiguously. Mass spectrometery has an advantage over UV detection coupled to HPLC in that three-dimensional data is also generated. In addition to signal strength, LC-MS-MS generate mass spectral data that can provide valuable information about the molecular weight, structure, identity, quantity, and purity of a sample. Mass spectral data adds specificity that increases confidence in the results of both qualitative and quantitative analyses by HPLC alone.

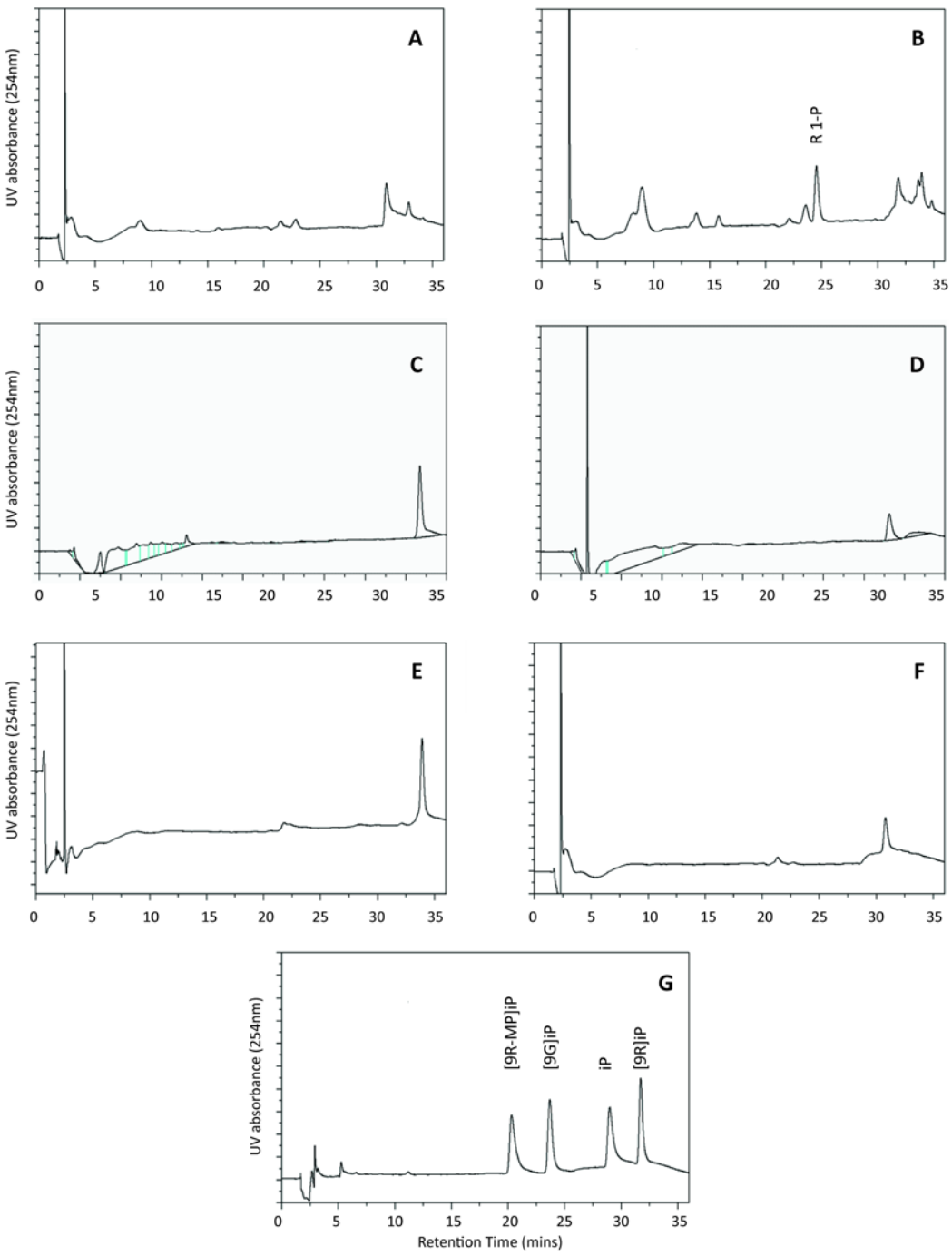

Figure 4.6 Chromatograms of HPLC separated isopentenyladenine-type (iP) products of reactions catalysed by recombinant StCKP1

Reactions **A, B, E** & **F** were carried out by addition of 10µg StCKP1 purified by gel filtration, reactions **D** & **E** were carried out with 10µg MBP purified from the same bacterial strain transformed with the empty pc2x vector (NEB). Substrate pairs were as follows: **A** & **C,** [9R]iP + Pi; **B** & **D**, iP + R 1-P; **E**, [9R]iP in absence of Pi; **F,** iP in absence of R 1-P. **G** shows 500pmol each of [9R-MP]iP, [9G]iP, iP, [9R]iP.

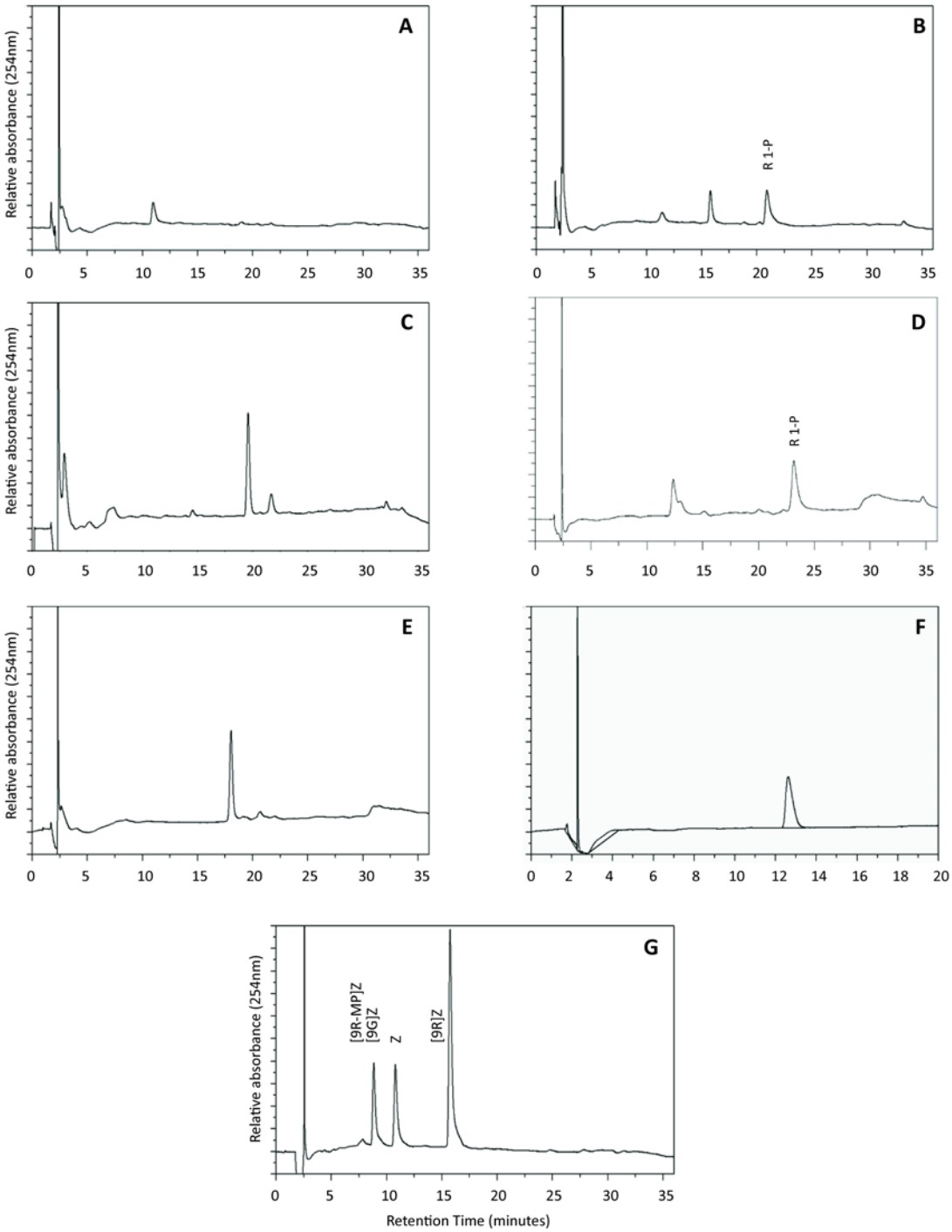

Figure 4.7 Chromatograms of HPLC separated zeatin-type (Z) products of reactions catalysed by recombinant StCKP1

Reactions **A**, **B**, **E** & **F** were carried out by addition of 10µg StCKP1 purified by gel filtration, reactions **D** & **E** were carried out with 10µg MBP purified from the same bacterial strain transformed with the empty pc2x vector (NEB). Substrate pairs were as follows: **A** & **C**, [9R]Z + Pi; **B** & **D**, Z + R 1-P; **E**, [9R]Z in absence of Pi; **F**, Z in absence of R 1-P. **G** shows 500pmol each of [9R-MP]Z, [9G]Z, Z, [9R]Z.

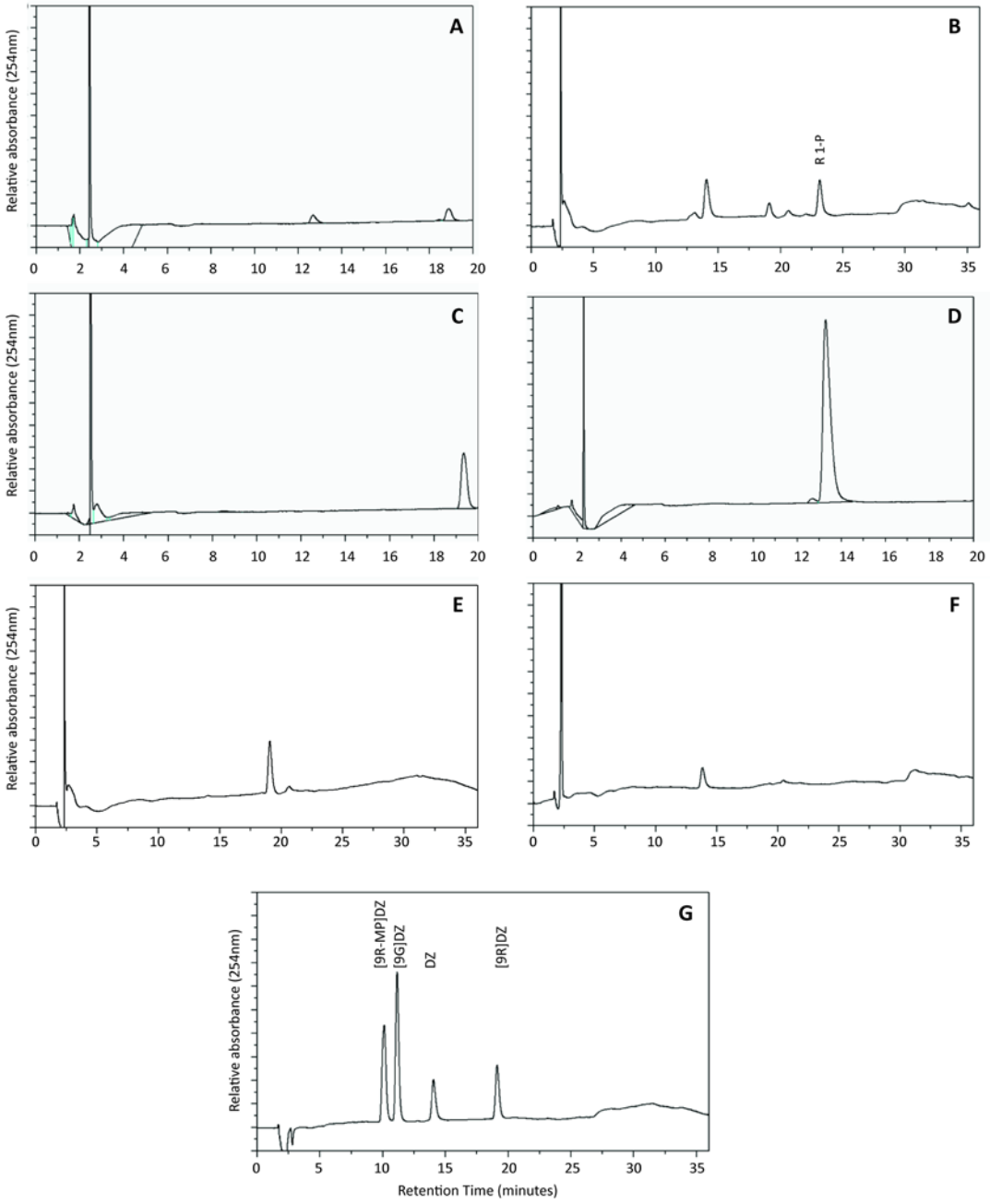

Figure 4.8 Chromatograms of HPLC separated dihydrozeatin-type (DZ) products of reactions catalysed by recombinant StCKP1

Reactions **A**, **B**, **E** & **F** were carried out by addition of 10µg StCKP1 purified by gel filtration, reactions **D** & **E** were carried out with 10µg MBP purified from the same bacterial strain transformed with the empty pc2x vector (NEB). Substrate pairs were as follows: **A** & **C**, [9R]DZ + Pi; **B** & **D**, DZ + R 1-P; **E**, [9R]DZ in absence of Pi; **F**, DZ in absence of R 1-P. **G** shows 500pmol each of [9R-MP]DZ, [9G]DZ, DZ, [9R]DZ.

Validation of the results of HPLC analysis included purifying a fresh preparation of StCKP1. Reactions were carried out pairing 20µM cytokinin riboside and 4mM K_2HPO_4 as inorganic phosphate donor as before (sections 2.7.3, 4.7 & 4.8). The products of reaction were taken to dryness, resuspended in acetonitrile and diluted to 200µl final volume using ammonium acetate. To each sample, a set of internal deuterium labelled cytokinin standards was added to give a retention time for all likely candidates for tandem mass spectrometry and also to estimate recovery. A gradient of acetonitrile in 10mM ammonium acetate (pH 3.4) was used to resolve cytokinin substrates and products of reaction. Initially the gradient was run isocratically at 5% solvent for 4 minutes, then rising to 14% at 20 minutes and further to 32% at 25 minutes with a flow rate of 200µl min^{-1} (section 2.6.3.2). Samples were run twice each, once carrying out multiple reaction monitoring (MRM) which looks at one diagnostic MS-MS parent-daughter ion pair per compound. This is most sensitive and quantitatively accurate. A second run was carried out in enhanced product ion (EPI) mode to give a more complete MS-MS spectra by letting the instrument find compounds eluted, and also by specifying a list of compound masses. EPI mode was much less sensitive than diagnostic analysis by MRM, but for the purposes of this validation was of greater use because confirmation of compound identity rather than accurate quantitation was of greater value.

Offering 20µM [9R]iP as a substrate for purified StCKP1 in the presence of an excess of inorganic phosphate, the overlaid extracted ion chromatogram (XIC) of the MRM traces generated for the reaction show peaks at 25.2 minutes and 26.8 minutes, depicted in grey and red respectively. These correspond to the molecular masses of iP (204amu) and [9R]iP (336amu). The peaks depicted in green and blue at 24.9 and 26.7 minutes correspond to internal standards of [$^2H_5$]-labelled iP and [$^2H_5$][9R]iP respectively (figure 4.9 A). Alongside data resolved by HPLC analysis, this indicates StCKP1 is catalysing phosphorolysis of [9R]iP at N^9 to release iP. EPI monitoring for compounds of with atomic masses of 336 ([9R]iP) and 204 (iP) was also carried out . Correlation of the overlaid XIC MRM traces and total ion chromatogram (TIC) of EPI at an atomic mass of 336 indicates the major compound of amu 336 is [9R]iP (figures 4.9 C). When analysed by mass spectrometry, the spectra produced has the same characteristic products of given intensities known for [9R]iP (figure 4.12 B), confirming the presence of the substrate. The products shown in this spectrum are of 204amu and 148amu and 136amu, corresponding to atomic masses of iP, Ade-C+ and Ade respectively (figure 4.9 D). Of greater interest is the TIC of EPI 204 which yields a chromatogram with a number of peaks of lesser magnitude than seen when analysing for [9R]iP (figure 4.9 E). The spectra produced for the product with a retention time of 25.2 minutes (figure 4.9 F), is the same retention time as for iP in the MRM trace, are the same for that of an iP standard (figure 4.9 B). This indicates that the product of reaction is iP which characteristically has a dominant product of mass spectrometry with a

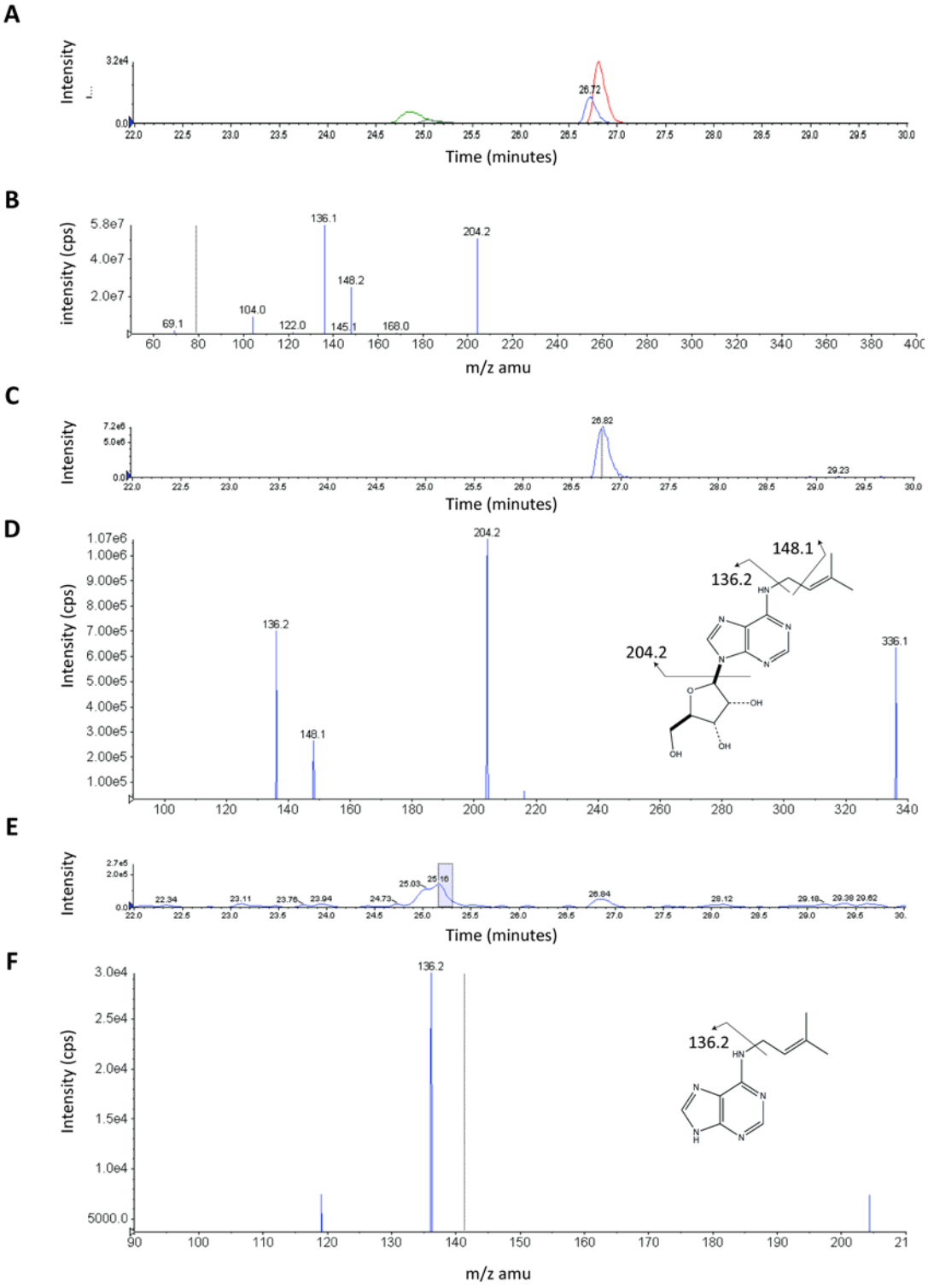

Figure 4.9 LC-MS-MS chromatograms and spectra of reaction products with [9R]iP as a substrate
A. MRM chromatogram of [9R]iP (red) and iP (grey) with internal deuterated standards d[9R]iP (blue) and diP (green). **B.** Mass spectrum of iP standard. **C**. EPI chromatogram of products of 336amu. **D.** Mass spectrum of EPI 336amu peak with 26.82 minute retention time. Inset: structure of parent ion [9R]iP and fragmentation to produce daugther ions. **E.** EPI chromatogram of products of 204amu. **F.** Mass spectrum of EPI 204amu peak with 25.10 minute retention time. Inset: structure of parent ion iP. Fragmentation to produce daughter ions is indicated by intersecting lines. Data presented are screen shots of output.

molecular mass of 136amu, corresponding to the atomic mass of Ade. The spectra produced for other compounds of 204amu were found to be non-specific, non-cytokinin compounds in the reaction mix (data not shown).

With 20µM [9R]Z as a substrate for purified StCKP1 in the presence of an excess of inorganic phosphate, the two XICs of the MRM traces generated for the reaction show peaks at 12.2 minutes and 17.25 minutes, depicted in blue on each trace. These correspond to the molecular masses of Z at 220amu and [9R]Z at 352amu. The earlier of the two peaks depicted in red on each of these traces at 12.08 and 17.1 minutes correspond to internal standards of $[^2H_5]$Z and $[^2H_5]$[9R]Z respectively. The second of the two red peaks corresponds to $[^2H_5]$DZ with an atomic mass of 227 and $[^2H_5]$[9R]DZ with an atomic mass of 359 (figures 4.10 A and B). Alongside data resolved by HPLC analysis, this indicates StCKP1 is catalysing ribosyl transfer in the presence of inorganic phosphate of [9R]Z at N^9 to release Z. EPI monitoring for compounds of with molecular masses of 352 ([9R]Z) and 220 (Z) was also carried out . Agreement between the XIC MRM chromatograms and the TIC of EPI for an atomic mass of 352 indicates the major compound, with an amu of 352, is [9R]Z (figure 4.10 D). When analysed by mass spectrometry, the spectrum produced is the same as that for [9R]Z (figure 4.13 C), confirming the presence of the substrate. The products shown in this spectrum are of 220amu and 202amu and 136amu, corresponding to Z, Ade-C+ and Ade respectively (figure 4.10 E). Of greater interest is the TIC of EPI 220 which yields a chromatogram with a number of peaks of lesser magnitude, although the peak with the same retention time as observed in XIC MRM for Z is dominant (figure 4.10 F). The spectrum produced for the product with a retention time of 12.2 minutes (figure 4.10 G), which is the same retention time as seen for Z in the MRM trace, are the same for that of Z standard (figure 4.10 C), indicating that the product of reaction is Z. As in the mass spectrum produced for the reaction production formed from iP, the dominant product of bombardment has an atomic mass of 136, corresponding to Ade. The spectra produced for other compounds of 220amu were found to be non-specific, non-cytokinin compounds in the reaction mix (data not shown).

Presenting 20µM [9R]DZ as a substrate for purified StCKP1 in the presence of an excess of inorganic phosphate, the two XICs of the MRM traces generated for the reaction show peaks at 13.02 minutes (figure 4.11 A) and 17.94 minutes (figure 4.11 B), depicted in blue on each trace. These correspond to the molecular masses of DZ at 222amu and [9R]DZ at 354amu. The second of the two peaks depicted in red on each of these traces at 12.66 and 17.75 minutes correspond to internal standards of $[^2H_5]$DZ and $[^2H_5]$[9R]DZ respectively. On each UV absorption trace, the earlier of the two red peaks correspond to $[^2H_5]$Z and $[^2H_5]$[9R]Z respectively . Confirming the HPLC results, this indicates

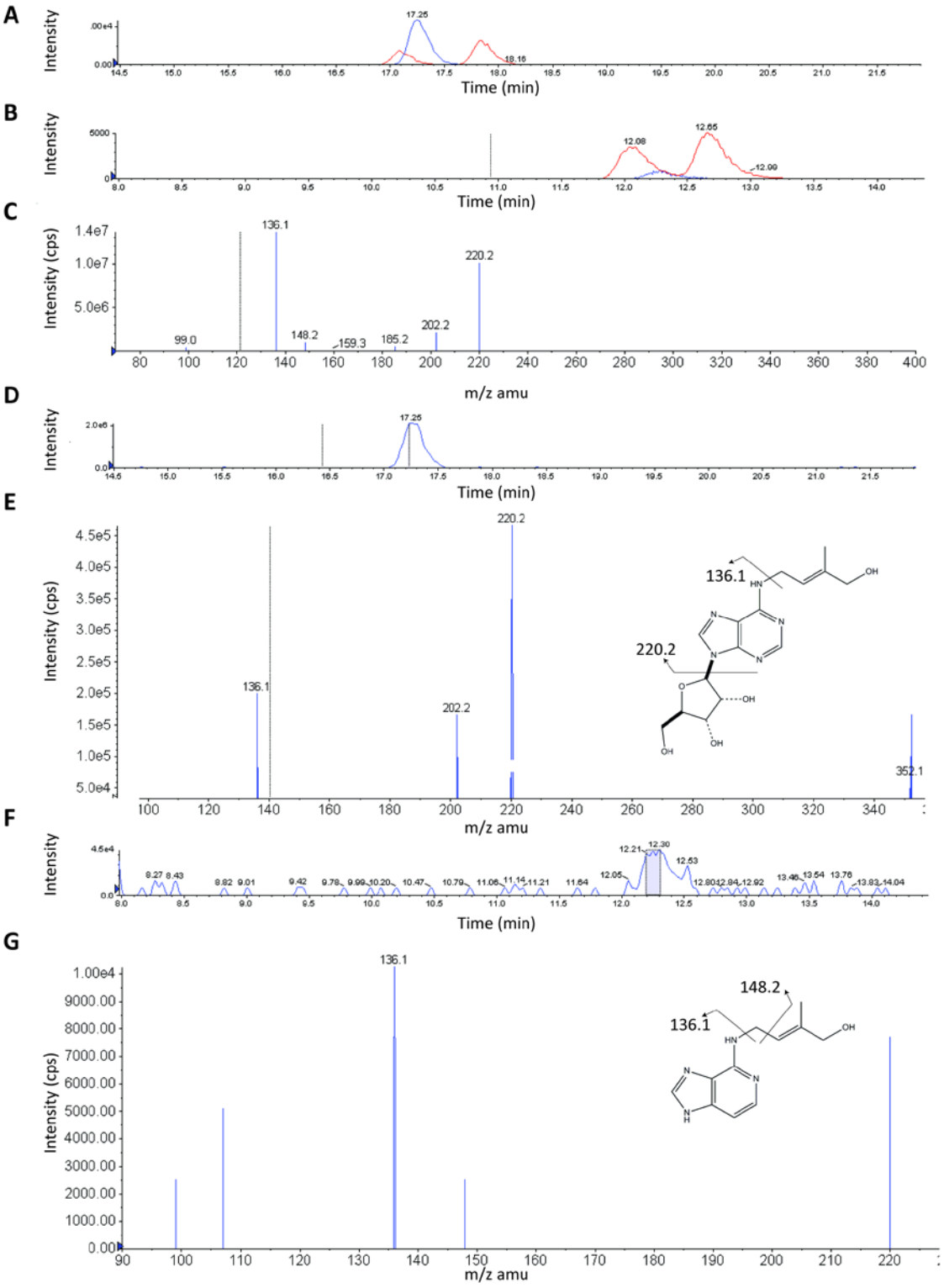

Figure 4.10 LC-MS-MS chromatograms and spectra of reaction products with [9R]Z as a substrate
A. MRM chromatogram of [9R]Z (blue) with d[9R]Z and d[9R]DZ internal standards (red) **B.** MRM chromatogram of Z (blue) with dZ and dDZ internal standards (red). **C.** Mass spectrum of Z standard. **D**. EPI chromatogram of products of 352amu. **E.** Mass spectrum of EPI 352amu peak with 17.25 minute retention time. Inset: structure of parent ion [9R]Z and fragmentation to produce daugther ions. **F.** EPI chromatogram of products of 220amu. **G.** Mass spectrum of EPI 220amu peak with 12.35 minute retention time. Inset: structure of parent ion Z. Fragmentation to produce daughter ions is indicated by intersecting lines. Data presented are screen shots of output.

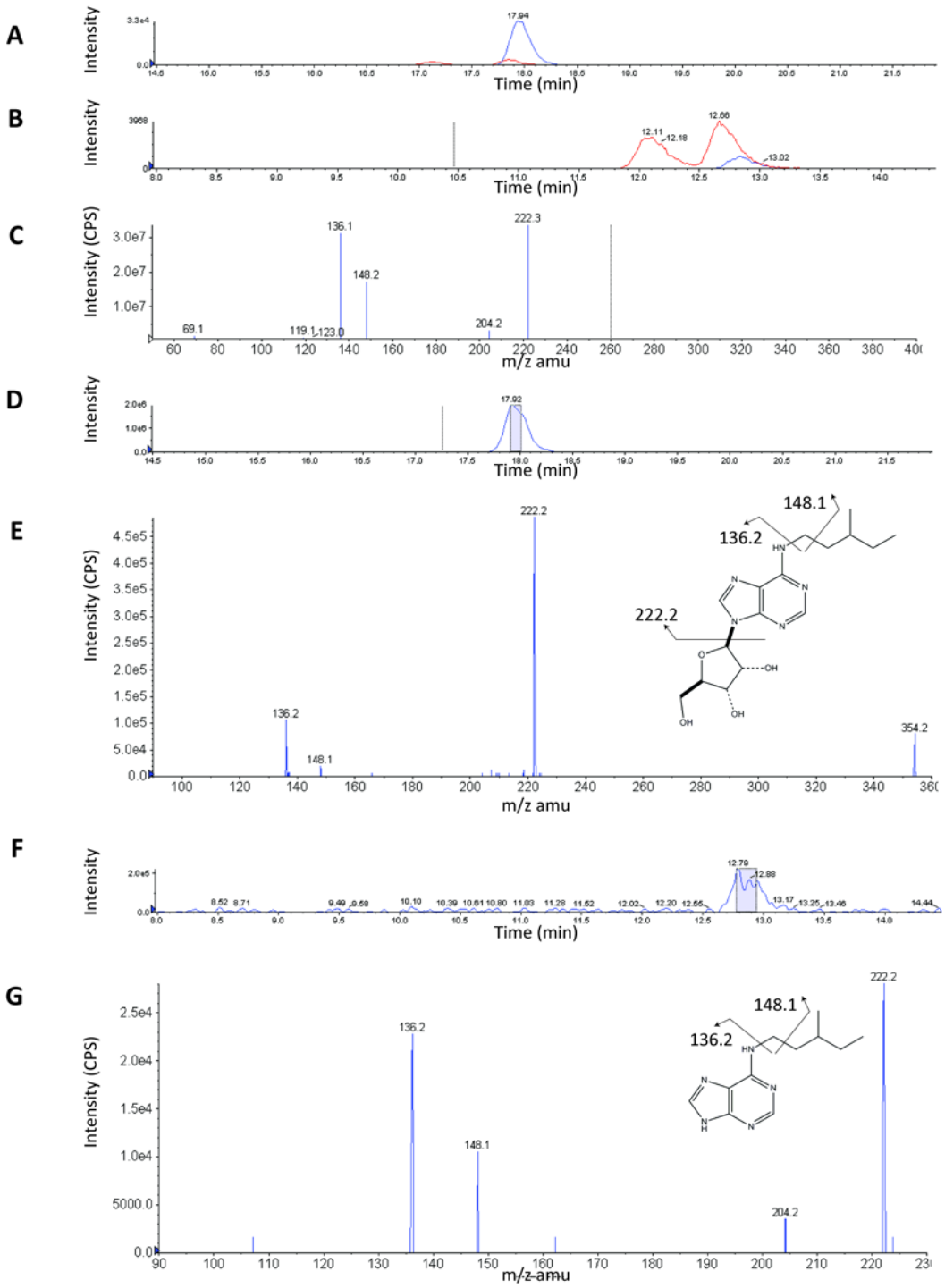

Figure 4.11 LC-MS-MS chromatograms and spectra of reaction products with [9R]DZ as a substrate
A. MRM chromatogram of [9R]DZ (blue) with d[9R]Z and d[9R]DZ internal standards (red) **B.** MRM chromatogram of DZ (blue) with dZ and dDZ internal standards (red). **C.** Mass spectrum of DZ standard. **D.** EPI chromatogram of products of 354amu. **E.** Mass spectrum of EPI 354amu peak with 17.94 minute retention time. Inset: structure of parent ion [9R]DZ and fragmentation to produce daugther ions. **F.** EPI chromatogram of products of 222amu. **G.** Mass spectrum of EPI 222amu peak with 12.80 minute retention time. Inset: structure of parent ion DZ. Fragmentation to produce daughter ions is indicated by intersecting lines. Data presented are screen shots of output.

StCKP1 is catalysing cleavage of [9R]DZ at N^9, in the presence of inorganic phosphate, to release DZ. EPI monitoring for compounds of molecular masses of 354 ([9R]DZ) and 222 (DZ) was also carried out . Agreement between the XIC MRM chromatogram and the TIC of EPI at an atomic mass of 354 (figure 4.11 D) indicates the major compound of amu 354 is [9R]DZ. When analysed by mass spectrometry, the spectrum produced is the same as that for [9R]DZ standard (figure 4.14 C), confirming the presence of the substrate. The products shown in this spectrum are of 222amu and 148amu and 136amu, corresponding to DZ, Ade-C+ and Ade respectively (figure 4.11 E). Of greater interest is the TIC of EPI 222 (figure 4.11 F) which yields a chromatogram with a number of peaks of lesser magnitude, although the peak with the same retention time as observed in XIC MRM for DZ is dominant. The spectrum generated from the product with a retention time of 12.8 minutes (figure 4.11 G), which is the same retention time as seen for DZ in the MRM trace, is the same for that of a DZ standard (figure 4.11 C), indicating that the product of reaction is DZ. As with the mass spectra produced for the reaction products formed from iP and Z, the dominant product of bombardment has an atomic mass of 136, corresponding to Ade. The spectra produced for other compounds of 220amu were found to be non-specific, non-cytokinin compounds in the reaction mix (data not shown).

In summary, validation of StCKP1 phosphorolytic activity carried out by LC-MS-MS agrees with the results of HPLC analysis. Two cytokinin types were found in each reaction mix, the substrate and a single product. When analysed by tandem mass spectrometry, the substrate was confirmed to be a cytokinin riboside by comparison with spectra produced for cytokinin riboside standards (figures 4.9 D, 4.10 E and 4.11 E). Spectra produced for the major product with an amu of that of the corresponding cytokinin base confirmed that the product of reaction was the corresponding base to the riboside substrate used (figures 4.9 F, 4.10 G and 4.11 G).

4.10 Determination of ribosyltransferase activity

Methods for determining ribosyltransferase activity were the same as for determination of phosphorolytic activity, with the cytokinin base as substrate and R 1-P. Reaction products of four different reactions were purified and diluted as described previously (section 4.7), and alongside a set of standards, containing base, riboside, ribotide and 9-glucoside for each of iP, Z and DZ cytokinin types respectively and were loaded onto a primed C18 HPLC column. The reaction products were eluted over a 35 minute methanol gradient (section 4.7 and figure 4.5) and traces were compared. With 20µM iP as a substrate in the presence of excess R 1-P, purified StCKP1 catalysed the formation of [9R]iP from the two substrates provided (figure 4.6 B). In the absence of inorganic phosphate or

R-1P, no reaction was detected (figure 4.6 F). Negative controls using MBP purified from pMalc2x vector showed no detectable activity (figure 4.6 D). When presented with 20µM Z, and in the presence of an excess of R 1-P, StCKP1 catalysed the equivalent reaction to that with iP as substrate (figure 4.7 B). Again, in the absence of inorganic phosphate (figure 4.7 F) or a negative control provided by purified MBP (figure 4.7 D), ribosyltransferase activity was not observed. When offered 20µM DZ with an excess of R 1-P in the reaction mix, the ribose moiety was again added at the N^9 position of DZ (figure 4.8 B) while in all other combinations no riboside synthesis was detected (figure 4.8 D&F)).

4.11 Validation of ribosyltransferase activity

Presenting 20µM iP as a substrate for purified StCKP1 in the presence of an excess of R 1-P as a ribosyl donor, the overlaid XIC of the MRM traces generated for the reaction show peaks at 25.2 minutes and 26.8 minutes, depicted in grey and red respectively. These correspond to the molecular masses of iP at 204amu and [9R]iP at 336amu. The peaks depicted in green and blue at 24.9 and 26.7 minutes correspond to internal standards of [$^2H_5$]-labelled iP and [9R]iP respectively (figure 4.12 A). Alongside data resolved by HPLC analysis, this indicates StCKP1 is catalysing conjugation of a ribosyl group to the N^9 of iP producing [9R]iP. EPI monitoring for compounds of with molecular masses of 336 ([9R]iP) and 204 (iP) was also carried out . Agreement between the overlaid XIC MRM traces and TIC of EPI at an atomic mass of 204 indicates the major compound with an amu of 204 is iP (figure 4.12 C). When analysed by mass spectrometry, the spectrum produced is the same as that for an iP standard (figure 4.9 B), confirming the presence of the substrate. The products shown in this spectrum are of 148amu and 136amu, corresponding to Ade-C+ and Ade respectively (figure 4.12 D). Of greater interest is the TIC of EPI 336 which yields a chromatogram with a number of peaks, although the peak of greatest magnitude has a retention time corresponding with [9R]iP (figure 4.12 E). The spectrum produced for the product is the same for that of an [9R]iP standard (figure 4.12 B), indicating that the product of reaction is [9R]iP. The dominant product of mass spectrometry has a molecular mass of 204amu, corresponding to the atomic mass of iP (figure 4.12 F). The spectra produced for other compounds of 336amu were found to be non-specific, non-cytokinin compounds in the reaction mix (data not shown).

Presenting 20µM Z as a substrate for purified StCKP1 in the presence of an excess of R 1-P as a ribosyl donor, the XIC of the MRM chromatograms generated for the reaction show peaks at 12.22 minutes (figure 4.13 A) and 17.24 minutes (figure 4.13 B), depicted in blue in both UV absorption

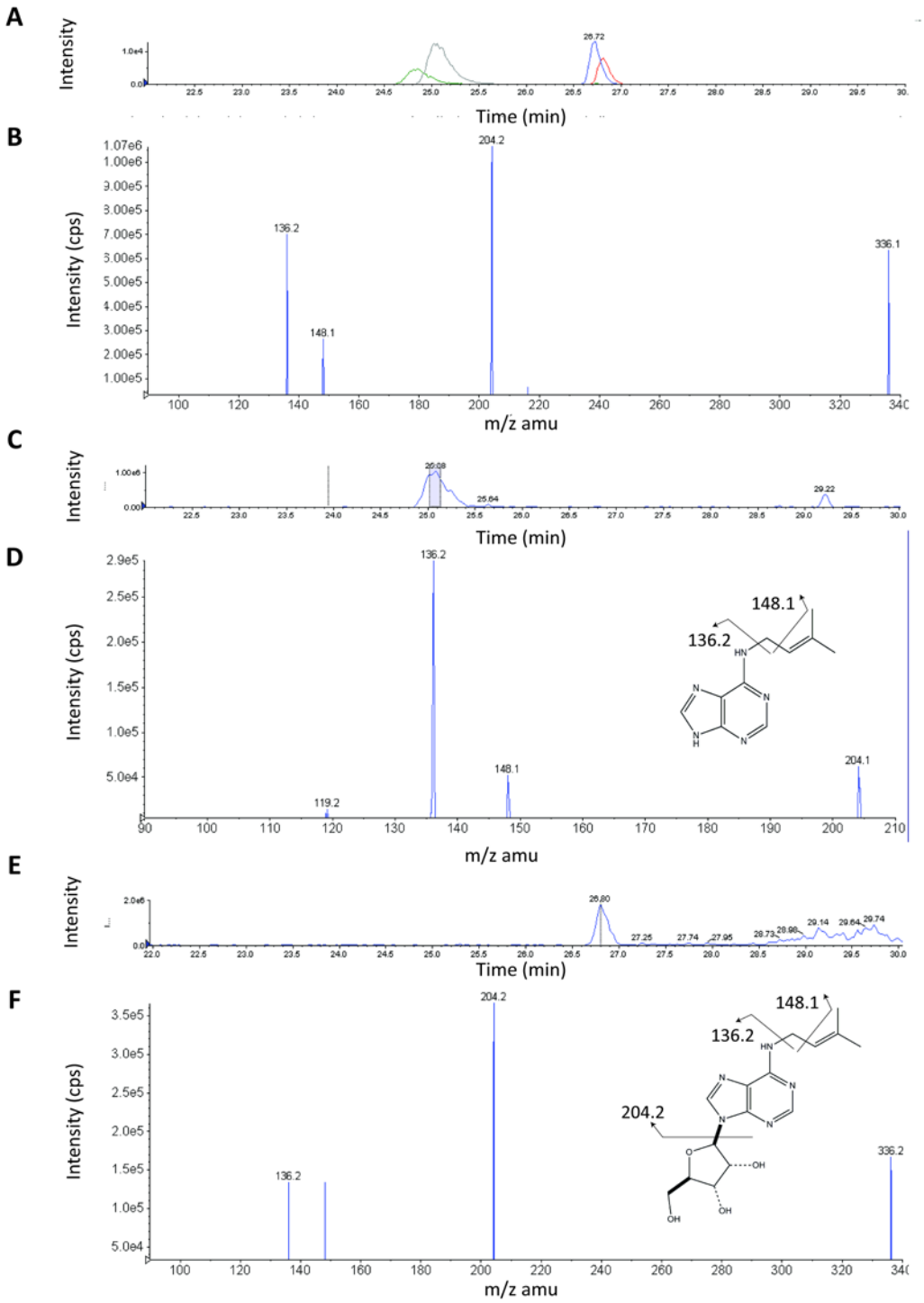

Figure 4.12 LC-MS-MS chromatograms and spectra of reaction products with iP as a substrate
A. MRM chromatogram of [9R]iP (red) and iP (grey) with internal deuterated standards d[9R]iP (blue) and diP (green). **B.** Mass spectrum of [9R]iP standard. **C.** EPI chromatogram of products of 204amu. **D.** Mass spectrum of EPI 204amu peak with 25.88 minute retention time. Inset: structure of parent ion iP and fragmentation to produce daugther ions. **E.** EPI chromatogram of products of 336amu. **F.** Mass spectrum of EPI 336amu peak with 26.80 minute retention time. Inset: structure of parent ion [9R]iP. Fragmentation to produce daughter ions is indicated by intersecting lines. Data presented are screen shots of output.

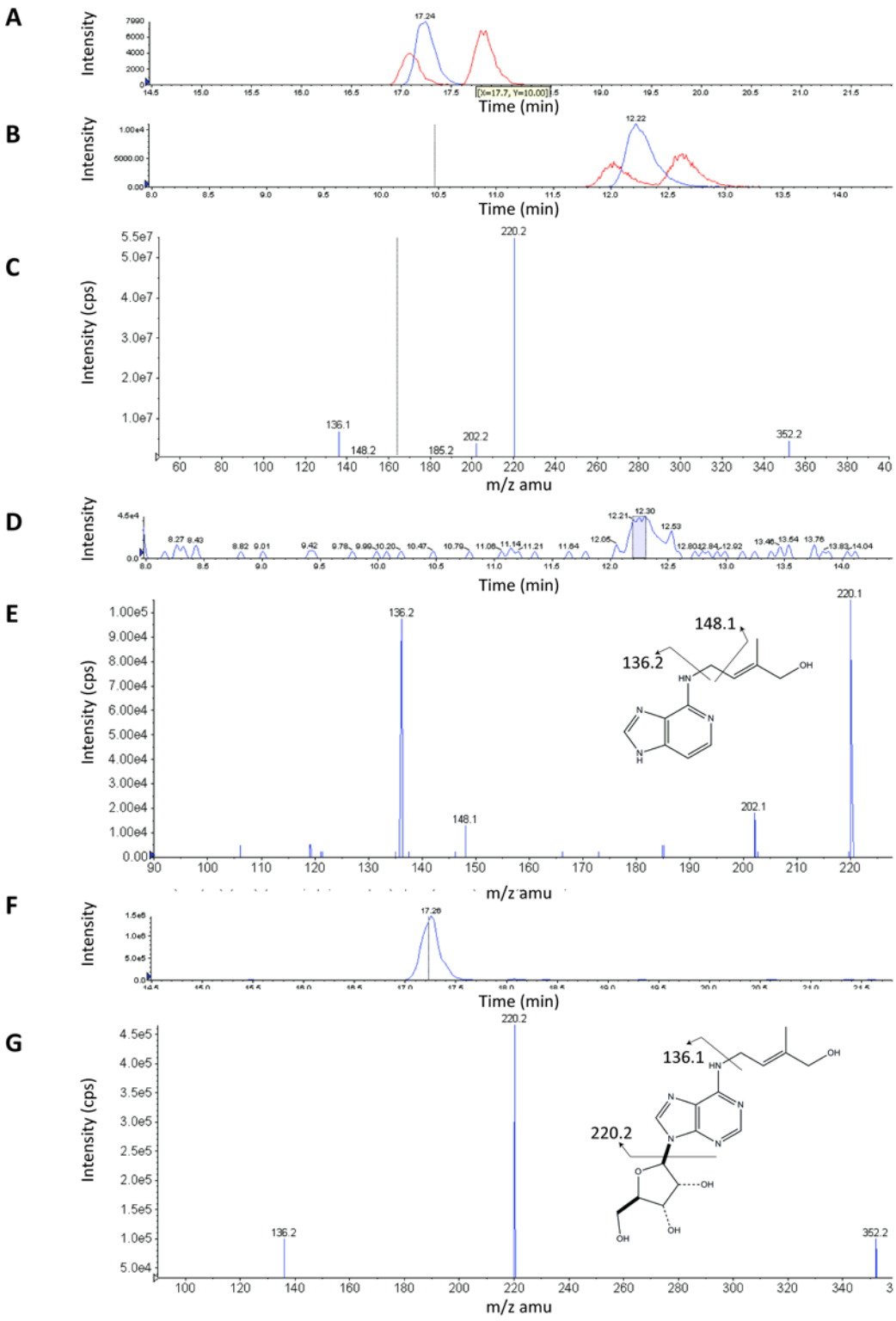

Figure 4.13 LC-MS-MS chromatograms and spectra of reaction products with Z as a substrate
A. MRM chromatogram of [9R]Z (blue) with d[9R]Z and d[9R]DZ internal standards (red) **B.** MRM chromatogram of Z (blue) with dZ and dDZ internal standards (red). **C.** Mass spectrum of [9R]Z standard. **D.** EPI chromatogram of products of 220amu. **E.** Mass spectrum of EPI 220amu peak with 12.25 minute retention time. Inset: structure of parent ion Z and fragmentation to produce daugther ions. **F.** EPI chromatogram of products of 352amu. **G**. Mass spectrum of EPI 352amu peak with 17.25 minute retention time. Inset: structure of parent ion [9R]Z. Fragmentation to produce daughter ions is indicated by intersecting lines. Data presented are screen shots of output.

traces. These correspond to the molecular masses of Z at 220amu and [9R]Z at 352amu. The earlier of the two peaks depicted in red on each of these traces at 12.08 and 17.1 minutes correspond to internal standards of [$^2H_5$]Z and [$^2H_5$][9R]Z respectively. The second of the two red peaks corresponds to [$^2H_5$]DZ with an atomic mass of 227 and [$^2H_5$][9R]DZ with an atomic mass of 359. Matching the HPLC results, this confirms that StCKP1 is catalysing conjugation of a ribosyl group to the N^9 of Z, producing [9R]Z. EPI monitoring for compounds of with molecular masses of 352 ([9R]Z) and 220 (Z) was also carried out. Agreement between the XIC MRM traces and TIC of EPI 352 which yields a chromatogram with a single dominant peak corresponding with [9R]Z (figure 4.13 F). The spectrum produced for the product (figure 4.13 G) is the same for that of an [9R]Z standard (figure 4.13 C), indicating that the product of reaction is [9R]Z. The dominant product of mass spectrometry has a molecular mass of 220amu, corresponding to the atomic mass of Z.

Offering 20µM DZ as a substrate for purified StCKP1 in the presence of an excess of R 1-P as a ribosyl, the XIC of the MRM chromatograms generated for the reaction show peaks at 12.85 minutes (figire 4.14 A) and 17.98 minutes (figure 4.14 B), depicted in blue in both traces. These correspond to the molecular masses of DZ at 222amu and [9R]DZ at 354amu. The second of the two peaks depicted in red on each of these traces at 12.7 and 17.8 minutes correspond to internal standards of [$^2H_5$]DZ and [$^2H_5$][9R]DZ respectively. The earlier of the two red peaks corresponds to [$^2H_5$]Z with an atomic mass of 225 and [$^2H_5$][9R]Z with an atomic mass of 357. Confirming results of HPLC analysis, this indicates StCKP1 is catalysing conjugation of a ribosyl group to the N^9 of DZ producing [9R]DZ. EPI monitoring for compounds of with molecular masses of 354 ([9RD]Z) and 223 (DZ) was also carried out. Agreement between the XIC MRM traces and TIC of EPI 354 yields a chromatogram with a single dominant peak corresponding to [9R]DZ (figure 4.14 F). The spectrum produced for the product (figure 4.14 G) is the same for that of an [9R]DZ standard (fiure 4.14 B), indicating that the product of reaction is [9R]DZ with the dominant product of mass spectrometry having a molecular mass of 222amu, corresponding to the atomic mass of DZ.

In summary, validation of StCKP1 ribosyltransferase activity carried out by LC-MS-MS agrees with the results of HPLC analysis. Two cytokinin types were found in each reaction mix, the substrate and a single product. When analysed by tandem mass spectrometry, the substrate was confirmed to be a cytokinin base by comparison with spectra produced for cytokinin base standards (figures 4.12 D, 4.13 E and 4.14 E). Spectra produced for the major product with an amu of that of the corresponding cytokinin riboside confirmed that the product of reaction was the corresponding riboside to the base substrate used (figures 4.9 F, 4.10 G and 4.11 G).

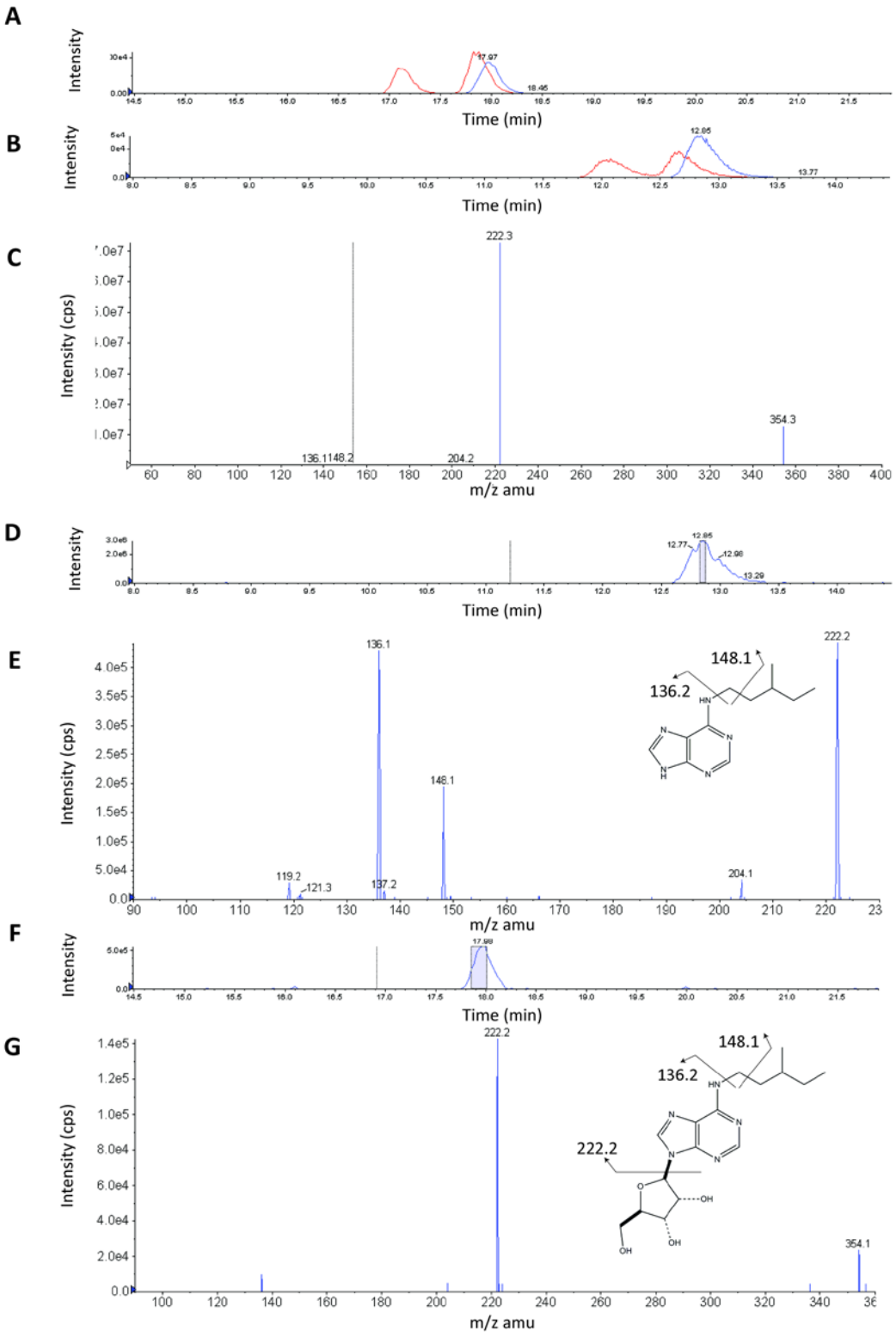

Figure 4.14 LC-MS-MS chromatograms and spectra of reaction products with DZ as a substrate
A. MRM chromatogram of [9R]DZ (blue) with d[9R]Z and d[9R]DZ internal standards (red) **B.** MRM chromatogram of DZ (blue) with dZ and dDZ internal standards (red). **C.** Mass spectrum of [9R]DZ standard. **D.** EPI chromatogram of products of 222amu. **E.** Mass spectrum of EPI 222amu peak with 12.85 minute retention time. Inset: structure of parent ion Z and fragmentation to produce daugther ions. **F.** EPI chromatogram of products of 354amu. **G.** Mass spectrum of EPI 354amu peak with 17.85 minute retention time. Inset: structure of parent ion [9R]Z. Fragmentation to produce daughter ions is indicated by intersecting lines. Data presented are screen shots of output.

4.12 Discussion

In summary, StCKP1 without its predicted transit peptide was over-expressed as the fusion protein MBP-CKP using the pMal expression system. A number of different bacterial host strains deficient in different proteases and some also offering enhanced availability of 'rare' tRNA codons were assayed for expression of MBP-CKP. Strain ER2508 was found to give the highest expression of MBP-CKP and yield of StCKP1 following cleavage from the fusion protein using factor Xa.

The data presented offer substantial evidence for the activity of StCKP1 as a nucleoside phosphorylase which participates in phosphorolysis of cytokinin ribosides to produce cytokinin bases, and also in the reverse reaction of riboside synthesis as a ribosyltransferase catalysing the conjugation of a ribosyl group to the N^9 position of the cytokinin base. This activity resembles that of adenosine phosphorylase, which catalyses the conversion of purine bases to nucleosides depended upon the addition of R 1-P, while the phosphorolysis of nucleosides was dependent upon the presence of inorganic phosphate (Chen and Petschow, 1978).

A crude quantification of substrate/product pairs identified by LC-MS-MS according to the ratio method outlined by Prinsen et al. (1995) supports the HPLC UV-chromatograms and mass spectra presented in identifying the requirement for inorganic phosphate in order for reactions catalysed by StCKP1 to proceed (figure 4.15). This quantification of products suggests that StCKP1 acts preferentially as a ribosyltransferase with the equilibrium lying towards phosphoribosylation rather than phosphorolysis (figure 1.3). The mass spectra were carefully analysed for signs of products from nucleotides, however there was no evidence to suggest StCKP1 acts, like LOG, as a phosphoribosylhydrolase (Kurakawa et al., 2007) or has the same activity as adenosine phosphoribosyltransfease previously identified (Chen et al., 1982b) when offered a cytokinin substrate. Specific activities of StCKP1 when incubated with 20µM cytokinin substrate and an excess of inorganic phosphate or ribosyl donor calculated from quantified LC-MS-MS data (figure 4.15) support this finding that StCKP1 is predominantly responsible for phosphoribosylation of cytokinin bases to form their corresponding riboside (figure 4.16). Chen and Kristopiet (1981a), when assaying for the activity of adenosine nucleosidase in partially purified wheat germ extracts calculated specific activities for [9R]iP and Ado as substrates and found them to be 0.027µM and 0.063µM respectively. These values are similar to those calculated for the cytokinin ribosides assayed in this study, giving confidence in the assay undertaken and results obtained.

During this analysis, a pilot experiment was carried out using LC-MS-MS analytical techniques to ascertain if StCKP1 is able to facilitate phophorolysis or phosphoribosylation of Ado and Ade

A

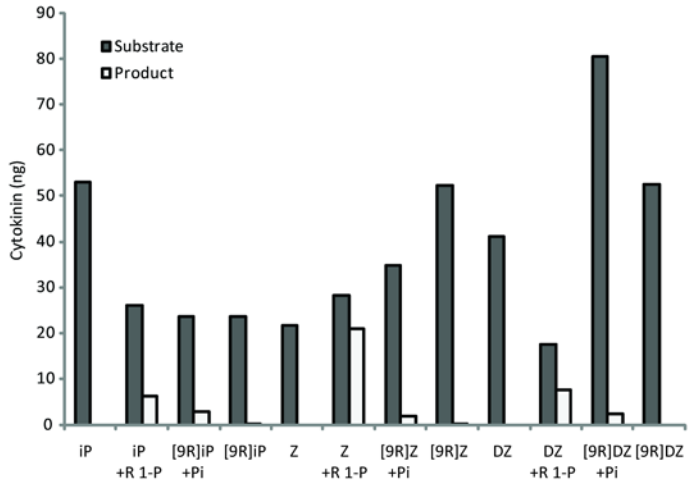

B

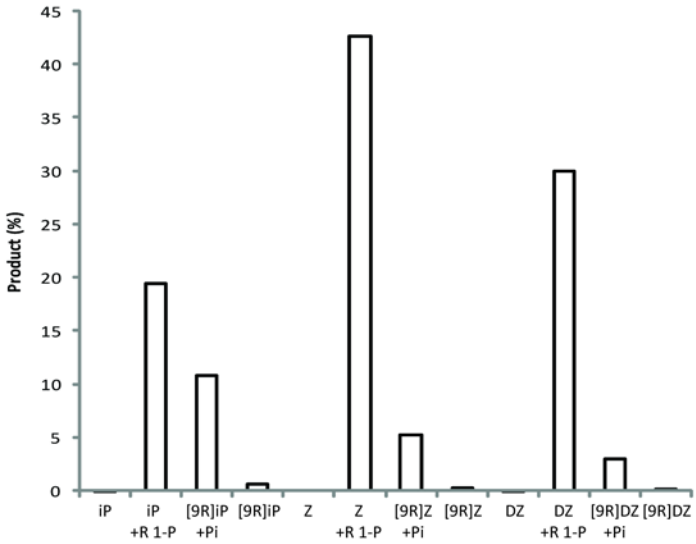

C

Substrate	Specific Activity (µmol/min/mg CKP)
iP	1.88E-02
[9R]iP	9.58E-04
Z	5.97E-02
[9R]Z	1.07E-03
DZ	2.12E-02
[9R]DZ	6.21E-05

Figure 4.15 Quantification of LC-MS-MS data
A. Amounts of cytokinin substrates and products as quantified by MRM analysis according to the methods of Prinsen et al. (1995) including correction for isotopic purity and application of a linear calibration curve. **B.** Percentage conversion. **C.** Calculated specific activities. Quantification was carried out on one sample for each reaction monitored.

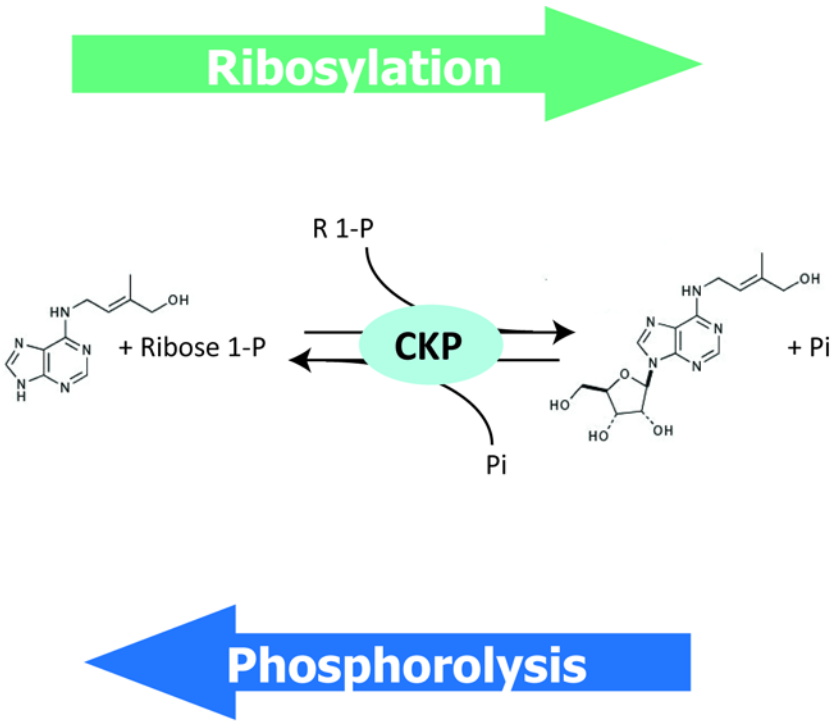

Figure 4.16 Schematic of StCKP1 catalysed interconversion between cytokinin base and riboside in the presence of inorganic phosphate (Pi)
Reaction shown with zeatin (Z) tyoe cytokinin substrates, although schematic equallly applicable to isopentenyladenine (iP) or dihydrozeatin (DZ) cytokinin types.

respectively. A small amount of a compound that resembled AMP in its spectrum was detected in a reaction mix containing Ade and R 1-P, indicating StCKP1 may possess adenosine kinase activity, however detection of Ade and its derivatives was not fully optimised on this machine and so the data cannot be regarded as firm.

The pMal expression system had been chosen as it seemed to be the best route to producing enough pure protein that could be used not only in enzyme assays for determination of activity, but also in the production of a polyclonal antibody. An antibody had previously been raised to a predicted synthetic peptide sequence of StCKP1 (Warnes, 2005), however it has proved to be difficult to use in detection of StCKP1 in plant extracts due to relatively low specificity. Thus data generated using anti-CKP requires further validation by other techniques and can only serve to support results generated by other means. Using affinity chromatography alone, a pure fraction of StCKP1 was not achieved. At best, purified StCKP1 would make up 60% of the purified protein. Using gel filtration to purify StCKP1 proved to be more effective, however the yield of protein returned was poor and insufficient for the production of an antiserum raised to a protein rather than a synthetic peptide.

To increase the degree of purification achieved other protein tagging methods could be investigated. Other solubility enhancing protein expression systems which generate tagged proteins in a bacterial expression vector are available, for example glutathione S-transferase (GST) (Smith and Johnson, 1988) and thioredoxin (TRX) (Lavallie et al., 1993). MBP as a solubility enhancer has been found to be more effective in comparison to these other proposed methods (Kapust and Waugh, 1999). However, to overcome the problems encountered here: bacterial proteases degrading purified proteins, and tRNA codons present in plants but rare in *E.coli*, it would be advantageous to use a poly (His) tag (S·Tag) on either the N or C terminal of StCKP1. This method has been used successfully in tagging proteins for Arabidopsis-based expression and purification (Dolja et al., 1998; Ling et al., 2000; Crofcheck et al., 2003; MacRae et al., 2004). It may even be advantageous to introduce a second tag, such as an MYC-Tag at the opposite terminus in order to allow a two step purification and ensure increased purity.

Chapter 5

Enzyme kinetics of StCKP1

5.1 Introduction

In the *de novo* biosynthesis of cytokinin using a crude system prepared from plant cells, a cytokinin ribotide, riboside and base were formed from known substrates of biosynthesis. This observation indicates that plant cells contain enzyme systems catalysing the formation of cytokinin base from its riboside (Chen and Melitz, 1979). To date only the phosphoribohydrolase OsLOG, identified by Kurakawa and co-workers (Kurakawa et al., 2007) has been identified to function specifically in the cytokinin metabolic pathway. No phosphoribohydrolytic activity could be measured for LOG when presented with AMP as substrate while the Michaelis constants (K_M) were determined to be 11.7µM and 22.0µM for [9R-MP]iP and [9R-MP]Z respectively. Schnorr et al. (1996) identified adenine phosphoribosyltransferase in Arabidopsis, ATapt2, which was found to have a higher degree of specificity towards BA over Ade as a substrate for conjugation, though this enzyme could use Ade as a substrate, in contrast to OsLOG. Other enzymes thought to be involved in cytokinin metabolism have been shown to have higher affinities for adenine and its derivatives adenosine and adenosine monophosphate (AMP). These include adenosine nucleosidase (Chen and Kristopeit, 1981a), adenosine phosphorylase (Chen and Petschow, 1978; Petschow and Chen, 1978), 5'-nucleotidase (Chen and Kristopeit, 1981b; Burch and Stuchbury, 1987), adenosine phosphoribosyltransferase (Chen et al., 1982b; Burch and Stuchbury, 1987; Moffatt et al., 1991), and adenosine kinase (Chen and Eckert, 1977) whose reactions and K_M values are summarised in figure 5.1. These enzymes show, in general, a low degree of specificity for the exact structure of the purine ring hence show activity for purines and N^6-substituted purine derivatives including, but not limited to, cytokinins. However, due to the similarity of cytokinins and unsubstituted purines, it seems likely that these enzymes are important in controlling the uptake and release of some cytokinins (Letham et al., 1982) as well as in the formation of biologically active forms (Laloue and Pethe, 1982).

Assays carried out in this study (sections 4.8-11), have confirmed that StCKP1 acts as a nucleoside phosphorylase, catalysing the phosphorolysis of cytokinin ribosides to yield the free base and also the reverse reaction in which a ribosyl moiety is conjugated at the N^9 position of the free base to produce a cytokinin riboside. An initial quantification from LC-MS-MS analysis of reaction products indicates that StCKP1 has a higher specific activity when presented with a free base substrate and an excess of ribose 1-phosphate (R 1-P) compared to its activity with a cytokinin riboside substrate and inorganic phosphate (Pi) (figure 4.16). Of the previously characterised enzymes, those catalysing same reaction as StCKP1 are adenosine nucleosidase (Chen and Kristopeit, 1981a) and adenosine phosphorylase (Chen and Petschow, 1978). Both enzymes were isolated from wheat germ preparations, with fractionated protein being selected, pooled and concentrated for assay on the

A

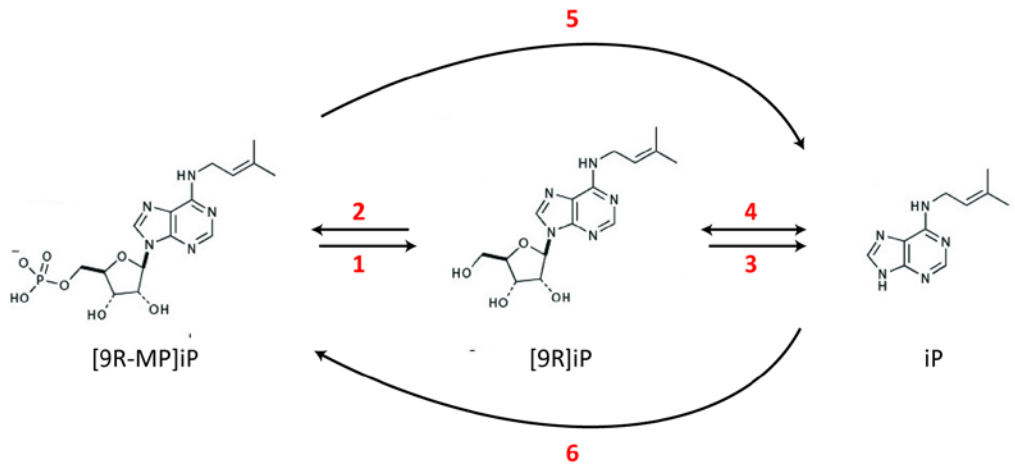

B

Enzyme Name	Activity	Substrate	Km (µM)	Reference
OsLOG	5	[9R-MP]iP [9R-MP]Z AMP	11.7 22.0 ND	(Kurakawa et al., 2007)
Adenosine Nucleosidase	3	[9R]iP Ado	14.0 6.8	(Chen and Kristopeit, 1981a)
Adenosine Phosphorylase	4	iP Ade	57.1 32.2	(Chen and Petschow, 1978; Petschow and Chen, 1978)
5′-nucleotidase FI 5′-nucleotidase FII	1	[9R-MP]iP AMP [9R-MP]iP AMP	3.5 3.2 12.8 11.5	(Chen and Kristopeit, 1981b; Burch and Stuchbury, 1987)
Adenosine Phosphoribosyltransferase	6	iP N^6-furfuryladenine BA Ade	130 110 154 74.0	(Chen et al., 1982; Burch and Stuchbury, 1987; Moffatt et al., 1991)
Adenosine Kinase	2	[9R]iP Ado	31.0 8.7	(Chen and Eckert, 1977)

Figure 5.1 Kinetic constants determined for enzymes involved in cytokinin metabolism
A. Schematic of cytokinin metabolism of isopentenyladenine type cytokinins, though applicable to zeatin and dihydrozeatin type cytokinins (figure 1.3). **B.** Kinetic constants for enzymes of cytokinin metabolism, numbered activities correspond to the reaction paths in A. ND - not detected. Kinetic constant values given were determined by the first reference cited if applicable.

basis of activity when presented with either an Ade or iP substrate for the latter and Ado or [9R]iP for the former. In determination of enzyme kinetics for each, activity was measured over a time course of between 60 and 120 minutes. ^{14}C labelled substrates were provided and, following the given time for reaction, the enzyme was precipitated by addition of an equal volume of 95% ethanol. Remaining substrate and products of reaction were separated by thin layer chromatography and visualised at 254nm. The strips containing radioactivity were cut out and scintillation counted to determine quantity of ^{14}C incorporated into the product formed and this data used to generate a time course from which initial rates of reaction were calculated.

Preliminary work carried out (Sedelnikova, pers. comm.) to determine the kinetic constants of StCKP1 for Ade, Ado, iP and [9R]iP substrates utilised spectrophotometry for Ade and Ado substrates and competitive ELISA for iP and [9R]iP substrates. Recombinant MBP-CKP was produced using the pMal system as previously described (section 4.3), and purified by two rounds of affinity chromatography (section 4.4). The assay was carried out under conditions previously described (section 4.7) and change in absorbance at 260nm monitored over time. The initial rate of reaction (V_0) was calculated from the initial slope of the plot for both Ade and Ado at a variety of concentrations. Taking the reciprocal of these values allowed an estimation of K_M to be made of 35µM and 250µM for Ade and Ado respectively (figure 5.2). This finding correlated with the specific activities previously calculated by LC-MS-MS analysis of StCKP1 catalysed reaction products in that StCKP1 appeared to have a higher activity with the purine base relative to the purine nucleoside as a substrate (figure 4.16).

Determination of the enzyme kinetics for both phosphorolysis and ribosyltransfer is of interest as enzyme affinity for both substrates, catalytic activity and kinetic evidence for control of activity by product/substrate activation or inhibition will provide insights into the role of StCKP1 in cytokinin catabolism. This information can then be used alongside expression data already gathered (sections 3.3 & 3.4.4) to determine the role of StCKP1 in tuberisation and the release of tuber dormancy. Also of interest are the kinetic parameters for Ade and Ado as to date all nucleoside phosphorylases involved in phosphorolysis and ribosyltransfer are primarily enzymes of the adenine salvage pathway (Chen, 1997) which are able to catalyse these reactions with cytokinin substrates due to a low degree of specificity for the substituents on the far side of the purine ring (Burch and Stuchbury, 1987).

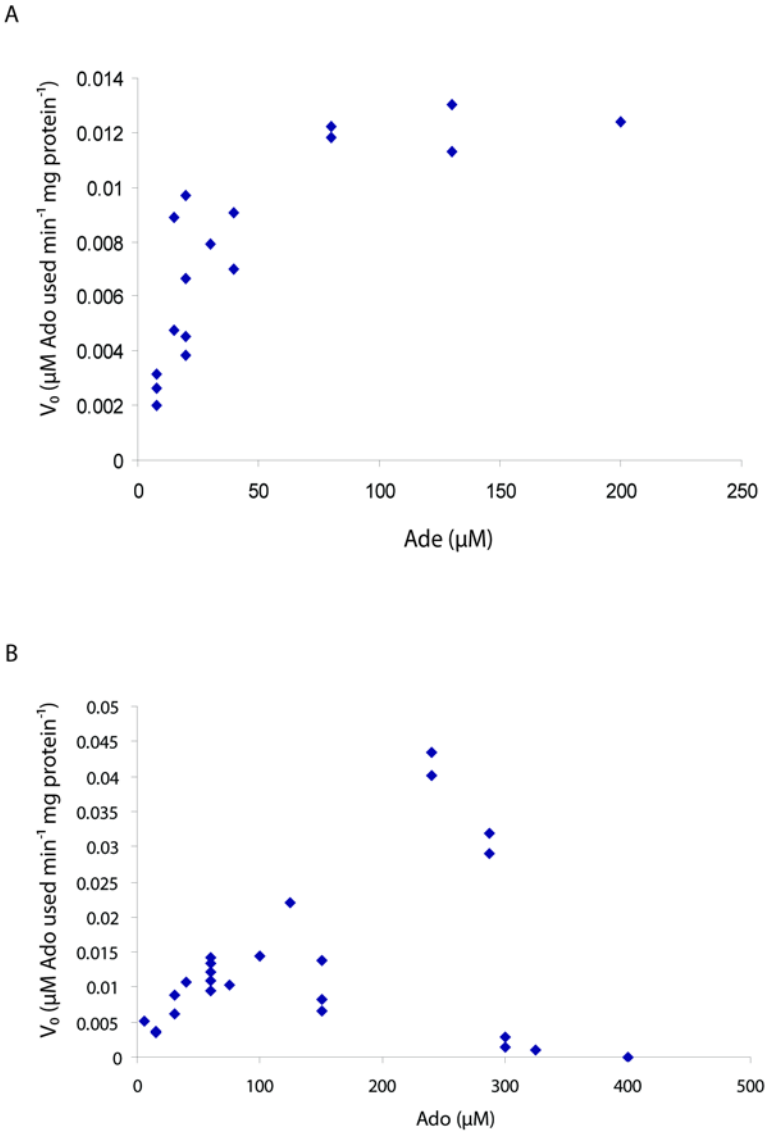

Figure 5.2 Preliminary assays of StCKP1 activity: relationship between initial rate of reaction and substrate concentration

A. Ribosylation of Ade by StCKP1 in the presence of excess R 1-P, K_M determined as 35µM. **B.** Phosphorolysis of Ado by StCKP1 in the presence of excess Pi. K_M determined as 250µM. Data O. Sedelnikova

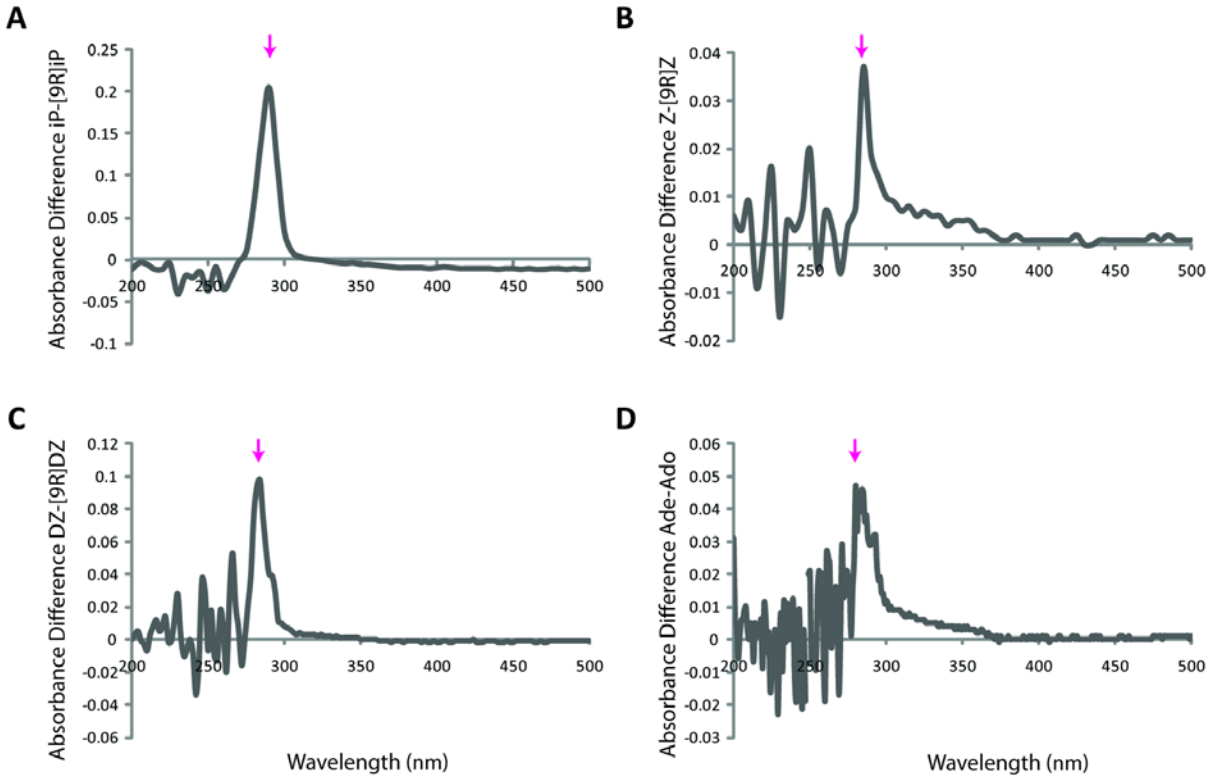

Figure 5.3 Absorbance differences between base and riboside
Scan of absorbance at 1nm intervals between 200nm and 500nm determined for 20µM of each iP, [9R]iP, Z, [9R]Z, DZ, [9R]DZ, Ade and Ado. Absorbance for riboside was subtracted from that obtained for the base at each wavelength. The maximum difference in absorbance at a given wavelength of base and riboside is indicated by an arrow. **A.** Absorbance difference between iP and [9R]iP – maximum difference at 285nm. **B.** Absorbance difference between Z and [9R]Z – maximum difference at 285nm. **C.** Absorbance difference between DZ and [9R]DZ – maximum difference at 285nm. **D.** Absorbance difference between Ade and Ado – maximum difference at 285nm.

5.2 Development of a continuous spectrophotometric assay

Assays previously used to determine the function and kinetic constants of nucleoside phosphorylases in plant tissue have been crude in their execution. Chen and Kristopeit (1981a)determined the kinetics of adenosine nucleosidase by discontinuous assay, taking time points every 5 minutes over a 60 minute period. Reactions were stopped by precipitation of the enzyme, ^{14}C labelled products were then separated from remaining labelled substrate using thin layer chromatography. Bands which fluoresced at 254nm and in line with cytokinin base and riboside standards were collected and radioactivity measured by scintillation counting. A purine nucleoside phosphorylase (PNP) has been identified in *Plasmodium falciparum* (Kicska et al., 2002) and subsequently an orthologue in *Toxoplasma gondii* (Chaudhary et al., 2006) was characterised. In both studies, enzyme activity with an Ado substrate was assayed and kinetic constants determined by spectrophotometric analysis of substrate disappearance at 274nm as at this wavelength Ado has a higher absorbance than Ade.

To investigate the possibility of using a continuous substrate disappearance assay and the converse product appearance assay, a spectrum of absorbance was determined for each of the substrate product pairs: Ade and Ado, iP and [9R]iP, Z and [9R]Z, and DZ and [9R]DZ, by scanning a 20µM solution of each compound in water every 1nm between 200 and 500nm (figure 5.3) using a BioTek Powerwave XS microplate spectrophotometer (BioTek, Winooski, VT, USA). Absorbance data collected was corrected for pathlength and against a blank containing water. The difference in corrected absorbance was then calculated for the region which the peak of absorbance spanned and the largest difference in absorbance selected (figure 5.3). For each of the cytokinins, a wavelength of 285nm was found to yield the largest difference in absorbance between base and riboside. The same wavelength was also found to give the largest difference in absorbance for Ade and Ado. A pilot assay with a 20µM initial substrate concentration, based on that of Moshides (1988), using conditions previously described (section 2.7.3) was carried out for each of the substrates with an excess of inorganic phosphate or ribosyl donor. Product appearance was found to be a viable method for measuring ribosyltransferase activity while substrate disappearance was not a viable method for determination of StCKP1 phosphoryoltic activity (figure 5.4).

5.3 Continuous assay of StCKP1 ribosyltransferase activity

The method used in determination of StCKP1 activity (section 2.7.3) was used to assay for the conjugation of a ribosyl group to the N^9 of cytokinin bases and adenine. StCKP1 was produced, cleaved and purified by two rounds of affinity chromatography as described previously (sections 4.3-

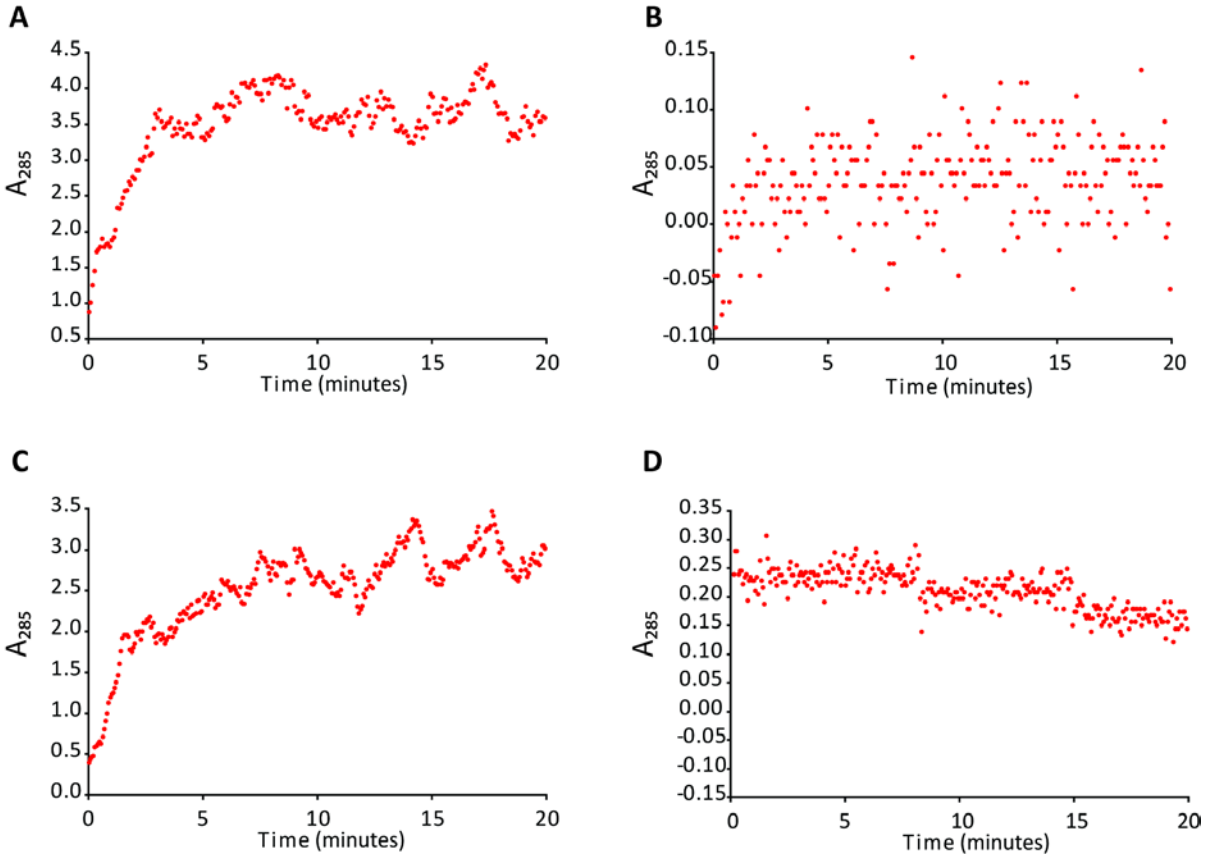

Figure 5.4 Pilot spectrophotometric assays
Pilot assays of 10µg purified StCKP1 carried out with 20µM substrate plus 4mM inorganic phosphate (Pi) or ribose 1-phosphate (R 1-P) donor. A. iP+R 1-P. B. [9R]iP+Pi. C. Z+R 1-P. D.[9R]Z+Pi. Data presented has been blank and pathlength corrected.

4.5.1). Affinity chromatography was chosen as a purification method over gel filtration with FPLC using a Superdex 2000 column due to the higher yield of protein returned. Affinity chromatography does not give as pure a product as purification by gel filtration, however the amount of protein returned by this purification method made it preferable as large amounts of enzyme were required for technical replicates with varying initial substrate concentrations. As previously ascertained, a bacterial extract twice purified by affinity chromatography containing only MBP as the dominant protein did not catalyse the reactions assayed (figures 4.6-4.8), and so contamination by MBP of the affinity chromatography purified StCKP1 would not affect the reaction. To determine how much of the protein being used in the assay was StCKP1, 10µg of the twice- affinity purified protein was run on a denaturing SDS polyacrylamide gel and stained with Coomassie blue. The intensity of the bands produced was estimated using Image J, and quantity of StCKP1 per 10µg total extract calculated (figure 5.5).

To test the sensitivity of the spectrophotometer to cytokinin substrates at different concentrations, a microplate was set up with a serial dilution of each of the different cytokinin substrates and expected products from 10nmol to 0.01nmol. It was found that 0.02nmol total cytokinin was at the lower limit of detection, and so it was decided that in order to assay dynamically for the conversion of base to riboside, a lower limit of initial substrate concentration would be 0.08µM to allow the riboside product to be detectable.

A master mix was produced which contained all the reaction components, including a 40mM excess of R 1-P as a ribosyl group donor, except the cytokinin base or adenine substrate and the StCKP1 protein. The master mix was added to different quantities of cytokinin or purine solution in a 96 well microplate to give final concentrations of between 320µM and 0.04µM depending on the substrate assayed. This mix was pre-warmed to 30°C for 10 minutes prior to addition of 10µg purified protein to give a final reaction volume of 50µl. The absorbance of the assay was immediately monitored every 5s at 285nm for a period of 10 to 20 minutes on a BioTek Powerwave XS microplate spectrophotometer. Data was processed using Gen5 software (BioTek), correcting absorbance values obtained against a blank containing no purified protein. All values were also pathlength corrected. Three samples were assayed and each was assayed three times.

For all cytokinin base substrates, the initial rate (V_0) was calculated from blank- and pathlength-corrected data for 9 initial substrate concentrations of 20, 10, 5, 2.5, 1.25, 0.63, 0.31, 0.16 and 0.08µM. The initial gradient of the reaction trace was taken to determine the change in OD units per second for the first 120s of the reaction, and this was further corrected by dividing by the gradient of

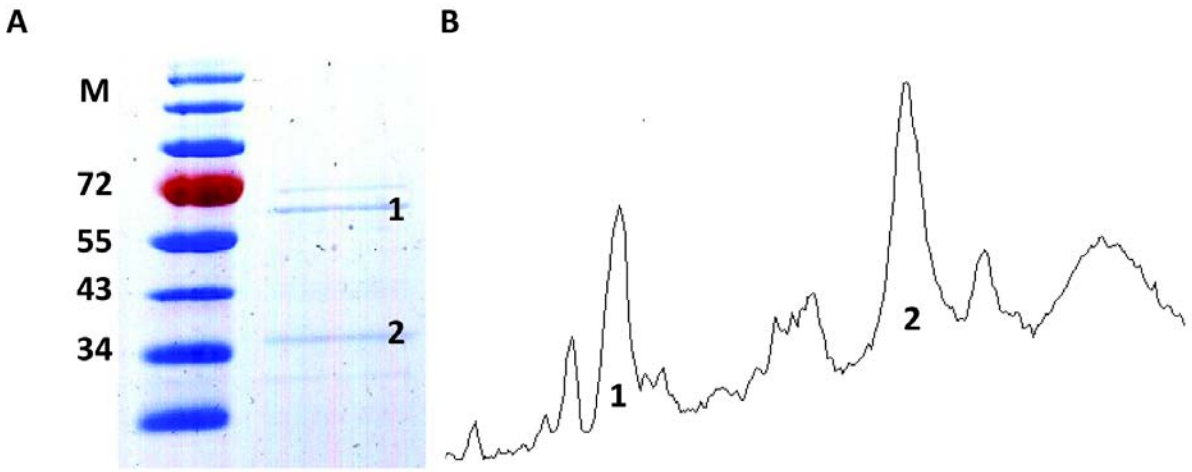

Figure 5.5 Affinity chromatography of purified expressed StCKP1
StCKP1 purified from the products of cleavage of MBP-CKP fusion protein by Xa protease. **A.** 5µg total protein from two rounds of affinity chromatography using 10ml amylose slurry which binds MBP at 3mg ml^{-1}. **B.** Quantification of bands using Image J gel analysis tool. **1:** MBP-CKP, **2:** StCKP1

the absorbance standard curve produced for each cytokinin to give pmol riboside formed per second, finally the V_0 was finally expressed as a specific activity per pmol CKP. The number of picomoles of CKP used was calculated according to equation 5-1:

Equation 5-1 Protein molar conversion

$$picomoles\ of\ protein\ = \frac{mass\ of\ protein\ (\mu g)}{Relative\ molecular\ mass\ (Da)}$$

The calculated values for V_0 were plotted against their respective initial substrate concentration. Using SigmaPlot (Systat software inc., Chicago, IL, USA), a curve was fitted to this data according to the Michaelis-Menten equation (Michaelis and Menten, 1913) as shown in equation 5-2:

Equation 5-2 Michaelis-Menten equation

$$V_0 = \frac{V\max\,[S]}{K_\mathrm{M} + [S]}$$

Kinetic constants determined in this study are summarised in table 5.1. The interconversion of iP to [9R]iP, as shown in figure 5.6 is catalysed by StCKP1 in the presence of an excess of ribosyl donor. The reaction products after 20 minutes of continuous assay of StCKP1 when presented with 20µM iP substrate were separated by HPLC and compared to standards to ascertain that the reaction monitored was as expected from previous assays (figure 4.6). The chromatogram showed two major peaks, one corresponding to iP substrate and the other to [9R]iP, the reaction product. The reaction time course indicated that ribosylation of iP by StCKP1 reached a maximum at 200 seconds then levelled off. The K_M and V_{max} were calculated from the curve fitted to the V_0/[iP] plot and further verified by taking the reciprocals of V_0 and initial [iP] by Lineweaver-Burk plot (Lineweaver and Burk, 1934). The K_M was calculated to be 0.053µM and the V_{max} was 0.408 pmol [9R]iP formed s^{-1} $pmol^{-1}$ CKP. This finding was significantly lower than the K_M value of 57.1µM reported by Chen and Petschow (1978) (figure 5.1).

The ribosylation of Z to form [9R]Z, as shown in figure 5.7 is catalysed by StCKP1 in the presence of an excess of R 1-P. The reaction products after 20 minutes of continuous assay of StCKP1 when presented with 20µM Z were separated by HPLC and compared to standards to confirm that the reaction monitored was as expected from previous assays (figure 4.7). The chromatogram showed two major peaks, one corresponding to Z substrate and the other to the product, [9R]Z. The reaction time course indicated that riboside synthesis by StCKP1 with Z and R 1-P substrates reached a maximum at 150s, then levelled off. The K_M and V_{max} were calculated from the curve fitted to the

Table 5.1 Michaelis constants, maximum initial velocities and catalytic efficiency
For both ribosylation and phosphorolysis of purine derivatives by StCKP1.

Compound	K_M (μM)	V_{max} (pmol s^{-1} $pmol^{-1}$ CKP)	Catalytic Efficiency (K_{CAT})
iP	0.053	0.408	7.70
Z	0.020	0.198	9.90
DZ	0.562	0.386	0.686
Ade	3.33	0.213	0.064
[9R]iP	13.31	0.027	0.002
[9R]Z	7.22	0.018	0.002
[9R]DZ	7.71	0.078	0.010
Ado	128	0.46	0.003

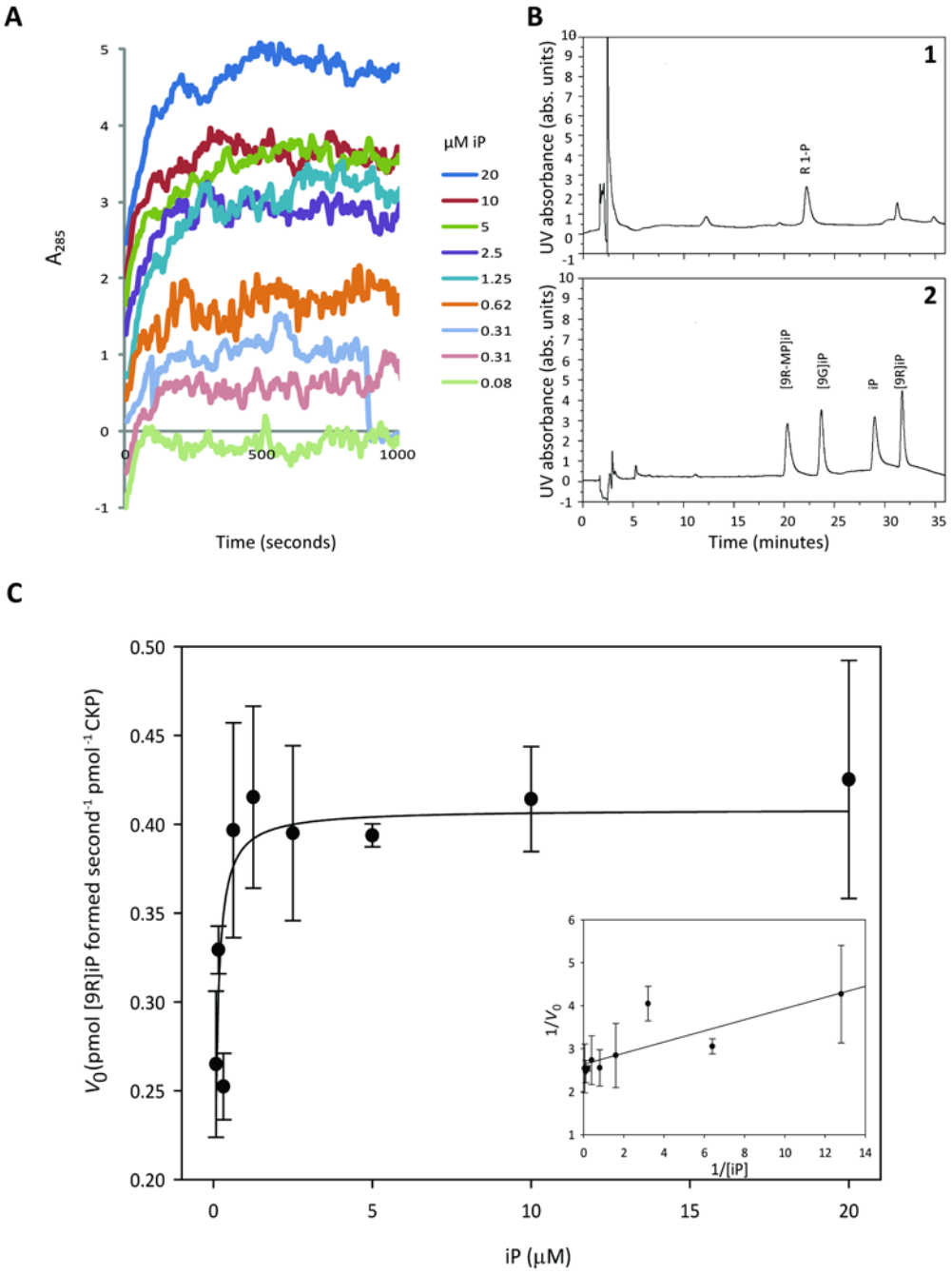

Figure 5.6 Spectrophotometric assay for ribosylation of isopentenyladenine
A. Change in absorbance with time for different concentrations of iP substrate. **B.** HPLC traces of: **1.** reaction products at 20mins. 1ml diluted reaction partitioned onto a C18 column and eluted using a methanol gradient , and **2.** 500pmol each [9R-MP]iP, [9G]iP, iP and [9R]iP standards. **C.** Initial rates of reaction determined by spectrophotometric assay plotted against initial iP concentration. Curve fitted according to equation $V_0 = \frac{V_{max}\,[iP]}{K_M + [iP]}$ to determine K_M as 0.053µM and V_{max} as 0.408pmol s^{-1} $pmol^{-1}$ CKP. Inset: Lineweaver-Burk plot of reciprocals to estimate K_M and V_{max}. Three replicates were carried out to determine initial rate, plotted as mean±SE.

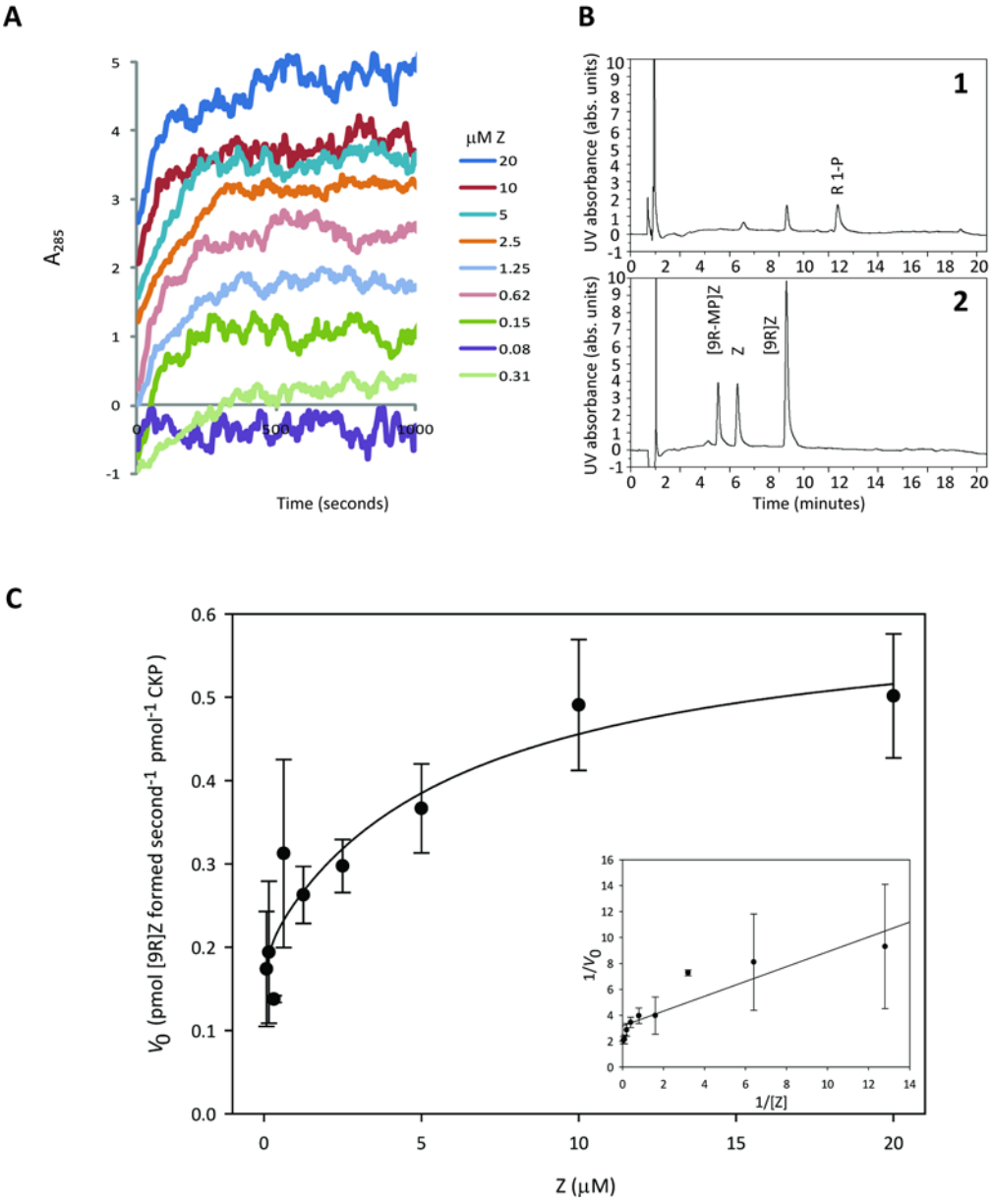

Figure 5.7 Spectrophotometric assay for ribosylation of zeatin

A. Change in absorbance with time for different concentrations of Z substrate. **B.** HPLC traces of: **1.** reaction products at 20mins. 1ml diluted reaction partitioned onto a C18 column and eluted using a methanol gradient , and **2.** 500pmol each [9R-MP]Z, [9G]Z, Z and [9R]Z standards. **C.** Initial rates of reaction determined by spectrophotometric assay plotted against initial Z concentration. Curve fitted according to equation $V_0 = \frac{V_{max}[Z]}{K_M+[Z]}$ to determine K_M as 0.020µM and V_{max} as 0.198pmol s^{-1} $pmol^{-1}$ CKP. Inset: Lineweaver-Burk plot of reciprocals to estimate K_M and V_{max}. Three replicates were carried out to determine initial rate, plotted as mean±SE.

V_0/[Z] plot and further verified by taking the reciprocals of V_0 and [Z] by Lineweaver-Burk plot (Lineweaver and Burk, 1934). The K_M was calculated to be 0.020μM and the V_{max} was found to be 0.198 pmol [9R]Z formed s^{-1} $pmol^{-1}$ CKP.

The conjugation of a ribosyl group at the N^9 of DZ to form [9R]DZ, as shown in figure 5.8 is catalysed by StCKP1 in the presence of an excess of ribosyl donor. The reaction products after 20 minutes of continuous assay of StCKP1 when presented with 20μM DZ were separated by HPLC and compared to standards to check that the reaction monitored was as expected from previous assays (figure 4.8). The chromatogram showed two major peaks, one corresponding to DZ substrate and the other to the product, [9R]DZ. The reaction time course indicated that riboside synthesis by StCKP1 with DZ and R 1-P substrates reached a maximum at 300s, then levelled off. The K_M and V_{max} were calculated from the curve fitted to the V_0/[DZ] plot and further verified by taking the reciprocals by Lineweaver-Burk plot (Lineweaver and Burk, 1934). The K_M was calculated to be 0.562μM and the V_{max} was 0.386 pmol [9R]DZ formed s^{-1} $pmol^{-1}$ CKP. However, when initial concentrations of DZ were in excess of 10μM, V_0 was dramatically reduced (figure 5.10) indicating that there may be a second, regulatory site present which binds DZ at a lower affinity than the active site. Substrate inhibition like that observed here may also be due to kinetic reasons as two substrate reactions result in competition between the two substrates, DZ and [9R]DZ for the active site.

The ribosylation of Ade by StCKP1 was of interest as an adenosine phosphorylase activity previously characterised to conjugate a ribosyl group to the N^9 of iP was found to have a higher affinity for Ade than its cytokinin structural homologue, iP (Chen and Petschow, 1978). For adenine, the initial rate (V_0) was calculated from blank, pathlength corrected data for 13 initial substrate concentrations of 320, 160, 80, 40, 20, 10, 5, 2.5, 1.25, 0.63, 0.31, 0.16 and 0.08μM. All further data analysis was carried out as previously described.

As figure 5.9 demonstrates, StCKP1 catalysed the ribosylation of Ade to form Ado in the presence of an excess of R 1-P. Unlike the time course of ribosylation seen with the cytokinin substrates assayed, continuous catalysis was observed until around 500s, before the curve reached a maximum and levelled off. HPLC separation of reaction products following 20 minutes of continuous assay with 20μM Ade initial substrate concentration indicate that the reaction monitored was the ribosylation of Ade to produce Ado as had been predicted. The chromatogram showed two peaks which corresponded to the retention times shown by Ade and Ado standards. The K_M and V_{max} were calculated from the curve fitted to the V_0/[Ade] plot and further verified by plotting the reciprocals by Lineweaver-Burk plot (Lineweaver and Burk, 1934). The K_M was calculated to be 3.33μM and the

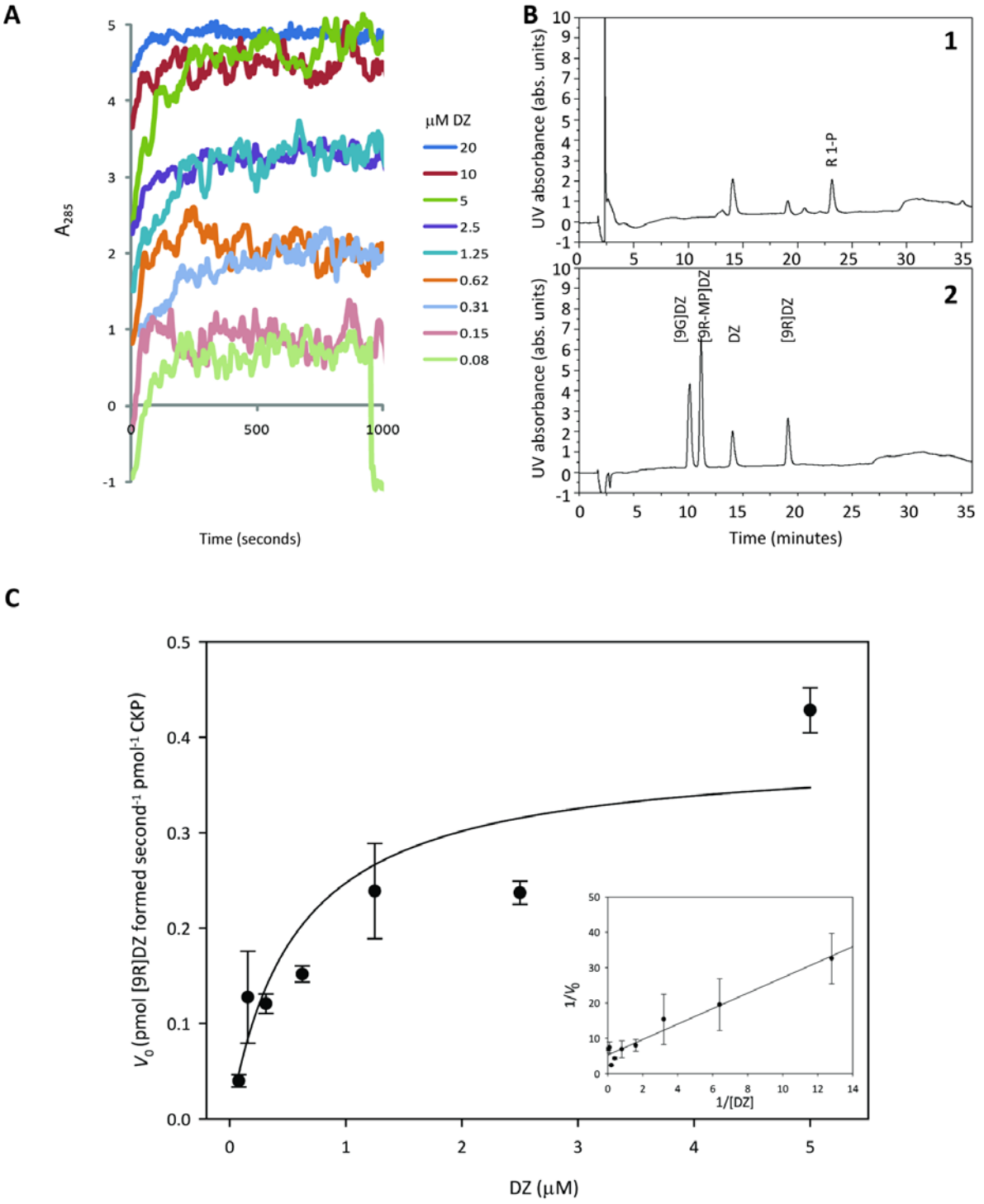

Figure 5.8 Spectrophotometric assay for ribosylation of dihydrozeatin

A. Change in absorbance with time for different concentrations of DZ substrate. **B.** HPLC traces of: **1.** reaction products at 20mins. 1ml diluted reaction partitioned onto a C18 column and eluted using a methanol gradient , and **2.** 500pmol each [9R-MP]DZ, [9G]DZ, DZ and [9R]DZ standards. **C.** Initial rates of reaction determined by spectrophotometric assay plotted against initial DZ concentration. Curve fitted according to equation $V_0 = \frac{V_{\max}[\mathrm{DZ}]}{K_M+[\mathrm{DZ}]}$ to determine K_M as 0.562µM and V_{max} as 0.386pmol s^{-1} $pmol^{-1}$ CKP. Inset: Lineweaver-Burk plot of reciprocals to estimate K_M and V_{max}. Three replicates were carried out to determine initial rate, plotted as mean±SE.

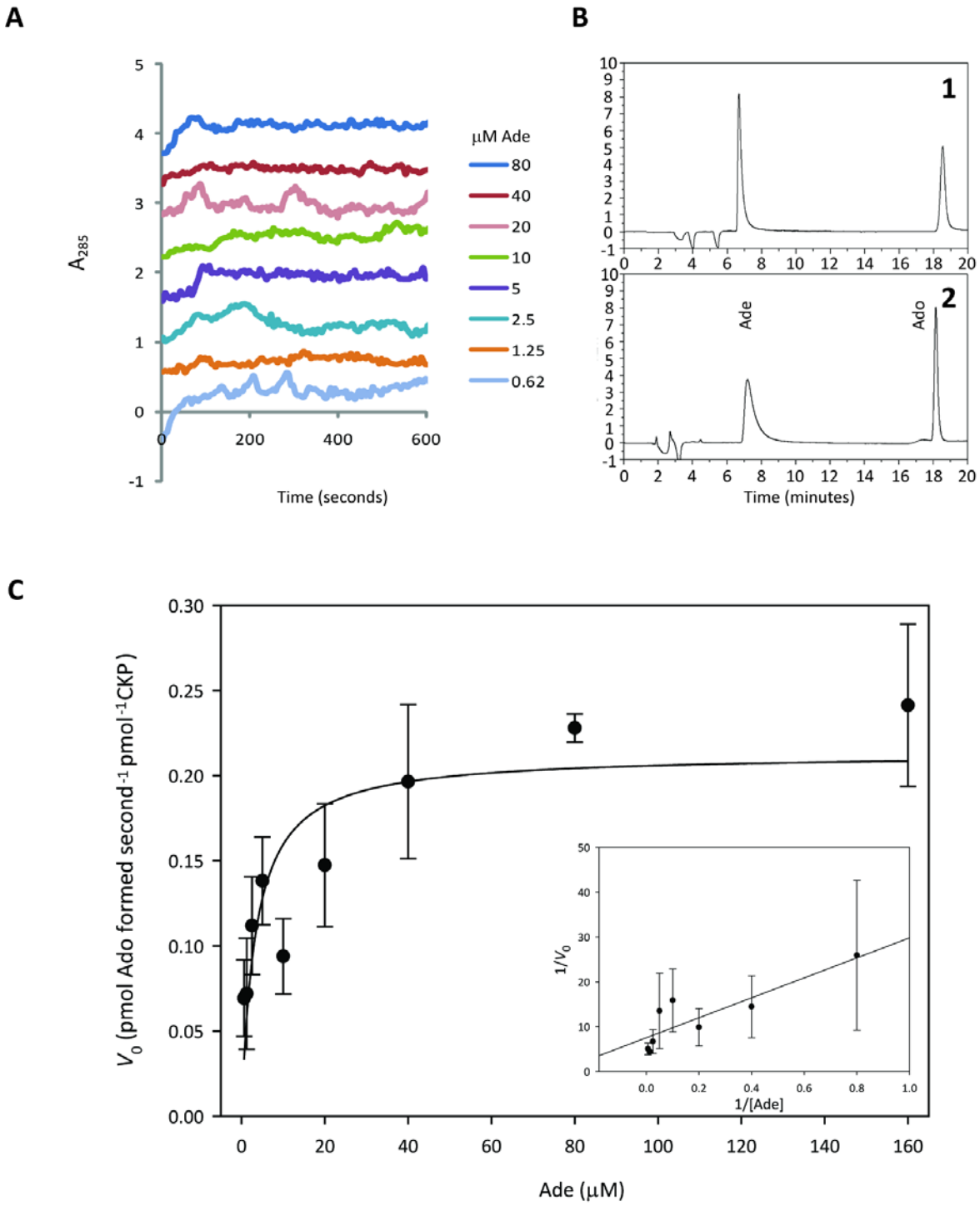

Figure 5.9 Spectrophotometric assay for ribosylation of adenine

A. Change in absorbance with time for different concentrations of Ade substrate. **B.** HPLC traces of: **1.** reaction products at 20mins. 1ml diluted reaction partitioned onto a C18 column and eluted using a methanol gradient , and **2.** 500pmol each Ade and Ado standards. **C.** Initial rates of reaction determined by spectrophotometric assay plotted against initial Ade concentration. Curve fitted according to equation $V_0 = \frac{V_{max}[Ade]}{K_M+[Ade]}$ to determine K_M as 3.33µM and V_{max} as 0.213pmol s^{-1} $pmol^{-1}$ CKP. Inset: Lineweaver-Burk plot of reciprocals to estimate K_M and V_{max}. Three replicates were carried out to determine initial rate, plotted as mean±SE.

V_{max} was 0.213 pmol Ado formed s^{-1} $pmol^{-1}$ CKP. This K_M is substantially lower than 32.2µM calculated for the wheat germ adenosine phoshorylase activity investigated by Chen and Petschow (1978), though interestingly is higher than the K_M of 0.052µM determined for iP in this study. This finding indicates that StCKP1 has a higher affinity for cytokinin substrates than for adenine equivalents although isn't exclusively selective for cytokinin substrates like LOG has been demonstrated to be (Kurakawa et al., 2007).

The levelling off seen in the ribosylation time course for all of the ribosylation reactions catalysed by StCKP1 could be due to end product inhibition, limiting substrate availability and/or the deterioration of the enzyme in aqueous solution at 30°C. Data gathered using Ade as a substrate indicates that StCKP1 is inhibited by either excess of substrate or product. Increasing the quantity of Ade substrate to an initial concentration of 320µM dramatically reduced the V_0 relative to that observed for an initial substrate concentration of 160µM (figure 5.10). This runs counter to the expectation that increasing [S] will increase V_0, and implies that if there were no inhibitory effects of substrate, the same V_0 might be achieved at a lower substrate concentration, i.e. the measured K_M would be lower. A two site inhibition curve for a second, regulatory site inhibiting activity was fitted to the data using equation 5-3:

Equation 5-3 Two site inhibition

$$V_0 = \left(\frac{V_{\max}[S]}{K_M + [S]}\right) - \left(\frac{V'_{\max}[S]}{K'_M + [S]}\right)$$

The output value for K_M was found to be 1.11µM which is lower than that determined by fitting a curve using the Michaelis-Menten equation. However, the K_M determined is still greater than those determined for cytokinin substrates, indicating a higher degree of specificity towards cytokinin substrates than Ade. The value determined for V_{max} was found to be 0.324 pmol Ado formed s^{-1} $pmol^{-1}$ CKP which is higher than that determined by the Michaelis-Menten equation. However, equation 5-3 assumes that inhibition occurs to the same extent no matter the initial substrate concentration. The fit of the curve to the data (figure 5.10 A) indicates that inhibition is likely to be due to a lower affinity regulatory site capable of binding the same substrate as the active site rather than binding with the same affinity, regardless of the initial substrate concentration.

Chen and Petschow (1978) found that 1mM Ado selectively inhibited the ribosylation of Ade by adenosine phosphorylase, but had little effect on ribosylation of other purine-derived substrates investigated. Shiio and Ishii (1969) demonstrated that end product inhibition is important in the

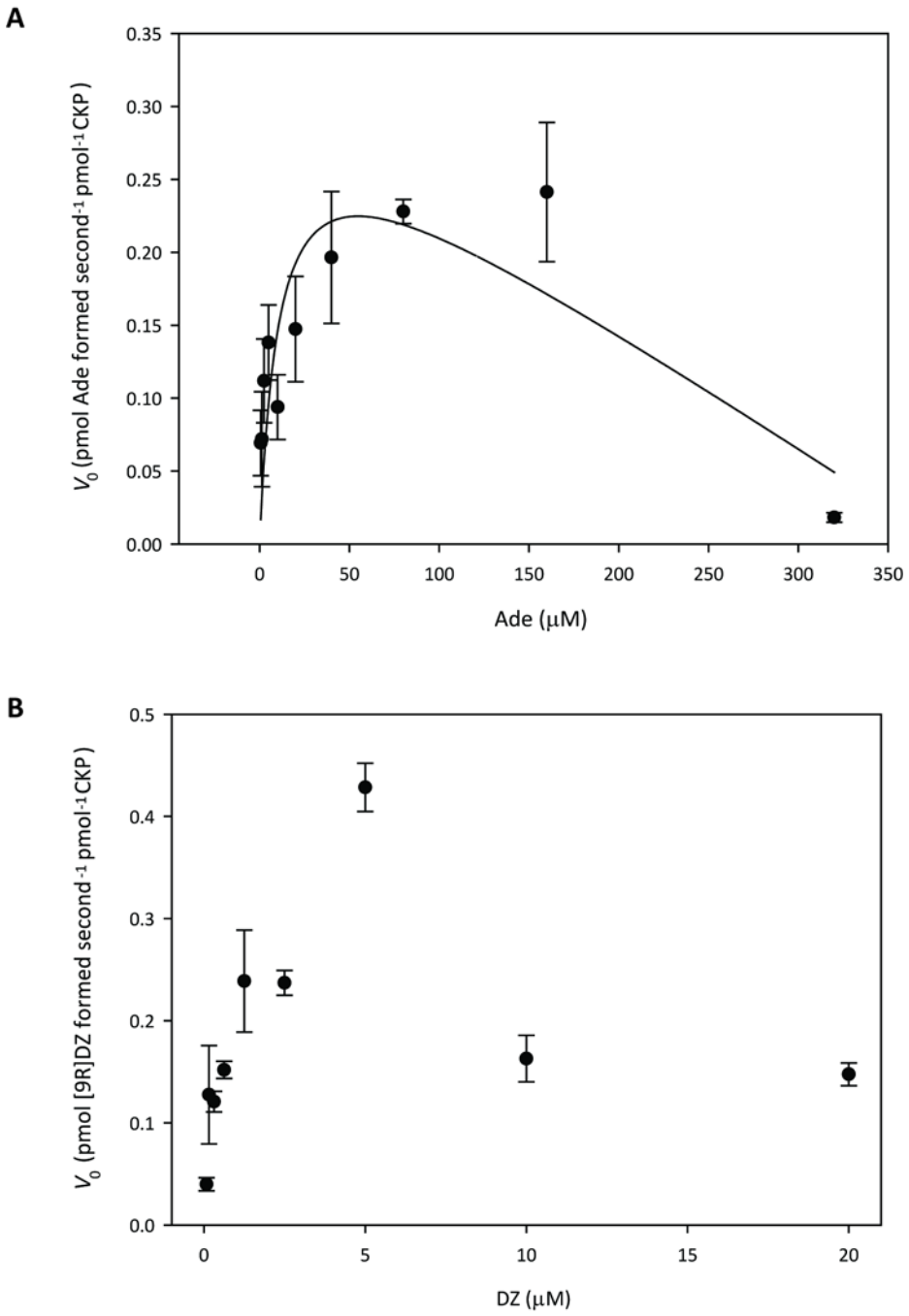

Figure 5.10 Inhibition of ribosylation

The ribosylation reaction catalysed by StCKP1 was found to be inhibited at increased initial substrate concentrations. **A.** Inhibition of ribosylation of Ade. Curve fitted according to the equation: $V_0 = \left(\frac{V_{\max}[\mathrm{Ade}]}{K_{\mathrm{M}}+[\mathrm{Ade}]}\right) - \left(\frac{V'_{\max}[\mathrm{Ade}]}{K'_{\mathrm{M}}+[\mathrm{Ade}]}\right)$ which models an inhibitory, second binding site. **B.** Inhibition of ribosylation of DZ. Three replicates were carried out to determine initial rate, plotted as mean±SE.

regulation of purine ribonucleotide biosynthesis, which may be the case for StCKP1 preventing an excess of cytokinin riboside entering the vascular transport system. Data gathered in this study suggests that a regulatory second site which binds the base is involved in regulation of StCKP1 activity. However, further investigation is required in order to determine if the inhibition seen in this study is due to an excess of product or substrate in the system and how this acts to regulate StCKP1.

5.4 Development of phosphorolytic assay

5.4.1 Cytokinin riboside substrates

As previously discussed (section 5.2), it was found through a pilot study that substrate disappearance measurement by continuous spectrophotometric assay was not a viable method for determination of StCKP1 phosphorolytic activity (figure 5.4). Phosphorolysis reactions carried out on the plate reader which did not yield the expected substrate disappearance curve were analysed by HPLC as previously described (section 4.7) to determine if the reaction previously demonstrated (section 4.8) had taken place. Figure 5.11 shows the chromatograms produced and cytokinin standards used to determine retention time of cytokinin substrates and products, indicating that the phosphorolysis of each [9R]iP, [9R]Z and [9R]DZ was being catalysed by StCKP1 to release the corresponding cytokinin base. Previous assays for quantifying adenosine phosphorylase activity (Chen and Petschow, 1978) and adenosine nucleosidase activity (Chen and Kristopeit, 1981a) used TLC analysis of discrete time points throughout dynamic assay to separate cytokinins and determined quantities of product and substrate remaining in the reaction mix. As has been previously demonstrated in this study (section 4.7) and numerous others (Strnad et al., 1992; Collier et al., 2003; Winwood et al., 2007), HPLC is a powerful method for both separating and determining absolute cytokinin content of a sample so it was decided to utilise HPLC to separate and quantify cytokinin content of phosphorolysis catalysed by StCKP1 in order to determine the initial rate of reaction over a range of initial substrate concentrations. To determine the range of initial substrate concentrations viable for analysis by HPLC, the same set of cytokinin standards used to determine sensitivity of the spectrophotometer was separated by HPLC and the UV absorbance traces integrated. It was found that 3.15nmol initial substrate was at the lower limit of detection and so this was used as the lowest initial substrate quantity for the purpose of this assay.

The reaction rates determined for ribosyltransferase activity (section 5.3) indicated that the V_0 is ideally determinable from the initial 200s of reaction, and a time point was taken every 30s from addition of 10µg StCKP1 twice purified by affinity chromatography (section 5.2) up to 6 minutes after addition, totalling 12 time points. The reaction components previously described (section 2.7.3)

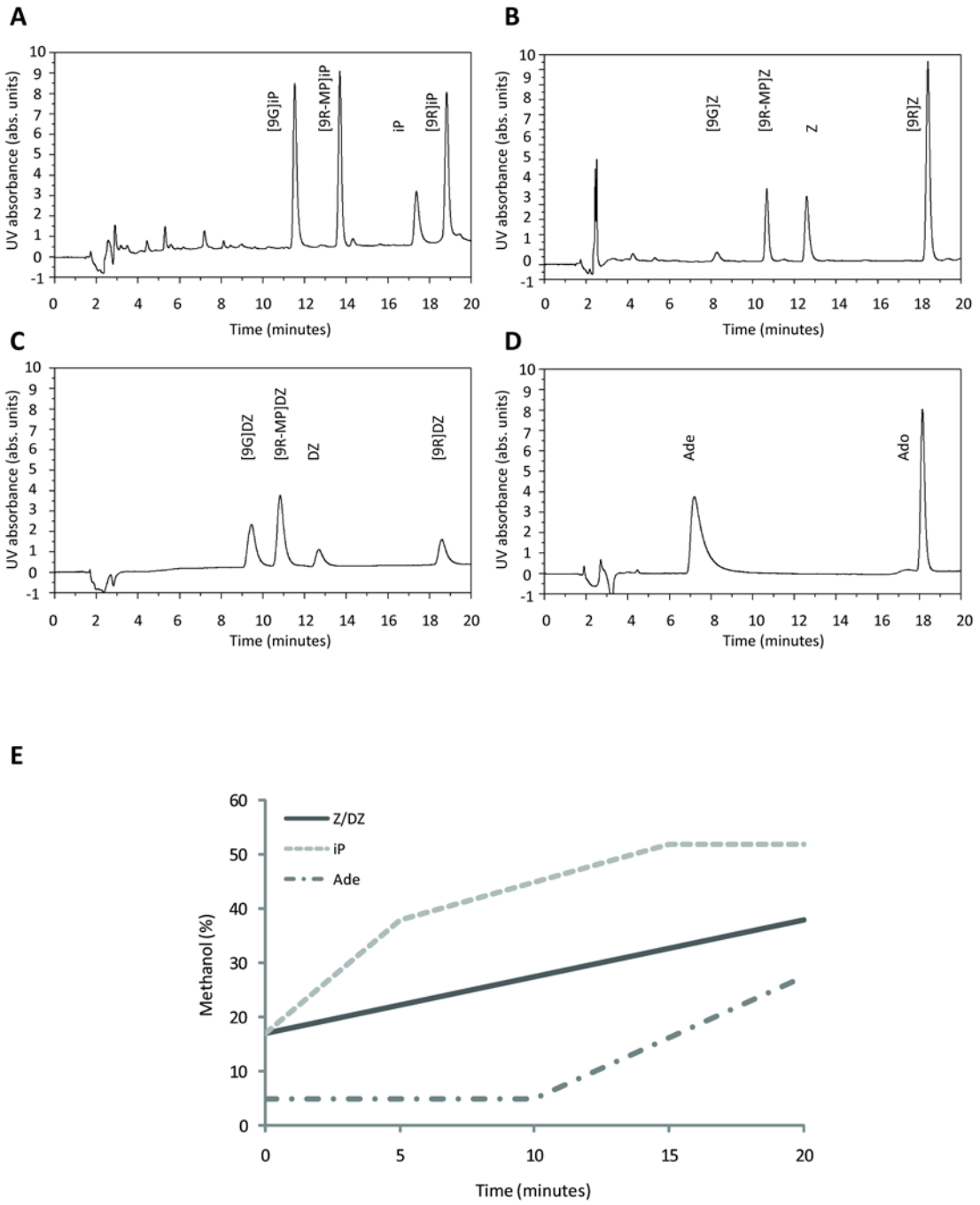

Figure 5.11 Cytokinin and aminopurine standards
500pmol each cytokinin or aminopurine analysed by HPLC. **A.** iP-type cytokinin standards. **B.** Z-type cytokinin standards. **C.** DZ-type cytokinin standards. **D.** Aminopurine standards. **E.** Gradients used to separate cytokinins and aminopurines. iP-, Z- and DZ-type cytokinin separation used mobile phase solvent containing 10% methanol and 4.6ml l^{-1} acetic acid, adjusted to pH3.6 with TEA. Aminopurine separation used mobile phase solvent containing 5% methanol, 4.6ml l^{-1} acetic acid, 200mM ammonium acetate and 0.5ml l^{-1} TEAA, adjusted to pH5.0. The gradient of methanol was produced by mixing of a second solvent containing 80% methanol and 6ml l^{-1} acetic acid.

were utilised with addition of 40mM K_2HPO_4 as inorganic phosphate donor. A master mix for 12.5 reactions designed to generate each of the initial substrate concentrations 20, 10, 5, 2.5, 12.5 and 0.63µM was prepared containing all components except StCKP1 protein. This mix was pre-warmed to 30°C for 10 minutes prior to addition of 125µg purified protein to give a final reaction volume of 625µl. At 30s intervals, 50µl of the reaction mix was removed and mixed into 250µl ice cold 96% ethanol to precipitate the protein and so halt the reaction. Before analysis by HPLC, any precipitate was removed from the reaction mix by filtering and the reaction mix diluted to contain less than 10% ethanol in order to allow cytokinins to partition into the stationary phase of the column. One ml of diluted reaction mix, minus protein, was loaded onto the column and retention times provided by traces compared relative to those of standards.

A methanol gradient adapted from that previously described (section 4.7, figure 4.5) with a 20 minute run time was used to separate cytokinins. For separation of Z and DZ-type cytokinins, the initial 20 minutes of this gradient was selected (figures 5.13 & 5.14), while for separation of iP-type cytokinins, the percentage of methanol was ramped up over a shorter period of time and the last 15 minutes of the gradient previously described was adopted for separation (figure 5.12). Peak area was determined for products of phosphorolysis and quantified relative to standard curves. V_0 for each initial substrate concentration was calculated from the initial gradient of the reaction curve produced. As with calculations to determine ribosyltransferase activity (section 5.3), this value was further corrected to express V_0 as a specific activity per pmol StCKP1. All kinetic data is presented in table 5.1.

In the presence of excess inorganic phosphate donor cleavage of the ribosyl group from [9R]iP was catalysed by StCKP1 as previously determined (sections 4.8 & 4.9). Figure 5.12 shows the separation by HPLC of products of reaction over a 6 minute period. Each chromatogram had two major peaks: one corresponding to [9R]iP, the substrate, and the other to the product, iP. The reaction time course indicated that phosphorolysis of [9R]iP to produce iP, catalysed by StCKP1, reached a maximum between 240 and 300s before beginning to level off. The K_M and V_{max} were calculated from the curve fitted to the V_0/[[9R]iP] plot and further verified by a reciprocal, Lineweaver-Burk plot (Lineweaver and Burk, 1934). The K_M was calculated to be 13.38µM and the V_{max} to be 0.027 pmol iP formed s^{-1} $pmol^{-1}$ CKP.

As previously demonstrated (sections 4.8 & 4.9) phosphorolysis of the ribosyl group from [9R]Z is catalysed by StCKP1. Figure 5.13 shows the separation of products of reaction by HPLC over a 6 minute reaction period. Each chromatogram had two major peaks: one corresponding to [9R]Z, the

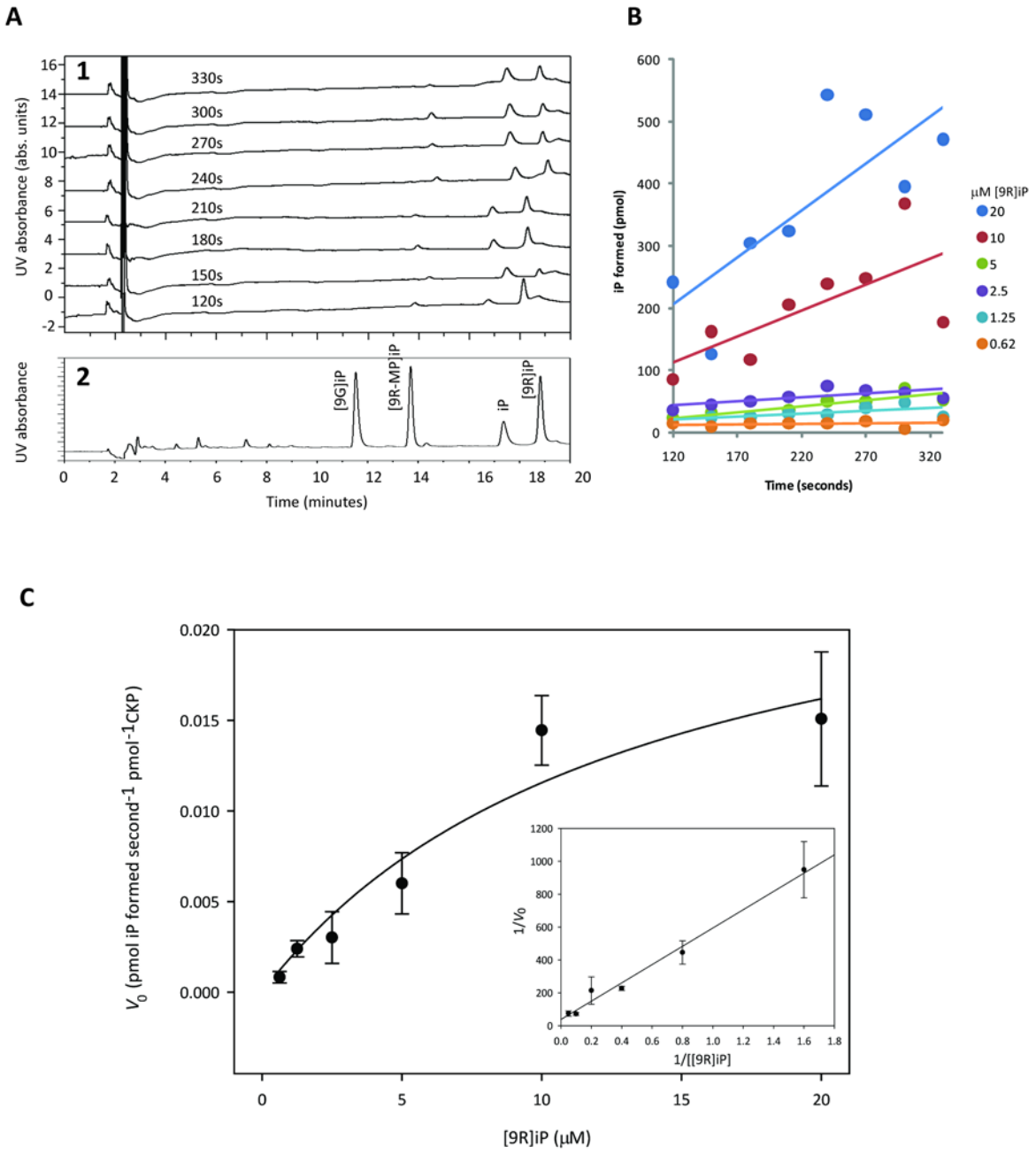

Figure 5.12 Phosphorolysis of isopentenyladenosine

A. Chromatograms of (1) time points from 120s to 330s separated by HPLC and quantified by integration relative to a standard curve produced for (2) iP standards. **B.** Quantified product plotted against time to determine initial rate of reaction (V_0), then **C**. plotted for different initial substrate concentrations. Curve fitted to the data according to the equation $V_0 = \frac{V_{max}[[9R]iP]}{K_M+[[9R]iP]}$ to determine K_M as 13.31µM and V_{max} as 0.027pmol s^{-1} pmol^{-1} CKP. Inset: Lineweaver-Burk reciprocal plot to estimate K_M and $V_{max.}$ Three replicates were carried out to determine initial rate, plotted as mean±SE.

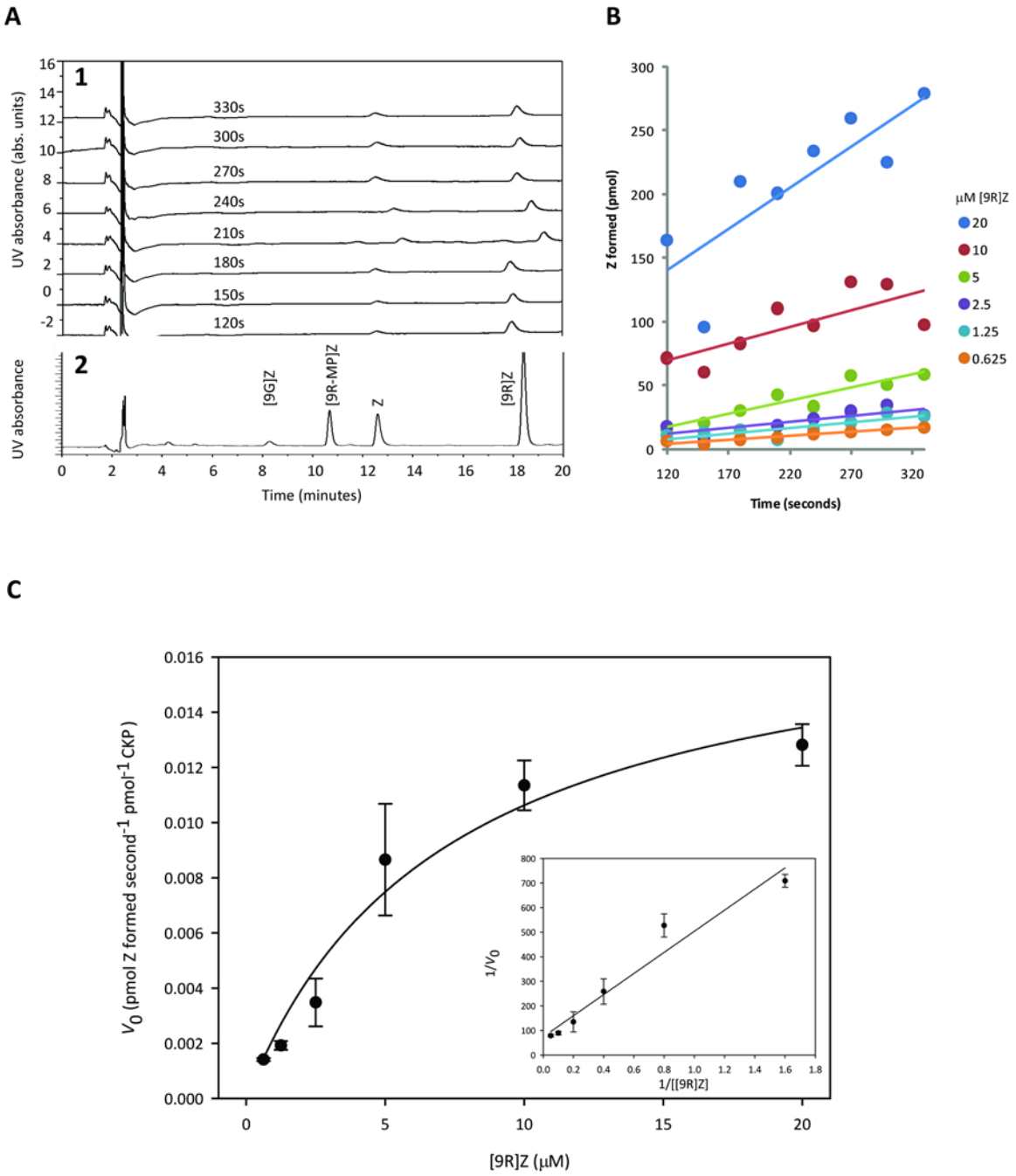

Figure 5.13 Phosphorolysis of zeatin riboside

A. Chromatograms of (1) time points from 120s to 330s separated by HPLC and quantified by integration relative to a standard curve produced for (2) Z standards. **B.** Quantified product plotted against time to determine initial rate of reaction (V_0), then **C**. plotted for different initial substrate concentrations. Curve fitted to the data according to the equation $V_0 = \frac{V_{max}[[9R]Z]}{K_M+[[9R]Z]}$ to determine K_M as 7.22µM and V_{max} as 0.018pmol s^{-1} pmol^{-1} CKP. Inset: Lineweaver-Burk reciprocal plot to estimate K_M and $V_{max.}$ Three replicates were carried out to determine initial rate, plotted as mean±SE.

substrate and the other to the product, Z. The reaction time course indicated that phosphorolysis of [9R]Z to produce Z reached a maximum just before 300s before beginning to level off. The K_M and V_{max} were calculated from the curve fitted to the V_0/[[9R]Z] plot and further verified by plotting the reciprocals of these in a Lineweaver-Burk plot (Lineweaver and Burk, 1934). The K_M was calculated to be 7.22µM and the V_{max} was 0.018 pmol Z formed s^{-1} $pmol^{-1}$ CKP.

Phosphorolytic cleavage of the ribosyl group from [9R]DZ to release DZ, previously demonstrated as catalysed by StCKP1 in the presence of an excess of inorganic phosphate (sections 4.8 & 4.9), was assayed over the same period used for phosphorolysis of [9R]iP and [9R]Z. Figure 5.14 shows the separation by HPLC of products of reaction over a 6 minute reaction period. Each chromatogram had two major peaks, one corresponding to [9R]DZ, the substrate and the other to the product, DZ. The reaction time course indicated that the rate of phosphorolysis of [9R]DZ to produce DZ reached a maximum between 240 and 270s before beginning to level off, possibly even going into decline. The K_M and V_{max} were calculated from the curve fitted to the V_0/[[9R]DZ] plot and further verified by plotting the reciprocals. The K_M was calculated to be 7.71µM and the V_{max} to be 0.078 pmol DZ formed s^{-1} $pmol^{-1}$ CKP.

5.4.2 Adenosine as substrate

The methanol gradient employed for separation of cytokinins was found to be insufficiently polar for retention of Ade on a C18 column. Reducing the initial methanol content of solvent A (section 2.6.3.1) to 5% and isocratic separation were tested in an attempt to retain Ade on the column. This had some success in that Ade eluted between 3 and 4 minutes post injection and a clear peak of UV absorption was visible on the chromatogram. However, the method was impractical as Ade was running too close to the injection peak, causing problems for the quantitation of Ade by integration. In order to buffer the solution further and retain Ade on the column for longer, the pH of solvent A was increased to pH 5.0 by addition of 50mM ammonium acetate and triethylammonium acetate (TEAA) as an ion pairing agent. However, the resulting solvent was too viscous for use below the maximum operating pressure of 40MPa. In order to overcome this problem, the concentration of ammonium acetate was raised to 200mM as ammonium acetate itself has ion pairing capacity. pH was adjusted to pH 5.0 by addition of 4.6ml acetic acid and 0.5ml TEAA was added as a further ion pairing agent. The final methanol gradient used to separate of Ade and Ado is shown in figure 5.15 and the solvents used were as follows: A. 5% methanol, 200mM ammonium acetate, 4.6ml l^{-1} acetic acid, 0.5ml l^{-1} TEAA, pH 5.0; B. 80% methanol, 6ml l^{-1} acetic acid; C. 100% methanol.

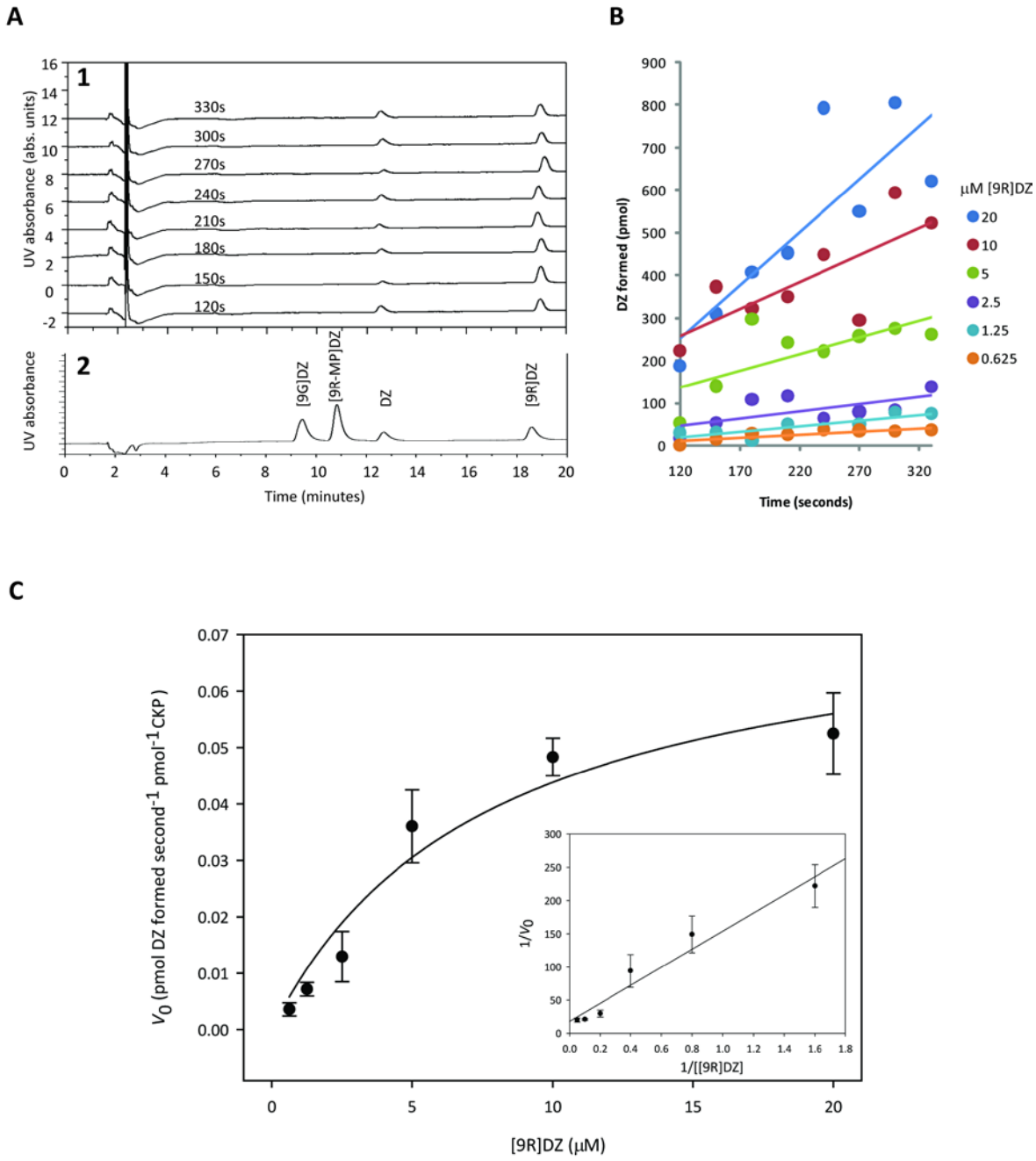

Figure 5.14 Phosphorolysis of dihydrozeatin riboside

A. Chromatograms of (1) time points from 120s to 330s separated by HPLC and quantified by integration relative to a standard curve produced for (2) DZ standards. **B.** Quantified product plotted against time to determine initial rate of reaction (V_0), then **C**. plotted for different initial substrate concentrations. Curve fitted to the data according to the equation $V_0 = \frac{V_{max}[[9R]DZ]}{K_M+[[9R]DZ]}$ to determine K_M as 7.71µM and V_{max} as 0.078pmol s^{-1} pmol^{-1} CKP. Inset: Lineweaver-Burk reciprocal plot to estimate K_M and $V_{max.}$ Three replicates were carried out to determine initial rate, plotted as mean±SE.

The methanol gradient developed for separation of Ade and Ado began with a lower initial methanol concentration than that used for separation of cytokinins, so sample preparation was adapted to ensure the products were suspended in a lower concentration of methanol than 5% at start of the gradient. The assay was carried out, stopped and filter sterilised as for cytokinin riboside substrates as previously described (section 5.4.1) using initial substrate concentrations of 320, 160, 80, 40, 20, 10, 5, 2.5, 1.25 and 0.62µM. Filter sterilised assay products were taken to dryness using a Univap centrifugal evaporator and refrigerated solvent trap and resuspended in 250µl HPLC grade water. Assay products from StCKP1 catalysed phosphorolysis of Ado were analysed on a Thermoscientific Spectrasystem HPLC and analysis carried out by Dr Michael Moulin with ChromQuest software. 100µl of the reaction was injected onto the column and absorbance of the eluate measured at 254nm. Data was subsequently corrected to calculate the total Ade content of the assay sample at each time point using a standard curve produced by injecting 100µl Ade standard at concentrations ranging from 500µM to 31.25µM. As with previous calculations to determine phosphorolytic activity (section 5.4.1), this value was further corrected to express V_0 as specific activity, i.e. activity per pmol StCKP1.

Phosphorolytic cleavage of the ribosyl group to form Ade from Ado was assayed over the same period used for phosphorolysis of cytokinin ribosides (section 5.4.1). Figure 5.15 shows the separation of reaction products by HPLC from 20µM initial substrate concentration over a 6 minute reaction period. Each chromatogram had two major peaks, one corresponding to Ado and the other to Ade. The reaction time course indicated that phosphorolysis of Ado to produce Ade reached a maximum at 240s before beginning to level off. The K_M and V_{max} were calculated from the curve fitted to the V_0/[Ado] plot and further verified a Lineweaver-Burk plot (Lineweaver and Burk, 1934). The K_M was determined to be 128µM and the V_{max} found to be 0.46 pmol Ade formed s^{-1} $pmol^{-1}$ CKP. The calculated K_M for Ado was found to be roughly twenty fold higher than that calculated for the cytokinin ribosides assayed in this study higher than the value of 6.8µM calculated for adenosine nucleosidase which carries out the hydrolysis of nucleosides but preferentially with Ado over cytokinin ribosides (Chen and Kristopeit, 1981a).

As for the ribosylation time courses, the levelling decrease in rate of reaction with time may be due to: end product inhibition, limited presence of substrate and/or the deterioration of the enzyme in aqueous solution at 30°C. For phosphorolysis of Ado, a significant reduction in V_0 was detected between 160 and 320µM initial substrate concentrations (figure 5.16). This finding matches results obtained by Sedelnikova (pers. comm.) who found a dramatic reduction in rate of reaction catalysed by StCKP1 with increasing initial substrate concentrations from 250µM to 300µM Ado (figure 5.2). A

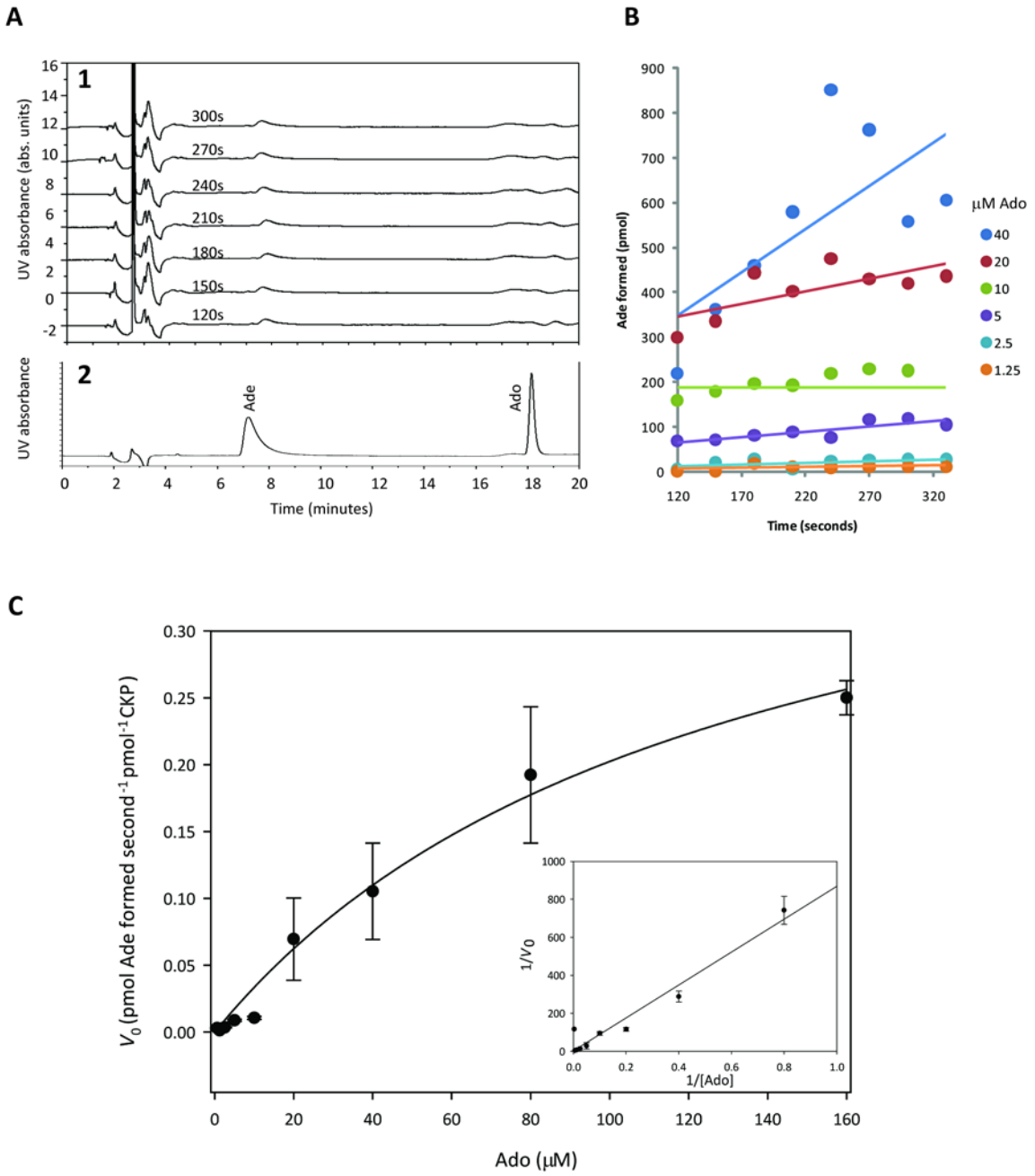

Figure 5.15 Phosphorolysis of adenosine

A. Chromatograms of (1) time points from 120s to 300s separated by HPLC and quantified by integration relative to a standard curve produced for (2) Aminopurine standards. **B.** Quantified product plotted against time to determine initial rate of reaction (V_0), then **C**. plotted for different initial substrate concentrations. Curve fitted to the data according to the equation $V_0 = \frac{V_{max}[Ade]}{K_M+[Ade]}$ to determine K_M as 128µM and V_{max} as 0.46pmol s^{-1} $pmol^{-1}$ CKP. Inset: Lineweaver-Burk reciprocal plot to estimate K_M and $V_{max.}$ Three replicates were carried out to determine initial rate, plotted as mean±SE.

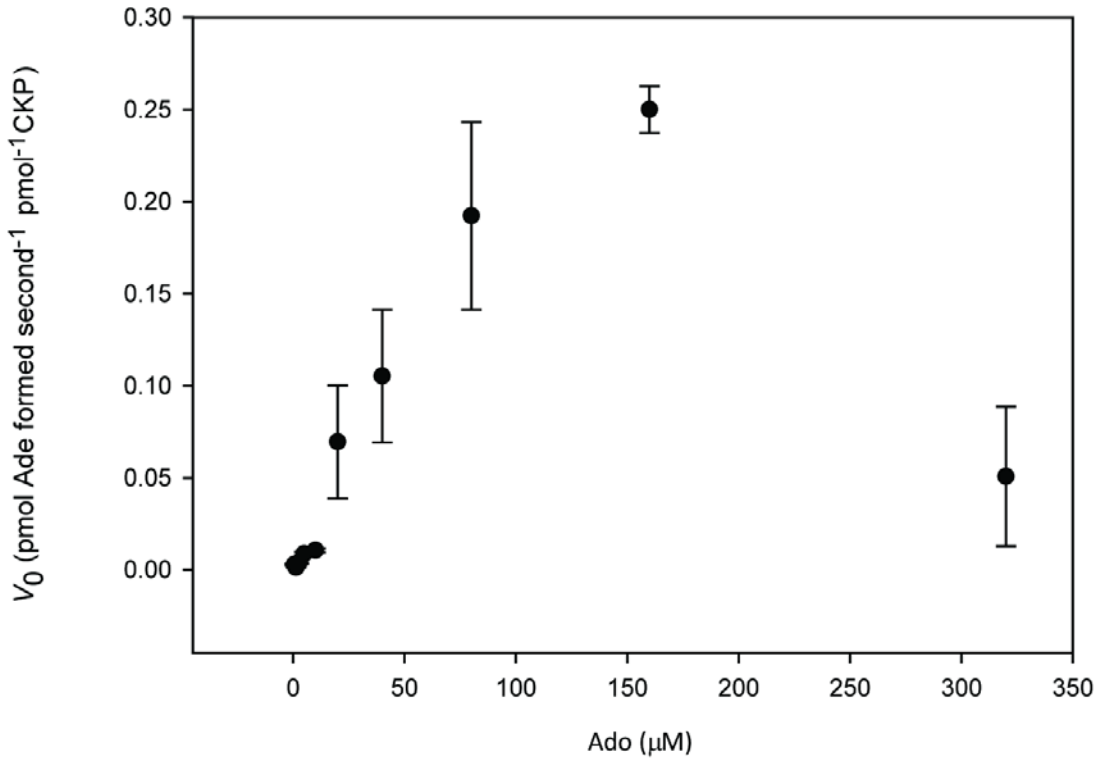

Figure 5.16 Substrate inhibition of phosphorolysis of adenosine
Phosphorolysis of Ado was inhibited at increased initial substrate concentration. Three replicates were carried out to determine initial rate (V_0) plotted as mean±SE

similar observation was also made by Chen and Kristopeit (1981a) who found adenosine nucleosidase to be completely inhibited by 250μM Ado. Like the curve shape produced for the ribosylation of Ade to produce Ado, a curve fitted according to Equation 5-3 did not give a close fit to the data, however this model may not be sufficient to describe inhibition by a lower affinity regulatory, second site.

5.5 Discussion

The kinetic parameters calculated from data collected (table 5.1) indicate that StCKP1 acts primarily in ribosylation of cytokinin bases to produce the corresponding riboside with the highest affinities for Z and iP as substrates. In the presence of inorganic phosphate, StCKP1 also catalyses deribosylation to produce the free base showing the highest affinity for [9R]Z, however is several orders of magnitude larger than the K_M determined for Z. StCKP1 has been shown to catalyse the phosphorolysis of Ado to produce Ade and also the reverse reaction of ribosylation of Ade, but with a higher calculated K_M, indicating a lower affinity of StCKP1 for Ade and Ado relative to that for the corresponding cytokinin species.

It was originally hoped that all kinetic data would be collected using a plate reader based assay for continuous measurement of substrate disappearance or product appearance. However, in practice this was not possible for measurement of the disappearance of riboside substrate. Measurement of the appearance of the riboside was achieved due to production of a compound with a higher absorbance at 285nm. By contrast measurement of the disappearance of the riboside which has a greater absorbance at 285nm, while the base with a lower absorbance was produced proved impractical as the plate reader, at 285nm lacked the sensitivity to measure a small difference between two comparatively large numbers. The difficulty was compounded by environmental challenge, in that to attain a reliable measure of absorbance, the pathlength must remain constant. Due to vibrations caused by movement and general laboratory practice, the pathlength may have varied, or there was an affect upon the precise wavelength measured throughout the period of measurement contributing to the error seen in ribosyltransferase assays carried out using the spectrophotometric method.

As a result, for measurement of phosphorolysis, samples were taken from a large initial reaction volume, stopped individually and assayed by HPLC in order to separate product from substrate for quantification. The data produced had much smaller errors than those for the spectrophotometric assay. However the sensitivity of the LC871 UV-VIS detector was insufficient for detection of initial substrate concentrations below 0.62μM preventing quantitation of V_0 for the lower initial

concentrations assayed using the spectrophotometer. It is also unclear as to how the change in reaction volume may have affected the rate of reaction as aliquots were taken throughout the duration of the reaction, for example, the apparent levelling off of the rate of reaction seen from plotting quantified product against time (figures 5.6 - 5.9) may be to some extent an artefact of changing the volume conditions during the assay.

Both of the methods for measurement of reaction rate have limitations. The continuous nature of the spectrophotometric assay meant more technical replicates could be carried out as the consumption of purified protein was comparatively low compared with the large amounts required for assay by HPLC separation and quantitation, limiting both the number of replicates and also the number of time points that could be taken over the substrate concentration range chosen. Also, the rate at which reactions could be carried out and analysed is another important factor as the number of time points assayed by HPLC was restricted by the number of samples that could be manually run. One day on the HPLC was the equivalent of 6 minutes of continuous assay on the plate reader, but producing 72 time points as opposed to 10 by HPLC analysis. Hence the need to weigh the sensitivity of assay against the number of time points taken is a crucial consideration in assay choice.

The inhibition observed for the ribosylation of adenine and DZ (figure 5.10), and for phosphorolysis of adenosine (figure 5.16) is in line with observations of Chen and co-workers (Chen and Petschow, 1978; Chen and Kristopeit, 1981a) who have shown that adenosine nucleosidase is subject to inhibition by addition of excess product to the reaction mix and that adenosine phosphorylase is inhibited by addition of an excess of its substrate. Combining these observations with what has been found for StCKP1 in this study and also in preliminary experimentation carried out by Sedelnikova (pers. comm.) (figure 5.2), suggests that StCKP1 has a regulatory second site with lower affinity for adenine or cytokinin base which can act to inhibit StCKP1 activity when either the substrate or product, depending on direction of reaction, reaches a critical concentration. The current study did not investigate this putative second regulatory site though it has led to preliminary experiments on the effect of pH on the reaction (Broadhurst, pers. comm.). pH optima can be used as an indication of the cellular site at which an enzyme is active, plus if multiple peaks are seen it may indicate the presence of a second site with a different pH optimum. Previous observations lead to the prediction that the second site may bind either the substrate or the product to inhibit activity at the catalytic site. The results obtained were consistent with the presence of a regulatory second site (data not shown). For the ribosylation of Z to [9R]Z at an initial substrate concentration of 5µM, a strong dip in specific activity was observed around pH 8, which may suggest that this pH is optimum for binding at the inhibitory site. However, the observation may be due to a pH-induced shift in relative

absorbance at 285nm, or the protonation state of phosphate so further investigation is required for confirmation.

The K_M determined for zeatin is of particular note as it is close to the K_D of 0.17µM determined for the original cytokinin-binding activity in extracts tuberising potato stolon tips (Thomson, 1994). These extracts were the source of the affinity purified protein whose sequence was identified as StCKP1 (James, pers. comm.). In order to determine if the protein characterised by Thomson and StCKP1 are the same, and because absolute purity has not been achieved through the production and cleavage of MBP-CKP followed by purification to yield a partially pure sample of StCKP1, StCKP1 is currently being expressed using a baculovirus insect based expression system in order to test the binding affinity of StCKP1 for each of the cytokinin and adenine substrates assayed in this investigation.

Chapter 6

Transgenic analysis, and analysis of *StCKP1* in other potato cultivars

6.1 Introduction

Manipulation of expression of genes involved in cytokinin biosynthesis (Macháčková et al., 1997; Zubko et al., 2005; Morris et al., 2006) and of genes involved in extracellular ATP salvage (Riewe et al., 2008) has resulted in changes in tuber dormancy, sprouting characteristics and in purine metabolism. In a study of extracellular ATP salvage in potato, Riewe et al. (2008) identified a cell wall-bound nucleosidase that is highly specific for adenosine. In their assays of ribose production using cell wall extract as an enzyme source, only adenosine was cleaved to produce adenine and ribose. All other purine substrates, which included [9R]Z, did not result in the liberation of detectable amounts of ribose using apoplastic enzymes. This is in stark contrast with assays carried out using intact isolated tuber discs in which zeatin and ribose were liberated from [9R]Z, indicating intracellular cytokinin hydrolytic activity is present in tuber tissue, in line with findings of Katahira and Ashihara (2006). When the activity of a second cell wall-bound enzyme, ATP diphosphohydrolase, was reduced by RNA interference (RNAi), adenosine nucleosidase activity was significantly reduced in RNAi lines to between 28 and 60% of the wild type level of activity.

There has been a history of expressing proteins involved in cytokinin biosynthesis and metabolism in the tuber to investigate control of tuber initiation and dormancy. Some of these were designed to affect cytokinin content directly, such as manipulation of *ipt* (Macháčková et al., 1997; Zubko et al., 2005), others were shown to affect tuber cytokinin content indirectly such as over-expression of *dxs* (Morris et al., 2006).

Perturbing isoprenoid biosynthesis via the methylerythritol phosphate (MEP) pathway, which produces the isoprenoid precursor, dimethylallyl diphosphate (DMAPP) required for cytokinin biosynthesis via the [9R-MP]iP-dependent pathway (Kakimoto, 2003b) and 1-hydroxy-2-methyl-2-(E)-butenyl 4 diphosphate (HMBPP) for the [9R-MP]iP–independent pathway (Astot et al., 2000), altered the biosynthesis of cytokinin and other plastidic isoprenoid-derived hormones including gibberellins and ABA, and altered dormancy, tuberisation and tuber morphology (Morris et al., 2006). Of particular note, *dxs*-over-expressing lines were found to have a six fold increase in [9R]Z content relative to wild type. However, this increase was only detected at harvest; after 10 weeks of storage [9R]Z levels had returned to wild type levels in transgenic tubers. *dxs*-over-expressing tubers were found to have a period of dormancy shorter than non-transformed controls and also were found to initiate tuberisation 30 days earlier than wild type Desiree. The authors concluded that, as the only isoprenoid-derived hormone to be significantly upregulated, the increase in post-harvest zeatin riboside is the most likely cause of the *dxs*-phenotype.

Other studies which have modified cytokinin biosynthesis in potato have done so by introducing the *isopentenyltransferase* (*ipt*) gene from Agrobacterium (Macháčková et al., 1997) and Petunia (*Sho*)(Zubko et al., 2005). Constitutive expression of Agrobacterium *ipt* was found to correlate predominantly with accumulation of [9R]Z, and also with increases in number of stolons and tubers formed. Like the observation of Morris et al. (2006), *in vitro* tuber formation also occurred earlier and at lower sucrose concentrations in explants expressing the *ipt* transgene compared with wild type (Macháčková et al., 1997). In contrast, constitutive expression of *Sho*, which shows homology with isopentenyltransferases and when expressed in tobacco enhances tissue content of iP derivatives (Zubko et al., 2002), the Petunia isopentenyltransferase did not cause a change in [9R]Z content but instead increased the levels of biologically inactive iP and Z glucosides. This probably reflects a prior increase in active cytokinins that have been inactivated by conjugation. Many of the phenotypic consequences of over-expression of *Sho* are similar to those described for over-expression of *ipt* and *dxs*, however by contrast with over-expression of *ipt*, over-expression of *Sho* resulted in a delay in tuber production by at least 2 months accompanied by a significant reduction in tuber size.

This *dxs*-induced increased post harvest cytokinin and shortening of the dormant period are in line with the observations of Hemberg (1970) who demonstrated treatment of innately dormant tuber buds with kinetin or zeatin results in the induction of sprouting. This finding was furthered by Turnbull (1982) who found artificially increasing cytokinin levels around the dormant bud by injection resulted in dormancy break within 48 hours of injection in tubers with an increased sensitivity to cytokinin. He found that potato tuber buds of 'Majestic' have periods of sensitivity to injected zeatin during the innate period of dormancy, with this zeatin being interconverted to zeatin riboside and accumulating around tuber buds. The first of these periods of sensitivity was in the first six weeks after tuber initiation, while the second was in the three weeks preceding the break of dormancy. In parallel with this, endogenous zeatin-type cytokinin was measured during tuber growth and storage (Turnbull and Hanke, 1985b). Early stage (less than 6 weeks after initiation) tubers contained naturally high contents of [9R]Z, with measured concentrations reaching 1300 pmol g^{-1}. At tuber maturity, [9R]Z content was found to be as low as 2% of the value at earlier stages, coinciding with a period in which sprouting could not be induced by exogenous application of cytokinin. Combining all the results, they concluded that cytokinins could be the primary trigger releasing tuber buds from innate dormancy. However the concentration of cytokinins in bud tissue offered no guide to the state of dormancy or its responsiveness to applied cytokinin. Koda (1982a) found a decrease in Z and [9R]Z immediately after harvest and an increase preceding the break of dormancy. The level of [9R-MP]Z showed an opposite pattern, building up during storage then going

into decline. On the basis of this, it was suggested that the increases in base and riboside content observed prior to the break of dormancy were the result of metabolism of the stored ribotide. Mauk & Langille (1978), consistent with the results presented by Koda (1982a), demonstrated [9R]Z levels to be 10-100 times greater than any other cytokinin detected in non-dormant tissues.

Assays carried out in this study (sections 4.8-11 and 5.3-4) have demonstrated that StCKP1 acts as a nucleoside phosphorylase, catalysing both the phosphorolysis of cytokinin ribosides to yield the free base and the reverse reaction in which a ribosyl moiety is conjugated at the N^9 position of the free base to produce a cytokinin riboside. For equivalent concentrations of the substrates, the synthetic direction was favoured in the assay, and K_{CAT} was 5000 times higher for this direction. *StCKP1* transcript has been shown to increase expression during the process of tuberisation and transition to a dormant state (section 3.3). This finding indicates that it is likely that StCKP1 contributes to the increase in zeatin riboside observed upon tuberisation and the reduction in transcript during dormancy correlates with the reduced cytokinin content of dormant tubers (Turnbull and Hanke, 1985b). It is hypothesised that altering the expression of *StCKP1* is likely to perturb the metabolism of cytokinin, resulting in a change in dormancy and tuberisation characteristics which may be of commercial value. To study the effect of increased expression of *StCKP1* on tuberisation and dormancy phenotypes, transgenic potato plants were prepared carrying a construct for constitutive expression of *StCKP1* in the Desiree background. A brief investigation was also carried out into the expression of *StCKP1* in other commercially important potato cultivars, information helpful for new cultivar breeding programs.

6.2 Constitutive expression of *StCKP1* in potatoes

6.2.1 Generation of 35SS::StCKP1 construct

The full coding region of StCKP1 had previously been cloned into pGADT7 AD by Barbara Warnes to produce pGADT7CKPCDS (table 2.2). Using methods described in section 2.4.1.3, the coding sequence of *StCKP1* was excised from pGADT7CKPCDS by restriction digest with *Eco*RI and *Bam*HI. The desired product of digestion was purified from a 1.2% agarose gel using the QIAquick PCR purification kit and quantified by UV spectrophotometry. The destination vector, pGreen0029:35SS (table 2.2, figure 6.1) was digested with the same enzymes and the cut ends dephosphorylated using CIAP before purifying and quantifying as before. Using a 3:1 molar ratio of insert to vector the cut pGreen0029:35SS backbone and *StCKP1* insert were ligated using NEB Quick Ligase to produce pG35SS::CKP (table 2.2, figure 6.1) and transformed into *E.coli* strain TBI. Colony PCR was carried out

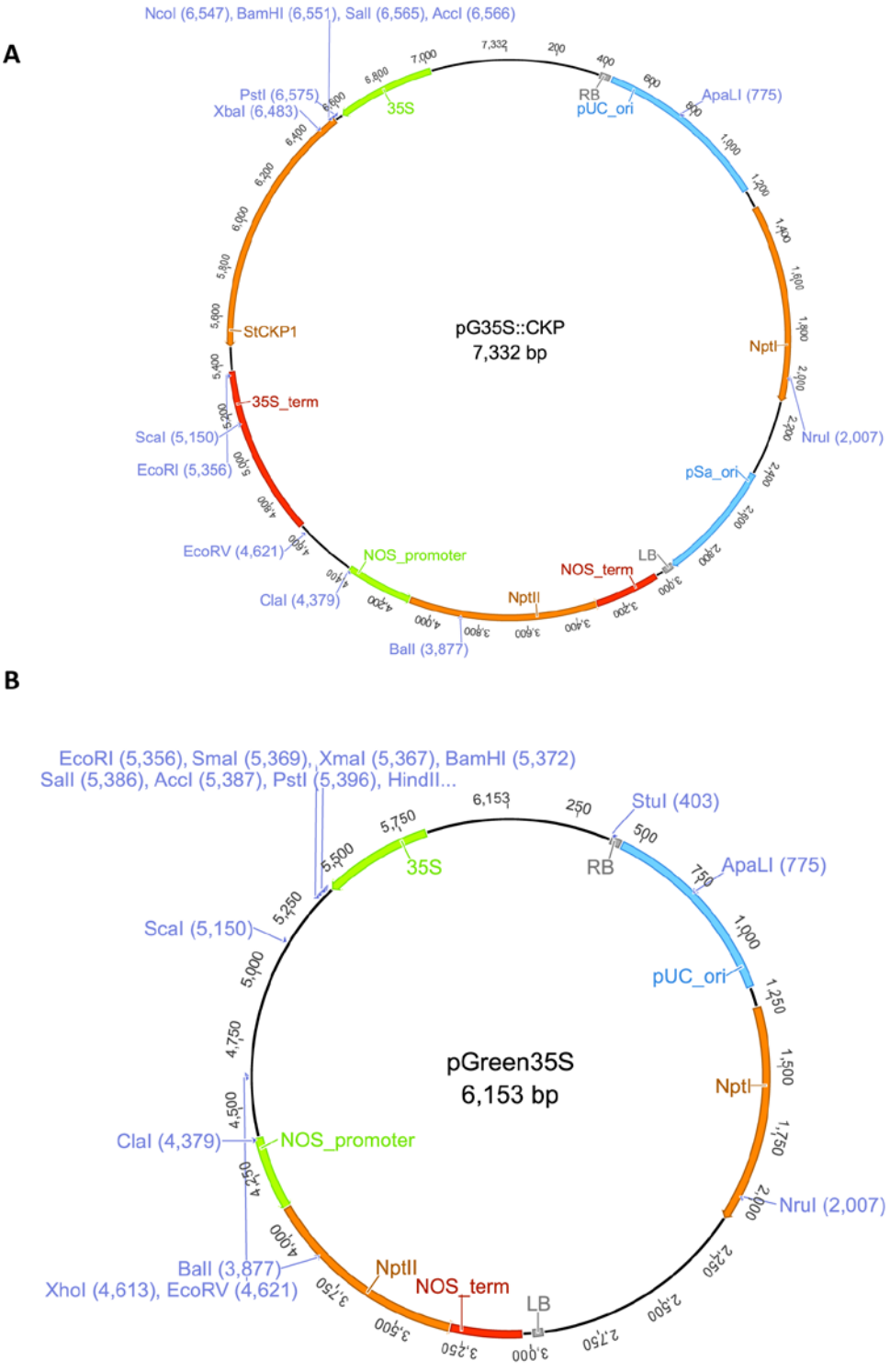

Figure 6.1 Map of pG35S::CKP plasmid used in the production of transgenic lines
A. pG35S::CKP constructed**. B.** pGreen35S plasmid from which pG35S::CKP was constructed is used as an empty vector transformation control

with 35S F and Nos R primers (table 2.3) on transformed bacteria to determine if ligation reactions had been successful. Two colonies yielding a product of 1400bp (as opposed to 200bp if unsuccessful) were selected, grown in LB liquid culture supplemented with 50mg l^{-1} kanamycin and used for plasmid preparation. The purified plasmids were subject to a restriction digest with *Eco*RI and *Bam*HI to confirm insertion of the *StCKP1* insert into the backbone before sequencing with 35SF, Nos R and C912 F primers (table 2.3).

6.2.2 Transformation of *S.tuberosum* and selection of transformants

pG35SS::CKP and pGreen0029::35SS plasmids were transformed into *A. tumefaciens* strain LBA4404 already harbouring the pSOUP plasmid as previously described (section 2.4.8), the latter of which as an empty vector transformation control. Transformed Agrobacterium were cultured on TYNGA containing kanamycin, tetracyclin and streptomycin at appropriate concentrations (appendix 1, table A1.6). Successful transformants were identified by colony PCR using two primer pairs C2F & C2R, and NptII F & NptII R (table 2.3) which had expected product sizes: 441bp and 500bp respectively. One positive colony for each of the transformations was selected and placed into 5ml liquid culture in TYNG supplemented with appropriate antibiotics. Transformation of *S.tuberosum* was carried out as described in section 2.4.9, using six plates of 20-25 explants per transformation and 50µg ml^{-1} kanamycin as a selective antibiotic.

After regeneration of 12 shoots and transfer to MS30 media containing selective antibiotics, leaf tissue was harvested and DNA extracted (section 2.3.1.2) to screen for positive transformants with two primer pairs: 35S F & C2R, and NptII F & NptII R (table 2.3), expected product sizes: 550bp and 500bp respectively. Of the constitutively expressing lines, all were found to be positive for the 35SS:StCKP1 construct while the empty vector control lines were found to be positive for the kanamycin resistance gene *Npt*II. 12 lines expressing the 35SS:StCKP1 construct and 4 empty vector lines were selected for further analysis. These positive transformants were each sub-cultured into two new pots of MS30 containing only kanamycin at a concentration of 50µg ml^{-1} as a selective antibiotic. One of these pots was sub-cultured every 6-8 weeks onto new MS30 media containing kanamycin while the other was allowed to mature for 7 weeks before transfer to pot culture on compost at the Plant Growth Facility for tuber production (section 2.2.1.2).

6.2.3 Quantification of expression of *StCKP1*

To determine *StCKP1* expression in each of the transgenic lines produced, transcript abundance of *StCKP1* was measured in leaves, previously ascertained by Warnes (2005) to contain a relatively low

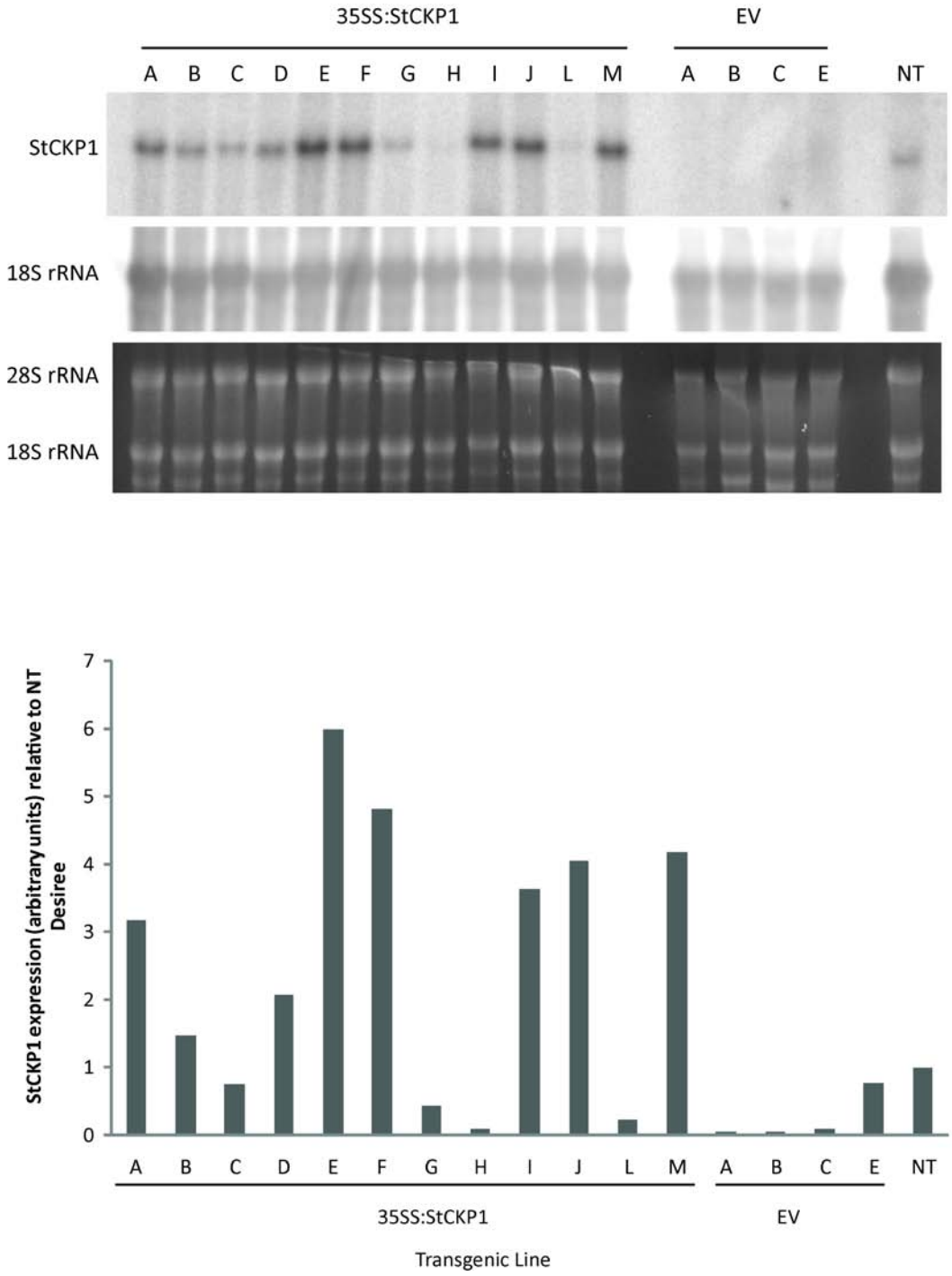

Figure 6.2 Quantification of *StCKP1* expression in leaves of shoot cultures of transgenic lines
Expression of *StCKP1* determined by RNA blotting was normalised relative to 18S rRNA as a loading control, then expressed relative to its expression in non-transformed Desiree. **NT** = non-transformed, **EV** = empty vector.

abundance of *StCKP1* transcript. RNA was extracted from 1g leaf tissue from each of the transgenic lines as previously described (section 2.3.8), and abundance of *StCKP1* transcript measured by RNA blotting. An [α-^{32}P]dCTP labelled DNA probe was synthesised using a 441bp fragment of *StCKP1* produced by PCR with C2F & C2R primers (table 2.3) (section 2.3.11). Abundance of *StCKP1* transcript was quantified by hybridisation of this DNA probe to 5µg extracted RNA immobilised on a nylon membrane, and normalised relative to abundance of 18S rRNA determined by hybridisation of an [α-^{32}P]dCTP labelled 18S probe. To determine the abundance of *StCKP1* in transgenic lines relative to untransformed Desiree (NT), expression data was normalised giving the wild type an arbitrary value of 1. Abundance of *StCKP1* in 35SS:StCKP1 lines was found to be up to 6 times that in wild type (figure 3.2). Lines A, B, D, E, F, I, J and M were designated over-expressing (OE). 35SS:StCKP1 lines C, G, H and L were found to have a lower abundance of transcript in leaves than in NT and so were designated as non-expressers (NE). Line E from the pG0029:35SS empty vector (EV) control lines was selected to use as a control alongside NT as expression of *StCKP1* was closest to that measured in wild type. However, for tuber phenotype studies, EV lines A and B were used due to availability of tissue.

6.3 Tuber phenotype

Transgenic lines were transferred from aseptic culture as previously described (section 6.2) and one plant for each line grown for 6 months until tubers had reached maturity, indicated by senescence of the aerial portions of the plant. Immediately after harvest, tubers were numbered, weighed and photographed for measurement of tuber dimensions. The total mass of all harvested tubers from a single plant was plotted against the number of tubers harvested from the same plant and a Pearson product-moment correlation coefficient calculated for each of OE and NE to give an r^2 value as a measure of the strength of linear dependence between tuber number and total tuber mass. For OE lines, the r^2 was found to be 0.698; for NE lines r^2 was calculated to be 0.924 after removal of outliers circled in figure 6.3. In order to determine whether the slopes of the regression lines fitted to the data, indicated by the calculated r^2 values, an analysis of covariance was carried out using the MiniTab 15 package (MiniTab Ltd, Coventry, UK) which returned a *P*-value of 0.383 indicating that the slopes of the regression lines were not significantly different from one another. A *P*-value of 0.596 was returned when investigating the intercepts of the regression lines, meaning the null hypothesis could not be rejected i.e. there was no significant difference between the intercepts of the regression lines for OE and NE transgenics. It was not possible to calculate the Pearson product-moment correlation coefficient for the EV lines or WT due to insufficient data points.

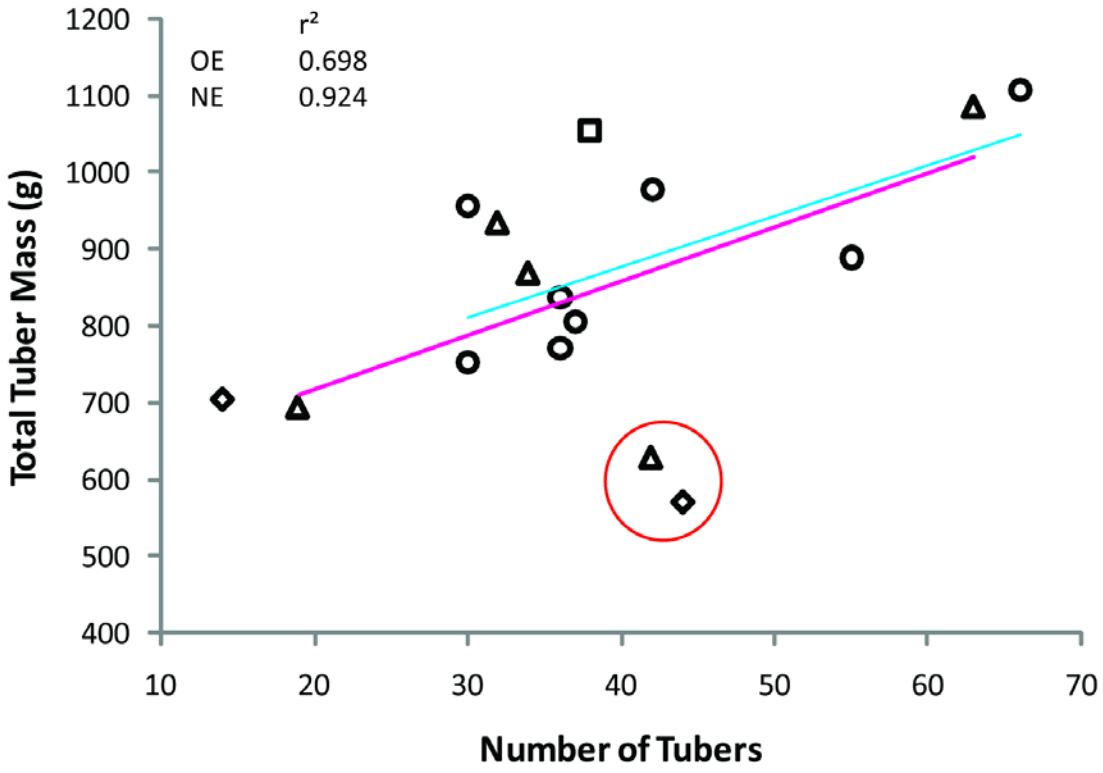

Figure 6.3 Relation of number of tubers produced by a single plant and mean mass of the tubers
The total mass of all harvested tubers from a single plant was plotted against the number of tubers harvested from the same plant. 35SS:StCKP1 lines found to over-express *StCKP1* are represented by (⭘), non-expressing (NE) 35SS:StCKP1 lines are represented by (▲), empty vector controls by (◆), and non-transformed Desiree by (◘). A Pearson product-moment correlation coefficient was calculated to give an r^2 value for the regression of OE (pink) and NE 35SS:StCKP1 lines (blue). Outliers not included in calculation of r^2 are circled in red. ANCOVA analysis gave P values of 0.383 for the slope and 0.596 for the intercept indicating no significant difference for the relationship of tuber mass versus number between OE and NE lines. It was not possible to calculate the Pearson product-moment correlation coefficient for the EV lines or WT as insufficient data points were available for analysis.

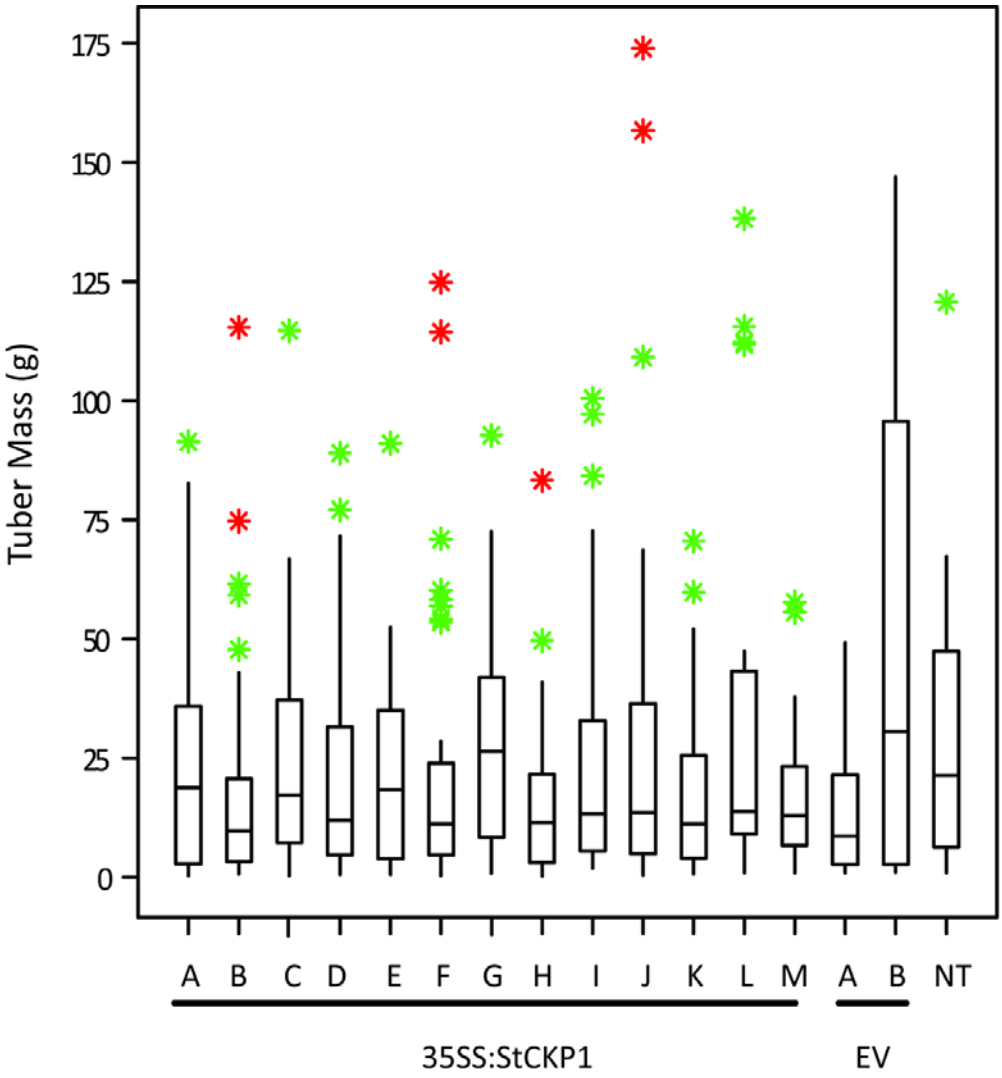

Figure 6.4 Variation in tuber mass range of newly harvested Desiree 35SS:StCKP1 lines compared with non-transformed (NT) and empty vector (EV) controls
The median, interquartile range, minimum and maximum masses of tubers harvested from a single plant were calculated using GenStat 11 and data plotted as a box-whisker plot. Outliers are marked *, extreme outliers *.

The median, interquartile range, minimum and maximum tuber masses were calculated using GenStat 11 and data plotted as a box-whisker plot (figure 6.4). Outliers are marked by green stars, extreme outliers by red stars. The plot indicates that within each line, there is a large range of tuber mass from a single plant. EV line B had unusual growth characteristics, possibly due to irregularities in the watering regime, and produced fewer tubers. It was excluded from the analysis. The observed differences in median values and interquartile ranges for tuber masses were not large enough to be significant at $P<0.05$. The calculated interquartile ranges can be used to assess the tuber size distribution, an accepted measure of the range of tuber masses expected for individual lines, which vary from the lowest value: 16.4g for line 35S M, up to 32.8g for line 35S A. The size distributions measured for different transgenic lines were similar to those previously measured for Desiree (Wurr et al., 1993). The calculated interquartile ranges for untransformed NT Desiree and the transgenic EV line A, are at the upper and lower bounds respectively of the size distribution range calculated for all the transgenic lines, so a difference in tuber size distribution between OE transgenic lines and controls due to expression of the 35SS:StCKP1 construct cannot be said to have had an effect on tuber mass.

The length and width were measured for each of the harvested tubers using Image J. Length was determined as the longest measurable span across the tuber axis. Tuber width was measured at right angles to length and taken halfway along the tuber length, not necessarily at the widest point. The calculated length to width ratios (figure 6.5) were higher in the transgenic lines expressing CKP than the EV transgenic controls and also the NT Desiree line. All tubers transgenic for the 35SS:StCKP1 construct were found to have a length:width ratio of more than 1.5 while the EV and NT tubers were all found to have a length:width ratio less than 1.5. In order to determine whether differences observed in the length:width ratios were significant, a one way analysis of variance (ANOVA) was carried out using MiniTab which gave a *P* value of <0.000, indicating there is a significant difference between means of calculated length:width ratios. To determine which of the means were significantly different from those of the NT Desiree tubers, a two way t-test was carried out between the NT Desiree and the transgenic lines produced. The *P* value for acceptance was corrected according to the Bonferroni correction to give a value for significance of <0.00417. All lines transgenic for the 35SS:StCKP1 construct were found to be significantly different from NT Desiree (marked on figure 6.5 by *) while EV transgenic control lines were found to be not significantly different.

An unusual finding was that 35S lines G and L, previously determined as not expressing the transgene in leaf tissue, had particularly large length:width ratios compared with NT Desiree and

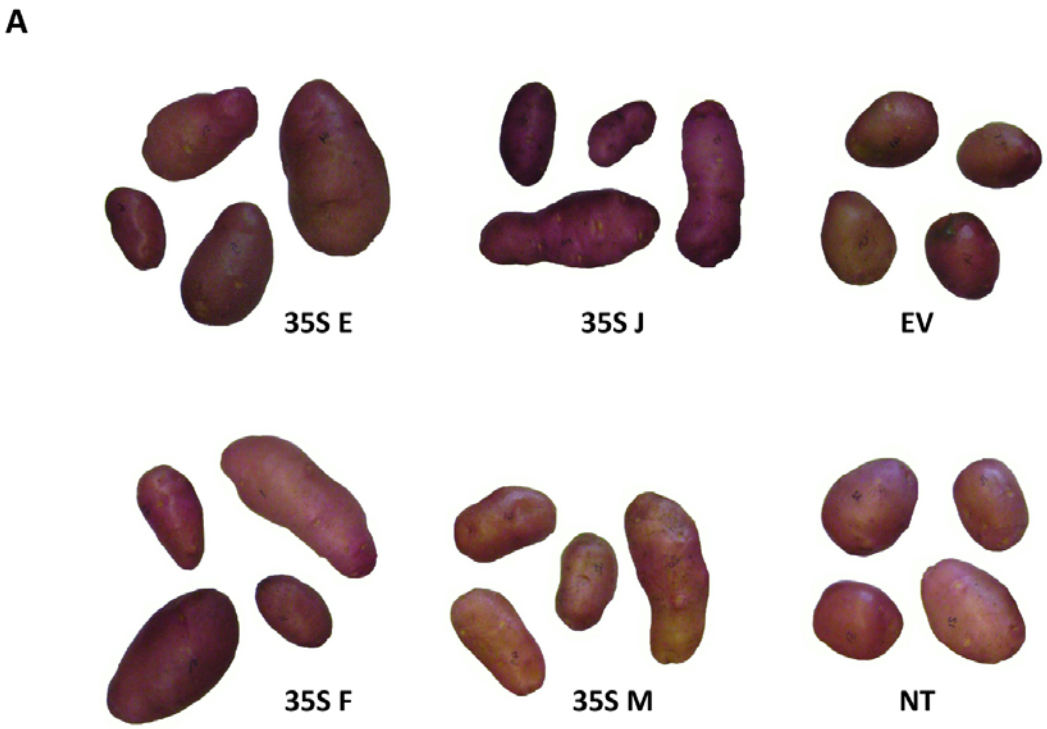

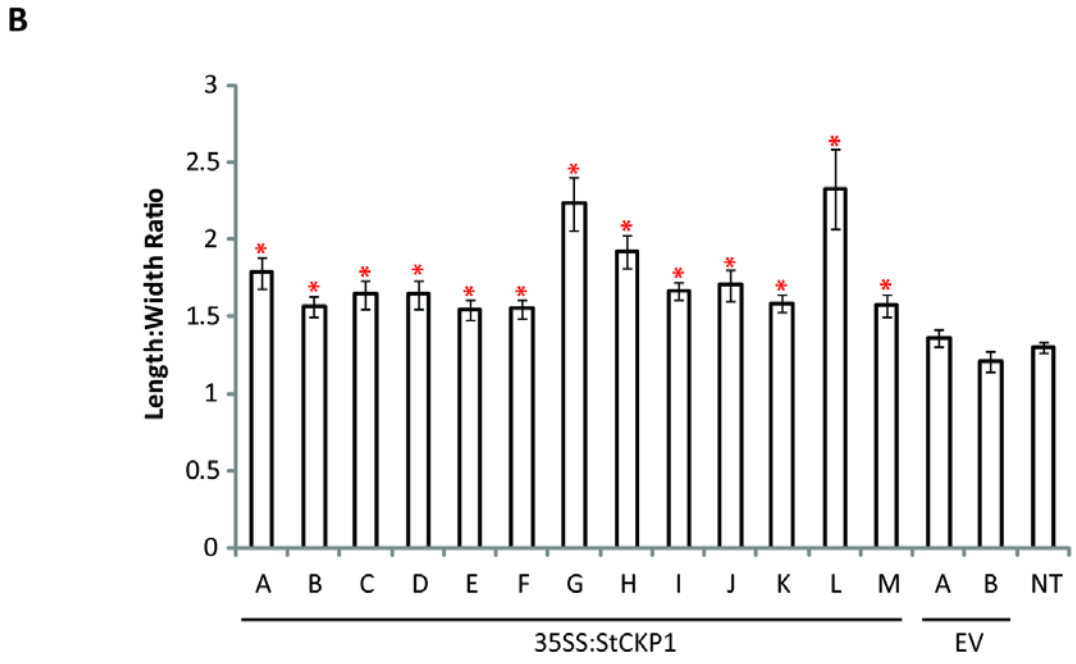

Figure 6.5 Variation in tuber morphology of newly harvested Desiree StCKP1 transgenic lines compared with non-transformed Desiree (NT) and empty vector (EV) controls
A. Comparison of tuber shape for controls (NT and EV) and over-expressing 35SS:*StCKP1* lines. **B.** Length to width ratios of the tested lines ±SE (n=14 to 66).

transgenic OE lines. It may be that the insertion site of the transgenic construct has interfered in the function of another gene or genes, resulting in an increased length to width ratio. It is known that numerous genes are involved in determination of tuber morphology (Vaneck et al., 1994; Morris et al., 2006; Kim et al., 2007), and so it may be that the construct has disrupted expression or activity one of these genes, resulting in altered tuber morphology. A more likely possibility is that the CaMV 35S promoter directed expression of *StCKP1* is different in leaves compared to the expression observed in tubers and other tissues. Thus observation of transgene expression in one tissue, here the stolon and subsequently formed tuber, may not be the same as the transcription measured in another tissue, in this case the leaf. It is also known that there is a threshold level of RNA which accumulates in a given tissue before the sequence triggers suppression. So a further possibility is that the threshold transcript level for triggering suppression might be higher in tuber tissues than leaves as if proteins are to accumulate to storage levels, more transcript is needed than in leaves. If 35S is equally active in leaves and tubers, this would mean that lines in which *StCKP1* is suppressed in leaves, *StCKP1* might not be suppressed in tubers. Further investigation by thermoasymmetric interlaced PCR out from the inserted DNA into the gDNA may give an insight into the position of insertion if sequence is available for the region. Analysis of transcript levels in tuber tissue would confirm whether the transgene is being expressed to a different level.

6.4 Tuber Dormancy

To assay dormancy characteristics of tubers in storage, tubers from each line were categorised according to mass into one of three size classes: 5-≤20g, 20-40g and >40g as used by Dr Christine Newell in an analysis of *StCKP1* silencing by a Potato Virus X (PVX) derived vector. Tubers weighing less than 5g were not used for assay of dormancy as tubers of this size are not commercially relevant and also may not have reached maturity at harvest. Up to five tubers of each size class were selected for each of two treatments to ensure an even distribution of tuber size throughout the assay. One set of tubers were placed directly in storage at 16°C in darkness while the other set were stored in darkness at 4°C for 21 days, a ‘chill’ treatment, prior to transfer to long-term storage at 16°C. The chill treatment was included because temperature is the most influential environmental factor involved in tuber bud dormancy break. There is evidence that chilling shortens dormancy in varieties with lengthy dormancy periods (Wurr and Allen, 1976; Harkett, 1981) and Turnbull and Hanke (1985a) showed that the effect of chill treatment on dormancy break in ‘Majestic’ is mediated by both cytokinin levels and the sensitivity of tubers to cytokinin. Newell (pers. comm.), using virus induced gene silencing (VIGS) to reduce *StCKP1* expression, showed that only the chill sensitive period of dormancy is shortened (figure 6.6).

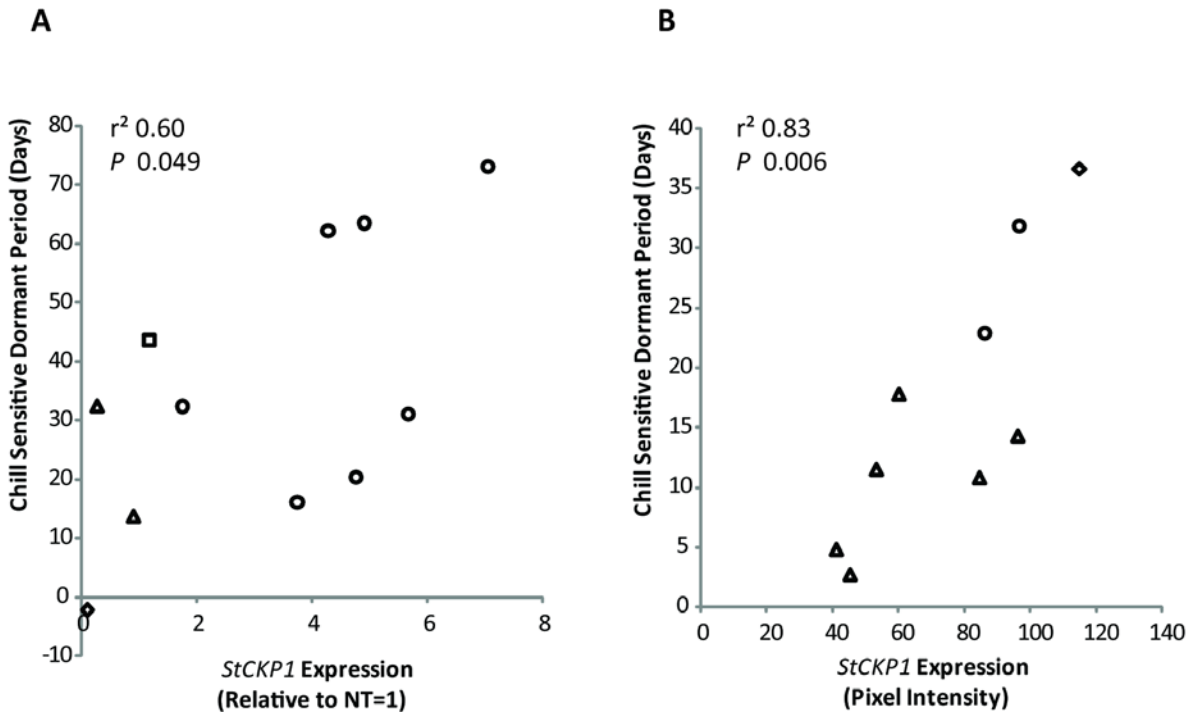

Figure 6.6 Duration of chill sensitive dormancy for *StCKP1* over-expressing and RNAi knock-down lines
A. Mean duration of chill sensitive dormancy of tubers harvested from a single plant for each of the 35SS:StCKP1 over-expressing (⭘), 35S:CKP non-expressing (▲), empty vector transgenic controls (◆), and non-transformed Desiree (◘). **B.** (Data Christine Newell) Mean duration of chill sensitive dormancy of tubers harvested from a single plant subject to VIGS: PVX::StCKP1 (▲), phytoene desaturase (PVX::PDS) (⭘), and empty vector VIGS control (◆).

Tubers were monitored twice weekly for signs of sprouting from apical and lateral tuber buds after lifting from soil. Buds were considered to have fully broken dormancy once sprouts had reached a length of 3mm. Morris et al. (2006) noted that *dxs*- over-expressing tubers appeared to have broken dormancy at harvest in that tuber buds had initiated sprout growth less than 3mm, however there was a 56 day lag before these sprouts began elongating beyond 3mm. At 250 days, tubers that had not sprouted were assigned a dormancy duration of 250 days. This applied to some tubers stored for the whole period at 16°C: two from each of lines 35S E, H, I and M, and one from line 35S F.

For each tuber set, including NE, EV and NT lines for 35SS:StCKP1 lines, and EV PDS lines for RNAi lines, the mean number of days post harvest until the tuber had broken dormancy was calculated. Data for each line are pseudoreplicated as all tubers from each line were produced by a single plant therefore SEs are invalid. To determine the duration of the chill sensitive period of dormancy relative to the insensitive dormant period, the mean dormant period for the tubers that had been given a 21 day 4°C treatment prior to storage at 16°C were subtracted from those that had not been given a chill treatment. The mean total dormant period and chill sensitive dormant period were plotted against the quantification of *StCKP1* expression in leaves of shoot cultures, as determined by RNA blot (section 6.2.3) and regression analyses carried out. Figure 6.6 shows the relationship between the duration of the chill-sensitive dormant period and the over-expression of *StCKP1* alongside the relationship between the chill-sensitive dormant period in lines in which *StCKP1* expression had been knocked-down by RNAi (data Christine Newell). The Pearson product-moment correlation coefficient was calculated to give an r^2 of 0.60 for over-expressing lines compared to the r^2 of 0.83 for the RNAi lines, indicating a positive correlation between level of *StCKP1* expression and duration of the chill sensitive period. Regression analyses were carried out on each of the data sets giving *P* values of 0.049 for the over-expressing lines and 0.006 for the RNAi lines, indicating the relationship between *StCKP1* expression and the duration of the chill sensitive dormant period is significant at $P<0.05$.

The relationship between *StCKP1* expression and the total duration of dormancy as determined by over-expression (this study) and RNAi (data Christine Newell) studies is shown in figure 6.7. The Pearson product-moment correlation coefficient was calculated to have an r^2 of 0.79 for over-expressing lines and 0.28 for RNAi lines, indicating that in over-expressing lines there is a positive correlation between *StCKP1* expression and the length of the dormant period while in RNAi lines, the length of the total dormant period is not significantly affected by a reduction in *StCKP1* transcript. Regression analyses carried out on the data yield *P* values of 0.003 and 0.462 for over-expressing and RNAi lines respectively indicating that the positive correlation between *StCKP1* over-expression and duration of dormancy is significant while there is no significant correlation ($P \leq 0.05$) between

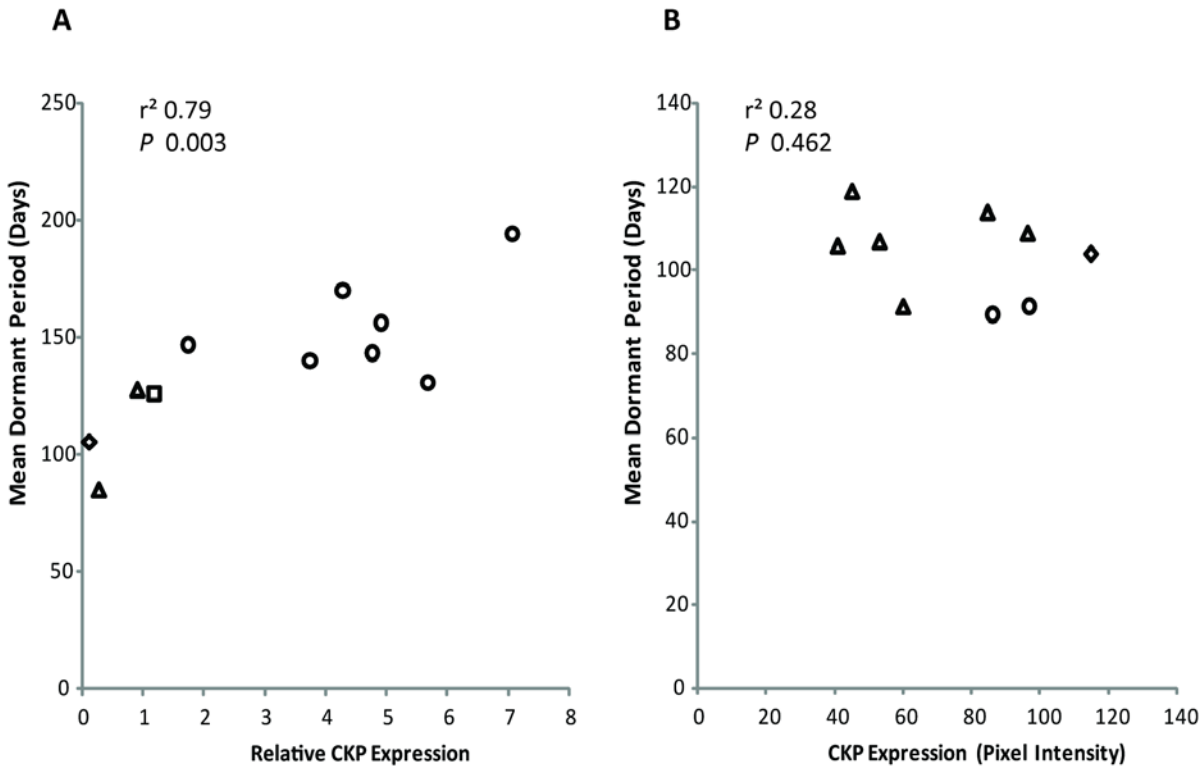

Figure 6.7 Duration of total dormancy in *StCKP1* over-expressing and RNAi knock-down lines
A. Mean duration of dormancy of tubers harvested from a single plant for each of the 35SS:StCKP1 over-expressing (⭘), 35SS:StCKP1 non-expressing (▲), empty vector transgenic controls (◆), and non-transformed Desiree (□). **B.** (Data Christine Newell) Mean duration of dormancy of tubers harvested from a single plant subject to VIGS: PVX::StCKP1 (▲), phytoene desaturase (PVX::PDS) (⭘), and empty vector VIGS control (◆)

StCKP1 knock-down and the total length of the dormant period. No effect of tuber size was observed on the total duration of dormancy or of the chill-sensitive period in over-expressing or RNAi knock down lines.

The relationship between *StCKP1* expression and the duration of chill-insensitive dormancy (calculated by subtracting the chill-sensitive period from the total dormant period) was analysed for over-expressing lines to determine if the increased length of the total dormant period was due to the effect of StCKP1 on the chill-sensitive period alone. The Pearson product moment correlation coefficient was calculated to give an r^2 of 0.38 and regression analysis yielded a *P* value of 0.249 indicating that there is no significant correlation ($P \leq 0.05$) between *StCKP1* over-expression and the chill-insensitive period of dormancy.

6.5 *In vitro* tuberisation

In view of the changes in tuber sprouting characteristics observed on over-expression of the *StCKP1* transgene (figures 6.6 and 6.7), the response of *StCKP1* OE lines was compared with that of EV and NT controls in an *in vitro* microtuberisation system. Microtuber induction was carried out using explants from 6 week old aseptic cultures on PMM+6% sucrose as previously described (section 2.2.1.5.1) using three different cytokinin supplements: 2.5mg l^{-1} BA, 2.5mg l^{-1} [9R]BA, and a no cytokinin, solvent control of dIH_2O. A combination of sucrose and cytokinin has been shown to be required for microtuber induction in Desiree, with a reduction in either resulting in retardation of tuberisation onset (Gopal et al., 1998). If the sucrose content of the media is increased sufficiently, cytokinin can be omitted. Sucrose is known to be the most critical stimulus for tuber formation (Donnelly et al., 2003) while exogenous cytokinin stimulates the process (Seabrook et al., 1993), promoting both microtuber initiation and growth, dependent on cultivar (Gopal et al., 1998). At sucrose concentrations below 8%, cytokinin has the effect of promoting microtuberisation for Desiree explants, thus 6% sucrose was selected in order to ensure a measurable response to addition of cytokinin to the medium. One plate was prepared per line per treatment, each with 12 nodal explants per plate. Explants were monitored daily for stolon induction, induction of tuberisation and full tuberisation. After 35 days of treatment, photographs were taken of each plate of microtubers and the length of each stolon measured using Image J. Stolon length was measured to the tip of either the untuberised apical stolon tip, passing any lateral microtubers, or to the apex of the terminal microtuber.

On PMM media containing no cytokinin, lines E, F and M over-expressing *StCKP1* were found to initiate tubers significantly earlier than EV and NT lines assayed. A one-way ANOVA was carried out

on the data which gave a P-value 0f 0.000, indicating a significant difference was to be found within the data. On completion of a two-way t-test between NT and the transgenic lines, lines E, F and M were found to have P-values less than the Bonferonni corrected P-value of 0.01 (marked with * on figure 6.8). This is in contrast to the explants subject to *in vitro* microtuberisation on media supplemented with cytokinin, BA or [9R]BA, in which induction of tuberisation in over-expressing lines was not significantly different ($P \leq 0.01$) to that observed in NT Desiree explants (figure 6.8). The inclusion of BA in the medium resulted in an increase in the percentage of stolons that tuberised. For example, for NT explants the degree of tuberisation increased from 58% to 100%, similar to the degree of tuberisation observed for OE lines in the absence of BA (table 6.1). When BA or [9R]BA was added to the microtuberisation media, tuberisation had occurred on all explants at 35 days, however when BA was omitted from the media, a greater proportion of the OE lines had undergone tuberisation at 35 days relative to the EV transgenic line and NT Desiree (Figure 6.9), indicating that cytokinin is a positive regulator of tuberisation of stolons at 6% (w/v) sucrose in NT Desiree. The number of tubers formed over the time course of induction on both 6% sucrose and 6% sucrose + BA treatments (figures 6.8 & 6.9) demonstrates the rate of tuber formation of OE, EV and NT lines. ANCOVA analysis of the calculated rates of tuber formation indicated that the rate of tuber production is faster in OE lines E (P=<0.000), F (P=<0.000) and M (P=<0.000) on media containing 6% sucrose relative to NT Desiree and EV transgenic control lines. In contrast, no significant difference in rate of tuber formation was found between OE, EV and NT lines when the media had been supplemented with BA or [9R]BA (at $P \leq 0.05$). Significant differences were found when comparing rates of tuber formation on 6% sucrose and 6% sucrose + BA in EV (P=0.037) and NT Desiree (P=0.001), while there was no significant difference to be found when comparing transgenic OE *StCKP1* lines induced on these two different media (at the $P \leq 0.05$ level).

Mean stolon lengths determined indicated that the addition of BA to the microtuber inducing PMM media, which contained 6% sucrose for all treatments, resulted in a significant reduction of mean stolon length in NT Desiree (P=0.001) and a non-significant reduction in transgenic EV control and lines 35S M and J and E. 35S F stolon length was increased by addition of BA to the media (table 6.1). This latter finding may be attributable to inhibitory effects of excess cytokinin upon tuberisation (Suttle, 2004). On media containing 6% sucrose, mean stolon length was significantly decreased (at $P \leq 0.01$) in OE transgenic lines 35S E (P=0.001), F (P=0.001) and M (P=0.01) while stolon lengths of explants of the EV transgenic control were found to be not significantly different from NT Desiree, indicating that over-expression of *StCKP1* results in shorter stolons, most likely due to the observed rate of tuberisation being faster than that of NT Desiree and EV transgenic controls (figure 6.10).

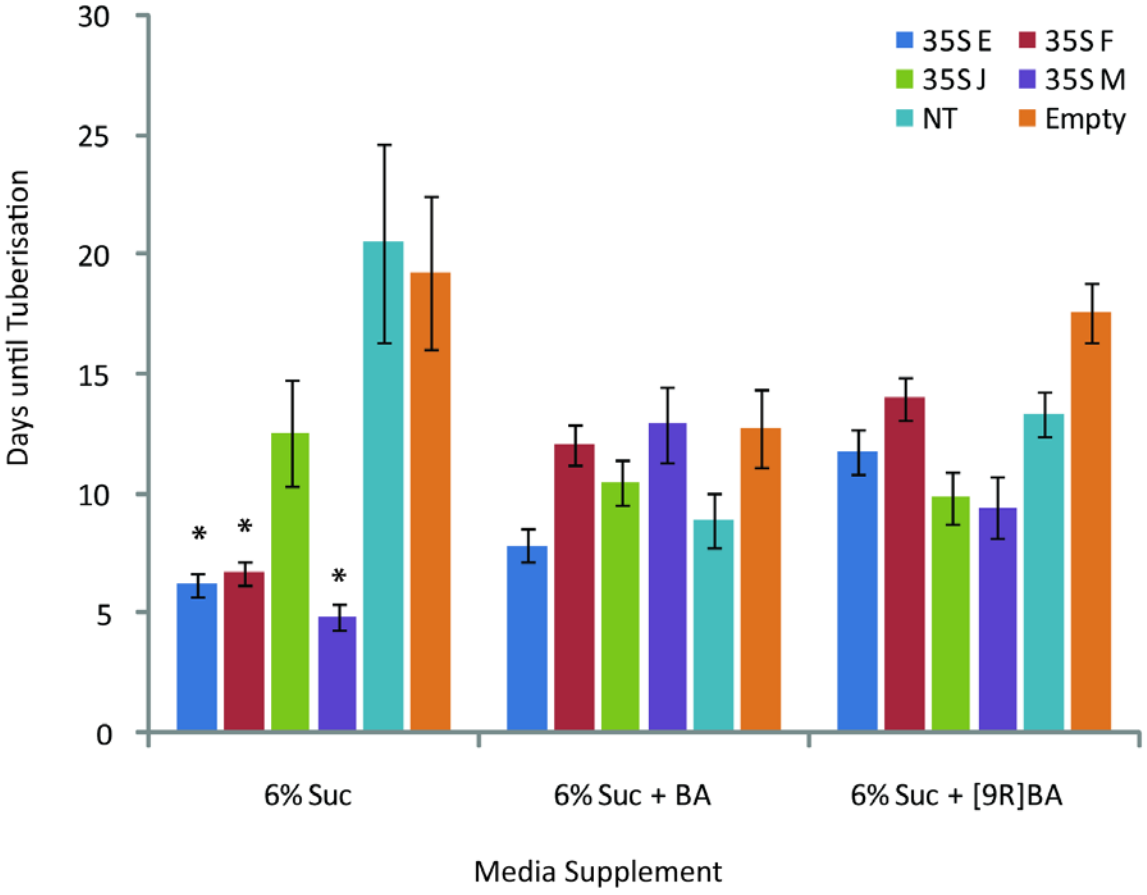

Figure 6.8 Effects of N-6 benzyladenine (BA) and N-6 benzyladenosine ([9R]BA) on *in vitro* tuberisation of *StCKP1* over-expressing transgenic lines compared with controls
Values are means ±SE (n=12). For each cytokinin treatment, lines tuberising significantly earlier than NT and EV controls (at P≤0.01) are marked with *.

Table 6.1 Effects of N-6-benzyladenine (BA) and N-6-benzyladenosine ([9R]BA) on *in vitro* tuberisation of *StCKP1* over-expressing tubers compared with controls.
Tuberisation after 35 days on PMM microtuber-inducing media is expressed as percentage (n=12), values for stolon length are means±SE (n=12). ND = not determined, EV = empty vector line E, NT = non-transformed

	Tuberisation at 35d (%)			Mean Stolon Length at 35d (mm)	
	6% Suc	6% Suc + BA	6% Suc + [9R]BA	6% Suc	6% Suc + BA
35S E	83	100	100	5.3±3.1	5.3±1.7
35S F	83	100	100	4.6±0.9	31.3±5.3
35S J	92	100	100	21.9±5.9	14.4±3.7
35S M	75	100	100	19.4±7.4	11.1±3.7
EV	50	100	100	17.2±5.8	13.69±4.5
NT	58	100	100	42.6±7.3	6.9±2.9

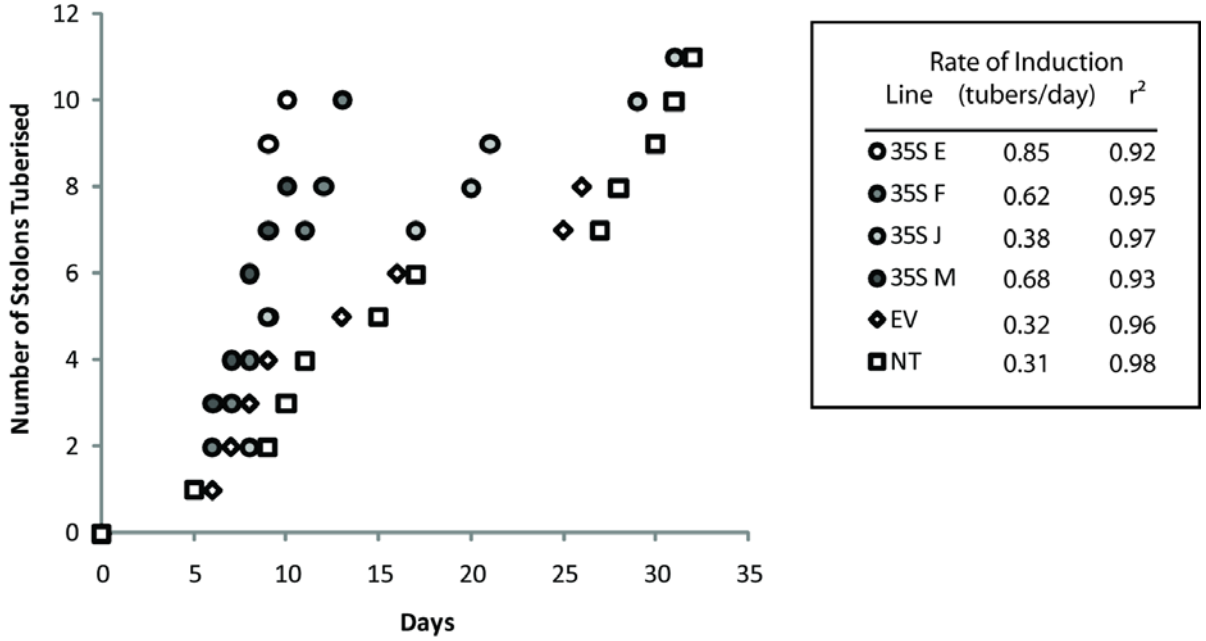

Figure 6.9 *In vitro* tuberisation: Effects of over-expression of *StCKP1*
Rate of tuber induction on microtuber inducing media (PMM) in the absence of cytokinin. r^2 calculated using the Pearson product moment correlation coefficient. ANCOVA analysis of the gradient of the regression gave significant *P*-values (at $P \leq 0.05$) for OE lines E, F and M.

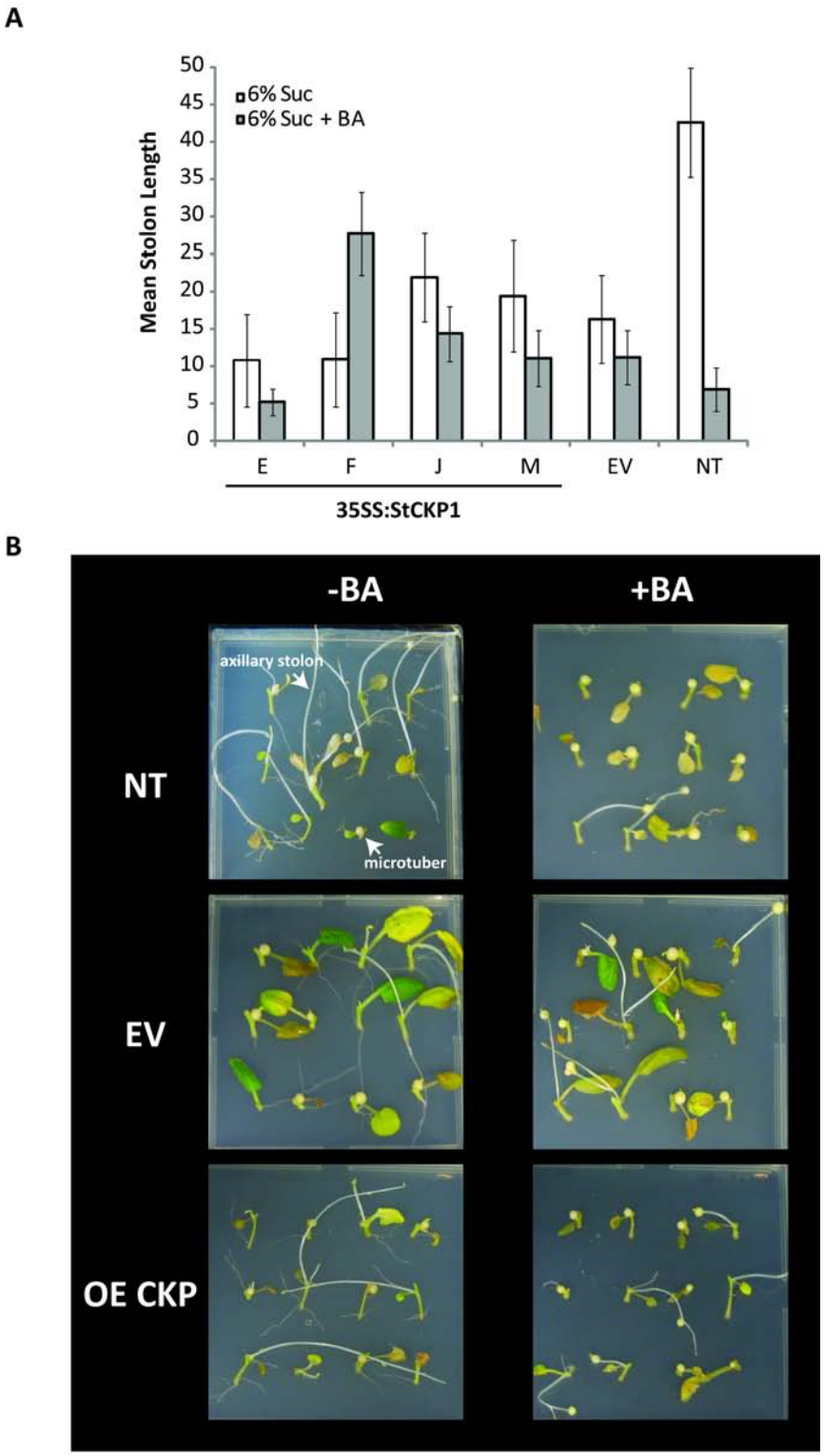

Figure 6.10 *In vitro* stolon growth of over-expressing and empty vector transgenic lines compared with non-transformed controls

A. Quantified mean stolon length ±SE (n=12) **B.** Nodes were grown in 100mm square Petri dishes on microtuber inducing media (PMM) in the presence (+BA) or absence (-BA) of the cytokinin benzyladenine for 35 days.

When induced on PMM supplemented with BA, only 35SF was found to have a mean stolon length significantly larger (P=0.001) than NT Desiree (at $P \leq 0.01$).

When supplemented with cytokinin, the rate of microtuber induction was increased in NT Desiree and EV transgenic control lines, while OE lines were found to have decreased rates relative to those induced on media not supplemented with cytokinin. No significant difference ($P \leq 0.05$) was found for the rates of microtuber induction between OE lines and NT and EV controls when growth media were supplemented with BA or [9R]BA.

Overall, the *in vitro* tuberisation characteristics of *StCKP1* OE explants in the absence of BA were similar to that observed for NT Desiree and EV control explants cultured in the presence of BA, as evident in figure 6.10. However, the large degree of variation seen in stolon length indicated by the calculated standard errors (table 6.1) indicates further experiments should be carried out to determine the effect of *StCKP1* on the characteristics of *in vitro* tuberisation.

6.6 Callus growth rate

To measure the effect of over-expression of *StCKP1* on the rate of tissue growth, 5mm sections of stem internode from 6 week old plantlets grown in aseptic culture were placed on G B-5 callus induction media and incubated as previously described (section 2.2.1.5.2). 4 stem sections were cultured per plate, and 4 plates cultured per line (n=16). Calli were transferred to fresh media every two weeks in order to prevent nutrient deficiency. Plates of callus were photographed after the first signs of callus production had begun 30 days after transfer of internodes to G B-5 media, further photographs were taken at a minimum interval of 7 days. Callus area was estimated using the area measurement tool in Image J and used to determine relative growth rate of each line. Relative growth rates were found to be between 7.1 and 9.5$mm^2\ d^{-1}$ (figure 6.11). ANCOVA analysis yields a P-value of 0.122 indicating no significant difference in relative growth rate between the OE and EV transgenic lines, and NT Desiree.

6.7 Cytokinins in transgenic callus

It is known that [^{3}H]DZ is taken up from liquid media and transported throughout the root and shoot system of tomato seedlings (Arthur et al., 2001), and so to determine the effect on cytokinin interconversion of over-expression of *StCKP1*, callus tissue was fed [^{3}H]iP and the products of interconversion analysed by HPLC and liquid scintillation counting. 1g 40 day old callus, induced from 5mm stem internodes on G B-5 medium, was added to 10ml G B-5 liquid media without hormone

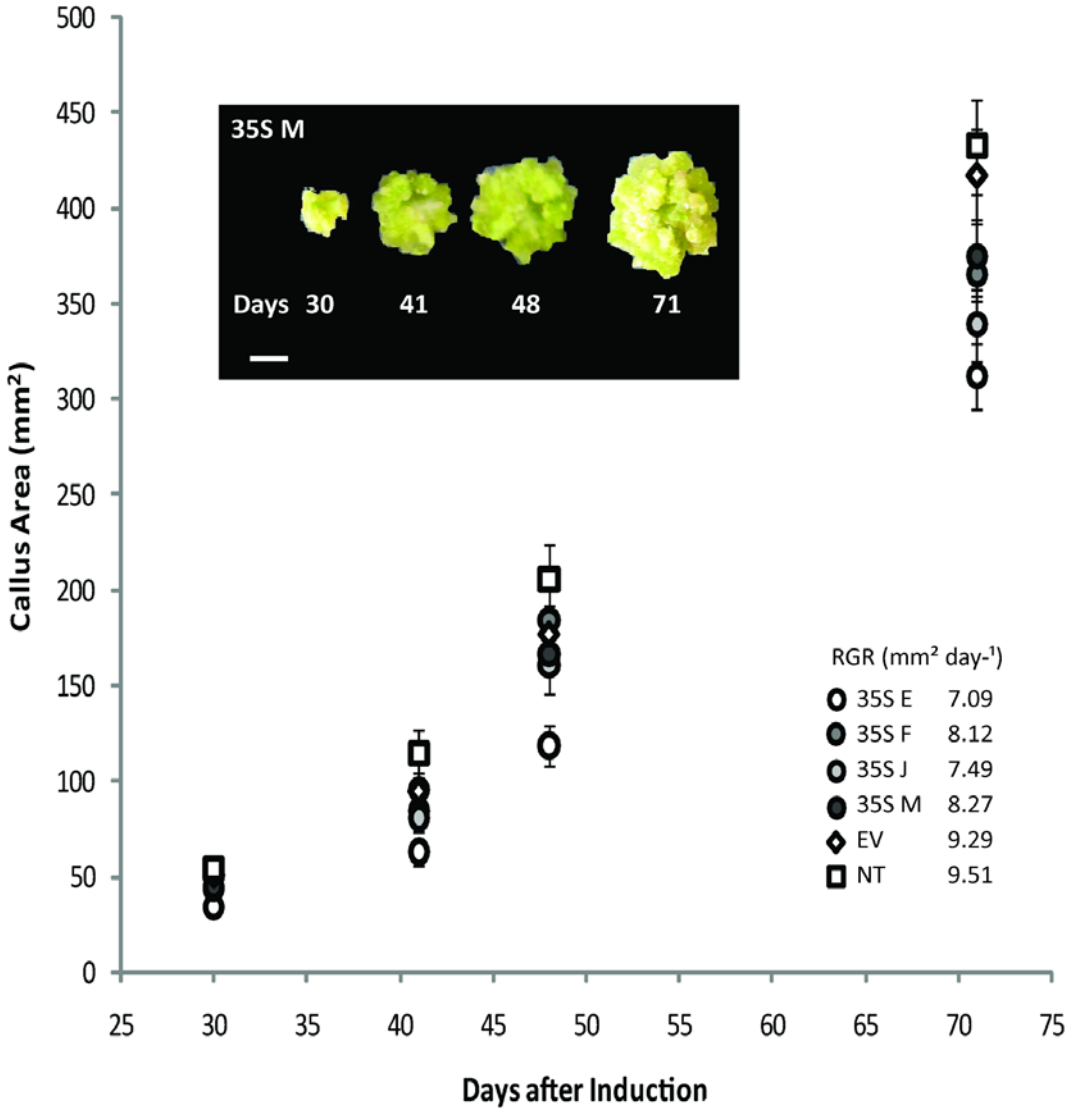

Figure 6.11 Callus Relative growth rate
Callus induced from 5mm stem internode sections on G B-5 media. Quantified mean area ±SE (n=16). ANCOVA analysis yielded no significant difference between slopes of NT Desiree and OE and EV transgenic lines. NT=Not transformed, EV=Empty vector, OE=Over-expressor. Scale bar = 10mm

supplement (3.86g l^{-1} G B-5+vitamins, 20g l^{-1} glucose, 0.5g l^{-1} MES, pH5.7) plus 10nM iP "cold carrier" supplemented with 2.5kBq [^{3}H]iP. Callus was incubated in the iP-supplemented media at 2Hz for 10 hours before separating callus from the media by filtration through 3 layers of GF/A grade glass filter paper (Whatman). Cytokinin was extracted from callus tissue as previously described (sections 2.6.1 and 2.6.2) and cytokinin remaining in the medium was extracted by Sep-Pak purification (section 2.6.2.2). Cytokinins were separated by HPLC in a methanol gradient as previously described (section 4.7) and 1ml fractions collected over 36 minutes. 3ml Optiphase Hi-safe 3 scintillation cocktail was added to each of the fractions and scintillation counted for 10 minutes to measure the [^{3}H] content. Total recovery was calculated by combining [^{3}H] counts for callus and media extracts and divided by initial [^{3}H] input to correct for losses in extraction; this value was used to correct the raw data for losses. Content of [^{3}H]cytokinin was determined by integration of data relative to elution times of standards and expressed as a percentage of total [^{3}H]cytokinin recovery using 3 biological replicates to calculate standard error.

Quantified cytokinin content is shown in table 6.2, which indicates that [^{3}H]iP was taken up from the medium and interconverted to other cytokinin types in all lines assayed. The extent of interconversion is apparently greater in transgenic OE lines harbouring the 35SS:StCKP1 construct as the fraction of [^{3}H] as labelled iP is lower in OE lines versus the EV transgenic control and NT Desiree lines. The mean ratio of cytokinin riboside to base showed that StCKP1 OE lines contain 3-fold more riboside than base while EV and NT control lines contain 2-fold more riboside than base. Of the compounds examined here, the predominant cytokinin types formed from [^{3}H]iP were Z, [9R]Z and [9R]DZ in all lines. The similar pattern observed in OE lines compared with EV and NT Desiree indicates that multiple enzymes are active in the interconversion of cytokinin bases, as previously identified (Chen and Petschow, 1978; Chen et al., 1982a; Burch and Stuchbury, 1987; Moffatt et al., 1991) and that over-expression of *StCKP1*, identified in this study as catalysing the ribosylation of cytokinin bases, does not have a major effect on interconversion in callus tissue. However, the similarity in this pattern indicates that over-expression of *StCKP1* has at most only a relatively minor affect on the fate of [^{3}H]iP in callus tissue, a finding that agrees with the lack of effect on vegetative phenotype of OE lines (section 6.6)

Zeatin-type cytokinin extracted from 1g 40 day old callus was quantified by ELISA. Cytokinin was extracted, including the addition of 830Bq [^{3}H]Z to quantify recovery, and purified as previously described (sections 2.6.1 and 2.6.2) and assayed by ELISA (section 2.7.1). Recovery was calculated by scintillation counting 50µl of the extract with 1ml Optiphase Hi-safe 3 scintillation cocktail (section 2.6.4) and used to correct for losses incurred in extraction and purification. A dilution series ranging

Table 6.2[^{3}H]-labelled cytokinin extracted from callus tissue after 10 hours incubation with 2.5kBq [^{3}H]iP
Cytokinin was extracted from callus tissue and from the incubation medium, then separated using HPLC. Total [^{3}H] recovery was calculated for media and callus and divided by initial [^{3}H]input to correct for losses in extraction. Cytokinin content was determined by integration relative to standards and expressed as a percentage of total cytokinin recovery ±SE (n=3). All recoveries were >0.12

Cytokinin	Line					
	35S E	35S F	35S J	35S M	EV	NT
iP	0.21±0.02	0.22±0.03	0.18±0.03	0.15±0.05	2.41±0.37	0.84±0.10
[9R]iP	0.17±0.03	0.16±0.04	0.11±0.01	0.11±0.03	0.69±0.05	0.05±0.009
[9R-MP]iP	2.39±0.59	1.61±0.45	1.71±0.27	2.03±0.42	5.71±2.14	8.59±1.25
[9G]iP	8.84±1.55	10.89±2.24	9.49±2.25	7.61±1.09	4.67±0.59	3.78±0.78
Z	11.85±0.33	7.59±3.28	12.56±1.21	12.71±1.05	5.85±0.82	14.30±3.17
[9R]Z	14.97±0.89	18.48±3.40	15.36±1.54	13.49±1.66	24.68±3.28	10.30±2.10
[9R-MP]Z	1.39±0.04	1.31±0.06	1.24±0.38	1.48±0.13	15.88±1.15	1.73±0.16
[9G]Z	1.47±0.08	1.53±0.02	1.30±0.22	1.67±0.16	3.21±0.93	1.57±0.38
DZ	2.71±0.12	2.64±0.26	3.05±0.31	2.64±0.05	2.53±0.41	6.85±1.75
[9R]DZ	28.45±1.70	34.79±6.55	28.42±2.92	25.83±3.54	14.01±1.50	22.52±5.43
[9R-MP]DZ	1.24±0.04	1.34±0.05	1.06±0.28	1.42±0.14	4.95±2.05	1.34±0.13
[9G]DZ	10.18±0.34	6.97±3.13	10.82±0.96	10.94±0.82	5.47±0.41	7.00±2.74
Ado	16.16±1.92	12.47±1.04	14.66±1.79	19.89±2.59	9.90±1.77	21.08±0.91

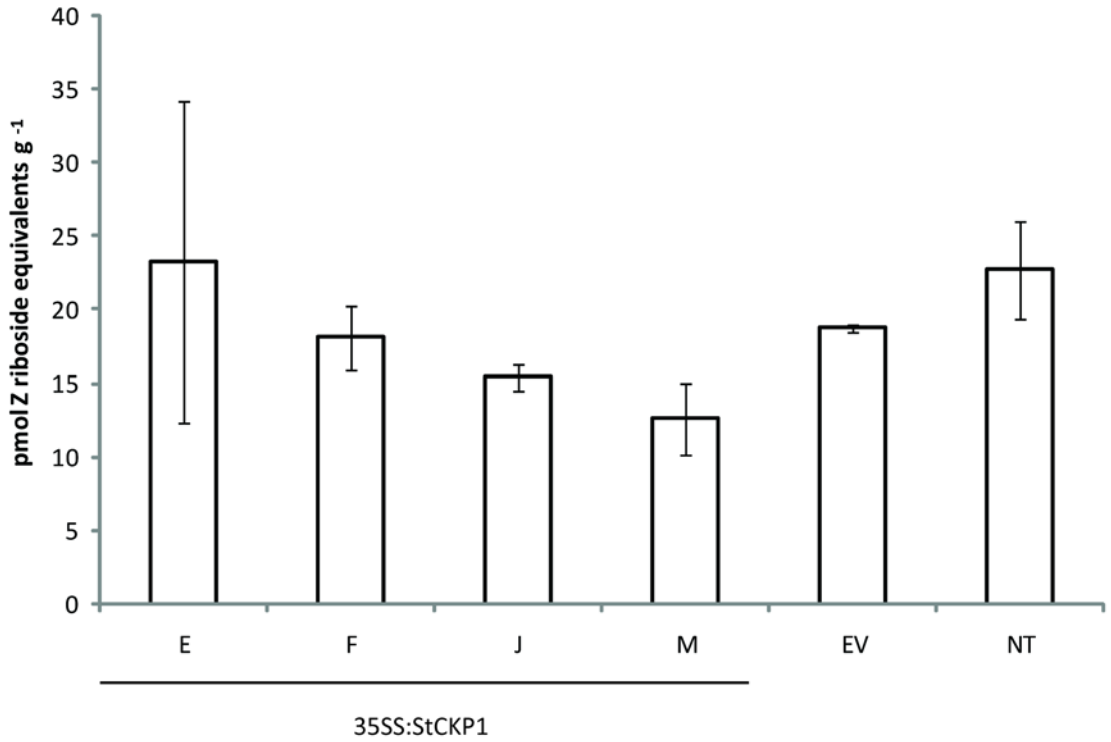

Figure 6.12 Content of cytokinin (pmol g-1 FM) in different lines of transgenic and control potato callus. Cytokinin content of 1g 40 day old callus, induced on G B-5 media, determined by ELISA. Result data presented is mean content of immunogenic zeatin-types in pmol [9R]Z equivalents g^{-1} FM ±SE (n=3). EV=Empty 35S vector transgenic control, NT= Non-transformed Desiree.

from 0.5 to 0.1 of each sample was made to test for interference by non-cytokinins in the extract, and a standard curve from 6250 to 12.2 fmol zeatin produced to allow for direct quantification. Figure 6.12 shows that there was no significant difference ($P \leq 0.05$) in the tissue content of zeatin type cytokinins in this tissue, which is unsurprising as OE of *StCKP1* does not directly perturb the biosynthetic pathway. However, there may be underlying differences in the amount of [9R]Z versus Z, indicated by feeding experiments (section 3.7) in which fed [^{3}H]iP was converted to [9R]iP and [9R]Z by callus tissue. Differences in [9R]Z compared to Z have also been observed in potatoes transgenic for a bacterial isopentenyltransferase relative to non transformed controls (Macháčková et al., 1997). Further analysis by HPLC-ELISA or LC-MS-MS would be pertinent to determine whether there are quantifiable differences between zeatin N^7 and N^9 conjugates, particularly N^7 glucosides, the content of which was shown by Zubko et al. (2005) to be increased in *Sho* over-expressing potatoes.

6.8 Transcript analysis in other potato cultivars

Manipulation of *StCKP1* transcript abundance by RNAi and 35S driven over-expression (section 6.4) affected the chill-sensitive period of tuber dormancy identified by Turnbull and Hanke (1985a, b). As the quantity of *StCKP1* transcript had an effect on duration of dormancy, in that the greater the *StCKP1* abundance the longer the dormant period governed by chilling, *StCKP1* may be a potentially useful early marker for predicting the duration of dormancy by molecular studies before long-term physiological studies are carried out on new cultivars.

Field grown stolons at various stages of tuberisation (before tuberisation, incipiently tuberising and tuberised) were harvested in July 2008 from Cambridge University Farm for the following commercially available cultivars: Accord, Anya, Carlingford, Charlotte, Desiree, Fambo, Hermes, Inca Dawn, Juliette, King Edward, Marfona, Maris Peer, Estima and Lady Rosetta; and from Babraham Home Farm in August 2008: Bonnie, Isle of Jura and Majestic. The known dormancy characteristics for each of these cultivars from the British Potato Variety Database (http:varieties.potato.org) and the European Cultivated Potato Database (www.europotato.org) is summarised in table 6.3 where a value of 9 indicates the longest period of innate dormancy.

RNA was extracted from 3 stolon tips from each available stage for each cultivar as previously described (section 2.3.8) and quantified by UV spectrophotometry (section 2.3.3). As figure 6.13 shows, much of the RNA extracted from field grown stolons was of poor quality, most likely due to contamination but also due to degradation of RNA in transit from field to laboratory. Two harvest approaches were taken, the former used in harvest of stolons from Cambridge University Farm was

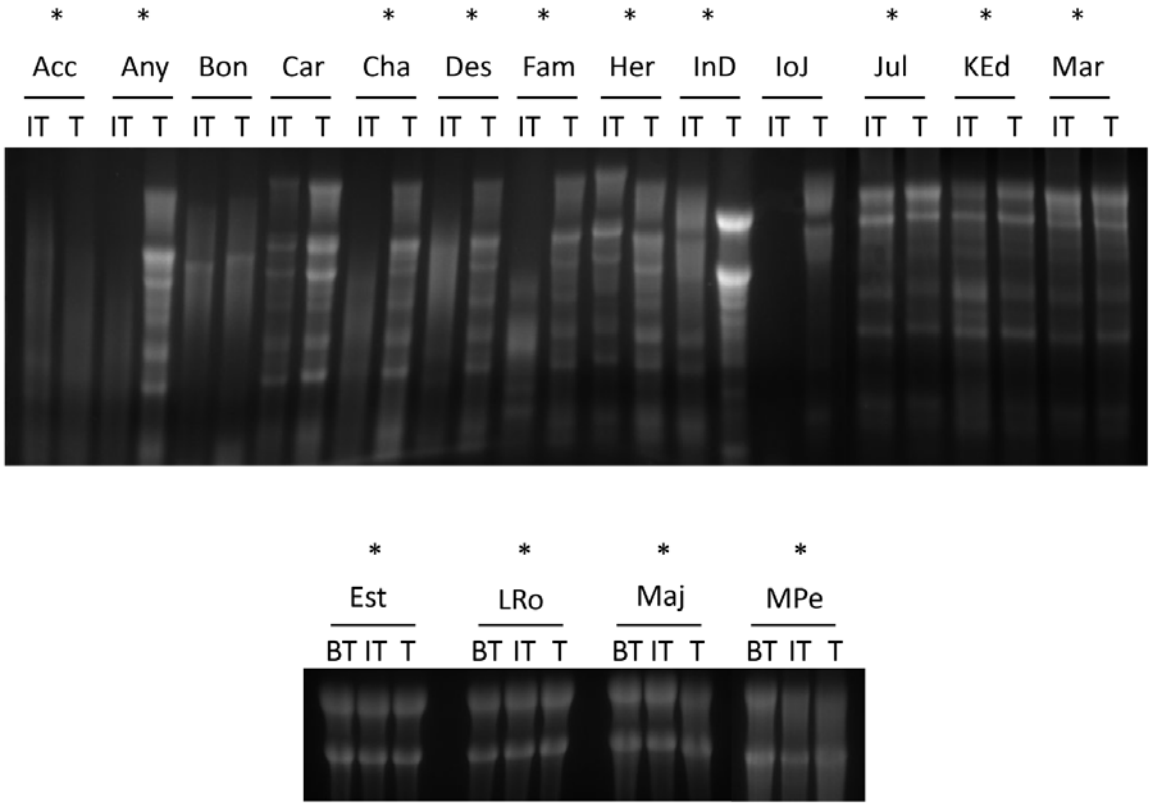

Figure 6.13 RNA extraction from multiple potato cultivars
RNA was extracted from field grown potatoes and run on a 1.2% (w/v) agarose gel after heating to 60°C in denaturing loading buffer. RNA visualised using ethidium bromide and UV illumination. Cultivars harvested from Cambridge University Farm are marked with *, unmarked cultivars were harvested from Babraham Home Farm. BT - Before tuberisation, IT - Incipient tuberisation, T - Tuberised. Cultivar abbreviations: Acc = Accord, Any = Anya, Bon = Bonnie, Car = Carlingford, Cha = Charlotte, Des = Desiree, Fam = Fambo, InD = Inca Dawn, IoJ = Isle of Jura, Jul = Juliette, KEd = King Edward, Mar = Marfona, Est = Estima, LRo = Lady Rosetta, Maj = Majestic, MPe = Maris Peer.

to wash stolons in the field with RO water and place in a dry shipper, pre-chilled using liquid nitrogen for transit before RNA extraction. The other approach utilised in the harvest of stolons was from cultivars grown at Babraham Home Farm and was to harvest the full potato plant for transport before harvesting stolons in the laboratory, snap freezing in liquid nitrogen, and storage at -80°C. It seems that neither of these approaches was particularly successful in yielding high quality RNA for hybridisation of radio-labelled probes and so quantification of transcript. However, of the successful extractions made, these were predominantly from the Cambridge University Farm harvest in which stolons were ensured to be free of contaminating soil before freezing for transport in a dry shipper.

RNA of suitable quality was used to assay for *StCKP1* transcripts in other cultivars at the previously defined stages of tuberisation (section 3.3.1). 10µg total RNA was used for an RNA blot with an [α-^{32}P]dCTP labeled probe synthesised using a 441bp fragment of *StCKP1* produced by PCR with C2F & C2R primers (table 2.3) (section 2.3.11). Abundance of *StCKP1* transcript was quantified by hybridisation of this DNA probe to extracted RNA immobilised on a nylon membrane, and normalised relative to abundance of 18S rRNA determined by hybridisation of an [α-^{32}P]dCTP labelled 18S probe synthesised by PCR using 18SF & 18SR primers (table 2.3).

RNA blotting indicates that *StCKP1* is expressed in tuberising stolons of the cultivars Estima, Lady Rosetta, Majestic, Maris Peer, Juliette, King Edward and Marfona. Interestingly the cultivars with longer dormancies shown in table 6.3, notably Lady Rosetta and Majestic, were found to have greater transcript abundance at both incipient tuberisation and while tuberising than those with a shorter dormant period, such as Maris Peer (figure 6.14). *StCKP1* transcript abundances fell once tubers had formed relative to transcript abundance at incipient tuberisation for Juliette, Estima, Lady Rosetta and Maris Peer. As demonstrated by the relationship between Desiree transcript and protein abundance (section 3.3, figures 3.7 & 3.8), StCKP1 protein may have a high stability and so a low turnover like the bark storage proteins with which StCKP1 shares similarity (Zhu and Coleman, 2001), thus although transcript decreases, protein abundance may remain high.

StCKP1 transcript abundance after tuberisation determined by RNA blotting was found to correlate significantly (r^2=0.76, P=0.048) with the mean dormancy classification given by the British and European cultivated potato databases. This finding indicates that there may be a link between StCKP1 and tuber dormancy, supported by the data from over-expression and knock-down by RNAi previously discussed (section 6.4). However, only a single estimate per cultivar has been carried out in this preliminary study and so to have greater confidence in this finding, further replicates are

Table 6.3 Dormancy characteristics of commercially available potato cultivars

Information collated from British Potato Variety Database (http:varieties.potato.org) and the European Cultivated Potato Database (www.europotato.org). [1] Department of Agriculture Food and Forestry, IRELAND, 2005; [2] Federal Research Centre of Agriculture, GERMANY, 2005; [3] Leibniz Institute of Plant Genetics and Crop Plant Research (IPK), GERMANY, 2005; [4] SASA, UNITED KINGDOM, 2005; [5] Pannon University, HUNGARY, 2005; [6] HZPC B.V., NETHERLANDS, 2005; [7] NEIKER-Instituto Vasco de Investigación y Des, SPAIN, 2005; [8] Nederlands Potato Consultative Foundation, NETHERLANDS, 2005

			Dormancy Rating (9=long dormancy period)									
				Source								
Variety	**Breeder**	**British Potato Variety Database**	**European Cultivated Potato Database**	**[1]**	**[2]**	**[3]**	**[4]**	**[5]**	**[6]**	**[7]**	**[8]**
Lady Rosetta	Meijer Research BV	5	Medium to long [3] Long [4, 8]			6	7				7
Maris Peer	PBI	4	Short to medium [4]				4				
Estima	?	5	Medium to long [3] Long [4, 8]			6				7	7
Accord	Meijer Research BV	No Data	No Data								
Anya	SCRI	No Data	No Data								
Carlingford	Cygnet PB	7	Medium [3] Medium to long [4]			5	6				
Charlotte	Unicopa	No Data	Medium to long [4, 6]				6		6		
Desiree	HZPC UK	5	Medium [3] Medium to long [4, 5, 8]			5	6	6		6	
Fambo	Meijer Research BV	7	Long [4]				7				
Hermes	Saatbah	7	Long to very long [3]			8					
Inca Dawn	SCRI	No Data	No Data								
Juliette	?	No Data	No Data								
King Edward	?	6	Medium [4] Medium to long [3]			6	5				
Marfona	Konst Research BV	4	Medium to long [3] Long [4, 8]			6	7				7
Bonnie	Cygnet PB	No Data	New Cultivar - No Data								
Isle of Jura	Cygnet PB	8	New Cultivar - No Data								
Majestic		9	Medium to long [4] Long [3]			7	6				

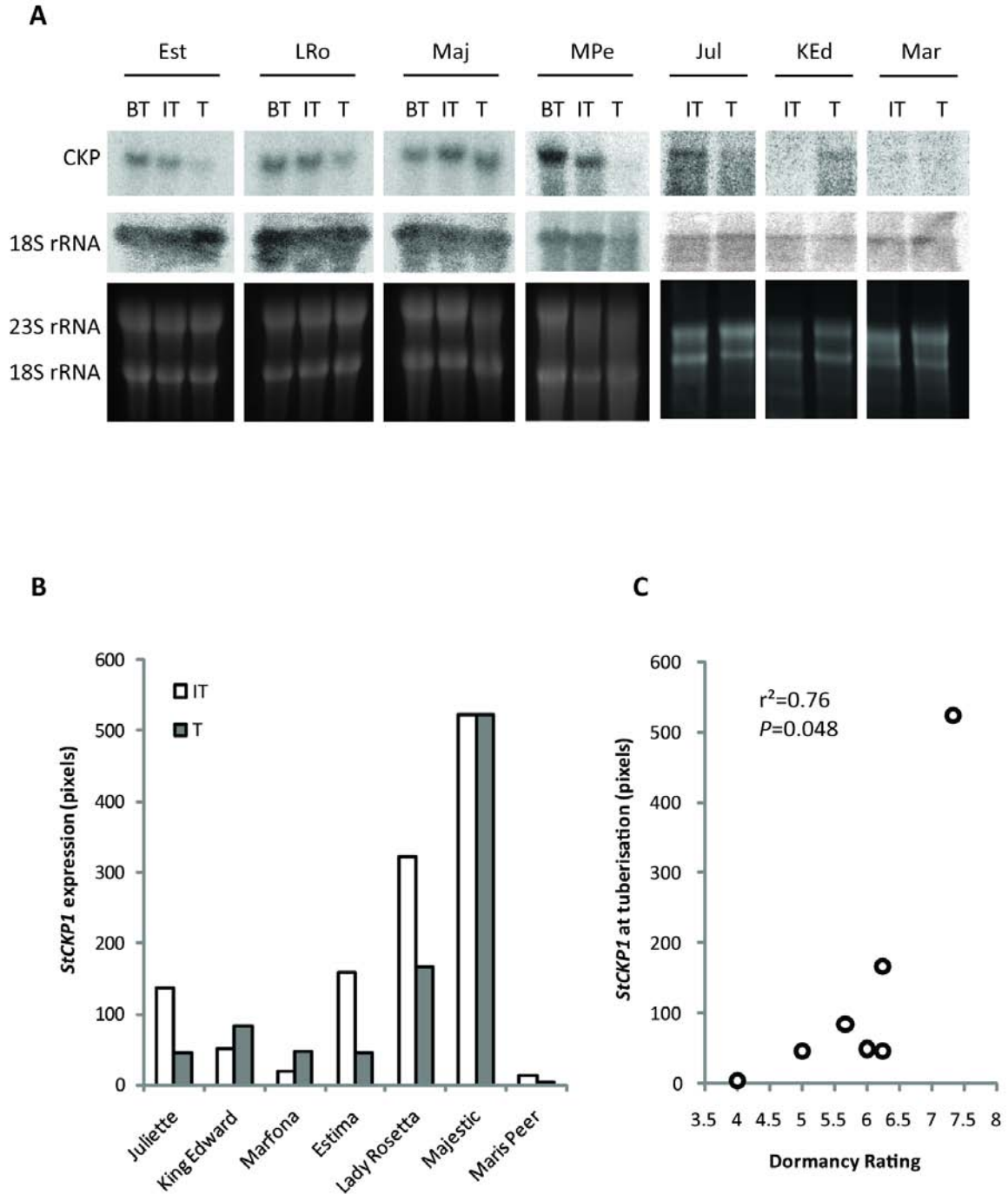

Figure 6.14 Analysis of *StCKP1* transcript in commercial potato cultivars
Membrane immobilised RNA extracted from field grown stolon tips at three defined stages of tuberisation (BT= Before tuberisation; IT= Incipient tuberisation; T= Tuberisation) was probed using radiolabelled cDNA probes synthesised to sequences from StCKP1 and 18S rRNA. A. Phospho-imaged RNA blots for StCKP1 (top), 18S rRNA (mid) and UV-visualised ethdium bromide RNA gels (bottom), each loaded with 10mg total RNA. B. Degree of hybridisation of radiolabelled StCKP1 DNA probes quantified using ImageQuant TL software and normalised relative to 18S rRNA probe hybridisation. C. Correlation of StCKP1 transcript abundance at tuberisation and dormancy ratings determined by calculating the average of dormancy ratings for each cultivar on the British potato variety database and the European cultivated potato database. Cultivar abbreviations: Jul = Juliette, KEd = King Edward, Mar = Marfona, Est = Estima, LRo = Lady Rosetta, Maj = Majestic, MPe = Maris Peer.

required. To ensure a better standard of RNA, it would be pertinent to use a bag induction system as used in this study for Desiree (section 2.2.1.3).

6.9 Discussion

Analysis of *StCKP1* expression in stolon tips of potato cultivars other than Desiree indicates that *StCKP1* transcript varies between these cultivars and that this variation has no notable effect on their growth or tuber morphology as these cultivars are considered to be commercially viable. Data collected from transgenic *StCKP1* over-expressing lines in this study indicate that increased abundance of *StCKP1* results in an increased length:width ratio of tubers, much like that found when the isoprenoid cytokinin biosynthetic pathway was perturbed by over-expression of a bacterial enzyme DXS which is involved in the biosynthesis of isoprenoid precursors (Morris et al., 2006). In their study, Morris et al. (2006) found that increasing the biosynthesis of isoprenoids resulted in increased cytokinin content of tubers relative to auxin, which together act to regulate the growth characteristics of tubers (Sergeeva et al., 2000). The increased length:width ratio observed in OE *StCKP1* tubers may imply that over-expression of *StCKP1* results in a change in ratio of active cytokinin to auxin, although preliminary measurements of zeatin-type cytokinins indicate there is no change in total cytokinin content of tissue expressing the 35SS:StCKP1 construct, at least for callus tissue.

Analysis of cytokinin interconversion in callus tissue indicates that *StCKP1* OE lines have increased ribosylation activity as cytokinin ribosides are found to be three-fold higher than bases, compared to the NT and EV control lines which contained a two-fold higher quantity of ribosides relative to bases. This observation indicates over-expression of StCKP1 is affecting the callus tissue biochemically in that there is a change in mean ratio of riboside to base relative to controls, however developmentally there is no measurable effect on the vegetative tissue. To make such a developmental difference, a change in the region of five- ten-fold between OE and controls would most likely be required. However, as AHK4 binds both cytokinin bases and ribosides it may be that a difference in the ratio of base to riboside doesn't cause a developmental difference.

Further analysis by HPLC-ELISA or LC-MS-MS is required in order to determine the proportions of total cytokinin made up by the active base and inactive N^7 and N^9 conjugates as over-expression of *StCKP1* is likely to alter the balance of cytokinin base and riboside as a result of its nucleoside phosphorylase activity identified in this study (chapter 4). Also of interest would be analysis of cytokinin content of tubers, and because cytokinin extraction is near impossible from microscopic but critical regions of tissue such as tuber buds, analysis of expression of cytokinin-inducible

response regulators, e.g. homologues of ARR5 (Aoyama and Oka, 2003), to monitor cytokinin activity in the tissue.

Further evidence for perturbation of active cytokinin levels came from *in vitro* tuberisation of stolon tips which was found to occur significantly earlier in *StCKP1* over-expressing lines analysed when cytokinin was absent from the media. When cytokinin was supplied, no significant difference was observed between over-expressing lines and non-transformed Desiree. Morris et al. (2006) found similar *in vitro* tuberisation characteristics for *dxs*-over-expressing lines, indicating that perturbation of active cytokinin production, either by altering the expression of enzymes active in the interconversion pathway or by perturbing biosynthesis results in an increased availability of active cytokinin and in consequence an increased rate of tuberisation. It is known that cytokinins, alongside gibberellins are the most important hormones involved in regulating tuberisation of stolon tips (Fernie and Willmitzer, 2001; Sarkar, 2008). Emerging data also suggests that, as in the regulation of tuber morphology, an appropriate ratio of cytokinin to auxin is required to promote tuberisation. Perturbation of this ratio through increasing the available active cytokinin by over-expression of *StCKP1*, a nucleoside phosphorylase which results in increased interconversion of cytokinin, is likely to affect this ratio and so result in earlier cessation of stolon growth and a shift to a sub-apical location for cell division.

As expected, an increased rate of tuberisation of NT Desiree and EV transgenic control lines was observed when media was supplemented with either BA or [9R]BA confirming the acceleratory effect of cytokinin on *in vitro* tuberisation previously observed (Levy et al., 1993; Gopal et al., 1998). However, a decrease in rate of tuberisation was observed for *StCKP1* OE lines when media was supplemented with cytokinin. This observation can be attributed to the inhibitory effect of an excess of active cytokinin. *ipt* over-expressing tubers are found to have increased 7- and 9-glucoside cytokinin conjugates relative to non transformed tubers (Zubko et al., 2005), indicating cytokinin inactivation occurs in tubers in which an excess of biologically active cytokinin is produced. Gális et al. (1995) found the onset of tuberisation in nodes of *ipt* transformed lines strongly expressing the transgene was completely inhibited by an external increase in cytokinin level which could not be overcome by application of auxin to return the unfavourable cytokinin-to-auxin ratio back to wild type levels. Lines weakly expressing the *ipt* transgene were not affected by application of cytokinin. They postulated that the reduction in the number of explants tuberising may be caused by excision of the node by cutting, causing injury which may induce developmentally specific native *ipt* promoters. This gene expression, in concert with the transgene can then lead to an increase in cytokinin content to a physiologically excessive level (Ainley et al., 1993). It may be that over-

expression *of StCKP1*, particularly in lines E, F and M may cause an increase in active cytokinin such that addition of exogenous cytokinin and that produced on wounding (Koda, 1982b) results in active cytokinin levels in the physiologically inhibitory range.

Abundance of *StCKP1* at tuberisation, the time of onset of dormancy, had a significant effect upon the duration of the dormant period. Mature Desiree plants infected with a PVX vector engineered to suppress *StCKP1* transcription showed a significant reduction in the duration of chill-sensitive period of dormancy correlating with a reduction of *StCKP1* in periderm tissue (Newell, pers. comm.). In line with these findings, over-expression of *StCKP1* by driving its transcription with the CaMV 35S promoter resulted in a significant increase in the duration of the chill-sensitive period of dormancy, which correlated with *StCKP1* transcript abundance in the leaves.

StCKP1 shares over 43% amino acid identity with nine storage proteins from poplar (*Poplus* sp.) and rice. BSPA is a well characterised storage protein in poplar which is involved in the storage of nitrogen from senescing leaves while the tree enters the dormant state, and its expression is known to be influenced by many environmental factors including photoperiod, nitrogen availability, temperature and wounding. Breakdown of these storage proteins is known to be regulated by temperature, in that after the moderate winter chilling requirements of 1000 hours at 2°C are met, BSP breakdown begins, releasing the stored N when days lengthen in the spring (Cooke and Weih, 2005). The shared homology with these bark storage proteins and vegetative storage proteins, and the role of StCKP1 in prolonging dormancy by increasing the chill-sensitive period indicates that StCKP1 may be involved in the sequestration of cytokinin, maintaining the tuber buds in a dormant state. Breakdown of StCKP1 appears to be regulated by temperature because in RNAi knock down lines and over-expressing lines, the duration of the chill sensitive phase of dormancy correlates with the abundance of *StCKP1*, determined for OE lines by leaf transcript analysis, and RNAi lines by periderm transcript analysis. Over-expression of *StCKP1* and RNAi knock down of *StCKP1* were also found to have no significant effect on the duration of dormancy following the 21d chill treatment. The results seem to indicate that even in warm or ambient storage, StCKP1 protein is slowly degraded so that eventually the level is low enough to allow sprouting. The more transcript there was initially, the more protein and so the longer it takes to break it all down. The chill treatment putatively accelerates its breakdown so that by the end of the chill-insensitive phase, there is insufficient StCKP1 to prevent sprouting. The chill insensitive phase of dormancy may be due to a sub fraction of StCKP1 that is not subject to chill accelerated destruction, or to a separate dormancy imposing process that runs in parallel and is chill-insensitive. Further investigation in which increased periods at 4°C are used to chill treat *StCKP1* over-expressing tubers into breakdown of StCKP1, thus

break of dormancy, would be of interest to determine the chill requirement of lines with protracted dormancy.

Tubers used to monitor dormancy for each transgenic line came from a single plant due to growth space constraints. This study has allowed the identification of over-expressing lines with dormancy traits of particular interest, notably 35S E, 35S I and 35S M which would benefit from further characterisation. Of particular interest would be to use tubers from these lines to produce more tubers vegetatively and investigate stability and vegetative propagation of the dormancy trait conferred by over-expression of StCKP1.

Data presented suggests that StCKP1 activates tuberisation and holds tubers in an innately dormant state by converting cytokinin bases to less active ribosides, preventing cytokinin interaction with receptors until the protein is broken down after a period of chilling. It is known that application of cytokinin bases to stolon tips causes premature tuberisation (Palmer and Smith, 1969). However, measurement of cytokinin in stolon tips and small bulking potatoes show [9R]Z to predominate (Van Staden and Dimalla, 1977) which may mean that [9R]Z is involved in the promotion of tuberisation and that conversion of the applied cytokinin base to the riboside required to trigger tuberisation. The high riboside content that persists until maturation of tubers post harvest may then contribute to maintaining tubers in a dormant state.

Chapter 7

Final Discussion

7.1 Introduction

Evidence collected to date suggests cytokinins play a key role in potato tuberisation and dormancy. The application of cytokinin to innately dormant tubers caused sprouting of tuber buds (Hemberg, 1970; Turnbull and Hanke, 1985a, b). At tuber initiation, a protein of 37kDa which binds cytokinin with a binding affinity (K_D) of 0.17μM is upregulated at the stolon tip at the same time as an eight-fold increase in cytokinin binding activity of the tuberising tip (Thomson, 1994) . This is in agreement with the observation that stolons treated with exogenous cytokinins showed indications of tuber formation after ten days of incubation (Palmer and Smith, 1969). Warnes (2005) obtained the full sequence of a 37kDa protein, StCKP1, previously isolated by its cytokinin-binding activity from tuberising stolon tips of the cultivar Majestic, known for its lengthy dormancy. Sequence similarities between StCKP1 and members of the phosphorylase superfamily (Mushegian and Koonin, 1994) led to a proposed role in cytokinin interconversion as nucleosidases have been postulated to play a role in production of the biologically active free base from the products of biosynthesis. This mass of accumulated circumstantial evidence suggests that the protein StCKP1 is part of the mechanism linking the hormone, cytokinin, to the process of tuber initiation at stolon tips and, later, the breakage of tuber dormancy controlled by cytokinin. This investigation set out to determine StCKP1 activity and investigate its role in tuberisation and tuber dormancy.

7.2 Discussion of results

The cytokinin content of stolon tips quantified for the three defined stages of tuberisation was found to be in line with previous observations of increasing cytokinin upon tuberisation of stolon tips (Mauk and Langille, 1978; Sattelmacher and Marschner, 1978; Turnbull and Hanke, 1985b) with zeatin riboside as the predominating active cytokinin at tuberisation. *StCKP1* transcript and protein content were also seen to increase upon tuberisation of stolon tips, although the precise stage at which each increased was different. Transcript abundance was detected as increasing upon tuberisation, whereas protein abundance increased at incipient tuberisation in agreement with the timing of the increase in cytokinin-binding activity by a 37kDa protein observed by Thomson (1994). This result indicates that either translation of *StCKP1*, or StCKP1 protein turnover/stability is likely to be subject to regulation independent of transcriptional regulation determined by activity of the promoter regions. As stolon tips tuberise, they enter the period of innate dormancy (Turnbull and Hanke, 1985b) and, much like the increase in the StCKP1 homolog BSPA (Zhu and Coleman, 2001; Cooke and Weih, 2005) during tuber bulking and before entering the overwinter period, StCKP1 may be accumulating as a storage protein for mobilisation upon break of dormancy. Although possessing the three motifs common to the phosphorylase superfamily (Mushegian and Koonin, 1994), no

activity has been determined for BSPA with the protein simply being annotated as a vegetative storage protein. However, as predicted by common motifs, StCKP1 was found to have nucleosidase activity interconverting cytokinin free base and riboside in a reversible reaction in the presence of suitable ribosyl or inorganic phosphate donor, with greater specificity for cytokinins than for aminopurine substrates. K_Ms determined for cytokinin substrates were found to be lower for the free base than the riboside for all cytokinin types assayed but particularly for iP and Z with K_Ms of 0.05 and 0.02µM respectively relative to their ribosides, [9R]iP and [9R]Z of 13 and 7µM.

Over-expression of StCKP1 resulted in an decreased time to tuberisation relative to non-transformed and empty vector controls when induced by sucrose in the absence of added cytokinin. However when supplemented with cytokinin, as either the free base or the riboside, no difference in the time to tuberisation between over-expressing lines and non-transformed Desiree was found. A similar decreased time to tuberisation in the absence of cytokinin supplement was also observed by Morris et al. (2006) who over-expressed bacterial *dxs*, which acts in the MEP pathway for the biosynthesis of isoprenoid substrates of IPTs. In both cases, the increase in rate of tuberisation can be seen as indirect evidence for perturbation of cytokinin levels with Morris et al. (2006) concluding the *dxs* phenotype is due to enhanced trans-zeatin riboside levels at the stolon apex and in the tuber relative to non-transformed Desiree. Tuber initiation has in commercial varieties of *S. tuberosum* been shown to be a response to an endogenous signal rather than due to environmental cues as, *in vivo,* plants subjected to different environmental conditions will initiate tuberisation at around the same time within 3-4 days. The timing of initiation was found to be variable between experiments and can be attributed to physiological age of the mother tuber post harvest (O'Brien et al., 1998) rather than to prevailing environmental conditions.

These results indicate that StCKP1 functions in control of tuberisation of stolon tips by altering the amount of biologically active cytokinin in the tissue. Upregulation of StCKP1 as stolon tips begin tuberising, even before physiological indications of tuberisation are visible, results in the conversion of cytokinin free base to the corresponding riboside, sequestering cytokinin by conjugation to produce the riboside. This sequestration results in tip-high cytokinin, maintaining the stolon tip as a sink for import of sucrose (Viola et al., 2001) but results in arrest of longitudinal cell division to promote swelling of the stolon apex by a combination of cell expansion and division. Over-expression indicates that it may not be the amount of cytokinin present in the stolon tip, but the ratio of biologically active to inactive conjugates that drives tuberisation causing the stolon apex to become prematurely dormant. Tuber dormancy is initiated upon tuberisation of the stolon apex (Coleman, 1987; Claassens and Vreugdenhil, 2000; Viola et al., 2007; Vreugdenhil, 2007) with the

apical bud of the forming tuber the first to become dormant. It is hypothesised here that tip high StCKP1 is one of the driving forces for tuberisation and so descent into the dormant state.

Analysis of transcript abundance indicated that *StCKP1* mRNA is present in periderm of dormant mature tubers after harvest. However, its abundance decreased as tubers break dormancy and begin sprouting, predominantly from apical buds. This behaviour is similar to that found for BSPA (Zhu and Coleman, 2001), one of a family of bark storage proteins known to accumulate in the inner bark, parenchyma and xylem rays during autumn and decline during spring growth (Wetzel et al., 1989). BSPs are thought to store nitrogen translocated from autumnal senescence for supply of nitrogen during commencement of growth the following spring. This observation of decline of BSPs during the transition to growth is in line with the observation of a decline in *StCKP1* transcript in the periderm of tubers on break of dormancy. Analysis of *StCKP1* promoters by promoter::GUS fusions indicates that it is pro2 that drives the expression of *StCKP1* in the periderm, resulting in the accumulation of *StCKP1* during onset of tuberisation and throughout the dormant period, while pro1 seems to be more active in tuber buds and might be responsible for expression of *StCKP1* during tuberisation as pro1 activity has been detected in stolon tips.

Over-expression of *StCKP1* resulted in an increased duration of dormancy after tubers had been subject to a 21 day chill treatment at 4°C. The amount of *StCKP1* transcript was found to positively correlate with the duration of dormancy. This was in line with findings of *StCKP1* knock down by RNAi in which a reduction in the duration of the dormant period relative to controls was observed following a chill treatment (Newell, pers. comm.). The breakdown of poplar bark storage protein, BSPA, is known to be regulated by winter chilling, requiring 1000 hours at 2°C for breakdown to begin, releasing sequestered N for mobilisation to winter buds for spring growth (Cooke and Weih, 2005). The shared homology with bark storage proteins and vegetative storage proteins, and the role of StCKP1 in prolonging dormancy indicates that StCKP1 may be involved in the sequestration of cytokinin, maintaining the tuber buds in a dormant state by either holding cytokinin as a riboside conjugate form, or simply by binding cytokinin bases, sequestering them from binding the cytokinin receptors CRE1/AHK4, AHK3 and AHK2. Breakdown of StCKP1 seems to be regulated by temperature. In RNAi knock-down lines the duration of dormancy in chilled tubers is 100d whatever the level of StCKP1 expression while in over-expressing lines, the increase in duration of dormancy following the chill treatment correlates with the increase in abundance of *StCKP1* relative to wild type, indicating that breakdown of StCKP1 allows cytokinin ribosides to be deribosylated by either by catalytic concentrations of StCKP1, the reaction being driven by increasing Pi, or by other enzymes

with ribohydrolase activity to form the free base which cause tuber buds to break their innate dormancy.

Analysis of the *StCKP1* promoter regions, pro1 and pro2 sequenced by Warnes (2005), by fusion with GUS indicates *StCKP1a* and *StCKP1b* expression is tuber-specific. Although, when over-expressed by the 35S promoter transcription is expected throughout the plant, the phenotype of *StCKP1* over-expressing lines was restricted to tuber development suggesting that control is not completely governed by either of pro1 or pro2. The StCKP1 sequence indicates a transit peptide is present at the N-terminal of the translated protein which may have a role in targeting the protein to regions of the cell where it can avoid protease activity prior to chilling which releases dormancy or after a given duration. A single trans-membrane domain is also predicted which indicates StCKP1 may be associated with the plasma membrane. This association is likely to be loose with the C-terminal domain remaining cytosolic as StCKP1 purified from stolon tips was in the soluble fraction (Warnes, 2005; James, pers. comm.) and pH optima determined indicate that StCKP1 is active within the cell rather than the cell wall or vacuole (Broadhurst, pers. comm.).

The total duration of dormancy was found to increase when *StCKP1* was over-expressed by prolonging the chill sensitive period but had no effect on the chill insensitive period, RNAi knock down of *StCKP1* also did not affect the chill insensitive period of dormancy, indicating increasing *StCKP1* above a certain threshold means more than the standard moderate period at reduced temperature alone is required for tuber buds to break dormancy. This contrasts with tubers over-expressing *ipt* which showed a reduction in the dormant period, with some tubers breaking dormancy before harvest (Zubko et al., 2005). The measured increase in availability of biologically active cytokinin is likely to drive the premature break of dormancy in *ipt*-over-expressing lines while in StCKP1 over-expressing lines, the availability of biologically active cytokinin is reduced. This reduction may be due to sequestration by StCKP1 binding cytokinin. Using stolon tips, Thomson (1994) measured 70pmol cytokinin binding sites g^{-1} FM and a cytokinin content of 40-60pmol g^{-1} FM indicating that there is an excess of binding sites to sequester all stolon tip cytokinin. As StCKP1 has been measured to accumulate to levels equivalent to those known for vegetative storage proteins, it is proposed that StCKP1 is responsible for binding cytokinin and maintaining bulking tubers in a dormant state. The measured K_D for CRE1/AHK4 was 8nm (Yamada et al., 2001) indicating that this receptor has a higher affinity for cytokinin than StCKP1 at 50nm and 20nm for iP and Z respectively. However, comparison of K_D and K_M is not a fair measure as K_M also includes the rate of conversion of substrate to product, assay of CRE1/AHK4 activity in bacteria which show Z half saturation for AHK4 activity just above 100nm, slightly higher for iP (Spichal et al., 2004) ,is likely to be a more robust

comparator indicating StCKP1 has a higher affinity than CRE1/AHK4 and AHK3 whose activity at Z half saturation was measured to be between 1 and 10µM (Spichal et al., 2004). When sufficient ribose 1-phosphate is available, StCKP1 may catalyse ribosylation of the bound base to release the riboside. AHK3 and AHK2 are the predominant cytokinin receptors in shoot tissue, and have been shown to bind only cytokinin base, thus interconversion of cytokinin bases to ribosides by StCKP1 may serve to prevent interaction with the dominant receptor types, effectively sequestering cytokinin for release by StCKP1 in the presence of sufficient Pi or by other ribohydrolytic enzymes upon break of dormancy.

StCKP1 transcript abundance measured in soil grown commercial cultivars was found to correlate positively with the dormancy rating attributed to each cultivar by the British and European Culitvated Potato Databases. The natural variation in *StCKP1* abundance between cultivars with dormant periods of differing duration indicates that StCKP1 and the length of the dormant period are linked. The phenotype of plants over-expressing *StCKP1* indicated that only developmental aspects of the tuber are altered, with early tuberisation, increased length to width ratio, and delay in break of dormancy, while vegetative aspects such as growth habit were unaffected. This finding raises the possibility of that StCKP1 abundance could provide an indicator of tuber dormancy in breeding programmes.

The results presented in this study have led to the development of a model for the control of tuberisation and tuber dormancy involving StCKP1 (figure 7.1). It is proposed that StCKP1 acts to sequester cytokinin by binding or conjugation at N^9 to produce cytokinin ribosides which may still enhance sink strength without being perceived by receptors. This sequestration of cytokinin causes the stolon apex to become dormant at the onset of tuberisation and remain dormant until StCKP1 is broken down. Breakdown of StCKP1 is caused by chilling, resulting in release of sequestered cytokinin riboside and its interconversion by enzymes which may include catalytic concentrations of StCKP1, with the phosphorolysis reaction driven by increasing Pi released from inositol 6-phosphate. Upon sprouting, StCKP1 transcription is relatively low in the elongating stolon, but once the endogenous signal for tuberisation is perceived, possibly in the form of a change in ratio of cytokinin riboside to base (Van Staden and Dimalla, 1977; Mauk and Langille, 1978), transcription is upregulated and the stolon apex again becomes dormant and tuberisation ensues.

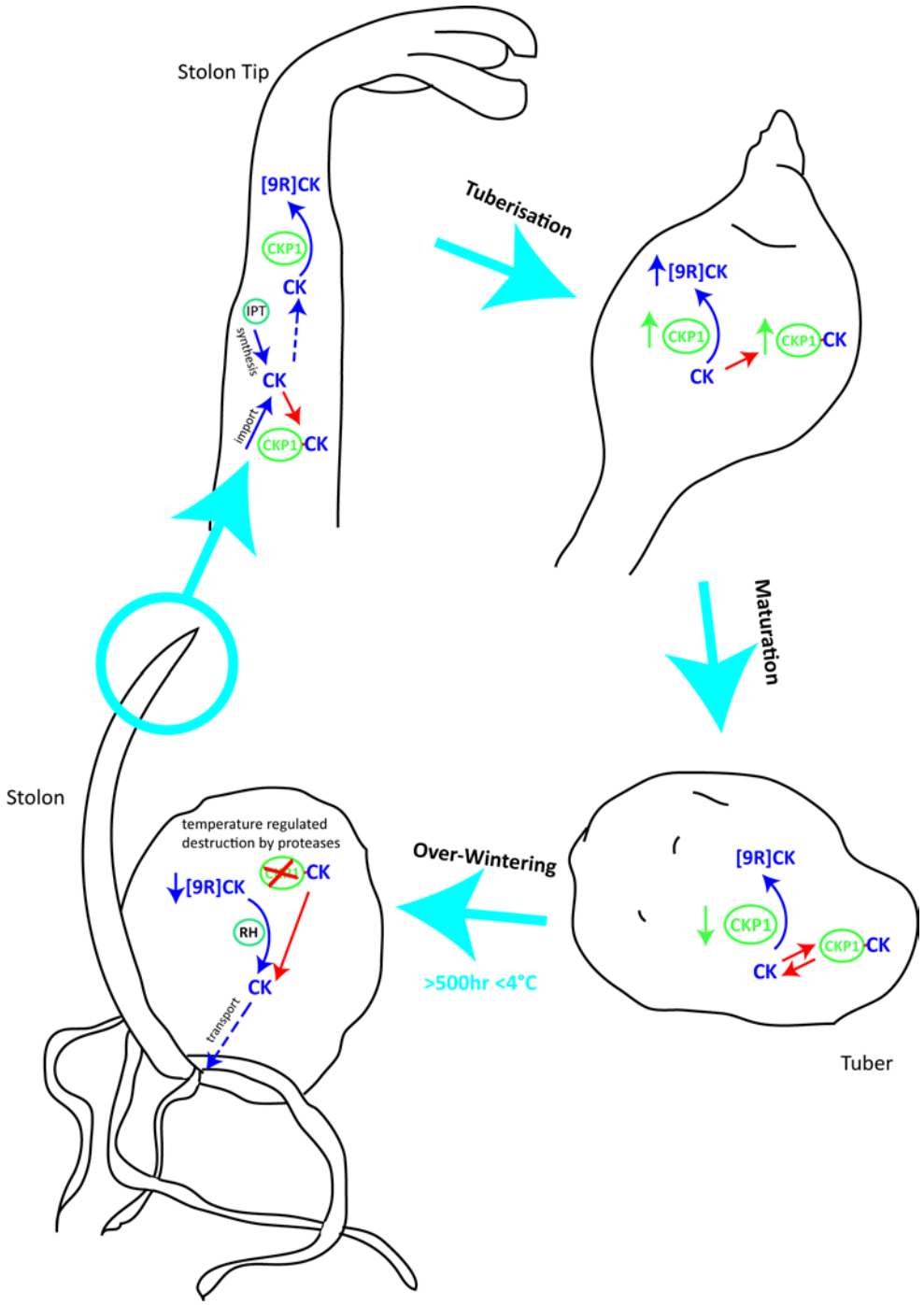

Figure 7.1 Proposed model for the involvement of StCKP1 in the tuber lifecycle
StCKP1 acts to sequester cytokinin by either conjugation at N9 to produce cytokinin ribosides (blue arrows), or by binding cytokinin (red arrows), enhancing sink strength without being perceived by receptors CRE1/AHK4, AHK3 and AHK2. This sequestration of cytokinin causes the stolon apex to become dormant at the onset of tuberisation and remain dormant until StCKP1 is broken down. Break down of StCKP1 is accelerated by chilling, resulting in release of cytokinin riboside for interconversion by enzymes with ribosylhydrolase like activity to release the free base. Upon sprouting, *StCKP1* transcription is relatively low in the elongating stolon, but once the endogenous signal for tuberisation is perceived, possibly in the form of a change in ratio of cytokinin riboside to base, transcription is upregulated and the stolon apex again becomes dormant and tuberisation ensues. CK = cytokinin, [9R]CK = cytokinin riboside, RH = Ribohydrolytic enzyme.

7.3 Future work

Much of the analysis of StCKP1 levels in this study has focussed upon transcript abundance, however immunoblotting using a polyclonal antibody raised to a synthetic peptide designed to the C-terminal domain (Warnes, 2005) indicates control of protein abundance is not dependent on transcript abundance. Thus analysis of StCKP1 protein abundance and activity *in vivo* is of particular interest. The data collected using anti-CKP may not be sufficiently robust as this antibody only exhibits a limited degree of specificity, labelling numerous bands of 30-50kDa in potato extracts. It would be pertinent to produce a new antibody, either to a synthetic peptide in the N-terminal domain, or by using purified recombinant StCKP1.

In concert with analysis of StCKP1 abundance *in vivo*, it would be of interest to measure cytokinin abundance in tuber buds, periderm and pith tissue throughout tuber development, dormancy and at the break of dormancy. As extraction and quantification of cytokinin from such small masses of tissue is impossible using current practise, an alternative strategy would be to monitor cytokinin levels indirectly, using as 'reporter' the transcript abundance of potato orthologs of the Arabidopsis Response Regulators (ARR) by either RT-PCR or RNA blotting. This method has been successfully implemented in *Oryza sativa* using the response regulators *OsRR1* and *OsRR5* (Kurakawa et al., 2007) and putative response regulator orthologs have been found by carrying out BLAST searches of the SGN EST database with ARR nucleotide sequences (Mielnichuk, pers. comm.)

Analysis of *StCKP1* transcript abundance in dormant tubers and in those that have exited dormancy reveals a change in abundance, particularly in the periderm. Promoter analysis using promoter::GUS fusion has been carried out in this study to ascertain the tissue specificity of promoters, but cannot be used to monitor *StCKP1* transcription non-invasively throughout development due to the inherent stability of GUS. Non-persistence of the reporter is required, such as promoter::luciferase fusions, used successfully for potato microtubers (Vreugdenhil et al., 2006).

7.4 Commercial application

Eliminating most of the post harvest losses in storage by reducing premature tuber sprouting, and also reducing the cost of storage by reducing the need for chemical sprout inhibitor application and low temperature storage is likely to increase the utility of potatoes. Reduction of the costs associated with storage and tuber dormancy may promote the potato from its current local scale of production to world crop status similar to that of wheat and maize. Each year, potatoes are stored for up to 10 months in stringently controlled conditions to minimise losses from: rotting, disease and

premature sprouting. Ware potatoes intended for direct human consumption or pre-consumption processing such as production of chips and crisps are stored at 8-12°C to reduce cold induced sweetening, while seed potatoes are stored at 2-4°C. However, when ware potatoes are taken out of cold storage, they quickly begin to sprout reducing their shelf life and acceptability to consumers and processors (Wiltshire and Cobb, 1996; Sonnewald, 2001; Suttle, 2004; Shahba et al., 2007). Tubers are also extensively treated with sprout suppressants such as CIPC which have been shown to have deleterious effects upon cell division in porcine brains. As StCKP1 has been shown to be involved in the control of tuber dormancy and its breakdown governed by chilling, increased expression of StCKP1 may offer a mechanism for increasing the period of tuber dormancy and for control of tuber sprouting post storage. As tubers lose dormancy in response to a period of chilling, tubers with a lengthened dormant period are still viable for commercial production as sprouting can be induced by a chill treatment. StCKP1 transcript or protein abundance in stolon tips at incipient tuberisation may be also used by breeders as an early indicator of tuber dormancy.

Appendix

1. Media, solutions, and supplements used in this study

All chemicals used were of the highest grade and obtained from Sigma-Aldrich (Gillingham, UK), BDN (Leicester, UK) or Fisher Scientific UK (Loughborough, UK) unless otherwise stated. For all solutions and solvent mixtures, the water used as a diluent was deionised and passed through a Millipore filtration system.

Murashige & Skoog (MS) powder plus vitamins and basal salts and Gamborg's B-5 (G B-5) powder plus vitamins were supplied by Duchefa Biochemie BV (Haarlem, Netherlands). ' MS+Vits' contains complete micro and macro elements and vitamins. 'MS salts' contains only complete micro and macro elements. Phytoagar was supplied by Duchefa Biochemie BV. All media was autoclaved prior to addition of filter sterilised hormones and/or antibiotics.

Antibiotics were supplied by Melford (Ipswich, UK) or Sigma-Aldrich. Plant hormones used to supplement media were supplied by Sigma-Aldrich and solubilised in deionised water unless otherwise stated before being filter sterilised using Millex 0.2µm pore syringe filter (Millipore, Billerica, MA, USA).

Table A1.1. Media for culture of and solutions for preparation of chemically competent bacteria

Nr	Media for bacterial culture	Components
1.1	Luria Broth (LB)	1%(w/v) tryptone 0.5%(w/v) yeast extract 1%(w/v) NaCl pH 7.0
1.2	LB Agar (LBA)	As 1.1 + 15g l^{-1} Bacto agar
1.3	TYNG	10gl^{-1} Tryptone 5gl^{-1} Yeast extract 5gl^{-1} NaCl 0.2gl^{-1}MES
1.4	TYNGA	As 1.3 + 15g l^{-1} Bacto agar
1.5	Rich Media (RM)	32gl^{-1} tryptone 20gl^{-1} yeast extract 5gl^{-1} NaCl
	Solutions for preparation of competent cells	
1.6	Transformation Buffer I (TBI)	30mM sodium acetate 50mM $MnCl_2$ 100mM RbCl 10mM $CaCl_2$ 15% (v/v) glycerol pH 5.8, filter sterile
1.7	Transformation Buffer II (TBII)	10mM NaMOPS 10mM RbCl 75mM $CaCl_2$ 15% (v/v) glycerol pH 6.5, filter sterile

Table A1.2. Media for potato transformation, regeneration and culture

	Media for potato transformation, regeneration and culture	**Components**
2.1	MS30	4.4g l^{-1} MS+Vits 30gl^{-1} sucrose pH 5.8 8gl^{-1} Phytoagar
2.2	M100	As 2.1 + 0.5mgl^{-1} thiamine-HCl 0.5 mgl^{-1} pyridoxine-HCl
2.3	MS10	4.4g l^{-1} MS+Vits 10gl^{-1} sucrose pH 5.8
	Media for potato transformation, regeneration and culture	**Components**
2.4	M400	As 2.3 + 8gl^{-1} Phytoagar 2mgl^{-1} zeatin 0.01mgl^{-1} NAA 0.1mgl^{-1} GA_3 400mgl^{-1} carbenicillin (50mgl^{-1} kanamycin)
2.5	M300	As 2.1 + 2mgl^{-1} NAA 1mgl^{-1} BA
2.6	M13	As 2.1 + 0.25mgl^{-1} BA 0.1mgl^{-1} GA_3 400mgl^{-1} carbenicillin 50mgl^{-1} kanamycin

Table A1.2 continued

	Media for potato transformation, regeneration and culture	**Components**
2.7	Gamborg's B5	3.86gl^{-1} G B-5+Vits 20gl^{-1} glucose 0.5gl^{-1} MES 0.5mgl^{-1} 2,4-D 1mgl^{-1} kinetin pH 5.7
2.8	PMM	4.6gl^{-1} MS basal salts 60gl^{-1} Sucrose pH 5.8 8gl^{-1} Phytoagar

Table A1.3 Solutions for nucleic acid extraction and manipulation

	Solutions for nucleic acid extraction	**Components**
3.1	CTAB Extraction Buffer	800mM NaCl
		220mM Tris-HCl pH 8.0
		140mM sorbitol
		22mM EDTA.Na_2
		0.8% (w/v) CTAB
		1% (w/v) Sarkosyl
3.2	Shorty Extraction Buffer	0.2M Tris-HCl pH 8.0
		0.4M LiCl
		25mM EDTA.Na_2
		1% (w/v) SDS
	Solutions for nucleic acid manipulation	**Components**
3.3	1x TE Buffer	10mM Tris-HCl pH 7.5
		1mM EDTA.Na_2
3.4	50x TAE Buffer	2M Tris-acetate
		50mM EDTA.Na_2
3.5	RNA Loading Dye	500µl formamide
		175µl formaldehyde
		50µl 10x MOPS
		50µl H_2O
		100µg EtBr
		Bromophenol blue
		Xylene Cyanol
3.6	10x MOPS	0.2M MOPS pH 7.0
		80mM sodium acetate
		10mM EDTA.Na_2
3.7	20x SSC	3M NaCl
		0.3M tri-sodium citrate
3.8	JOB Buffer	50mM Tris-HCl pH 8.0
		10mM EDTA.Na_2
		2% (w/v) SDS

Table A1.3 continued

	Solutions for nucleic acid manipulation	**Components**
3.9	Stripping solution	1% (w/v) SDS
		0.1x SSC
		40mM Tris-HCl pH 7.5

Table A1.4. Solutions for protein extraction and manipulation

	Solutions for protein extraction & purification	**Components**
4.1	Protein Extraction Buffer	100mM NaH_2PO_4
		10mM β-Mercaptoethanol
		0.1% (w/v) Triton X-100
4.2	pMal column buffer	20 mM Tris-pH 7.4
		200 mM NaCl
		1 mM EDTA.Na_2
4.3	pMal elution buffer	10mM maltose
		in 4.2
	Solutions for protein manipulation	**Components**
4.4	2x SDS-PAGE Loading Buffer	0.25M Tris-HCl pH 6.8
		20% (v/v) glycerol
		4% (w/v) SDS
		pH 7.2-7.6
4.5	Tris-glycine electrophoresis buffer	25mM Tris
		250mM glycine pH 8.3
		0.1% SDS
4.6	Coomassie Blue Stain	0.25g Coomassie Brilliant Blue R250
		90ml methanol:H_2O (1:1 v/v)
		10ml glacial acetic acid
4.7	Coomassie Destaining Solution	40% (v/v) Methanol
		10% (v/v) Acetic acid
4.8	Semi-Dry Transfer Buffer	25mM Tris-HCl pH 8.3
		192mM glycine
		20% (v/v) methanol
		0.02% (w/v) SDS
4.9	Ponceau Stain	0.1% (w/v) Ponceau S
		in 5% (v/v) acetic acid
4.10	Phosphate Buffered Saline + Tween (PBST)	10mM NaH_2PO_4.H2O
		130mM NaCl
		pH 7.0
		0.1%(v/v) Tween 20

Table A1.4 continued

	Solutions for protein manipulation	**Components**
4.11	PBST + Milk (PBSTM)	1% (w/v) Marvel skimmed milk powder in 4.9
4.12	Xa Cleavage Buffer	100mM NaCl 20mM Tris 5mM $CaCl_2$
4.13	MUG Stop Buffer	200mM Na_2CO_3.10H2O in 4.1
4.14	GUS Staining Solution	100mM phosphate buffer, pH 7.0 0.5mM $K_2Fe(CN)_6$ 0.5mM $K_4Fe(CN)_6$ 10mM EDTA 0.5mg ml^{-1} X-GlcA

Table A1.5. Solutions for ELISA

	Solutions for ELISA	**Components**
5.1	Tris Buffered Saline (TBS)	50mM Tris-HCl pH 7.4 0.15M NaCl
5.2	TBS + Tween 20 (TBS+T)	As 5.1 + 0.1% (v/v) Tween 20

Table A1.6. Table of stock and final antibiotic concentrations (used in bacterial culture)

	Antibiotic	**Stock Solution**	**Final Concentration**
6.1	Kanamycin	100mg ml^{-1}	50µg ml^{-1}
6.2	Carbenicillin	200mg ml^{-1}	100µg ml^{-1}
6.3	Tetracyclin	10mg ml^{-1}	34 µg ml^{-1}
6.4	Streptomycin	100 mg ml^{-1}	30 µg ml^{-1}

Table A1.7. Hormone stock concentrations, unless otherwise stated, solution made in dIH_2O

	Hormone/Supplement	**Stock Solution**
7.1	Benzyladenine (BA)	1mg ml^{-1}
7.2	Benzyladenosine ([9R]-BA)	1mg ml^{-1}
7.3	Zeatin (Z)	2mg ml^{-1}
7.4	Kinetin	0.05mg ml^{-1}
7.5	NAA	0.01mg ml^{-1} & 0.1mg ml^{-1}
7.6	2,4-D	1mg ml^{-1} in absolute ethanol
7.7	Gibberellic Acid (GA_3)	0.1mg ml^{-1}

References

Ainley, W.M., McNeil, K.J., Hill, J.W., Lingle, W.L., Simpson, R.B., Brenner, M.L., Nagao, R.T., and Key, J.L. (1993). Regulatable endogenous production of cytokinins up to toxic levels in transgenic plants and plant tissues. Plant Molecular Biology **22,** 13-23.

Albertini, S., Friederich, U., Holderegger, C., and Wurgler, F.E. (1988). The *invitro* porcine brain tubulin assembly assay - effects of a genotoxic carcinogen (aflatoxin-B1), 8 tumor promoters and 9 miscellaneous substances. Mutation Research **201,** 283-292.

Anantharaman, V., and Aravind, L. (2001). The CHASE domain: a predicted ligand-binding module in plant cytokinin receptors and other eukaryotic and bacterial receptors. Trends in Biochemical Sciences **26,** 579-582.

Andersen, J.B., Sternberg, C., Poulsen, L.K., Bjorn, S.P., Givskov, M., and Molin, S. (1998). New unstable variants of green fluorescent protein for studies of transient gene expression in bacteria. Applied and Environmental Microbiology **64,** 2240-2246.

Aoyama, T., and Oka, A. (2003). Cytokinin signal transduction in plant cells. Journal of Plant Research **116,** 221-231.

Arthur, G.D., Jager, A.K., and van Staden, J. (2001). Uptake of [^{3}H]DHZ by tomato seedlings. South African Journal of Botany **67,** 661-666.

Ashikari, M., Sakakibara, H., Lin, S.Y., Yamamoto, T., Takashi, T., Nishimura, A., Angeles, E.R., Qian, Q., Kitano, H., and Matsuoka, M. (2005). Cytokinin oxidase regulates rice grain production. Science **309**, 741-745.

Astot, C., Dolezal, K., Nordstrom, A., Wang, Q., Kunkel, T., Moritz, T., Chua, N.H., and Sandberg, G. (2000). An alternative cytokinin biosynthesis pathway. Proceedings of the National Academy of Sciences of the United States of America **97,** 14778-14783.

Auer, C.A. (2002). Discoveries and dilemmas concerning cytokinin metabolism. Journal of Plant Growth Regulation **21,** 24-31.

Barnes, M.F., Tien, C.L., and Gray, J.S. (1980). Biosynthesis of cytokinins by potato cell-cultures. Phytochemistry **19,** 409-412.

Bassil, N.V., Mok, D.W.S., and Mok, M.C. (1993). Partial-purification of a *cis-trans* isomerase of zeatin from immature seed of *Phaseolus vulgaris* L. Plant Physiology **102,** 867-872.

Bishopp, A., Mahonen, A.P., and Helariutta, Y. (2006). Signs of change: hormone receptors that regulate plant development. Development **133,** 1857-1869.

Blackhall, N. (1992). Callus suspension culture of *Arabidopsis*. In *Arabidopsis*: The Complete Guide, D. Flanders and C. Dean, eds (Norwich, UK: John Innes Centre), pp. 1/2–2/2.

Bradford, M.M. (1976). Rapid and sensitive method for quantitation of microgram quantities of protein utilizing principle of protein-dye binding. Analytical Biochemistry **72,** 248-254.

Bradshaw, N. (2006). Food Standards Agency - Pesticide residue minimisation crop guide: potatoes S. Ogilvy, ed (Wolverhampton: ADAS).

Burch, L.R., and Stuchbury, T. (1987). Activity and distribution of enzymed that interconvert purine-bases, ribosides and ribotides in the tomato plant and possible implications for cytokinin metabolism. Physiologia Plantarum **69,** 283-288.

Burkle, L., Cedzich, A., Dopke, C., Stransky, H., Okumoto, S., Gillissen, B., Kuhn, C., and Frommer, W.B. (2003). Transport of cytokinins mediated by purine transporters of the PUP family expressed in phloem, hydathodes, and pollen of *Arabidopsis*. Plant Journal **34,** 13-26.

Burton, W.G., van Es, A., and Hartmans, K.J. (1992). The physics and physiology of storage. In The Potato Crop: the scientific basis for improvement P. Harris, ed (London, UK: Chapman & Hall), pp. 608-709.

Campbell, M.A., Suttle, J.C., and Sell, T.W. (1996). Changes in cell cycle status and expression of p34(cdc2) kinase during potato tuber meristem dormancy. Physiologia Plantarum **98,** 743-752.

Chaudhary, K., Ting, L.M., Kim, K., and Roos, D.S. (2006). *Toxoplasma gondii* purine nucleoside phosphorylase biochemical characterization, inhibitor profiles, and comparison with the *Plasmodium falciparum* ortholog. Journal of Biological Chemistry **281,** 25652-25658.

Chen, C., Melitz, D.K., Petschow, B., and Eckert, R.L. (1980). Isolation of cytokinin-binding protein from plant tissues by affinity chromatography. European Journal of Biochemistry **108,** 379-387.

Chen, C.M. (1997). Cytokinin biosynthesis and interconversion. Physiologia Plantarum **101,** 665-673.

Chen, C.M., and Eckert, R.L. (1977). Phosphorylation of cytokinin by adenosine kinase from Wheat-Germ. Plant Physiology **59,** 443-447.

Chen, C.M., and Petschow, B. (1978). Metabolism of Cytokinin - Ribosylation of Cytokinin Bases by Adenosine Phosphorylase from Wheat Germ. Plant Physiology **62,** 871-874.

Chen, C.M., and Melitz, D.K. (1979). Cytokinin biosynthesis in a cell-free system from cytokinin-autotrophic tobacco tissue-cultures. FEBS Letters **107,** 15-20.

Chen, C.M., and Kristopeit, S.M. (1981a). Metabolism of Cytokinin: Deribosylation of Cytokinin Ribonucleoside by Adenosine Nucleosidase from Wheat Germ Cells. Plant Physiology **68,** 1020-1023.

Chen, C.M., and Kristopeit, S.M. (1981b). Metabolism of Cytokinin : Dephosphorylation of Cytokinin ribonucleotife by 5'-Nucleotidases from Wheat Germ cytosol. Plant Physiology **67,** 494-498.

Chen, C.M., Melitz, D.K., and Clough, F.W. (1982a). Metabolism of cytokinin - Phosphoribosylation of cytokinin bases by adenine phosphoribosyl transferase from wheat-germ. Archives of Biochemistry and Biophysics **214,** 634-641.

Chen, C.M., Melitz, D.K., and Clough, F.W. (1982b). Metabolism of cytokinin: phosphoribosylation of cytokinin bases by adenine phosphoribosyltransferase from wheat germ. Archives of Biochemistry and Biophysics **214,** 634-641.

Claassens, M.M.J., and Vreugdenhil, D. (2000). Is dormancy breaking of potato tubers the reverse of tuber initiation? Potato Research **43,** 347-369.

Coleman, W.K. (1987). Dormancy release in potato tubers - a review. American Potato Journal **64,** 57-68.

Collier, M.D., Sheppard, L.J., Crossley, A., and Hanke, D.E. (2003). Needle cytokinin content as a sensitive bioindicator of N pollution in Sitka spruce. Plant Cell and Environment **26,** 1929-1939.

Cooke, J.E.K., and Weih, M. (2005). Nitrogen Storage and Seasonal Nitrogen Cycling in Populus: Bridging Molecular Physiology and Ecophysiology. New Phytologist **167,** 19-29.

Cornell, K.A., and Riscoe, M.K. (1998). Cloning and expression of *Escherichia coli* 5 '-methylthioadenosine/S-adenosylhomocysteine nucleosidase: Identification of the pfs gene product. Biochimica Et Biophysica Acta-Gene Structure and Expression **1396,** 8-14.

Crofcheck, C., Loiselle, M., Weekley, J., Maiti, I., Pattanaik, S., Bummer, P.M., and Jayt, M. (2003). Histidine tagged protein recovery from tobacco extract by foam fractionation. Biotechnology Progress **19,** 680-682.

Dent, R.M. (1996). Cytokinin O-glucosides: Neglected products of cytokinin metabolism. In Department of Plant Sciences (Cambridge: University of Cambridge).

Dolja, V.V., Peremyslov, V.V., Keller, K.E., Martin, R.R., and Hong, J. (1998). Isolation and stability of histidine-tagged proteins produced in plants via potyvirus gene vectors. Virology **252,** 269-274.

Donnelly, D., Coleman, W., and Coleman, S. (2003). Potato microtuber production and performance: A review. American Journal of Potato Research **80,** 103-115.

Ealick, S.E., Rule, S.A., Carter, D.C., Greenhough, T.J., Babu, Y.S., Cook, W.J., Habash, J., Helliwell, J.R., Stoeckler, J.D. (1990). Three-dimensional structure of Human Erythrocytic Purine Nucleoside Phosphorylase at 3.2A resolution. Journal of Biological Chemistry **265**, 1812-1820.

Ellinger, S., Mach, M., Korn, K., and Jahn, G. (1991). Cleavage and purification of prokaryotically expressed HIV GAG and ENV fusion proteins for detection of HIV antibodies in the ELISA. Virology **180,** 811-813.

Erlanger, B.F., and Beiser, S.M. (1964). Antibodies specific for ribonucleosides and ribonucleotides and their reaction with DNA. Proceedings of the National Academy of Sciences of the United States of America **52,** 68.

Espinosa, A., Iglesias, J.M., Bou, J., and Prat, S. (2004). Gibberellin and daylength control of potato tuberisation. Acta Physiologiae Plantarum **26,** 5-5.

Ewing, E.E., and Struik, P.C. (1992). Tuber formation in potato: induction, initiation and growth. Horticultural Reviews **14,** 89-197.

Farre, E.M., Bachmann, A., Willmitzer, L., and Trethewey, R.N. (2001). Acceleration of potato tuber sprouting by the expression of a bacterial pyrophosphatase. Nature Biotechnology **19,** 268-272.

Fernie, A.R., and Willmitzer, L. (2001). Molecular and biochemical triggers of potato tuber development. Plant Physiology **127,** 1459-1465.

Ferreira, F.J., and Kieber, J.J. (2005). Cytokinin signaling. Current Opinion in Plant Biology **8,** 518-525.

Gális, I., Macas, J., Vlasák, J., Ondřej, M., and Van Onckelen, H. (1995). The effect of an elevated cytokinin level using the ipt gene and N 6-benzyladenine on single node and intact potato plant tuberization in vitro. Journal of Plant Growth Regulation **14,** 143-150.

Golovko, A., Sitbon, F., Tillberg, E., and Nicander, B. (2002). Identification of a tRNA isopentenyltransferase gene from Arabidopsis thaliana. Plant Molecular Biology **49,** 161-169.

Gomez-Roldan, V., Fermas, S., Brewer, P.B., Puech-Pages, V., Dun, E.A., Pillot, J.P., Letisse, F., Matusova, R., Danoun, S., Portais, J.C., Bouwmeester, H., Becard, G., Beveridge, C.A., Rameau, C., and Rochange, S.F. (2008). Strigolactone inhibition of shoot branching. Nature **455**, 189-194.

Gopal, J., Minocha, J.L., and Dhaliwal, H.S. (1998). Microtuberization in potato (*Solanum tuberosum* L.). Plant Cell Reports **17,** 794-798.

Gray, J., Gelvin, S.B., Meilan, R., and Morris, R.O. (1996). Transfer RNA is the source of extracellular isopentenyladenine in a Ti-plasmidless strain of Agrobacterium tumefaciens. Plant Physiology **110,** 431-438.

Hare, P.D., and van Staden, J. (1997). The molecular basis of cytokinin action. Plant Growth Regulation **23,** 41-78.

Harkett, P.J. (1981). External factors affecting length of dormancy period in potato. Journal of the Science of Food and Agriculture **32,** 102-103.

Hellens, R.P., Edwards, E.A., Leyland, N.R., Bean, S., and Mullineaux, P.M. (2000). pGreen: a versatile and flexible binary Ti vector for *Agrobacterium*-mediated plant transformation. Plant Molecular Biology **42,** 819-832.

Hemberg, T. (1970). Action of some cytokinins on rest-period and content of acid growth-inhibiting substances in potato. Physiologia Plantarum **23,** 850-858.

Herrmann, K.M., and Weaver, L.M. (1999). The shikimate pathway. Annual Review of Plant Physiology and Plant Molecular Biology **50,** 473-503.

Heyl, A., and Schmulling, T. (2003). Cytokinin signal perception and transduction. Current Opinion in Plant Biology **6,** 480-488.

Hirose, N., Takei, K., Kuroha, T., Kamada-Nobusada, T., Hayashi, H., and Sakakibara, H. (2007). Regulation of cytokinin biosynthesis, compartmentalization and translocation. Journal of Experimental Botany **59,** 75-83.

Hoekema, A., Hirsch, P.R., Hooykaas, P.J.J., and Schilperoort, R.A. (1983). A binary plant vector strategy based on separation of VIR-Region and T-Region of the *Agrobacterium tumefaciens* Ti-plasmid. Nature **303,** 179-180.

Hutchison, C.E., and Kieber, J.J. (2002). Cytokinin signaling in Arabidopsis. Plant Cell **14 Suppl,** S47-59.

Hutchison, C.E., Li, J., Argueso, C., Gonzalez, M., Lee, E., Lewis, M.W., Maxwell, B.B., Perdue, T.D., Schaller, G.E., Alonso, J.M., Ecker, J.R., and Kieber, J.J. (2006). The Arabidopsis histidine phosphotransfer proteins are redundant positive regulators of cytokinin signaling. Plant Cell **18**, 3073-3087.

Hwang, I., and Sheen, J. (2001). Two-component circuitry in *Arabidopsis* cytokinin signal transduction. Nature **413,** 383-389.

Hwang, I., and Sakakibara, H. (2006). Cytokinin biosynthesis and perception. Physiologia Plantarum **126,** 528-538.

Inoue, T., Higuchi, M., Hashimoto, Y., Seki, M., Kobayashi, M., Kato, T., Tabata, S., Shinozaki, K., and Kakimoto, T. (2001). Identification of CRE1 as a cytokinin receptor from *Arabidopsis*. Nature **409**, 1060-1063.

Jackson, S.D. (1999). Multiple signalling pathways control tuber induction in potato. Plant Physiology **119,** 1-8.

Jackson, S.D., Heyer, A., Dietze, J., and Prat, S. (1996). Phytochrome B mediates the photoperiodic control of tuber formation in potato. Plant Journal **9,** 159-166.

Jameson, P.E., McWha, J.A., and Haslemore, R.M. (1985). Changes in cytokinins during initiation and development of potato tubers. Physiologia Plantarum **63,** 53-57.

Jefferson, R.A., Klass, M., Wolf, N., and Hirsh, D. (1987). Expression of chimeric genes in *Caenorhabditis elegans*. Journal of Molecular Biology **193,** 41-46.

Kakimoto, T. (1996). CKI1, a histidine kinase homolog implicated in cytokinin signal transduction. Science **274,** 982-985.

Kakimoto, T. (2003a). Perception and signal transduction of cytokinins. Annual Review of Plant Biology **54,** 605-627.

Kakimoto, T. (2003b). Biosynthesis of cytokinins. Journal of Plant Research **116,** 233-239.

Kamada-Nobusada, T., and Sakakibara, H. (2009). Molecular basis for cytokinin biosynthesis. Phytochemistry **70,** 444-449.

Kaminek, M., Paces, V., Corse, J., and Challice, J.S. (1979). Effect of stereospecific hydroxylation of N^6-(delta-2-isopentenyl)adenosine on cytokinin activity. Planta **145,** 239-243.

Kapust, R.B., and Waugh, D.S. (1999). *Escherichia coli* maltose-binding protein is uncommonly effective at promoting the solubility of polypeptides to which it is fused. Protein Science **8,** 1668-1674.

Kasahara, H., Takei, K., Ueda, N., Hishiyama, S., Yamaya, T., Kamiya, Y., Yamaguchi, S., and Sakakibara, H. (2004). Distinct isoprenoid origins of cis- and trans-zeatin biosyntheses in Arabidopsis. Journal of Biological Chemistry **279,** 14049-14054.

Katahira, R., and Ashihara, H. (2006). Profiles of purine biosynthesis, salvage and degradation in disks of potato (*Solanum tuberosum* L.) tubers. Planta **225,** 115-126.

Kicska, G.A., Tyler, P.C., Evans, G.B., Furneaux, R.H., Kim, K., and Schramm, V.L. (2002). Transition state analogue inhibitors of purine nucleoside phosphorylase from *Plasmodium falciparum*. Journal of Biological Chemistry **277,** 3219-3225.

Kim, M., Kim, H., Kim, H., Kim, Y., Baek, K., Park, Y., Joung, H., and Jeon, J. (2007). Growth and tuberization of transgenic potato plants expressing sense and antisense sequences of Cu/Zn superoxide dismutase from lily chloroplasts. Journal of Plant Biology **50,** 490-495.

Koda, Y. (1982a). Changes in levels of butanol-soluble and water-soluble cytokinins during the life-cycle of potato tubers. Plant and Cell Physiology **23,** 843-849.

Koda, Y. (1982b). Effects of storage temperature and wounding on cytokinin levels in potato tubers. Plant and Cell Physiology **23,** 851-857.

Krauss, A. (1985). Interaction of nitrogen nutrition, phytohormones and tuberisation. In Potato Physiology, P.H. Li, ed (London, UK: Academic Press), pp. 209-231.

Kumar, D., and Wareing, P.F. (1972). Factors controlling stolon development in the potato plant. New Phytologist **71,** 639-648.

Kurakawa, T., Ueda, N., Maekawa, M., Kobayashi, K., Kojima, M., Nagato, Y., Sakakibara, H., and Kyozuka, J. (2007). Direct control of shoot meristem activity by a cytokinin-activating enzyme. Nature **445**, 652-655.

Laloue, M., and Pethe, C. (1982). Dynamics of cytokinin metabolism in tobacco cells. In Plant Growth Substances, P.F. Wareing, ed (London: Academic Press), pp. 185-195.

Lang, G.A., Early, J.D., Martin, G.C., and Darnell, R.L. (1987). Endodormancy, paradormancy, and ecodormancy - Physiological terminilogy and classification for dormancy research. Hortscience **22,** 371-377.

Lavallie, E.R., Diblasio, E.A., Kovacic, S., Grant, K.L., Schendel, P.F., and McCoy, J.M. (1993). A thioredoxin gene fusion expression system that circumvents inclusion body formation in the *Escherichia coli* cytoplasm. Bio-Technology **11,** 187-193.

Leshem, B., and Clowes, F.A.L. (1972). Rates of mitosis in shoot apices of potatoes at the beginning and end of dormancy. Annals of Botany **36,** 687-691.

Letham, D.S. (1994). Cytokinins as phytohormones: sites of biosynthesis, translocation, and function of translocated cytokinin. In Cytokinins - Chemistry, activity and function, D.W.S. Mok and M.C. Mok, eds (Boca Raton: CRC Press.

Letham, D.S., Tao, G.Q., and Parker, C.W. (1982). An overview of cytokinin metabolism. In Plant Growth Substances, P.F. Wareing, ed (London: Academic Press), pp. 143-153.

Levy, D., Seabrook, J.E.A., and Coleman, S. (1993). Enhancement of tuberisation fo axillary shoot buds of potato (*Solanum tuberosum* L.) cultivars cultured *in vitro*. Journal of Experimental Botany **44,** 381-386.

Lineweaver, H., and Burk, D. (1934). The Determination of Enzyme Dissociation Constants. Journal of the American Chemistry Society **56,** 658-666.

Ling, R., Colon, E., Dahmus, M.E., and Callis, J. (2000). Histidine-tagged ubiquitin substitutes for wild-type ubiquitin in *Saccharomyces cerevisiae* and facilitates isolation and identification of in vivo substrates of the ubiquitin pathway. Analytical Biochemistry **282,** 54-64.

Macháčková, I., Sergeeva , L., Ondřej, M., Zaltsman, O., Konstantinova, T., Eder, J., Ovesná, J., Golyanovskaya, S., Rakitin, Y., and Aksenova, N. (1997). Growth pattern, tuber formation and hormonal balance in *in vitro* potato plants carrying *ipt* gene. Plant Growth Regulation **21**, 27-36.

MacRae, A.F., Preiszner, J., Ng, S., and Bolla, R.I. (2004). Expression of His-tagged Shigella IpaC in Arabidopsis. Journal of Biotechnology **112,** 247-253.

Marchler-Bauer, A., and Bryant, S.H. (2004). CD-Search: protein domain annotations on the fly. Nucleic Acids Research **32,** W327-W331.

Marchler-Bauer, A., Anderson, J.B., Cherukuri, P.F., DeWweese-Scott, C., Geer, L.Y., Gwadz, M., He, S.Q., Hurwitz, D.I., Jackson, J.D., Ke, Z.X., Lanczycki, C.J., Liebert, C.A., Liu, C.L., Lu, F., Marchler, G.H., Mullokandov, M., Shoemaker, B.A., Simonyan, V., Song, J.S., Thiessen, P.A., Yamashita, R.A., Yin, J.J., Zhang, D.C., and Bryant, S.H. (2005). CDD: a conserved domain database for protein classification. Nucleic Acids Research **33**, D192-D196.

Marchler-Bauer, A., Anderson, J.B., Derbyshire, M.K., DeWeese-Scott, C., Gonzales, N.R., Gwadz, M., Hao, L.N., He, S.Q., Hurwitz, D.I., Jackson, J.D., Ke, Z.X., Krylov, D., Lanczycki, C.J., Liebert, C.A., Liu, C.L., Lu, F., Lu, S.N., Marchler, G.H., Mullokandov, M., Song, J.S., Thanki, N., Yamashita, R.A., Yin, J.J., Zhang, D.C., and Bryant, S.H. (2007). CDD: a conserved domain database for interactive domain family analysis. Nucleic Acids Research **35**, D237-D240.

Marchler-Bauer, A., Anderson, J.B., DeWeese-Scott, C., Fedorova, N.D., Geer, L.Y., He, S.Q., Hurwitz, D.I., Jackson, J.D., Jacobs, A.R., Lanczycki, C.J., Liebert, C.A., Liu, C.L., Madej, T., Marchler, G.H., Mazumder, R., Nikolskaya, A.N., Panchenko, A.R., Rao, B.S., Shoemaker, B.A., Simonyan, V., Song, J.S., Thiessen, P.A., Vasudevan, S., Wang, Y.L., Yamashita, R.A., Yin, J.J., and Bryant, S.H. (2003). CDD: a curated Entrez database of conserved domain alignments. Nucleic Acids Research **31**, 383-387.

Martinez-Garcia, J.F., Virgos-Soler, A., and Prat, S. (2002). Control of photoperiod-regulated tuberization in potato by the *Arabidopsis* flowering-time gene CONSTANS. Proceedings of the National Academy of Sciences of the United States of America **99,** 15211-15216.

Mason, M.G., Mathews, D.E., Argyros, D.A., Maxwell, B.B., Kieber, J.J., Alonso, J.M., Ecker, J.R., and Schaller, G.E. (2005). Multiple type-B response regulators mediate cytokinin signal transduction in Arabidopsis. Plant Cell **17**, 3007-3018.

Mauk, C.S., and Langille, A.R. (1978). Effect of induction on zeatin riboside levels in katahdin potato plant. American Potato Journal **55,** 386-386.

Michaelis, L., and Menten, M.L. (1913). Kinetics of invertase action. Biochemische Zeitschrift **49,** 333-369.

Miyawaki, K., Matsumoto-Kitano, M., and Kakimoto, T. (2004). Expression of cytokinin biosynthetic isopentenyltransferase genes in *Arabidopsis*: tissue specificity and regulation by auxin, cytokinin, and nitrate. Plant Journal **37,** 128-138.

Miyawaki, K., Tarkowski, P., Matsumoto-Kitano, M., Kato, T., Sato, S., Tarkowska, D., Tabata, S., Sandberg, G., and Kakimoto, T. (2006). Roles of *Arabidopsis* ATP/ADP isopentenyltransferases and tRNA isopentenyltransferases in cytokinin biosynthesis. Proceedings of the National Academy of Sciences of the United States of America **103**, 16598-16603.

Moffatt, B., Pethe, C., and Laloue, M. (1991). Metabolism of benzyladenine is impaired in a mutant of *Arabidopsis thaliana* lacking adenine phosphoribosyl transferase activity. Plant Physiology **95,** 900-908.

Mohlmann, T., Mezher, Z., Schwerdtfeger, G., and Neuhaus, H.E. (2001). Characterisation of a concentrative type of adenosine transporter from Arabidopsis thaliana (ENT1,At). Febs Letters **509,** 370-374.

Mok, D.W.S., and Mok, M.C. (2001). Cytokinin metabolism and action. Annual Review of Plant Physiology and Plant Molecular Biology **52,** 89-118.

Mok, M.C. (1994). Cytokinins and plant development - An overview. In Cytokinins – Chemistry, Activity, and Function, M.C. Mok and D.W.S. Mok, eds (Boca Raton CRC Press), pp. 155-166.

Mok, M.C., Martin, R.C., and Mok, D.W.S. (2000). Cytokinins: Biosynthesis, metabolism and perception. In Vitro Cellular & Developmental Biology-Plant **36,** 102-107.

Morris, S.E., Turnbull, C.G.N., Murfet, I.C., and Beveridge, C.A. (2001). Mutational analysis of branching in pea. Evidence that Rms1 and Rms5 regulate the same novel signal. Plant Physiology **126,** 1205-1213.

Morris, W.L., Ducreux, L.J.M., Hedden, P., Millam, S., and Taylor, M.A. (2006). Overexpression of a bacterial 1-deoxy-D-xylulose 5-phosphate synthase gene in potato tubers perturbs the isoprenoid metabolic network: implications for the control of the tuber life cycle. Journal of Experimental Botany **57,** 3007-3018.

Moshides, J.S. (1988). Enzymic determination of the free cholesterol fraction of high-density lipoprotein in plasma with the use of 2,4,6-tribromo-3-hydrobenzoic acid. Clinical Chemistry **34,** 1799-1804.

Mucci, L.A., and Adami, H.O. (2009). The Plight of the Potato: Is Dietary Acrylamide a Risk Factor for Human Cancer? Journal of the National Cancer Institute **101,** 618-621.

Mushegian, A.R., and Koonin, E.V. (1994). Unexpected sequence similarity between nucleosidases and phosphoribosyl transferases of different specificity. Protein Science **3,** 1081-1088.

Nishimura, C., Ohashi, Y., Sato, S., Kato, T., Tabata, S., and Ueguchi, C. (2004). Histidine kinase homologs that act as cytokinin receptors possess overlapping functions in the regulation of shoot and root growth in Arabidopsis. Plant Cell **16,** 1365-1377.

O'Brien, P.J., Allen, E.J., and Firman, D.M. (1998). A review of some studies into tuber initiation in potato (Solanum tuberosum) crops. Journal of Agricultural Science **130,** 251-270.

Oka, A. (2003). New insights into cytokinins. Journal of Plant Research **116,** 217-220.

Palmer, C.E., and Smith, O.E. (1969). Cytokinins and tuber initiation in the potato *Solanum tuberosum* L. Nature **221,** 279-280.

Petschow, B.W., and Chen, C.M. (1978). Ribosylation of cytokinin bases by adenosine phosphorylase from plant cells. Plant Physiology **61,** 11-11.

Prinsen, E., Kaminek, M., and van Onckelen, H.A. (1997). Cytokinin biosynthesis: a black box? Plant Growth Regulation **23,** 3-15.

Prinsen, E., Redig, P., Vandongen, W., Esmans, E.L., and Vanonckelen, H.A. (1995). Quantitative analysis of cytokinins by electrospray tandem mass-spectrometry. Rapid Communications in Mass Spectrometry **9,** 948-953.

Rashotte, A.M., Mason, M.G., Hutchison, C.E., Ferreira, F.J., Schaller, G.E., and Kieber, J.J. (2006). A subset of Arabidopsis AP2 transcription factors mediates cytokinin responses in concert with a two-component pathway. Proceedings of the National Academy of Sciences of the United States of America **103,** 11081-11085.

Riefler, M., Novak, O., Strnad, M., and Schmulling, T. (2006). Arabidopsis cytokinin receptor mutants reveal functions in shoot growth, leaf senescence, seed size, germination, root development, and cytokinin metabolism. Plant Cell **18,** 40-54.

Riewe, D., Grosman, L., Fernie, A.R., Zauber, H., Wucke, C., and Geigenberger, P. (2008). A Cell Wall-Bound Adenosine Nucleosidase is Involved in the Salvage of Extracellular ATP in *Solanum tuberosum*. Plant and Cell Physiology **49,** 1572-1579.

Riggs, P. (2000). Expression and purification of recombinant proteins by fusion to maltose-binding protein. Molecular Biotechnology **15,** 51-63.

Rodriguez-Falcon, M., Bou, J., and Prat, S. (2006). Seasonal control of tuberization in potato: Conserved elements with the flowering response. Annual Review of Plant Biology **57,** 151-180.

Romanov, G.A., Lomin, S.N., and Schmulling, T. (2006). Biochemical characteristics and ligand-binding properties of Arabidopsis cytokinin receptor AHK3 compared to CRE1/AHK4 as revealed by a direct binding assay. Journal of Experimental Botany **57,** 4051-4058.

Sambrook, J., Fritsch, E.F., and Maniatis, T. (1989). Molecular Cloning: A Laboratory Manual. (New York: Cold Spring Harbor Laboratory Press).

Sarkar, D. (2008). The signal transduction pathways controlling in planta tuberization in potato: an emerging synthesis. Plant Cell Reports **27,** 1-8.

Sattelmacher, B., and Marschner, H. (1978). Cytokinin activity in stolons and tubers of *Solanum tuberosum* during period of tuberisation. Physiologia Plantarum **44,** 69-72.

Schmulling, T. (2001). CREam of cytokinin signalling: receptor identified. Trends in Plant Science **6,** 281-284.

Schnorr, K.M., Gaillard, C., Biget, E., Nygaard, P., and Laloue, M. (1996). A second form of adenine phosphoribosyltransferase in *Arabidopsis thaliana* with relative specificity towards cytokinins. Plant Journal **9,** 891-898.

Seabrook, J.E.A., Coleman, S., and Levy, D. (1993). Effect of photoperiod on *in vitro* tuberisation of potato (*Solanum tuberosum* L.). Plant Cell Tissue and Organ Culture **34,** 43-51.

Sergeeva, L.I., de Bruijn, S.M., Koot-Gronsveld, E.A.M., Navratil, O., and Vreugdenhil, D. (2000). Tuber morphology and starch accumulation are independent phenomena: Evidence from ipt-transgenic potato lines. Physiologia Plantarum **108,** 435-443.

Shahba, M.A., Stushnoff, C., McSay, A.E., Holm, D., and Davidson, R. (2007). Effect of temperature on storage properties, dormancy, soluble sugar content and alpha-galactosidase activity of seven new potato (*Solanum tuberosum* L.) cultivars. Journal of Food Agriculture & Environment **5,** 116-121.

Shiio, I., and Ishii, K. (1969). Regulation of purine ribonucleotide synthesis by end product inhibition. Journal of Biological Chemistry **66,** 175-181.

Smith, D.B., and Johnson, K.S. (1988). Single-step purification of polypeptides expressed in *Escherichia coli* as fusions with glutathione S-transferase. Gene **67,** 31-40.

Sonnewald, U. (2001). Control of potato tuber sprouting. Trends in Plant Science **6,** 333-335.

Spichal, L., Rakova, N.Y., Riefler, M., Mizuno, T., Romanov, G.A., Strnad, M., and Schmulling, T. (2004). Two cytokinin receptors of *Arabidopsis thaliana*, CRE1/AHK4 and AHK3, differ in their ligand specificity in a bacterial assay. Plant and Cell Physiology **45,** 1299-1305.

Stadler, R.H., Blank, I., Varga, N., Robert, F., Hau, J., Guy, P.A., Robert, M.C., and Riediker, S. (2002). Acrylamide from Maillard reaction products. Nature **419**, 449-450.

Strnad, M., Peters, W., Beck, E., and Kaminek, M. (1992). Immunodetection and identification of N^6-(O-hydroxybenzylamino)purine as a naturally occuring cytokinin in *Populus X canadensis moench* cv Robusta Leaves. Plant Physiology **99,** 74-80.

Sun, J.P., Hirose, N., Wang, X.C., Wen, P., Xue, L., Sakakibara, H., and Zuo, J.R. (2005). Arabidopsis SOI33/AtENT8 gene encodes a putative equilibrative nucleoside transporter that is involved in cytokinin transport in planta. Journal of Integrative Plant Biology **47,** 588-603.

Sun, T.P., and Gubler, F. (2004). Molecular mechanism of gibberellin signaling in plants. Annual Review of Plant Biology **55,** 197-223.

Suttle, J.C. (1996). Dormancy in tuberous organs: Problems and perspectives. In Plant Dormancy: Physiology, Biochemistry & Molecular Biology, G.A. Lang, ed (Wallingford, UK: CAB International), pp. 133-143.

Suttle, J.C. (2004). Physiological regulation of potato tuber dormancy. American Journal of Potato Research **81,** 253-262.

Suttle, J.C., and Banowetz, G.M. (2000). Changes in cis-zeatin and cis-zeatin riboside levels and biological activity during potato tuber dormancy. Physiologia Plantarum **109,** 68-74.

Suzuki, T., Miwa, K., Ishikawa, K., Yamada, H., Aiba, H., and Mizuno, T. (2001). The Arabidopsis sensor His-kinase, AHK4, can respond to cytokinins. Plant and Cell Physiology **42,** 107-113.

Takei, K., Sakakibara, H., and Sugiyama, T. (2001). Identification of genes encoding adenylate isopentenyltransferase, a cytokinin biosynthesis enzyme, in *Arabidopsis thaliana*. Journal of Biological Chemistry **276,** 26405-26410.

Takei, K., Yamaya, T., and Sakakibara, H. (2004). Arabidopsis CYP735A1 and CYP735A2 encode cytokinin hydroxylases that catalyze the biosynthesis of *trans*-Zeatin. Journal of Biological Chemistry **279,** 41866-41872.

Taya, Y., Tanaka, Y., and Nishimura, S. (1978). 5'-AMP is a direct precursor of cytokinin in *Dictyostelium discoideum*. Nature **271,** 545-547.

Taylor, M.A., Wright, F., and Davies, H.V. (1994). Characterisation of the cDNA clones of 2 beta-tubulin genes and their expression in the potato plant (*Solanum tuberosum* L.). Plant Molecular Biology **26,** 1013-1018.

Terzaghi, W.B., and Cashmore, A.R. (1995). Light-regulated transcription. Annual Review of Plant Physiology and Plant Molecular Biology **46,** 445-474.

Thomson, J.P. (1994). Towards a receptor for cytokinins. In Department of Plant Sciences (Cambridge: University of Cambridge).

To, J.P., and Kieber, J.J. (2008). Cytokinin signaling: two-components and more. Trends in Plant Science **13,** 85-92.

To, J.P.C., Haberer, G., Ferreira, F.J., Deruere, J., Mason, M.G., Schaller, G.E., Alonso, J.M., Ecker, J.R., and Kieber, J.J. (2004). Type-A *Arabidopsis* response regulators are partially redundant negative regulators of cytokinin signaling. Plant Cell **16**, 658-671.

Triccas, J.A., Pinto, R., and Britton, W.J. (2002). Destabilized green fluorescent protein for monitoring transient changes in mycobacterial gene expression. Research in Microbiology **153,** 379-383.

Turnbull, C.G.N. (1982). Cytokinins and potato dormancy. In Department of Plant Sciences (Cambridge: University of Cambridge).

Turnbull, C.G.N., and Hanke, D.E. (1985a). The control of bud dormancy in potato tubers - evidence for the primary roles of cytokinins and a seasonal pattern of changing sensitivity to cytokinin. Planta **165,** 359-365.

Turnbull, C.G.N., and Hanke, D.E. (1985b). The control of bud dormancy in potato tubers - Measurement of the seasonal pattern of changing concentrations of zeatin-cytokinins. Planta **165,** 366-376.

Ueguchi, C., Sato, S., Kato, T., and Tabata, S. (2001). The AHK4 gene involved in the cytokinin-signaling pathway as a direct receptor molecule in Arabidopsis thaliana. Plant and Cell Physiology **42,** 751-755.

Van Staden, J., and Dimalla, G.G. (1977). The distribution of cytokinins in tuberizing potatoes. Annals of Botany **41,** 741-746.

Van Staden, J., and Dimalla, G.G. (1978). Endogenous cytokinins and breaking of dormancy and apical dominance in potato tubers. Journal of Experimental Botany **29,** 1077-1084.

Vaneck, H.J., Jacobs, J.M.E., Stam, P., Ton, J., Stiekema, W.J., and Jacobsen, E. (1994). Mulitple alleles for tuber shape in diploid potato detected by qualitative and quantitative genetic-analysis using RFLPs. Genetics **137,** 303-309.

Viola, R., Pelloux, J., van der Ploeg, A., Gillespie, T., Marquis, N., Roberts, A.G., and Hancock, R.D. (2007). Symplastic connection is required for bud outgrowth following dormancy in potato (*Solanum tuberosum* L.) tubers. Plant Cell and Environment **30,** 973-983.

Viola, R., Roberts, A.G., Haupt, S., Gazzani, S., Hancock, R.D., Marmiroli, N., Machray, G.C., and Oparka, K.J. (2001). Tuberization in potato involves a switch from apoplastic to symplastic phloem unloading. Plant Cell **13,** 385-398.

Visser, R.G.F. (1991). Regeneration and transformation of potato by *Agrobacterium tumefaciens*. In Plant Tissue Culture Manual: fundamentals and applications, K. Lindsey, ed (Berlin: Springer), pp. 1-9.

Vreugdenhil, D. (2007). The Canon of Potato Science: 39. Dormancy. Potato Research **50,** 371-373.

Vreugdenhil, D., and Struik, P.C. (1989). An integrated view of the hormonal regulation of tuber formation in potato (*Solanum tuberosum*). Physiologia Plantarum **75,** 525-531.

Vreugdenhil, D., Claassens, M.M.J., Verhees, J., van der Krol, A.R., and van der Plas, L.H.W. (2006). Ethanol-inducible gene expression: non-transformed plants also respond to ethanol. Trends in Plant Science **11,** 9-11.

Warnes, B.J. (2005). Cytokinins and Potato Tuber Development. In Department of Plant Sciences (Cambridge: University of Cambridge).

Wee, E.G.T., Sherrier, D.J., Prime, T.A., and Dupree, P. (1998). Targeting of active sialyltransferase to the plant Golgi apparatus. Plant Cell **10,** 1759-1768.

Werner, T., Motyka, V., Strnad, M., and Schmulling, T. (2001). Regulation of plant growth by cytokinin. Proceedings of the National Academy of Sciences of the United States of America **98,** 10487-10492.

Wetzel, S., Demmers, C., and Greenwood, J.S. (1989). Seasonally fluctuating bark proteins are a potential form of nitrogen storage in 3 temperate hardwoods. Planta **178,** 275-281.

Wilkins, C.G. (2004). Analysis of genes regulating plant perception of cytokinins. In Department of Plant Sciences (Cambridge: University of Cambridge).

Wiltshire, J.J.J., and Cobb, A.H. (1996). A review of the physiology of potato tuber dormancy. Annals of Applied Biology **129,** 553-569.

Winwood, J., Pate, A.E., Price, A.J., and Hanke, D.E. (2007). Effects of long-term, free-air ozone fumigation on the cytokinin content of mature beech trees. Plant Biology **9,** 265-278.

Wurr, D., Fellows, J., Lynn, J., and Allen, E. (1993). The impact of some agronomic factors on the variability of potato tuber size distribution. Potato Research **36,** 237-245.

Wurr, D.C.E., and Allen, E.J. (1976). Effects of cold treatments on sprout growth of three potato varieties. Journal of Agricultural Science **86,** 221-224.

Xu, X., Vreugdenhil, D., and van Lammeren, A.A.M. (1998). Cell division and cell enlargement during potato tuber formation. Journal of Experimental Botany **49,** 573-582.

Yamada, H., Suzuki, T., Terada, K., Takei, K., Ishikawa, K., Miwa, K., Yamashino, T., and Mizuno, T. (2001). The Arabidopsis AHK4 histidine kinase is a cytokinin-binding receptor that transduces cytokinin signals across the membrane. Plant and Cell Physiology **42,** 1017-1023.

Yonekura-Sakakibara, K., Kojima, M., Yamaya, T., and Sakakibara, H. (2004). Molecular characterization of cytokinin-responsive histidine kinases in maize: Differential ligand preferences, response to cis-zeatin and the subcellular localizations. Plant and Cell Physiology **45,** S41-S41.

Zhu, B.L., and Coleman, G.D. (2001). The poplar bark storage protein gene (Bspa) promoter is responsive to photoperiod and nitrogen in transgenic poplar and active in floral tissues, immature seeds and germinating seeds of transgenic tobacco. Plant Molecular Biology **46,** 383-394.

Zubko, E., Macháčková, I., Malbeck, J., and Meyer, P. (2005). Modification of cytokinin levels in potato via expression of the *Petunia hybrida Sho* gene. Transgenic Research **14,** 615-618.

Zubko, E., Adams, C.J., Macháčková, I., Malbeck, J., Scollan, C., and Meyer, P. (2002). Activation tagging identifies a gene from *Petunia hybrida* responsible for the production of active cytokinins in plants. Plant Journal **29,** 797-808.

Zuckerman, L. (1998). The Potato: How the Humble Spud Rescued the Western World. (London, UK: Macmillan).